Finite Difference Approximations of Second Order Quasi-linear Elliptic and Hyperbolic Stochastic Partial Differential Equations

Robert J. Pefferly Jr.
9600206

Doctor of Philosophy
University of Edinburgh
2001

ACKNOWLEDGEMENTS

I would like thank both Dr. Jessica Gaines and Dr. Sandy Davie for their eternal patience, care, concern, and help over these past few years. Without their guidance and recommendations completing this thesis would have been an impossible task. Thank you from the bottom of my heart. I would also like to acknowledge the Edinburgh University Mathematics Department and Luleå Universitet Software Engineering Department for their efforts in creating an environment encouraging learning and professional development.

Mor and Mormor, words cannot express my gratitude.

This work was funded in part by the United States-United Kingdom Fulbright Organisation.

Table of Contents

Chapter 1

Introduction

> In principle the accurate solution of the governing equations with appropriate boundary and initial conditions will reveal all required information in any particular problem. However, the equations of motion are so complex that only rarely can exact solutions be found, and any method of approximation of the equations requires first an understanding of the broad, general, physical principles with which any approximation must be consistent. [53, page 22]

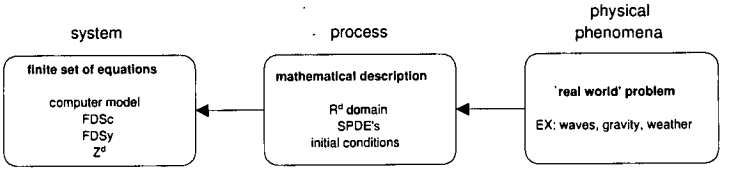

Figure 1.1: Levels of abstraction for physical problems

The definitions of 'equation' and 'space' are taken in the usual sense and given a 'physical phenomena' that one wishes to investigate:

•A 'process' is a mathematical description of the phenomena that involves partial differential equations and the initial conditions necessary to 'solve' the problem.

•A 'system' is a finite set of simultaneous equations and initial conditions that are used to model a process. The implementation and/or solution of this system will be called a 'numerical evaluation,' 'approximation,' or 'estimate.'

A partial differential equation, PDE, expresses the relationship between a function and its derivatives with respect to different state variables over a continuous space. When using PDE's, improvements can be made by adding non-deterministic (stochastic) elements to the equations to account for the seemingly random fluctuations between a 'good' deterministic model and the phenomena the process is describing. These fluctuations are due to the circumstances that:

•There generally is a measurement error in any mechanical device.
•There is incomplete or non-exact information about the initial conditions.
•Numerical methods utilise a finite number of decimal places, thus initial conditions and subsequent iterations introduce round off errors.
•Processes are often a truncation or idealization of a phenomenon that might utilise incomplete theory or disregard necessary variables.

The stochastic partial differential equations, SPDE's, considered in this text are interpreted in the Walsh distribution valued stochastic process sense using a standard Brownian sheet; refer to [60, Chapter 2]. SPDE's interpreted using a Kondratiev space or a nuclear covariance will not be considered; refer to [34, Chapter 1], [41], and [60]. As per standard notation, 'pathwise' solutions are dependent upon a single generation of a stochastic space, while 'non-pathwise' solutions are dependent upon the statistical properties of a stochastic space. As discussed in [2], when initial conditions are imposed on a process where a solution exists, is unique, and depends continuously on the data; then the initial conditions and process will be labeled 'well posed.' Given a well posed problem:
•$F(\cdot)$ denotes a 'solution' that identically satisfies a process on an a priori domain and $\widehat{F}(\cdot)$ denotes a numerical approximation to $F(\cdot)$. One can assume without loss of generality that $\{\Omega, \mathcal{F}, \mathbb{P}\}$ is common for both a process and system.
•The second order quasi-linear SPDE's of Chapters 2 - 4 can be expressed as:

$$a\frac{\partial^2 F(x,y,z)}{\partial^2 x} + b\frac{\partial^2 F(x,y,z)}{\partial x \partial y} + c\frac{\partial^2 F(x,y,z)}{\partial^2 y} + \beta\frac{\partial^2 F(x,y,z)}{\partial^2 z} + r\frac{\partial^2 F(x,y,z)}{\partial x \partial z} + s\frac{\partial^2 F(x,y,z)}{\partial y \partial z} = g\left(F'(x,y,z), F(x,y,z), x, y, z, \dot{W}(x,y,z)\right), \tag{1.1}$$

where one of the coordinates can be utilised as time. Specific importance is placed on the two dimensional form of (1.1):

$$a\frac{\partial^2 F(x,y)}{\partial x^2} + b\frac{\partial^2 F(x,y)}{\partial x \partial y} + c\frac{\partial^2 F(x,y)}{\partial y^2} = g\left(\frac{\partial F(x,y)}{\partial x}, \frac{\partial F(x,y)}{\partial y}, F(x,y), x, y, \dot{W}(x,y)\right) \tag{1.2}$$

with characteristic functions, $\xi(x,y)$ and $\zeta(x,y)$, being solutions to the DE:

$$\frac{dy}{dx} = \frac{1}{2a}\left(b \pm \sqrt{b^2 - 4ac}\right). \tag{1.3}$$

(1.2) is classified with respect to the discriminant, $\alpha = b^2 - 4ac$, such that $F(x,y)$ is 'elliptic' if $\alpha < 0$, 'hyperbolic' if $\alpha > 0$, and 'parabolic' if $\alpha = 0$. Thus, solutions to (1.3) are (real valued/complex conjugate) in (hyperbolic/elliptic) processes.

•The Quasi-Geostrophic SPDE's of Chapter 5 can be expressed as:

$$\frac{\partial \mathcal{Q}(X)}{\partial t} + \mathrm{J}(F(X), \mathcal{Q}(X)) = v\left(\nabla^2 F(X), F(X), X\right) + \omega(X)\dot{W}(X) \quad (1.4)$$

where $X = (x, y, z, t)$, ∇^2 is the Laplacian operator of Notation 3.1.1, $\mathrm{J}(\cdot)$ is the Jacobian of Notation 5.1.1, and $\mathcal{Q}(\cdot)$ is a functional of $\nabla^2 F(\cdot)$; refer to (5.2).

Various methods have been developed to solve these processes in closed form, but often the solutions involve complicated mathematical devices and/or trivial circumstances. In discretising a process, systems redefine and simplify the problem by transforming an equation of continuous change into a finite number of equations and unknowns. Thus, numerical approximations are often necessary when modeling a process with non-trivial conditions, since:

•One is confronted with having to evaluate and possibly solve partial differential equations where closed form solutions can rarely be identified.

•Even when closed form solutions exist, often their computational demands drastically outweigh the demands of an acceptable numerical evaluation.

Assuming numerical evaluations will be performed; estimates involving SPDE's aid a researcher by providing easily controlled 'realistic' models for experimentation. These models allow one to test theories, obtain information on phenomena that might not be readily available, and provide a non-invasive means of collecting data as compared to physical models involving intrusive measuring devices.

1.1 Background and notation

#.#.#	Chapter.Section.Number
Equation	(Chapter.Number)
Reference	[Bibliography Number, Loation]

A summary of variables can be found in Appendix A with selected proofs listed in Appendix B, algorithms in Appendix C, and figures in Appendix D. The following notation will apply throughout the thesis and notation will be omitted if it does not clarify the problem or detracts from the discussion:

•$\{\alpha, \beta, a, b, c, r, s\}$ denote real variables and $\{j, k, l, m, n, o\}$ denote integer counting variables. $i = \sqrt{-1}$ and is not an integer counting variable.

•$\{f(\cdot), g(\cdot), h(\cdot), u(\cdot), v(\cdot), \omega(\cdot), \Upsilon(\cdot), \xi(\cdot), \zeta(\cdot)\}$ denote real valued functions.

•$g(a_1, \cdots, a_n)\,|_{(r_1,\cdots,r_n)}$ denotes a function evaluated at $(r_1, \cdots, r_n)$.

•α_{text} denotes a function or variable dependent upon '*text*.'

•$|\alpha|$ denotes the absolute value of a function or variable.

•$\{[A],[B]\}$ denote matrices where $[I]$ is the identity matrix, $[0]$ is the zero matrix, and the inverse and transpose of A are denoted by $[A^{-1}]$ and $\left[A^T\right]$, respectively.
•$[V]$ is a vector and Table 1.1 denotes standard norms which satisfy: $0 \leq \|V\|$, $\|V_j + V_k\| \leq \|V_j\| + \|V_k\|$, and $\|\varpi V\| = |\varpi| \, \|V\|$. When l has a superscript, such as l^1, then l is a norm notation and not an integer counting variable.

Norm	Notation	Definition
Absolute or l^1	$\|V\|_1$	$\sum_{j=1}^{n} \|\alpha_j\|$
Euclidean or l^2	$\|V\|_2$	$\left(\sum_{j=1}^{n} \|\alpha_j\|^2\right)^{\frac{1}{2}}$
Maximum or l^∞	$\|V\|_\infty$	$\max_{1 \leq j \leq n} \|\alpha_j\|$

Table 1.1: Standard norm notation where $\left[V^T\right] = [\alpha_1, \cdots, \alpha_n]$

1.1.1 Domains in continuous space

Notation 1.1.1. *Let* $\mathtt{card}\,(\cdot)$ *and* $\complement\,(\cdot)$ *denote the cardinality and complement of a set or space.*

All processes will assume Euclidean space, $\mathbb{R}^d$, where $d \in \{1,2,3,4\}$ and $\mathbb{R}^d_{+t}$ denotes the half space $\mathbb{R}^{d-1} \times [0,\infty]$. A geometric point, $\wp \in \mathbb{R}^d$, is taken in the usual sense with a Cartesian coordinate defining its position vector from the origin, $[0]$. Position vectors $\{X,Y\}$ use a standard orthonormal basis and dot product and refer to an appropriate subset of space dimensions, $\{x,y,z,t\}$, where t is the dimension designated as time. A 'set of points' is any non-empty set of $\mathbb{R}^d$ points and a 'polygonally connected domain' is a set of points that forms a closed sub-space of $\mathbb{R}^d$, where any two points can be joined by a series of connected line segments lying wholly within the domain. The standard definitions of 'convex,' 'open,' and 'closed' apply and $\mathtt{S}\,(X,\beta)$ is a 'neighborhood' defined by a d-dimensional sphere centered on $\wp$ with a radius $\beta > 0$; refer to Figure 1.2. The following applies to all polygonally connected domains considered in this text:
•The words 'polygonally connected' will be omitted.
•An 'interior point,' $\wp_{\mho}$, has at least one non-empty neighborhood lying wholly within the domain. The 'interior' of the domain, $\mho$, is the set of all interior points and is an open sub-space.
•A 'boundary point,' $\wp_{\delta\mho}$, contains at least one interior and one non-interior point in every non-empty neighborhood. The 'boundary' of a domain, $\delta\mho$, is the set of all boundary points and is a closed sub-space.

•An 'exterior point,' has at least one non-empty neighborhood lying wholly within the compliment of the domain. The 'exterior' is the set of all exterior points; i.e. the open subspace, $\complement(\mho \cup \delta\mho) = \{\mathbb{R}^d - (\mho \cup \delta\mho)\}$.

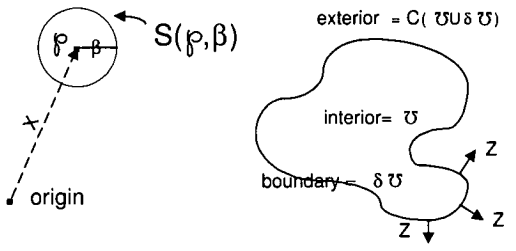

Figure 1.2: $\mathbb{R}^2$ Domain and notation

1.1.1.1 Continuity and singularities

As per standard notation, a variable or function is 'bounded' if there exists a positive real constant strictly less than infinity, K, such that $|\alpha| \leq K$. Given $[X - Y]$ is a difference vector and θ is bounded such that $0 \leq \theta \leq 1$; then a function is labeled 'Hölder continuous over a domain with exponent θ' if

$$\sup_{\{X,Y\}\in\mho} \frac{|g(X) - g(Y)|}{||X - Y||_2^{\theta}} \leq K \tag{1.5}$$

is true. If $\mho$ is arbitrary, then $g(\cdot)$ is Hölder continuous with exponent θ and if (1.5) only holds for a given neighborhood, $Y \in \mathsf{S}(X, \beta) \subset \mho$, then $g(\cdot)$ is 'locally continuous.' If $\theta = 1$ then $g(\cdot)$ is 'Lipschitz continuous,' if $\theta = 0$ then $g(\cdot)$ is bounded, and 'piecewise continuous' will be defined in the usual sense.

Notation 1.1.2. *$f(X) \in \mathfrak{C}^{(n)}$ denotes that the function $f(\cdot)$ can be differentiated at least n times, where the derivatives exist and are bounded.*

A singularity is a non-regular point where there is a sudden change in the initial conditions, driving noise, nature of a process, or a PDE becomes singular. Singularities are often referred to as shock waves, heat sinks, point sources, re-entrant corners, or points of ill-formed conditions, where examples include: a standard Kroneker delta function (δ_{text}), a 'unit source' and/or 'pulse' (refer to Figure D.7), 'large jumps' in a stochastic space, and a point of intersection where boundary conditions contradict each other or have a non-smooth interior angle greater that π.

1.1.2 Discretised space

Definition 1.1.3. $\mathbb{Z}^d_{\Delta x} \subset \mathbb{R}^d$, *where* $\mathbb{Z}^d_{\Delta x}$ *is a set of points with a minimum* l^2 *distance between any two distinct points greater than a positive constant,* Δx.

d	$\mathbb{Z}^d$	Notation	Definition - s represents either z or t
1	Uniform	g_j	$g(x_j) = g(j\Delta x)$
2	Uniform	$g_{j,k}$	$g(x_j, s_k) = g(j\Delta x, k\Delta s)$
3	Uniform	$g_{j,k,l}$	$g(x_j, y_k, s_l) = g(j\Delta x, k\Delta y, l\Delta s)$
4	Uniform	$g_{j,k,l,m}$	$g(x_j, y_k, z_l, t_m) = g(j\Delta x, k\Delta y, l\Delta z, m\Delta t)$

Table 1.2: $\mathbb{Z}^d_{\Delta x}$ Notation

A 'uniform' $\mathbb{Z}^d_{\Delta x}$ is a common discretisation that fulfills Definition 1.1.3 and is often referred to as a standard 'net' or 'mesh.' Discretisation points are uniformly distributed throughout the domain and are mapped to an ordered d-tuple (j, k, l, m), which equates to the $\mathbb{R}^d$ coordinate, $X = (j\Delta x, k\Delta y, l\Delta z, m\Delta t)$. Let $\mathbb{Z}^d$ represent $\mathbb{Z}^d_{\Delta x}$, where Δx is assumed and:

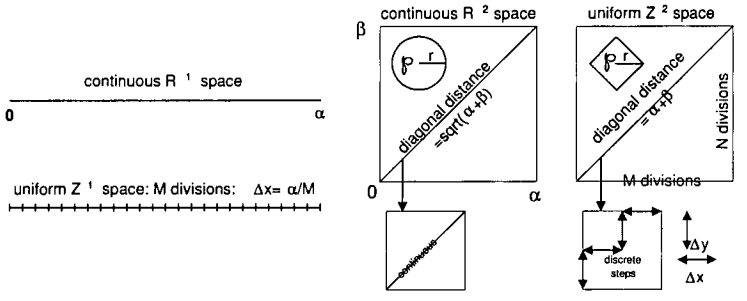

Figure 1.3: R^d and uniform $\mathbb{Z}^d$ spaces

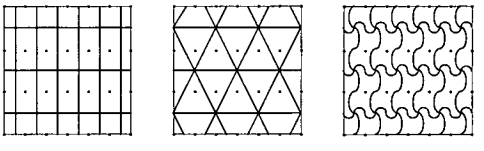

Figure 1.4: Example D allocations for a uniform $\mathbb{Z}^2$

•notation for $\mathbb{Z}^d$ will remain consistent with $\mathbb{R}^d$, where $\mathbb{Z}^d$ discretised variables / functions are listed in Table 1.2 and $\{\Delta x, \Delta y, \Delta z, \Delta t\} = \{\Delta x, \lambda_y \Delta x, \lambda_z \Delta x, \lambda_t \Delta x\}$.
•$\{M, N\}$ denote the finite number of divisions of a bounded $\mathbb{R}^1$ region and are often limited to values of $2^n + 1$, such that $\Delta x = \frac{\alpha}{2^n}$.
•$\mathtt{S}_2(\wp, r)$ and $\mathtt{S}_1(\wp, r)$ use the l^2 and l^1 norms and appear as a d-dimensional ball

Operator	Difference wrt. x_j	Definition
average difference	$\Delta_a g_{j,k,l,m}$	$\frac{g_{j+1,k,l,m}-g_{j-1,k,l,m}}{2}$
backward difference	$\Delta_b g_{j,k,l,m}$	$g_{j,k,l,m} - g_{j-1,k,l,m}$
central difference	$\Delta_c g_{j,k,l,m}$	$g_{j+\frac{1}{2},k,l,m} - g_{j-\frac{1}{2},k,l,m}$
forward difference	$\Delta_f g_{j,k,l,m}$	$g_{j+1,k,l,m} - g_{j,k,l,m}$

Table 1.3: Finite difference operators wrt x

or diamond, respectively; refer to Figure 1.3.

•$\mathtt{D}$ is a closed and bounded sub-domain of $\mho$ and let $\mathtt{D}_{\wp}$ denote the region of $\mathbb{R}^d$ space that is mapped to $\wp$; refer to Figure 1.4. The $\mathtt{D}_{\wp}$ regions do not have to be mutually exclusive subspaces.

•'adjacent' points are non-boundary points, Y, where $\min\left(\|Y, \wp_{\delta\mho}\|_2\right) \leq \lambda\Delta x$.

1.2 Numerical approximations

This thesis will concentrate on the mean square convergence of finite difference evaluations preformed on a uniform $\mathbb{Z}^d$ that discretise equations via Taylor expansions or Hölder continuous conditions. Using the Lax Equivalence Theorem, given a well posed linear problem and a discretisation scheme that satisfies consistency and stability conditions, then these are necessary and sufficient conditions for convergence. For an introduction to the 'basic principles of discretisation methods,' refer to [17, Chapter 2].

1.2.1 Finite difference operators

The first order finite difference operators of Table 1.3 are commutative, associative, and distributive over addition; refer to [17], [18], [33], or [39]. Higher order operators are composed by repeated application of the first order operators and are labeled 'equivalent' if they produce the same results when applied to any function in which both operators are defined. Thus, $\Delta^n f(X) = \Delta\left(\Delta^{n-1} f(X)\right)$ and the following second order operators are equivalent:

$$\Delta_b \Delta_f g(x_j) = \Delta_f \Delta_b g(x_j) = \Delta_c^2 g(x_j) = g_{j+1} - 2g_j + g_{j-1}. \tag{1.6}$$

Difference operators can also be applied to functions of multiple dimensions:

$$\Delta_{ff} g(x_j, y_k) = \Delta_{bb} g(x_{j+1}, y_{k+1}) = g_{j+1,k+1} - g_{j+1,k} - g_{j,k+1} + g_{j,k}. \tag{1.7}$$

Since a partial derivative is the limit of a difference quotient, a 'consistent' scheme is equivalent to the partial derivatives of the SPDE as $\Delta x \to 0$. Although

it is numerically impossible for $\Delta x = 0$, one should be able to approximate a partial derivative to any desired degree of accuracy using $\mathbb{Z}^d$ points that are 'close enough.' For example, let $r \in [x_j, x_{j+1}]$ and $s \in [x_{j-1}, x_{j+1}]$ such that:

$$\frac{\partial g(X)}{\partial x} |_{X=x_j} = \lim_{\Delta x \to 0} \frac{\Delta_f g(x_j)}{\Delta x} + O(\Delta x) = \frac{g_{j+1} - g_j}{\Delta x} + \frac{\Delta x}{2} \frac{\partial^2 g(r)}{\partial x^2} \tag{1.8}$$

$$\frac{\partial^2 g(X)}{\partial x^2} |_{X=x_j} = \lim_{\Delta x \to 0} \frac{\Delta_c^2 g(x_j)}{\Delta x^2} + O(\Delta x^2) = \frac{g_{j-1} - 2g_j + g_{j+1}}{\Delta x^2} + \frac{\Delta x^2}{12} \frac{\partial^4 g(s)}{\partial x^4}. \tag{1.9}$$

Using functionals of surrounding discretised points to approximate derivatives, the template for a numerical scheme will be expressed as a 'computational molecule' where the influence from Y to X is denoted by $\vartheta(Y;X)$ and:

•the standard definitions of 'explicit' and 'implicit' will be utilised.

•a computational molecule is a 'weighted average' if $\sum_{X \in \mathbb{Z}^d} \vartheta(Y;X) = 1$.

•$\widehat{F}(X) = \sum_{Y \in \mathbb{Z}^d} \vartheta(Y;X) \widehat{F}(Y)$ and for each $\cdot = \{l, m\}$ combination, a molecule is denoted by: $\begin{bmatrix} \vartheta(j-1,k+1,\cdot;j,k,\cdot) & \vartheta(j,k+1,\cdot;j,k,\cdot) & \vartheta(j+1,k+1,\cdot;j,k,\cdot) \\ \vartheta(j-1,k,\cdot;j,k,\cdot) & \vartheta(j,k,\cdot;j,k,\cdot) & \vartheta(j+1,k,\cdot;j,k,\cdot) \\ \vartheta(j-1,k-1,\cdot;j,k,\cdot) & \vartheta(j,k-1,\cdot;j,k,\cdot) & \vartheta(j+1,k-1,\cdot;j,k,\cdot) \end{bmatrix}$.

1.2.2 Finite Difference Schemes (FDSc)

Notation 1.2.1. *An expression, β is 'Big-Oh' with respect to Δx^r, when $\lim_{\Delta x \to 0} \frac{|\beta|}{\Delta x^r} \leq K$ and will be denoted by $\beta = O(\Delta x^r)$; refer to [39, page XXII].*

A FDSc approximation for (1.1) is derived by using a computational molecule to estimate the partial derivatives of a SPDE via

$$\begin{bmatrix} \widehat{F}(\wp_{\mho})_n \\ F(\wp_{\delta\mho}) \end{bmatrix} = \begin{bmatrix} FDSc_{\mho} & FDSc_{\delta\mho} \\ 0 & I \end{bmatrix} \begin{bmatrix} \widehat{F}(\wp_{\mho})_{n-1} \\ F(\wp_{\delta\mho}) \end{bmatrix} + O(\Delta x^2)[g(\cdot)]; \tag{1.10}$$

where $\widehat{F}(X)_n$ denotes a numerical approximation to $F(X)$ utilising the n^{th} iteration of a difference scheme on a discretised domain. For notational ease, denote (1.10) as $\left[\widehat{F}_n\right] = \beth\left(FDSc, \left[\widehat{F}_{n-1}\right], [F_{\delta\mho}], [g(\cdot)]\right)$, where $\beth(\cdot)$ is a system involving the FDSc matrix, previous approximations of $\widehat{F}(\cdot)$, boundary conditions, and driving functionals.

Example 1.2.2. *The canonical d=2 explicit elliptic computational molecules depicted on the far left of Figure 1.5 are the weighted averages*

- $\begin{bmatrix} 0 & \frac{1}{4} & 0 \\ \frac{1}{4} & 0 & \frac{1}{4} \\ 0 & \frac{1}{4} & 0 \end{bmatrix}$, *such that* $\vartheta = \frac{1}{4}$ *and* $\widehat{F}_{j,k} = \frac{1}{4}\left(\widehat{F}_{j+1,k} + \widehat{F}_{j-1,k} + \widehat{F}_{j,k+1} + \widehat{F}_{j,k-1}\right)$.
- $\begin{bmatrix} \frac{1}{20} & \frac{1}{5} & \frac{1}{20} \\ \frac{1}{5} & 0 & \frac{1}{5} \\ \frac{1}{20} & \frac{1}{5} & \frac{1}{20} \end{bmatrix}$, *such that* $\vartheta = \frac{1}{5}$ *or* $\frac{1}{20}$ *and* $\widehat{F}_{j,k} = \frac{1}{5}\left(\widehat{F}_{j+1,k} + \widehat{F}_{j-1,k} + \widehat{F}_{j,k+1}\right.$

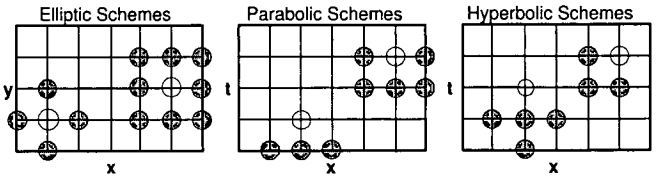

Figure 1.5: FDSc computational molecules for (1.2).

$$+\widehat{F}_{j,k-1}\Big) + \tfrac{1}{20}\left(\widehat{F}_{j+1,k+1} + \widehat{F}_{j+1,k-1} + \widehat{F}_{j-1,k+1} + \widehat{F}_{j-1,k-1}\right).$$

These molecules yield the $[FDSc_{\mho}]$ *matrices*

$$\begin{bmatrix} \ddots & 0 & 0 & \cdots & \frac{1}{4} & 0 & \frac{1}{4} & 0 & 0 & \cdots & \frac{1}{4} & 0 & 0 \\ 0 & \frac{1}{4} & 0 & \cdots & 0 & \frac{1}{4} & 0 & \frac{1}{4} & 0 & \cdots & 0 & \frac{1}{4} & 0 \\ 0 & 0 & \frac{1}{4} & \cdots & 0 & 0 & \frac{1}{4} & 0 & \frac{1}{4} & \cdots & 0 & 0 & \ddots \end{bmatrix} \text{ and}$$

$$\begin{bmatrix} \ddots & \frac{1}{5} & \frac{1}{20} & 0 & 0 & \cdots & \frac{1}{5} & 0 & \frac{1}{5} & 0 & 0 & \cdots & \frac{1}{20} & \frac{1}{5} & \frac{1}{20} & 0 & 0 \\ 0 & \frac{1}{20} & \frac{1}{5} & \frac{1}{20} & 0 & \cdots & 0 & \frac{1}{5} & 0 & \frac{1}{5} & 0 & \cdots & 0 & \frac{1}{20} & \frac{1}{5} & \frac{1}{20} & 0 \\ 0 & 0 & \frac{1}{20} & \frac{1}{5} & \frac{1}{20} & \cdots & 0 & 0 & \frac{1}{5} & 0 & \frac{1}{5} & \cdots & 0 & 0 & \frac{1}{20} & \frac{1}{5} & \ddots \end{bmatrix}$$

with appropriate entries of $\left\{0, \frac{1}{4}, \frac{1}{5}, \frac{1}{20}\right\}$ *for the* $[FDSc_{\delta\mho}]$ *matrix.*

1.2.2.1 Other schemes

Predictor-Corrector methods are often used to reduce computational effort by combining the numerical benefits of different computational molecules. These methods utilise at least two FDSc matrices to create an approximation where, $\left[\widehat{F}_k\right] = \beth\left(FDSc1, FDSc2, \left[\widehat{F}_{k-\frac{1}{2}}\right], \left[\widehat{F}_{k-1}\right], [F_{\delta\mho}], [g(\cdot)]\right)$. Thus:

1. Use a FDSc (usually explicit) to derive an estimate for $\left[\widehat{F}_{k-\frac{1}{2}}\right] = \beth\left(FDSc1, \left[\widehat{F}_{k-1}\right], \left[g\left(\widehat{F}_{k-1}\right)\right]\right)$.
2. Use $\left[\widehat{F}_{k-\frac{1}{2}}\right]$ to derive a 'more accurate estimate' for the driving functionals, $\left[g\left(\widehat{F}_{k-\frac{1}{2}}\right)\right]$.
3. Use another FDSc (usually implicit) to derive $\left[\widehat{F}_k\right] = \beth\left(FDSc2, \left[\widehat{F}_{k-\frac{1}{2}}\right], \left[g\left(\widehat{F}_{k-\frac{1}{2}}\right)\right]\right)$.
4. Repeat if necessary.

In using different FDSc's, improvements can be made by focusing upon the strengths of an FDSc and overcoming its pitfalls with the benefits of another FDSc. For example, a non-consistent but stable FDSc with a small spectral radius can be combined with another FDSc to create an overall consistent scheme. Due to the amount of material covering this topic over the past century, a discussion of popular methods such as explicit Adams-Bashforth methods, implicit Adams-Moulton methods, and n^{th} order Runge-Kutta methods will be omitted.

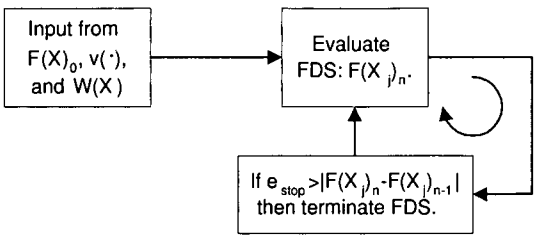

Figure 1.6: Picard-Lindelöf FDSy schematic - closed loop feedback system

Finite Element Systems and Spectral Methods (collectively labeled FESy) discretise processes using trial functions; refer to [10], [17, Chapter 4], or [19, Section 12.5] for an introduction. Although often more accurate than finite difference systems due to the superior handling of boundary conditions and error propagation, FESy experience minor difficulties in the stochastic setting as discussed in [1]. Due to the reliance upon FESy in the deterministic literature, deriving results for FESy will be addressed in future work.

1.2.3 Finite Difference Systems (FDSy)

Since numerical approximations are derived from well posed initial conditions and driving functionals, a FDSy approximation will be the reduction of (1.10) where:
$\begin{bmatrix} \widehat{F}(\wp_{\mho})_{\infty} \\ F(\wp_{\delta\mho}) \end{bmatrix} = \begin{bmatrix} FDSc_{\mho} & FDSc_{\delta\mho} \\ 0 & I \end{bmatrix} \begin{bmatrix} \widehat{F}(\wp_{\mho})_{\infty} \\ F(\wp_{\delta\mho}) \end{bmatrix} + O(\Delta x^2)[g(\cdot)]$ gives
$0 = \begin{bmatrix} FDSc_{\mho} - I & FDSc_{\delta\mho} \\ 0 & I - I \end{bmatrix} \begin{bmatrix} \widehat{F}(\wp_{\mho})_{\infty} \\ F(\wp_{\delta\mho}) \end{bmatrix} + O(\Delta x^2)[g(\cdot)]$,
which is used to create a system of equations that approximates a process via
$0 = \begin{bmatrix} -I & FDSy_{\delta\mho} \\ 0 & I - I \end{bmatrix} \begin{bmatrix} \widehat{F}(\wp_{\mho})_{\infty} \\ F(\wp_{\delta\mho}) \end{bmatrix} + [FDSy_{\mho}][g(\cdot)]$, such that
$\begin{bmatrix} \widehat{F}(\wp_{\mho})_{\infty} \\ F(\wp_{\delta\mho}) \end{bmatrix} = \begin{bmatrix} 0 & FDSy_{\delta\mho} \\ 0 & I \end{bmatrix} \begin{bmatrix} \widehat{F}(\wp_{\mho})_{\infty} \\ F(\wp_{\delta\mho}) \end{bmatrix} + [FDSy_{\mho}][g(\cdot)]$, or simply

$$\left[\widehat{F}(\wp_{\mho})_{\infty}\right] = [FDSy_{\delta\mho}][F(\wp_{\delta\mho})] + [FDSy_{\mho}][g(\cdot)]. \tag{1.11}$$

Thus, the FDSc and FDSy approximations are equivalent. Using a consistent FDSc, direct methods 'exactly' approximate a system on a domain using Gaussian elimination or an algebraic reduction to derive a FDSy. This method is preferred when deriving an approximation, but considering the size and density of the sparse FDSc matrices, evaluating their inverses is generally not a viable alternative. The algebraic reduction of a FDSc to derive a FDSy will be used in Chapter 2.

The 'method of successive approximations' involves a Picard-Lindelöf iteration scheme that relies upon multiple iterations of a FDSc to derive a FDSy. Thus, $\left[\widehat{F}_n\right] = \beth\left(FDSc, \left[\widehat{F}_{n-1}\right], [g(\cdot)]\right)$ will be repeated a number of times to derive

the FDSy matrix; refer to Figure 1.6. Although computationally expensive, this method is easily implemented on a computer for a variety of boundary conditions and domains and this will be the technique used in Chapters 3 - 5.

1.2.3.1 FDSy Illustration

Due to the quasi-linear format of (1.1), a one-dimensional linear function, $\Upsilon(x)$, will be considered without a loss of generality. Thus, on the uniform domain $[x_0, x_N]$, there exists a linear difference equation

$$a_j\widehat{\Upsilon}_{j+2} + b_j\widehat{\Upsilon}_{j+1} + c_j\widehat{\Upsilon}_j = a_j\Delta_f^2\widehat{\Upsilon}_j + (2a_j + b_j)\,\Delta_f\widehat{\Upsilon}_j + (a_j + b_j + c_j)\,\widehat{\Upsilon}_j, \quad (1.12)$$

such that $\widehat{\Upsilon}_k = \omega_k + \widehat{\Upsilon}_0 u_k + \widehat{\Upsilon}_1\, v_k$. If the discretised solution is satisfied for arbitrary values of Υ_0 and Υ_1; then ω_j must be a particular solution of Υ_j while u_j and v_j satisfy the associated homogeneous difference equations of (1.12). Multiplying the difference equations by v_{j+1} and u_{j+1}, respectively, and subtracting yields the relation $a_j\beta_{j+1} = c_j\beta_j$, where $\beta_j = u_j v_{j+1} - u_{j+1}v_j$ and:
•If $\{a_j \neq 0, c_j \neq 0\}$ then the general solution involves two independent arbitrary constants on the domain and Υ_j is uniquely determined by its two initial values, Υ_0 and Υ_1. Hence, an algebraic reduction of the direct FDSc yields an FDSy approximation, $\left[\widehat{\Upsilon}_k\right] = [FDSy1]\left[\widehat{\Upsilon}_1\right] + [FDSy2]\left[\widehat{\Upsilon}_0\right] + [K]$.
•If $\{a_j \neq 0, c_j = 0\}$, then $\beta_{j+1} = \beta_{j+2} = \cdots = 0$ and the $\widehat{\Upsilon}_k$ are constant multiples for $k \geq j$. Hence, the general solution involves one arbitrary constant and the respective boundary points $\{\Upsilon_0, \Upsilon_N\}$. The FDSy is often determined via an iterative FDSc, which eventually yields, $\left[\widehat{\Upsilon}_k\right] = [FDSy]\left[\widehat{\Upsilon}_0, \widehat{\Upsilon}_N^T\right] + [K]$.

Remark 1.2.3. *Due to the nature of the $\{a_j \neq 0, c_j = 0\}$ system, a linear combination of boundary and adjacent points can also be utilised.*

1.2.4 Error, convergence, and stability

Since the exact solution to a process is unknown; the crux of approximating a process lies in applying a finite difference scheme to create an accurate, convergent, and stable numerical estimate. A local error is unavoidably introduced at each discretisation step, thus use a consistent scheme such that errors remain sufficiently small and try to assure that the accumulation of all errors in an approximation either decay or remain bounded. A system is stable if approximations remain uniformly bounded functions of the initial state and the cumulative effect of all round off errors remains negligible as $\Delta x \to 0$. Conversely, a system is unstable if there exists initial disturbances for which the approximation becomes unbounded and/or global errors are uncontrollable. It is desirable for a scheme to

Convergence	Definition
almost sure	$\mathbb{P}\left(\lim_{\Delta x\to 0} \mathfrak{eg} \to 0\right) = 1$
mean square	$\lim_{\Delta x\to 0} \mathbb{E}\left(\mathfrak{eg}^2\right)^{\frac{1}{2}} \to 0$
stochastic	$\lim_{\Delta x\to 0} \mathbb{P}\left(\mathfrak{eg} \geq \beta\right) \to 0$

Table 1.4: Standard convergence definitions.

be asymptotically stable such that small changes in the initial conditions produce relatively small changes in the approximation.

Notation 1.2.4. *Let* $\mathfrak{es}(X)$ *denote a 'stopping error,' which is an a prioi value used to terminate an iterative FDSc once successive Picard-Lindelöf iterations yield* $\mathfrak{es}(X) \geq \left|\widehat{F}_{\Delta x}(X)_n - \widehat{F}_{\Delta x}(X)_{n-1}\right|$*; refer to Figure 1.6.*

Notation 1.2.5. *Let* $\mathfrak{e}\left(FDSy, FDSc, \widehat{F}(X), \Delta x, n, \mathfrak{es}(X)\right) = F(X) - \widehat{F}_{\Delta x}(X)_n$ *denote the 'error' and* $\mathfrak{eg}\left(\widehat{F}(X)\right) = \left|\mathfrak{e}\left(\widehat{F}(X)\right)\right| = \left|F(X) - \widehat{F}_{\Delta x}(X)_n\right|$ *denote the 'global error,' where* $(FDSy, \cdots, \mathfrak{es}(X))$ *will be omitted unless necessary.*

Notation 1.2.6. *The rate of convergence for a FDSy to a solution is denoted as* $\mathrm{RC}\left(\widehat{F}(X), s, \Delta x\right) = \frac{1}{\ln(s)} \ln\left(\lim_{\Delta x\to 0}\left(\mathfrak{eg}(F(X), s\Delta x) \times \mathfrak{eg}(F(X), \Delta x)^{-1}\right)\right)$
$= \frac{1}{\ln(s)} \ln\left(\lim_{\Delta x\to 0}\left(\left|F(X) - \widehat{F}_{s\Delta x}(X)\right| \times \left|F(X) - \widehat{F}_{\Delta x}(X)\right|^{-1}\right)\right)$.

Notation 1.2.7. *Denote the covariance, expectation, probability, variance, and Lebesgue measure via* $\{\mathbb{C}(\cdot), \mathbb{E}(\cdot), \mathbb{P}(\cdot), \mathbb{V}(\cdot), \mathfrak{M}(\cdot)\}$*, respectively.*

The standard definition of 'pathwise' (strong) convergence will be used, where a scheme is labeled convergent, if, for any well posed problem, the approximation approaches the solution of the SPDE as $\Delta x \to 0$; refer to Table 1.4. Convergence will relate to the asymptotic behavior of a finite sequence of random variables where mean square convergence will be the focus of this thesis; i.e., given $\mathbb{E}\left(\alpha(X)^2\right) < \infty$, then show $\lim_{n\to\infty} \mathbb{E}\left(\left|\alpha(X) - \widehat{\alpha}(X)_n\right|^2\right)^{\frac{1}{2}} = 0$. One can evaluate $\lim_{\Delta x\to 0} \mathbb{E}\left(\mathfrak{eg}^2\right)^{\frac{1}{2}}$ directly or utilise:

- $\lim_{\Delta x\to 0} \mathbb{E}\left(\mathfrak{eg}^2\right)^{\frac{1}{2}} = \lim_{\Delta x\to 0} \mathbb{E}\left(|\mathfrak{e}|^2\right)^{\frac{1}{2}} = \lim_{\Delta x\to 0} \mathbb{E}\left((\mathfrak{e})^2\right)^{\frac{1}{2}} = \lim_{\Delta x\to 0} \left(\mathbb{V}(\mathfrak{e}) + \mathbb{E}(\mathfrak{e})^2\right)^{\frac{1}{2}}$.
- $\lim_{\Delta x\to 0} \mathbb{E}\left(\mathfrak{eg}^2\right)^{\frac{1}{2}} = \lim_{\Delta x\to 0} \left(\mathbb{V}(\mathfrak{eg}) + \mathbb{E}(\mathfrak{eg})^2\right)^{\frac{1}{2}} = \lim_{\Delta x\to 0} \left(\mathbb{V}(|\mathfrak{e}|) + \mathbb{E}(|\mathfrak{e}|)^2\right)^{\frac{1}{2}}$.

Since $F(X)$ is rarely, if ever, known then this value must also be approximated using a 'very accurate' estimate; i.e., $\widehat{F}_{\theta\Delta x}(X)_m$ where θ is close to 0 and $m > n$ and/or $\mathfrak{es}_m < \mathfrak{es}_n$. The following notation will be utilised for numerical results:
- $\widehat{\mathfrak{e}}\left(\widehat{F}(X), \theta, \beta, \Delta x, m, n\right) = \widehat{F}_{\theta\Delta x}(X)_m - \widehat{F}_{\beta\Delta x}(X)_n$.

$\bullet \widehat{\mathfrak{eg}}\left(\widehat{F}(X)\right) = \left|\widehat{\mathfrak{e}}\left(\widehat{F}(X)\right)\right| = \left|\widehat{F}_{\theta\Delta x}(X)_m - \widehat{F}_{\beta\Delta x}(X)_n\right|.$

$\bullet \widehat{\mathrm{RC}}\left(\widehat{F}(X), \theta, \beta, \Delta x, m, n\right)$

$= \frac{1}{\ln(\beta)} \ln\left(\lim_{\Delta x \to 0}\left(\left|\widehat{F}_{\theta\Delta x}(X)_m - \widehat{F}_{\beta\Delta x}(X)_n\right| \times \left|\widehat{F}_{\theta\Delta x}(X)_m - \widehat{F}_{\Delta x}(X)_n\right|^{-1}\right)\right).$

1.3 Wiener process

As discussed in [60], a stochastic process models a random phenomena and two-dimensional Gaussian white noise will be interpreted in the canonical Walsh distribution sense with mean 0 and a Dirac delta covariance function. Let $\mathbb{W}(\mathtt{D})$ represent a l^2 Gaussian measure with orthogonal increments on Borel subsets of $\mathbb{R}^2_{+t}$, such that $\left\{\mathbb{W}(\mathtt{D}) \sim \mathcal{N}(0, \mathfrak{M}(\mathtt{D})); \mathtt{D} \in \mathcal{B}\left(\mathbb{R}^2_{+t}\right)\right\}$ is a mean 0 Gaussian process with a covariance function $\mathbb{C}(\mathbb{W}(\mathtt{D}_1), \mathbb{W}(\mathtt{D}_2)) = \mathfrak{M}(\mathtt{D}_1 \cap \mathtt{D}_2)$ and $\mathcal{B}\left(\mathbb{R}^2_{+t}\right)$ is the set of Borel subsets with a finite Lebesgue measure. The process $\mathbb{W}$ is carried by a probability space $\left\{\Omega, \mathcal{F}, (\mathcal{F}_t)_{t\geq 0}, \mathbb{P}\right\}$ with a filtration, $\mathcal{F}$, satisfying the usual conditions:

•for each $t \geq 0$, $\left\{\mathbb{W}(\mathtt{D}); \mathtt{D}_\tau \subset \mathbb{R}^d \cap \{\tau \geq t\}\right\}$ is independent of $\mathcal{F}_t$.

•$\mathbb{W}(\mathtt{D})$ is $\mathcal{F}_t$-measurable whenever $\mathtt{D} \subset \mathbb{R}^2 \cap \{0 \leq \tau \leq t\}$.

Remark 1.3.1. *Refer to Section C.2 for numerical examples on how one can generate and refine example spaces.*

1.3.1 Stochastic integration

In evaluating processes of measurable functions subject to stochastic noise, the Riemann-Stieltjes integral must be abandoned and Lebesgue integration utilised such that meaningful results can be obtained. In order to accommodate Chapter 2, two-dimensional stochastic integration will be the focus of this section; refer to [9], [13], and [60, Chapter 2]. Given a real valued step function, $h_N(x,y) = \sum_{j=1}^{N} \alpha_j 1_{\mathtt{D}_j}$ which is a countably finite linear combination of real coefficients and indicator functions that is well defined on $\{\Omega, \mathcal{F}, \mathbb{P}\}$, let $\{\mathtt{D}_1, \cdots, \mathtt{D}_N\}$ be a series of disjoint rectangles. Thus for a step function, $\iint h_N(x,y)\, d\Upsilon = \sum_{j=1}^{N} \alpha_j 1_{\mathtt{D}_j} \Upsilon$:

•a deterministic integral would be $\iint h_N(x,y)\, dxdy = \sum_{j=1}^{N} \alpha_j \mathfrak{M}(\mathtt{D}_j)$.

•a stochastic integral would be $\iint h_N(x,y)\, dW(x,y) = \sum_{j=1}^{N} \alpha_j \mathbb{W}(\mathtt{D}_j)$.

The representation of $h(x,t)$ via a step function is not unique, but given $h(x,t)$ is a general adapted piecewise continuous function on the domain, one can find a sequence of adapted step functions converging to h, i.e., $\lim_{N\to\infty} h_N \to h$

on the filtration $\mathcal{F}_t$. Thus, assuming that $\iint\limits_{\mho\cup\delta\mho} h(x,t)^2\,dxdt < \infty$, one can define

$$\iint h(x,y)\,dW(x,y) \;=\; \lim_{N\to\infty}\iint h_N(x,y)\,dW(x,y) \;=\; \lim_{\max(\mathfrak{M}(\mathtt{D}))\to 0}\sum_{j=1}^{N}\alpha_j\mathbb{W}(\mathtt{D}_j),$$

where $\alpha_j = h(\min(\{x,t\}\in \mathtt{D}_j))$.

Remark 1.3.2. *As per standard notation, let*

• $\int f(X)\,dW(X)$ *denote the Itô integral which is a non-anticipating sum that is utilised due to its martingale properties.*

• $\int f(X)\circ dW(X)$ *denote the Stratonovich integral which is an anticipating sum that is used in engineering literature due to similar properties with 'normal' Riemann-Steiltjes Calculus.*

• *The Brownian Sheet,* $W(X)$*, can be defined by* $W(X) = \mathbb{W}(\mho_X)$ *where the domain is an appropriately selected sub-domain of* $\mathbb{R}^d$*. In the case of Chapter 2,* $W(x,t) = \mathbb{W}(DoI(x,t))$*, where* (x,t) *is the apex of a suitable triangle in* $\mathbb{R}^2_{+t}$*.*

Hence, the process is stationary, separable, and measurable and the Brownian sheet is a homogeneous Markov diffusion process with paths that are almost surely continuous and nowhere differentiable; refer to [9], [34], [39], or [60].

Chapter 2

Hyperbolic equations in one space dimension

2.1 Introduction

Notation 2.1.1. *The second order $d = 2$ hyperbolic operator is denoted by $\mathfrak{H}^2(F(x,t), C) = \frac{\partial^2 F(x,t)}{\partial t^2} - C^2 \frac{\partial^2 F(x,t)}{\partial x^2}$, where C is the 'wave speed' or 'speed of propagation.'*

This chapter concentrates on quasi-linear second-order hyperbolic SPDE's in $\mathbb{R}^2_{+t}$ of the canonical form

$$\mathfrak{H}^2(F(x,t), C) = \upsilon(F(x,t), x, t) + \omega(F(x,t), x, t) \frac{\partial^2 W(x,t)}{\partial x \partial t}, \tag{2.1}$$

where an initial state and velocity are given at $t = 0$; or equivalently

$$\frac{\partial^2 F(\xi,\zeta)}{\partial \zeta \partial \xi} = \upsilon_2(F(\xi,\zeta), \xi, \zeta) + \omega_2(F(\xi,\zeta), \xi, \zeta) \frac{\partial^2 W(\xi,\zeta)}{\partial \zeta \partial \xi}, \tag{2.2}$$

with an initial state given along $\xi\zeta = 0$. (2.1) will be referred to as the 'general' noise case, with the following cases addressed throughout the chapter:
•deterministic, $\omega(F(X), X) = 0$,

$$\mathfrak{H}^2(F(x,t), C) = \upsilon(F(x,t), x, t). \tag{2.3}$$

•additive noise, $\omega(F(X), X) = \omega(X)$,

$$\mathfrak{H}^2(F(x,t), C) = \upsilon(F(x,t), x, t) + \omega(x,t) \frac{\partial^2 W(x,t)}{\partial x \partial t}. \tag{2.4}$$

•multiplicative noise, $\omega(F(X), X) = F(X)\omega(X)$,

$$\mathfrak{H}^2(F(x,t), C) = \upsilon(F(x,t), x, t) + \omega(x,t) F(x,t) \frac{\partial^2 W(x,t)}{\partial x \partial t}. \tag{2.5}$$

As discussed in [33] and [46]; dispersion and dissipation will be introduced to (2.1) via $\{\upsilon(\cdot), \omega(\cdot)\}$ including functionals of the lower order terms $\left\{F(x,t), \frac{\partial F(x,t)}{\partial x}\right.$,

$\frac{\partial F(x,t)}{\partial t}\Big\}$. The transformation between (2.1) and (2.2) is accomplished using the real valued solutions to (1.3), where

$$\xi(x,t) = x - Ct \text{ and } \zeta(x,t) = x + Ct \tag{2.6}$$

are called 'linear propagation functions' or 'characteristic curves.' This transformation follows from $\mathfrak{H}^2(F(x,t),C) = 0$ being a combination of the first order equations $\left\{\frac{\partial(Cf(x,t))}{\partial t} = C\frac{\partial g(x,t)}{\partial x}, C\frac{\partial f(x,t)}{\partial x} = \frac{\partial g(x,t)}{\partial t}\right\}$, or equivalently

$$\frac{\partial f(x,t)}{\partial t} = \frac{\partial g(x,t)}{\partial x} \text{ and } \frac{\beta \partial f(x,t)}{\partial x} = \frac{\alpha \partial g(x,t)}{\partial t}; \tag{2.7}$$

where $f(x,t) = \frac{\partial F(x,t)}{\partial x}$, $g(x,t) = \frac{\partial F(x,t)}{\partial t}$, and $C = \sqrt{\frac{\beta}{\alpha}}$. The PDE's of (2.7) are the 'conservation of slope' and 'conservation of momentum' equations, respectively. The scalars $\{\zeta(x,t), \xi(x,t)\}$ satisfy $\left\{\frac{\partial \zeta(x,t)}{\partial t} = C\frac{\partial \zeta(x,t)}{\partial x}, \frac{\partial \xi(x,t)}{\partial t} = -C\frac{\partial \xi(x,t)}{\partial x}\right\}$, where $\begin{bmatrix} 0 & C \\ C & 0 \end{bmatrix}$ and $\begin{bmatrix} 0 & 1 \\ \frac{\beta}{\alpha} & 0 \end{bmatrix}$ have eigen values $\pm C$ and eigen vectors $\{[1,1],[-1,1]\}$; i.e. $\zeta(x,t)$ and the invariant $\xi(x,t)$ are functions of $x \pm Ct$. Due to these propagation properties, solutions, initial conditions, and internal disturbances do not have to be $\mathfrak{C}^{(1)}$ and singularities almost surely exist when using a Brownian sheet.

2.1.1 Summary of results

As per Theorem 2.3.8, numerical approximations built using a canonical five point computational molecule are convergent to the d'Alembert solution with $\mathtt{RC}(FDSy = (2.17), F(X) = (2.8)) = \frac{1}{2}$. Refer to Section 2.3.4 for numerical results and Section D.1 for a listing of figures.

2.1.2 Hyperbolic Assumed Initial Conditions (HAIC)

The following initial conditions assure that hyperbolic processes are well posed:

Assumption 2.1.2. *Utilise the closed and bounded domains of Section 2.1.2.1.*

Assumption 2.1.3. *Dirichlet boundary conditions* $\left\{F(x,0), \frac{\partial F(x,t)}{\partial t}\Big|_{t=0}\right\}$ *are given, where the initial state and velocity are Hölder continuous functions with* $\theta \geq \frac{1}{2}$.

Assumption 2.1.4. *A Brownian sheet is utilised.*

Assumption 2.1.5. $v(\cdot)$ *and* $\omega(\cdot)$ *are real valued measurable functions on* $\mathbb{R}^2_{+t}$ *and they are globally Lipschitz continuous with coefficients* K_v *and* K_ω.

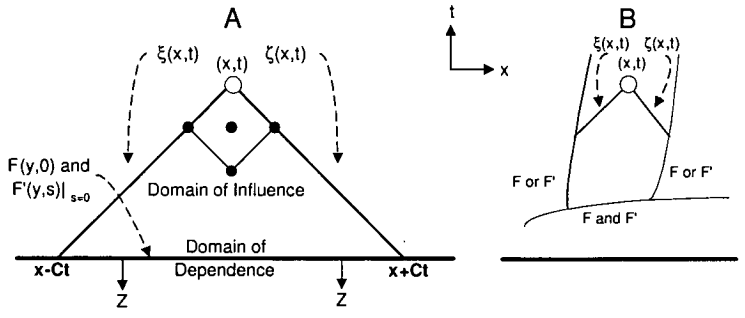

Figure 2.1: Initial Conditions

2.1.2.1 Domains

Notation 2.1.6. *The variables* $\{r, s\}$ *will be used in the same manner as* t *such that the coordinate pairs* $\{(x,t),(y,s),(z,r)\} \in \mathbb{R}^2_{+t}$.

Definition 2.1.7. *The Domain of Dependence (DoD) is the closed* $\mathbb{R}^1$ *interval bounded by (2.6), where the DoD* $(x,t) = \{(y,s) \mid s = 0, y \in [\xi(x,t), \zeta(x,t)]\}$.

Definition 2.1.8. *The Domain of Influence (DoI) is the bounded and open interior enclosed by the DoD* (x,t) *and (2.6), such that the DoI* $(x,t) = \{(y,s) \mid s \in (0,t],$ $y \in [\xi(x,t-s), \zeta(x,t-s)]\}$.

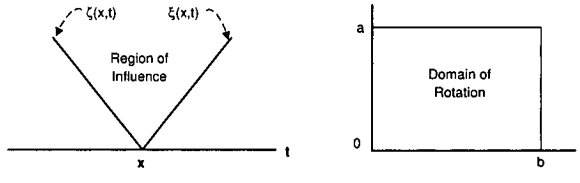

Figure 2.2: Region of Influence and Domain of Rotation

Definition 2.1.9. *The Region of Influence (RoI) is the unbounded region outlined by (2.6), such that the RoI* $(x,t) = \{(y,s) \mid s \in [t,\infty), y \in [\zeta(x,t), \xi(x,t)]\}$.

Definition 2.1.10. *When using (2.2), the Domain of Rotation,* $DoR(b,a)$, *is the rectangular domain in the positive quadrant bounded by the origin and axes.*

Figure 2.1-A represents the domains utilised in this chapter and Figure 2.1-B is a special case that has been partially solved along the lower and side boundaries. The union of the *DoD* and *DoI* is a closed, bounded, and convex domain, where the $DoD(x,t)$ contains information regarding the initial state of the system, while the $DoI(x,t)$ contains information regarding the forcing terms of (2.1).

Solutions on semi-infinite strips are applicable since waves propagating along (2.6) are reflected at the boundaries; refer to [31, Chapters 17 and 18], [33, page 239] and [46, Chapter 3] with analogous results for the stochastic case proved in [12]. Results for domains restricted to the positive quadrant of $\mathbb{R}^2$ are applicable via a transformation forcing $\Delta x = \Delta t$, shifting, and rotating the basis by $-\frac{\pi}{4}$ to yield a *DoR*; refer to [20], [30], [44], and [56].

2.1.3 The hyperbolic process

The motivation for solving hyperbolic processes in one space dimension is to model wave equations analogous to the vibrating string problem where, in zero gravity, a string of infinite length, constant density, and uniform tension is disturbed. These processes involve pulses, vibrations, and the flow of information or energy such as: water waves in a straight and narrow channel, linearized supersonic airflow, sound waves along a pipe, longitudinal vibrations and torsional oscillations of a rod, transmission of an electric signal along a low-resistance cable, transmission of a signal from a transmitter to a receiver, the flux of information according to Shannon's model, waves in hydro-magnetics, and one-dimensional transmission of S and P waves of an earthquake. Stochastic functionals can be used to represent:
•external disturbances to a transmission line or noise in a communication channel.
•energy introduced to waves via 'rain' or some other force.
•dispersed energy sources in models of turbulence.

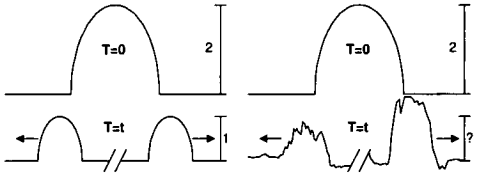

Figure 2.3: Deterministic versus stochastic wave propagation; T = time

Remark 2.1.11. *The communications and electrical engineering fields often utilise smoother than white noise, colored noise, or bounded stochastic noise in place of Assumption 2.1.4, such that large singularities almost surely do not exist; refer to [35, Chapter 6]. Many non-pathwise stochastic spaces also ensure that large singularities do not exist; refer to [39].*

The d'Alembert solution, (2.8) expresses solutions to (2.3) and (2.4) when $v(\cdot) = v(x,t)$ or numerical approximations to $F(x,t)$ when either $v(\cdot)$ or $\omega(\cdot)$ are multiplicative or general functions. If one wishes to approximate hyperbolic

processes involving (2.8) and non-additive functionals, then either a Predictor-Corrector or Picard-Lindelöf iteration scheme must be implemented.

$$F(x,t) = \frac{F(\zeta(x,t),0) + F(\xi(x,t),0)}{2} + \frac{1}{2C} \int\limits_{DoD(x,t)} \frac{\partial F(y,s)}{\partial s} \mid_{s=0} dy$$

$$+\frac{1}{2C} \iint\limits_{DoI(x,t)} \upsilon(F(y,s),y,s)\, dyds + \frac{1}{2C} \iint\limits_{DoI(x,t)} \omega(F(y,s),y,s)\, dW(y,s). \quad (2.8)$$

2.1.3.1 The deterministic process

Derivations of solutions as well as proofs of existence, uniqueness, and boundedness for (2.3) can be found in research literature from the earlier half of this century and most rigorous undergraduate physics and calculus texts published over the past quarter century. Refer to [38, Sections 10.7 and 10.8] for an overview of the deterministic system and [31, Chapters 17 and 18] for a discussion of physical properties. [46, Chapter 3] and [33, Sections 3.12 through 3.14] address the FDSy setting and for a FESy illustration, consider $\mathfrak{H}^2(F(x,t),C) = 0$ on the positive quadrant with 0 endpoint conditions, $\mathfrak{M}(DoD(x,t)) = L$, $x \in [0,L]$, and $a = \frac{\pi}{L}$. Derive a FESy via a separation of variables with a Fourier series to yield initial conditions, $F(x,0) = \sum\limits_{n=1}^{\infty} c_n \sin(nx)$ and $\frac{\partial F(x,t)}{\partial t} \mid_{t=0} = \sum\limits_{n=1}^{\infty} b_n \sin(nx)$, where progressive and standing wave solutions are represented as $F(x,t) = \sum\limits_{n=1}^{\infty} \frac{c_n}{2} (\sin(an\zeta(x,t)) + \sin(an\xi(x,t))) - \sum\limits_{n=1}^{\infty} \frac{b_n}{2an} (\cos(an\zeta(x,t)) - \cos(an\xi(x,t)))$ and $F(x,t) = \sum\limits_{n=1}^{\infty} \sin(nx) \left(\frac{c_n}{2} \cos(anCt) + \frac{b_n}{2an} \sin(anCt)\right)$. Assuming a general solution of $F(x,t) = h(\zeta(x,t)) + g(\xi(x,t))$ for (2.3) with non-zero boundary conditions, then $F(x,0) = h(x) + g(x)$ and $\frac{1}{C} \frac{\partial F(x,t)}{\partial t} \mid_{t=0} = h'(x) - g'(x)$. Since, $2C(h(\zeta(x,t)) + g(\xi(x,t))) = h(\zeta(x,t)) + g(\zeta(x,t)) + h(\xi(x,t)) + g(\xi(x,t))$ $+ \int\limits_{DoD(x,t)} h'(z) - g'(z)\, dz$, this yields the d'Alembert solution $\{(2.8), \omega(\cdot) = 0\}$, where $\frac{1}{2C}$ is a scaling factor accounting for the propagation of disturbances along (2.6) in both the $-x$ and $+x$ directions; refer to Figure 2.3.

2.1.3.2 The stochastic process

Solutions to (2.1) are not differentiable due to the 'roughness' of the Brownian sheet driving the stochastic process, thus (2.1) and (2.2) are just formal representations. The existence and uniqueness of solutions to (2.1) on $\mathbb{R}^2_{+t}$, where $C = 1.0$, is proved in [13] with further results on the positive quadrant shown in [20], [30], [51], and [56]. Although not addressed in this text:

•[44] discusses hyperbolic processes along a strip in the positive quadrant using

a variety of initial conditions.

•[50] proves the long time existence for $\{(2.1),\ v(\cdot)=0, 0<\alpha<\frac{1}{2}\}$ and $\omega(x,t)$ is locally continuous with $|\omega(F(x,t),x,t)| \leq K(|F(x,t)|+1)\log(|F(x,t)|+2)^{\alpha}$.

•Cabana, Orsingher, and [60, Chapter 3] address $\{(2.4), v(\cdot)=0, \omega(x,t)=1\}$ and discuss how a Brownian sheet is a hyperbolic system. This equivalence to the vibrating string problem explains the propagation of singularities parallel to an axis as covered in [12] and [60].

•[15] discusses hyperbolic equations in $\mathbb{R}^3_{+t}$ of the form $\frac{\partial^2 F(x,y,t)}{\partial t^2} - C_x^2\frac{\partial^2 F(x,y,t)}{\partial x^2} - C_y^2\frac{\partial^2 F(x,y,t)}{\partial y^2} = v(F(x,y,t),x,y,t) + \frac{\omega(F(x,y,t),x,y,t)\partial^3 W(x,y,t)}{\partial x\partial y\partial t}$.

> There are few results concerning the wave equation driven by random noise in two (or more) dimensions ... One reason for this is that if $W(x,y,t)$ is white noise, even the linear equation $\{v(\cdot)=0, \omega(\cdot)=1\}$ has no solution in the space of real-valued measurable stochastic processes (refer to [60]). Given that white noise can be viewed as a random variable with values in a space of distributions, the linear equation has of course a distribution-valued solution ... and is not readily amenable to numerical calculations. [15, Section 1]

2.1.3.3 Results of [13]

[13, Sections III - V] provide an instructive and intuitive discussion of the nature of the stochastic process and initial conditions which solve (2.8) on the positive quadrant, $\mathbb{R}^2_{+t}$ half plane, and semi-infinite strips.

Definition 2.1.12. *[13, Definition II.1]: Let $h(x)$ be a $\mathcal{F}_0$-measurable stochastic process with continuous sample paths and let $g(x) : \mathcal{B}_f(\mathbb{R}) \to l^2(\{\Omega,\mathcal{F},\mathbb{P}\})$ be a σ-finite random l^2 measure with a $\mathfrak{F}$. A continuous process $F(x,t)$ is $\mathcal{F}_t$-measurable and a weak solution of (2.1) with initial conditions $\{h(\cdot), g(\cdot)\}$ if:*

$$\begin{aligned}\iint_{DoI(x,t)} v(F(y,s),y,s)\,f(y,s)\,dyds + \iint_{DoI(x,t)} \omega(F(y,s),y,s)\,f(y,s)\,dW(y,s)\\ = \int_{DoD(x,t)} \frac{\partial f(y,s)}{\partial s}|_{(y,0)}\,h(y)\,dy - \int_{DoD(x,t)} f(y,0)\,g(dy)\\ + \iint_{DoI(x,t)} \mathfrak{H}^2(f(y,s),1.0)\,F(y,s)\,dyds\end{aligned} \tag{2.9}$$

almost surely for each $f(x) \in \mathfrak{C}^{\infty}$ with compact support in $\mathbb{R}^2_{+t}$.

Lemma 2.1.13. *[13, Proposition II.2]: Assuming $v(\cdot)$ and $\omega(\cdot)$ are locally Lipschitz, then there exists at most one weak solution.*

Proof. Refer to Appendix B. □

Lemma 2.1.14. *[13, Proposition II.3]: Given Assumption 2.1.5, then for each $\mathcal{F}_0$-measurable continuous process $F(x,t)_0$ satisfying: $\iint\limits_{DoI(x,t)} \mathbb{E}\left(\left|F(y,s)_0\right|^2\right) dyds < \infty$, there exists a unique continuous solution to the integral equation $F(x,t) = F(y,s)_0 + \frac{1}{2C} \iint\limits_{DoI(x,t)} v(F(y,s),y,s)\, dyds + \frac{1}{2C} \iint\limits_{DoI(x,t)} \omega(F(y,s),y,s)\, dW(y,s)$.*

Proof. Refer to Appendix B. □

Remark 2.1.15. *Let $\mho_\dagger = DoI(x,t) \cup DoD(x,t)$; the maximal inequality implies that the above solution satisfies $\mathbb{E}\left(\sup\limits_{(y,s)\in\mho_\dagger} |F(x,t)|^p\right) < \infty$, provided $\infty > \iint\limits_{\mho_\dagger} |F(y,s)_0|^p\, dyds$. When $F(x,t)_0 = \frac{1}{2C} \int\limits_{DoD(x,t)} \frac{\partial F(y,s)}{\partial s}\,|_{s=0}\, dy + \frac{F(\zeta(x,t),0)+F(\xi(x,t),0)}{2}$, the uniqueness result of Corollary 2.1.17 can also be proved as an elegant 'consequence' of Lemma 2.1.13 and Lemma 2.1.16; refer to [13, pg. 477].*

Lemma 2.1.16. *[13, Proposition II.4]: Given Assumptions 2.1.3 and 2.1.5, then the unique solution of the integral equation (2.8) is a weak solution of (2.1) in the sense of Definition 2.1.12.*

Proof. Refer to Appendix B. □

Corollary 2.1.17. *Given Assumptions 2.1.3 and 2.1.5, then there exists a unique solution to (2.8).*

Proof. Refer to Appendix B. □

2.1.3.4 Results of [20]

Expanding upon the results of Carmona and Fouque, [20] extends the existence and uniqueness results to the nonlinear equation

$$\frac{\partial^2 F(x,y)}{\partial x \partial y} = \frac{1}{\alpha} f\left(\frac{x}{\alpha}, \frac{y}{\alpha}\right) g(F(x,y),x,y) + h(F(x,y),x,y) \tag{2.10}$$

with initial conditions $F(0,s) = F(r,0) = 1$, where α tends to 0 and $\{x,y\} \geq 0$, such that (x,y) lies in the positive quadrant. The random field $f(r,s) = \sum\limits_{k=1}^{\infty}\sum\limits_{l=1}^{\infty} W_{k,l} 1_{[k-1,k)\times[l-1,l)}(r,s)$, where W is an iid family of bounded and centered random variables driven by a two-parameter Wiener process.

2.1.3.5 Results of [30, Section 4] and [51, Sections 3 and 4]

Using 'semi-martingales,' $\mathcal{SM}$, on the positive quadrant with zero boundary conditions along the axes, [30] proves existence, uniqueness, and the Markov Property for the nonlinear equation

$$\begin{aligned}\frac{\partial^2 F(x,y)}{\partial x \partial y} &= \upsilon_1(F(x,y),x,y)\frac{\partial F(x,y)}{\partial x}\frac{\partial F(x,y)}{\partial y} \\ &+\upsilon_2(F(x,y),x,y)+\omega(F(x,y),x,y)W(x,y). \end{aligned} \tag{2.11}$$

$W(x,y)$ is a two-parameter Gaussian white noise which is formally a Gaussian process with mean zero and auto-covariance
$\mathbb{E}(W(r_x,r_y)W(s_x,s_y)) = \delta(r_x - s_x)\delta(r_y - s_y)$.

Lemma 2.1.18. *Given Assumption 2.1.5, then there is a unique adapted sample continuous random process, $F(x,y)$, that fulfills $\frac{\partial^2 F(x,y)}{\partial x \partial y} = \upsilon(F(x,y),x,y) + \omega(F(x,y),x,y)\frac{\partial^2 W(x,y)}{\partial x \partial y}$; where $F(x,y) \in \mathcal{SM}^{\infty}$ and is Markov relative to $\mathcal{F}_{F(x,y)}$.*

Proof. [30, Theorem 4.1, page 459] □

Lemma 2.1.19. *Given $\{\upsilon_1(\cdot),\upsilon_2(\cdot),\omega(\cdot)\} \in \mathfrak{C}^{(4)}$, then there is a unique solution to the Stratonovich version of (2.11) contained in $\mathcal{SM}_w$. The solution is actually $\mathcal{SM}_{\infty}$ and is Markov relative to $\mathcal{F}_{F(x,y)}$. If $h(\cdot) \in \mathfrak{C}^{(6)}$, $h(0) = 0$, and $h'(\cdot)$ is strictly positive and bounded, then the Markov process $h(Y)$ satisfies the Stratonovich integral solution for (2.11).*

Proof. [30, Theorem 4.2, page 461]. □

[51] proves existence, uniqueness, and non-explosion for (2.2) driven by $W(x,y)$, where (x,y) lies in the positive quadrant and initial conditions are given along the axes. The results of [51] are an extension of [30] and presented in a more 'user-friendly version.'

Lemma 2.1.20. *Consider an Ito version of (2.2), where $\upsilon(\cdot) = 0$ with the additional function along the characteristics $\left\{\frac{\partial u(x,y)}{\partial x} = a(\cdot)\frac{\partial F(x,y)}{\partial x}, \frac{\partial v(x,y)}{\partial y} = a(\cdot)\frac{\partial F(x,y)}{\partial y}\right\}$ and regular $\mathcal{SM}$ initial conditions. Assuming that the functionals have a uniform bound and are Lipschitz continuous, then there exists a unique solution. Moreover, for all $\theta \leq \frac{1}{2}$ and $\alpha \geq 1.0$; then $\mathbb{E}\left(\sup_{DoR(x,y)} \frac{\|F(X)-F(Y)\|_2^{\alpha}}{\|X-Y\|_2^{\theta\alpha}}\right) \leq K$.*

Proof. [51, Theorem 3.2.2, page 304]. □

Lemma 2.1.21. *Consider a Stratonovich version of (2.2) with $\upsilon(\cdot) \neq 0$ and containing lower order terms of $F(x,y)$ and regular $\mathcal{SM}$ initial conditions. For an unknown $\mathcal{SM}$ and $F(X)$ with known $\mathcal{SM}$'s $\{u(x,y),v(x,y)\}$, there exists a unique solution.*

Proof. [51, Theorem 3.2.6, page 318]. □

2.1.3.6 Results of [56]

[56] proves existence, uniqueness, and smoothness for the nonlinear equation

$$\frac{\partial^2 F(x,y)}{\partial x \partial y} = \upsilon_1(x,y)\frac{\partial F(x,y)}{\partial x} + \upsilon_2(x,y)\frac{\partial F(x,y)}{\partial y} + \upsilon_3(F(x,y),x,y) + \omega(F(x,y),x,y)\frac{\partial^2 W(x,y)}{\partial x \partial y} \tag{2.12}$$

with initial conditions given along the axes (boundary), where (x,y) lies in the positive quadrant. Although not as robust as the results of [51], the presentation is easier to read and the results listed in [56, Section 5] provide an introduction to the Green's function of Chapters 3 - 5.

2.2 Discretisation of the process

Notation 2.2.1. *In accordance with Section 1.1, denote the Domain of Dependence, Domain of Influence, Region of Influence, and (2.6) in*
•$\mathbb{R}^2_{+t}$ *by* $\{DoD(x_j,t_k), DoI(x_j,t_k), RoI(x_j,t_k), \xi(x_j,t_k), \zeta(x_j,t_k)\}$.
•$\mathbb{Z}^2_{+t}$ *by* $\{DoD_{j,k}, DoI_{j,k}, RoI_{j,k}, \xi_{j,k}, \zeta_{j,k}\}$.

Due to the propagation properties of (2.6), the FDSy and FDSc should include functionals used to derive solutions to (2.1). Hence $\mathbb{R}^2_{+t}$ must be discretised such that (2.6) are adequately modeled using $\{\xi_{j,k}, \zeta_{j,k}\}$ and the discretised $\{DoD, DoI, RoI\}$ map to their respective $\mathbb{R}^2_{+t}$ counterparts. As addressed in [54], the respective size of Δx and Δt help determine if a system is stable and accurate, since the slopes of (2.6) are $\pm\frac{1}{C}$ and the slopes of $\{\xi_{j,k}, \zeta_{j,k}\}$ are $\pm\frac{\lambda}{C} = \pm\frac{\Delta t}{\Delta x}$. Thus, the magnitude of λ must be bounded as to not introduce new properties to the $\mathbb{Z}^2$ model and ensure that the conservation principles of (2.7) are upheld. Referring to Figure 2.4:

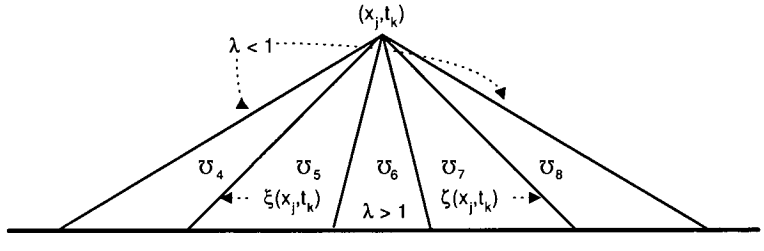

Figure 2.4: CFL Condition: $\mho$. are closed and bounded sub-domains.

•When $\lambda < 1$, the approximation speed is too fast and the space-time discretised grid enforces a slope less than $\pm\frac{1}{C}$. Regardless of the magnitude of Δx, $DoI_{j,k} = \sum_{j=4}^{8} \mho_j$ and the numerical scheme is stable, but the accuracy is questionable due to the inclusion of $\mho_4$ and $\mho_8$.

•When $\lambda > 1$, the approximation becomes violently unstable and is inaccurate due to the non-inclusion $\mho_5$ and $\mho_7$ in $DoI_{j,k}$.

•When $\lambda \neq 1$, $\mathbb{Z}^2_{(x,t)} \neq \mathbb{Z}^2_{(\xi,\zeta)}$ and $\{\xi_{j,k}, \zeta_{j,k}\} \neq \{\xi(x_j, t_k), \zeta(x_j, t_k)\}$ such that there is an inadequate mapping of the continuous domains in $\mathbb{Z}^2$.

•When $\lambda = 1$, $C\Delta t = \Delta x$ and $\mathbb{Z}^2_{(x,t)} = \mathbb{Z}^2_{(\xi,\zeta)}$ such that the discretised and continuous characteristic functions are equivalent.

In addition to the slope of the characteristics and magnitude of λ, there is also the problem of how to map sub-domains $\{\mathtt{D}, \mathbb{W}(\mathtt{D})\}$ in order to utilise the driving functionals of the process in the system. Thus, use the following:

Definition 2.2.2. $\mathtt{D}_{j,k} = \left\{ (y,s) \mid \begin{array}{l} \xi(y,s) \in [\xi(x_j, t_{k+1}), \xi(x_j, t_{k-1})] \\ \zeta(y,s) \in [\zeta(x_j, t_{k-1}), \zeta(x_j, t_{k+1})] \end{array} \right\}$ *where* $\mathfrak{M}(\mathtt{D}_{j,k}) = \iint_{\mathtt{D}_{j,k-1}} dyds = 2\Delta x \Delta t$ *with diagonals* $2\Delta x$ *and* $2\Delta t$*; refer to Figure 2.5.*

Notation 2.2.3. *Centered on* (x_j, t_{k-1})*, let* $\iint_{\mathtt{D}_{j,k-1}} \Upsilon(\alpha, \beta)$ *be equivalent to:*

- $\int_{\zeta_{j,k-2}}^{\zeta_{j,k}} \int_{\xi_{j,k}}^{\xi_{j,k-2}} \Upsilon(\alpha, \beta)$ *when using* (ζ, ξ) *coordinates.*
- $\int_{t_{k-2}}^{t_{k-1}} \int_{x_j - C(s-t_{k-2})}^{x_j + C(s-t_{k-2})} \Upsilon(\alpha, \beta) + \int_{t_{k-1}}^{t_k} \int_{x_j - C(t_k - s)}^{x_j + C(t_k - s)} \Upsilon(\alpha, \beta)$ *when using* (x, t) *coordinates.*

2.2.1 Canonical finite difference scheme

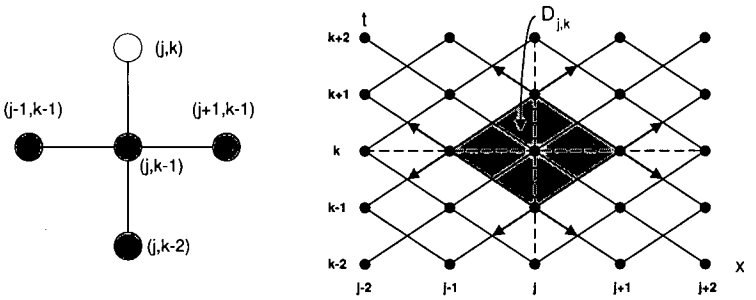

Figure 2.5: 5 Point FDSc and rhombic discretisation scheme

From Section 1.2.2, (2.6), and Figure 2.5, since disturbances propagate through

space as a function of time, a FDSc estimate will be of the form

$$\left[\widehat{F}_{j,k+1}\right] = [FDSc1]\left[\widehat{F}_{j,k}\right] + [FDSc2]\left[\widehat{F}_{j,k-1}\right] + O\left(\Delta x^2\right)[\upsilon_{j,k-1}] + K\left[\mathbb{W}\left(\mathtt{D}_{j,k}\right)\right][\omega_{j,k-1}]. \tag{2.13}$$

Referring to Definition 2.2.2 and Figure 2.5, the diamond shaped region between two consecutive $\mathbb{Z}^2$ points is assigned to each grid point; thus a $\frac{\lambda}{2C}$ factor will assure that the discretised domain is properly weighted. Use (1.9) to construct the consistent and canonical explicit five point FDSc for (2.1), where the forcing terms used to calculate $\widehat{F}_{j,k}$ are mapped to $\{\mathtt{D}_{j,k-1}, \upsilon_{j,k-2}, \omega_{j,k-2}\}$ to ensure that the $DoI_{j,k}$ is not overstated.

Notation 2.2.4. *Let* $[A_n]$ *denote the following matrix with* n *rows and* $n+2$ *columns* $[A_n] =$

$$\begin{bmatrix} \lambda^2 & 2\left(1-\lambda^2\right) & \lambda^2 & 0 & 0 & \cdots & 0 \\ 0 & \lambda^2 & 2\left(1-\lambda^2\right) & \lambda^2 & 0 & \cdots & 0 \\ & & & \ddots & & & \\ 0 & \cdots & 0 & 0 & \lambda^2 & 2\left(1-\lambda^2\right) & \lambda^2 \end{bmatrix}$$

and let $[\mathbb{W}(\mathtt{D}_{j,k})]$ *denote a square diagonal matrix centered on* $\mathbb{W}(\mathtt{D}_{j,k})$*, such that*

$$[\mathbb{W}(\mathtt{D}_{j,k})] = \begin{bmatrix} \ddots & & & & \\ & \mathbb{W}(\mathtt{D}_{j-1,k}) & 0 & 0 & \\ & 0 & \mathbb{W}(\mathtt{D}_{j,k}) & 0 & \\ & 0 & 0 & \mathbb{W}(\mathtt{D}_{j+1,k}) & \\ & & & & \ddots \end{bmatrix}.$$

Lemma 2.2.5. *The canonical five point direct FDSc for (2.1) is*

$$\left[\widehat{F}_{j,k}\right] = [A_n]\left[\widehat{F}_{j,k-1}\right] - [I]\left[\widehat{F}_{j,k-2}\right] + \frac{\lambda\mathfrak{M}(\mathtt{D})}{2C}\left[\upsilon\left(\widehat{F}_{j,k-2}, x_j, t_{k-2}\right)\right] + \frac{\lambda}{2C}\left[\mathbb{W}\left(\mathtt{D}_{j,k-1}\right)\right]\left[\omega\left(\widehat{F}_{j,k-2}, x_j, t_{k-2}\right)\right]. \tag{2.14}$$

Proof. Rearrange (2.1) such that $0 = -\mathfrak{H}^2\left(F\left(x,t\right), C\right) + \upsilon\left(F\left(y,s\right), y, s\right)$ $+\omega\left(F\left(y,s\right), y, s\right)\frac{\partial^2 W(y,s)}{\partial x \partial t}$ and use (1.9) to construct a consistent explicit FDSc where $-\frac{F_{j,k}-2F_{j,k-1}+F_{j,k-1}}{\Delta t^2} + C^2\frac{F_{j+1,k}-2F_{j,k-1}+F_{j-1,k}}{\Delta x^2} + \upsilon\left(F_{j,k-2}, x_j, t_{k-2}\right)$ $+\omega\left(F_{j,k-2}, x_j, t_{k-2}\right)\frac{\mathbb{W}\left(\mathtt{D}_{j,k-1}\right)}{2\Delta x \Delta t} \approx 0$. Solving for $\widehat{F}_{j,k}$ gives

$$\widehat{F}_{j,k} = \lambda^2\left(\widehat{F}_{j+1,k-1} + \widehat{F}_{j-1,k-1}\right) + 2\left(1-\lambda^2\right)\widehat{F}_{j,k-1} - \widehat{F}_{j,k-2} + \frac{\lambda\mathfrak{M}\left(\mathtt{D}_{j,k-1}\right)}{2C}\upsilon\left(\widehat{F}_{j,k-2}, x_j, t_{k-2}\right) + \frac{\lambda}{2C}\omega\left(\widehat{F}_{j,k-2}, x_j, t_{k-2}\right)\mathbb{W}\left(\mathtt{D}_{j,k-1}\right) \tag{2.15}$$

which reduces to $\widehat{F}_{j,k} = \widehat{F}_{j+1,k-1} + \widehat{F}_{j-1,k-1} - \widehat{F}_{j,k-2}$

$$+\frac{\mathfrak{M}\left(\mathtt{D}_{j,k-1}\right)}{2C}\upsilon\left(\widehat{F}_{j,k-2}, x_j, t_{k-2}\right) + \frac{1}{2C}\omega\left(\widehat{F}_{j,k-2}, x_j, t_{k-2}\right)\mathbb{W}\left(\mathtt{D}_{j,k-1}\right) \tag{2.16}$$

when $\lambda = 1$. Using (2.15), the ϑ values yield the computational molecule $\begin{bmatrix} 0 & 0 & 0 \\ \lambda^2 & 2\left(1-\lambda^2\right) & \lambda^2 \\ 0 & -1 & 0 \end{bmatrix}$ and the $\{[A_n], -[I]\}$ FDSc combination. □

2.2.1.1 Other computational molecule's

•Rotated: As depicted in Figure 1.5, another scheme can be constructed using (2.2) in the DoR, such that $\widehat{F}(\xi(x_{j+1},t_{k+1}),\zeta(x_{j+1},t_{k+1}))$
$=\widehat{F}(\xi(x_j,t_{k+1}),\zeta(x_j,t_{k+1}))+\widehat{F}(\xi(x_{j+1},t_k),\zeta(x_{j+1},t_k))-\widehat{F}(\xi(x_j,t_k),\zeta(x_j,t_k))$.
•Problematic: Although consistent, when discretising the derivative in space as a central derivative and the derivative in time is a backwards derivative such that $(1+2\lambda^2)\widehat{F}_{j,k}=2\widehat{F}_{j,k-1}-\widehat{F}_{j,k-2}+\lambda^2\left(\widehat{F}_{j+1,k}+\widehat{F}_{j-1,k}\right)$, the resulting FDSc experiences stepwise over-stability; refer to [33, Section 3.13].
•Higher order: Explicit and implicit schemes can be created such that stability is achieved for $\lambda\geq 1$. For example, $\frac{1}{\Delta t^2}\left(\widehat{F}_{j,k+1}-2\widehat{F}_{j,k}+\widehat{F}_{j,k-1}\right)$
$=\frac{1}{12\Delta x^2}\left(-\widehat{F}_{j+2,k}+16\widehat{F}_{j+1,k}-30\widehat{F}_{j,k}+16\widehat{F}_{j-1,k}-\widehat{F}_{j-2,k}\right)$.

2.2.2 Expansion of terms

When $\lambda=1$, (2.16) yields the solution if exact values are available for $F(x,0)$, $F(x,\Delta t)$, and the integrals of the driving functionals over each $\mathtt{D}$. When $\lambda\neq 1$, the inherent error introduced results from the expansion/contraction of the discretised domain and the weighting of the driving functionals.

Lemma 2.2.6. *Analogous to the deterministic problem, if $\lambda=1$, then*
$F(x_j,t_k)=\lambda^2(F_{j+1,k-1}+F_{j-1,k-1})+2(1-\lambda^2)F_{j,k-1}-F_{j,k-2}$
$+\frac{1}{2C}\iint\limits_{\mathtt{D}_{j,k-1}}\upsilon(F(y,s),y,s)\,dyds+\frac{1}{2C}\iint\limits_{\mathtt{D}_{j,k-1}}\omega(F(y,s),y,s)\,dW(y,s)$.

Proof. Refer to Appendix B. □

Remark 2.2.7. *Lemma 2.2.6 fails when $\lambda\neq 1$; refer to Appendix B.*

Notation 2.2.8. *A Modified Pascal Row, MPR $\binom{m}{\cdot}$, is the transpose of a binomial coefficient vector intermixed with 0's. This can be viewed as Pascal's Triangle with entries separated by 0's.*

$MPR\binom{0}{\cdot}=$ 1
$MPR\binom{1}{\cdot}=$ 1 0 1
$MPR\binom{2}{\cdot}=$ 1 0 2 0 1
$MPR\binom{3}{\cdot}=$ 1 0 3 0 3 0 1
$MPR\binom{4}{\cdot}=$ 1 0 4 0 6 0 4 0 1

Lemma 2.2.9. *When $\lambda=1$,* $\left[\prod_{j=1}^{m}\left[A_{n+2(j-1)}\right]\right]=[\,MPR\,\binom{m}{\cdot}]$.

Proof. Refer to Appendix B. □

Notation 2.2.10. *Referring to Figure 2.6, the points that are blackened lie on $\{\xi_{j,k+1-2l}\cap\zeta_{j,k-1+2l}\}$, where $l\in\{0,1,...,k-1\}$. Let*

• $\sum_{DoD_{j,k}}^{n}$ *denote the* k *additions along* $\wp_{\mathbb{Z}^2} \in DoD_{j,k}$ *where* $n = (j-k+1+2l) \in [j-k+1, j+k-1]$.

• $\sum_{DoI_{j,k}}^{n}$ *denote the* $\frac{k(k-1)}{2}$ *additions in the* $DoI_{j,k}$ *that lie on either* $\xi_{j,k-1-2l}$ *or* $\zeta_{j,k-1-2l}$. $\wp_{\mathbb{Z}^2} \in DoD_{j,k}$ *will be excluded from this set of points.*

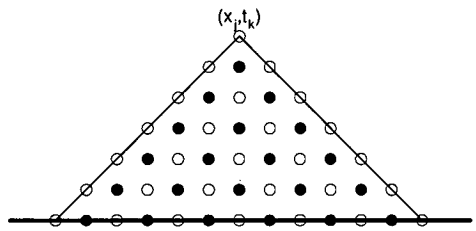

Figure 2.6: Alternating $\mathbb{Z}^2$ points that lie on either $\xi_{j,k-1-2l}$ or $\zeta_{j,k-1-2l}$

Lemma 2.2.11. $\int_{DoD_{j,k}} u(y,0)\,dy = \sum_{DoD_{j,k}}^{n} \left(\int_{x_{n-1}}^{x_{n+1}} u(y,0)\,dy \right)$ *and let* $\Upsilon(z,r)$ *denote either* $dzdr$ *or* $dW(z,r)$, *such that* $\iint_{DoI_{j,k}} u(v(y,s),y,s)\,\Upsilon(z,r)$

$= \sum_{DoI_{j,k}}^{n} \left(\iint_{\mathtt{D}_n} u(v(y,s),y,s)\,\Upsilon(z,r) \right)$.

Proof. Refer to Appendix B. □

Corollary 2.2.12. $\mathfrak{M}(DoI_{j,k}) = \left(\frac{k}{2} + \sum_{l=1}^{k-1} l \right) \mathfrak{M}(\mathtt{D}) = \frac{k^2}{2} \mathfrak{M}(\mathtt{D})$ *and*

$\mathfrak{M}\left(DoI_{j,k} - \sum_{DoD(j;k)}^{n} \mathtt{D}_{n,0} \right) = \frac{k^2-k}{2} \mathfrak{M}(\mathtt{D})$.

Proof. Refer to Appendix B. □

Definition 2.2.13. *Referring to Figure 2.7, define the subspaces:*

•$L_1(y,s)$ *as the set of points* $(z,r) = (z \in [\xi(y,s), \xi(x_j,t_{k-2})], r = 0)$.

•$L_2(y,s)$ *as the set of points* $(z,r) = (z \in [\zeta(x_j,t_{k-2}), \zeta(y,s)], r = 0)$.

•$\mho_1(y,s)$ *as the set of points* $(z,r) \in [\xi(y,s), \xi(x_j,t_{k-2})]$, *where* $r > 0$ *and* $\zeta(z,r) \leq \zeta(x_{j-1},t_{k-1})$.

•$\mho_2(y,s)$ *as the set of points* $(z,r) \in [\zeta(x_j,t_{k-2}), \zeta(y,s)]$, *where* $r > 0$ *and* $\xi(z,r) \geq \xi(x_{j+1},t_{k-1})$.

•$\mho_3(y,s)$ *as the correction of* $\mho_1(y,s)$ *and* $\mho_2(y,s)$ *in* $\mathtt{D}_{j,k-1}$, *where* $\mho_3(y,s) = \{DoI(y,s) \cap \mathtt{D}_{j,k-1}\}$.

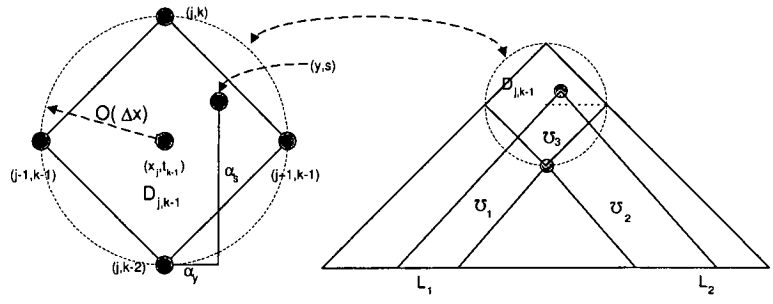

Figure 2.7: Example subdomains for integration

Notation 2.2.14. *Let* $\left\{ \underset{L_1(y,s)}{\int}, \underset{L_2(y,s)}{\int}, \underset{\upsilon_1(y,s)\upsilon_2(y,s)\upsilon_3(y,s)}{\iint}, \underset{\upsilon_1(y,s)\upsilon_2(y,s)\upsilon_3(y,s)}{\iint}, \underset{\upsilon_1(y,s)\upsilon_2(y,s)\upsilon_3(y,s)}{\iint} \right\}$ *denote integration over the domains depicted in Definition 2.2.13, where* $\underset{DoI(x_j,t_{k-2})}{\overset{DoI(y,s)}{\iint}} = \underset{\upsilon_1(y,s)+\upsilon_2(y,s)+\upsilon_3(y,s)}{\iint}$.

Lemma 2.2.15. *Expanding* $F(y,s)$ *around* $F(x_j,t_{k-1})$ *yields* $F(y,s) = F(x_j,t_{k-2}) + f(y,s) + g(y,s) + h(y,s)$, *where:*

- $f(y,s) = -\frac{F(\xi(x_j,t_{k-2}),0)+F(\zeta(x_j,t_{k-2}),0)}{2} + \frac{F(\xi(y,s),0)+F(\zeta(y,s),0)}{2}$
  $+\frac{1}{2C}\left(\underset{L_1(y,s)}{\int} \frac{\partial F(z,r)}{\partial r} \mid_{r=0} dz + \underset{L_2(y,s)}{\int} \frac{\partial F(z,r)}{\partial r} \mid_{r=0} dz \right)$.
- $g(y,s) = \frac{1}{2C} \underset{DoI(x_j,t_{k-2})}{\overset{DoI(y,s)}{\iint}} \upsilon(F(z,r),z,r)\, dzdr$.
- $h(y,s) = \frac{1}{2C} \underset{DoI(x_j,t_{k-2})}{\overset{DoI(y,s)}{\iint}} \omega(F(z,r),z,r)\, dW(z,r)$.

Proof. Refer to Appendix B and Figure 2.7. □

2.2.3 Finite difference system

As alluded to in Figure 2.3, hyperbolic processes can be visualized as the propagation of singularities over a domain. The following examples represent the propagation of a pulse of magnitude 2; i.e., a $2\delta_{(0,0)}$ singularity. The diagrams of Figure 2.8 utilise the canonical FDSc (2.14), where $\{\Delta x = 0.5, \lambda = 1, \upsilon(x,t) = 0\}$ and the same Brownian sheet is used to drive each system.

- Deterministic propagation where $\mathfrak{H}^2(F(x,t),1) = 0$.
- Additive noise propagation where $\mathfrak{H}^2(F(x,t),1) = 0.1\frac{\partial^2 W(x,t)}{\partial x \partial t}$.
- Multiplicative noise propagation where $\mathfrak{H}^2(F(x,t),1) = 0.1F(x,t)\frac{\partial^2 W(x,t)}{\partial x \partial t}$.
- General noise propagation where $\mathfrak{H}^2(F(x,t),1) = 0.1\cos(5\pi F(x,t))\frac{\partial^2 W(x,t)}{\partial x \partial t}$.

To demonstrate how the FDSc matrix is used and give an introduction as to how a FDSy matrix is formulated, utilise the domain of Figure 2.6, where

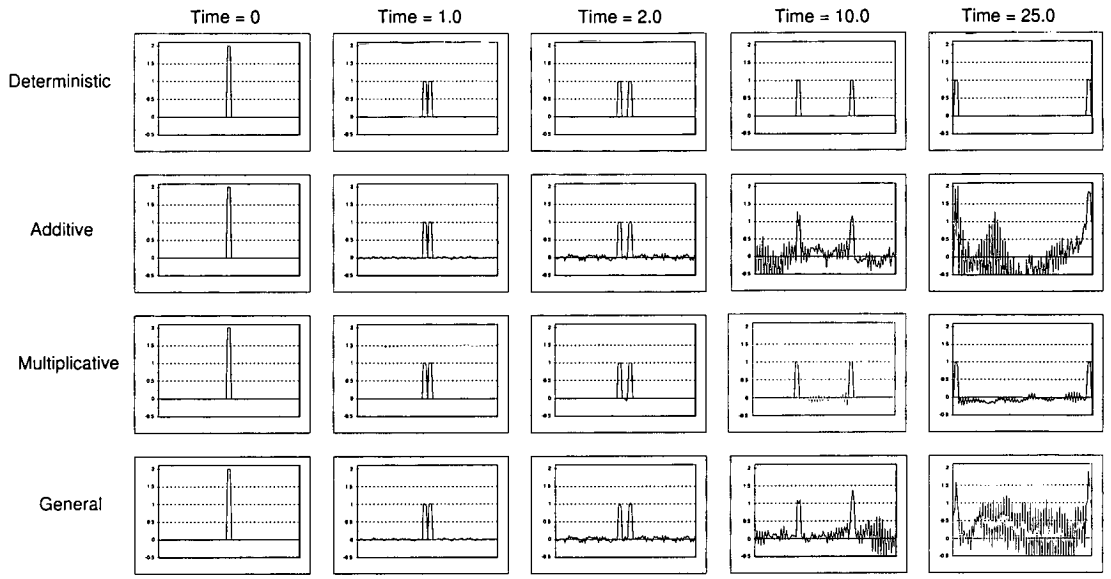

Figure 2.8: Propagation of a pulse

$(x_j, t_k) = (x_0, t_6)$; from (1.10) and (2.14):

$$\bullet \widehat{F}_{0,6} = \begin{bmatrix} \lambda^2 & 2(1-\lambda^2) & \lambda^2 \end{bmatrix} \begin{bmatrix} \widehat{F}_{-1,5} \\ \widehat{F}_{0,5} \\ \widehat{F}_{1,5} \end{bmatrix} - \widehat{F}_{0,4} + \tfrac{\lambda}{2C}\mathfrak{M}(\mathtt{D}) \left[\upsilon\left(\widehat{F}_{0,4}, 0, 4\Delta t\right) \right]$$
$$+ \tfrac{\lambda}{2C}\mathbb{W}(\mathtt{D}_{0,5}) \left[\omega\left(\widehat{F}_{0,4}, 0, 4\Delta t\right) \right].$$

$$\bullet \begin{bmatrix} \widehat{F}_{-1,5} \\ \widehat{F}_{0,5} \\ \widehat{F}_{1,5} \end{bmatrix} = \begin{bmatrix} \lambda^2 & 2(1-\lambda^2) & \lambda^2 & 0 & 0 \\ 0 & \lambda^2 & 2(1-\lambda^2) & \lambda^2 & 0 \\ 0 & 0 & \lambda^2 & 2(1-\lambda^2) & \lambda^2 \end{bmatrix} \begin{bmatrix} \widehat{F}_{-2,4} \\ \widehat{F}_{-1,4} \\ \widehat{F}_{-0,4} \\ \widehat{F}_{1,4} \\ \widehat{F}_{2,4} \end{bmatrix}$$
$$- \begin{bmatrix} \widehat{F}_{-1,3} \\ \widehat{F}_{0,3} \\ \widehat{F}_{1,3} \end{bmatrix} + \tfrac{\lambda}{2C}\mathfrak{M}(\mathtt{D}) \begin{bmatrix} \upsilon\left(\widehat{F}_{-1,3}, -\Delta x, 3\Delta t\right) \\ \upsilon\left(\widehat{F}_{0,3}, 0, 3\Delta t\right) \\ \upsilon\left(\widehat{F}_{1,3}, \Delta x, 3\Delta t\right) \end{bmatrix}$$
$$+ \tfrac{\lambda}{2C} \begin{bmatrix} \mathbb{W}(\mathtt{D}_{-1,4}) & 0 & 0 \\ 0 & \mathbb{W}(\mathtt{D}_{0,4}) & 0 \\ 0 & 0 & \mathbb{W}(\mathtt{D}_{1,4}) \end{bmatrix} \begin{bmatrix} \omega\left(\widehat{F}_{-1,3}, -\Delta x, 3\Delta t\right) \\ \omega\left(\widehat{F}_{0,3}, 0, 3\Delta t\right) \\ \omega\left(\widehat{F}_{1,3}, \Delta x, 3\Delta t\right) \end{bmatrix}.$$

As addressed in Section 1.2.3.1, these relations yield an expression for $\widehat{F}_{0,6}$ in terms of $\left\{ \left[\widehat{F}_{j,0}\right], \left[\widehat{F}_{j,1}\right] \right\}$ and values of $\{\upsilon(\cdot), \omega(\cdot), \mathbb{W}(\mathtt{D})\}$ over the $DoI_{0,6}$. When $\lambda = 1$, the $\{\mathfrak{M}(\mathtt{D}), \mathbb{W}(\mathtt{D})\}$ sub-domains will only be evaluated on the blackened dots of Figure 2.6, while the empty circles represent $\left\{\widehat{F}, \upsilon(\cdot), \omega(\cdot)\right\}$ values used in the approximation of $\widehat{F}_{0,6}$. Due to the propagation properties of the characteristic functions, an algebraic reduction of a FDSc using (2.15) will be utilised.

Notation 2.2.16. *Define $P(m,n)$ such that n is the number of rows and:*

$$P(m,n) = \sum_{j=0}^{k} (-1)^j \binom{m-j-1}{m-2j-1} \left[\prod_{o=1}^{m-2k-1} [A_{n+2(o-1)}] \right] \text{ where } k = \begin{cases} \frac{m-1}{2} \text{ if } m \text{ is odd} \\ \frac{m}{2} - 1 \text{ if } m \text{ is even} \end{cases}$$

$$\text{or } P(m,n) = \begin{cases} \sum_{j=l}^{2l} (-1)^j \binom{j}{2(j-l)} \left[\prod_{o=1}^{2(j-l)} [A_{n+2(o-1)}] \right] \text{ where } m = 2l+1 \\ \sum_{j=l}^{2l-1} (-1)^{j+1} \binom{j}{2(j-l)+1} \left[\prod_{o=1}^{2(j-l)+1} [A_{n+2(o-1)}] \right] \text{ where } m = 2l \end{cases}$$

$$\text{or } P(m,n) = \begin{cases} \sum_{j=0}^{l} (-1)^j \binom{2l-j}{2(l-j)} \left[\prod_{o=1}^{2(l-j)} [A_{n+2(o-1)}] \right] \text{ where } m = 2l+1 \\ \sum_{j=0}^{l-1} (-1)^j \binom{2l-j-1}{2(l-j)-1} \left[\prod_{o=1}^{2(l-j)-1} [A_{n+2(o-1)}] \right] \text{ where } m = 2l \end{cases}$$

Lemma 2.2.17. $P(k+1,n) = [A_n] P(k,n+2) - [I] P(k-1,n)$.

Proof. Refer to Appendix B. □

Corollary 2.2.18. *Using (2.16), when $\lambda = 1$ then*

$$P(k,n) = \begin{bmatrix} 1 & 0 & 1 & 0 & \cdots & 1 & 0 & 1 & 0 & \dots & 0 \\ & & & & & \ddots & & & & & \\ 0 & \dots & 0 & 1 & 0 & 1 & 0 & \cdots & 1 & 0 & 1 \end{bmatrix}.$$

Proof. Refer to Appendix B. □

Lemma 2.2.19. *FDSy approximation vectors to (2.8) are expressed as:*

$$\left[\widehat{F}_{j,k}\right] = P(k,n) \left[\widehat{F}_{j,1}\right] + \frac{\lambda \mathfrak{M}(\mathtt{D})}{2C} \sum_{l=1}^{k-1} P(l,n) \left[v\left(\widehat{F}_{j,k-l-1}, x_j, (k-l-1)\Delta t\right)\right]$$

$$-P(k-1,n) \left[\widehat{F}_{j,0}\right] + \frac{\lambda}{2C} \sum_{l=1}^{k-1} P(l,n) \left[\mathbb{W}(\mathtt{D}_{j,k-l})\right] \left[\omega\left(\widehat{F}_{j,k-l-1}, x_j, (k-l-1)\Delta t\right)\right]. \tag{2.17}$$

Proof. Refer to Appendix B. □

Corollary 2.2.20. *Given values of $\{[\Upsilon_{j,1}], [\Upsilon_{j,0}]\}$, relations of the form*

$\Upsilon_{j,k} = \begin{bmatrix} \lambda^2 & 2(1-\lambda^2) & \lambda^2 \end{bmatrix} \begin{bmatrix} \Upsilon_{j-1,k-1} \\ \Upsilon_{j,k-1} \\ \Upsilon_{j+1,k-1} \end{bmatrix} - \Upsilon_{j,k-2} + f(\Upsilon_{j,k-2})$ *or equivalently*

$[\Upsilon_{j,k}] = [A_n][\Upsilon_{j,k-1}] - [I][\Upsilon_{j,k-2}] + [I][f(\Upsilon_{j,k-2})]$ *can be expressed as:*

$$[\Upsilon_{j,k}] = P(k,n)[\Upsilon_{j,1}] - P(k-1,n)[\Upsilon_{j,0}] + \sum_{l=1}^{k-1} P(l,n)[f(\Upsilon_{j,k-l-1})]. \tag{2.18}$$

Proof. Refer to Appendix B. □

Corollary 2.2.21. *Given* $\{[\Upsilon_{j,1}], [\Upsilon_{j,0}]\}$ *and* $\lambda = 1$, *(2.18) is expressed as*

$$\Upsilon_{j,k} = \sum_{l=0}^{k} \Upsilon_{j-k+2l,1} - \sum_{l=0}^{k-1} \Upsilon_{j-k+2l+1,0} + \sum_{l=1}^{k-1} \sum_{m=0}^{l-1} f\left(\Upsilon_{j-l+2m+1,k-l-1}\right). \quad (2.19)$$

Proof. Refer to Appendix B. This result can also be used to verify Lemma 2.2.11 and Corollary 2.2.12. □

2.3 Errors and convergence

An expression is $O(\Delta x^r)$ if its absolute value is less than $K\Delta x^r$, where K depends upon the driving functionals, initial conditions, and size of the domain.

Assumption 2.3.1. *Throughout this section, assume* $\lambda = \frac{C\Delta t}{\Delta x} = 1$, *such that* $\{\xi_{j,k}, \zeta_{j,k}\} = \{\xi(x_j, t_k), \zeta(x_j, t_k)\}$; *refer to the CFL condition of [54].*

2.3.1 Initial conditions

Assumption 2.3.2. $\left\{\widehat{F}_{j,1}, \widehat{F}_{j,0}\right\}$ *are derived from the initial conditions* $\left\{F(x,t)\,|_{t=0}, \frac{\partial F(x,t)}{\partial t}\,|_{t=0}\right\}$. *Unless otherwise stated,* $\mathbb{W}_{j,0}$ *has been included in the evaluation of* $\widehat{F}_{j,1}$, $\mathfrak{e}_{j,0}$*'s are iid, and* $\max_{DoD(x,t)} \left(\mathbb{E}\left(\mathfrak{e}\mathfrak{g}_{j,0}^2\right), \mathbb{E}\left(\mathfrak{e}\mathfrak{g}_{j,1}^2\right)\right) \leq K_{DoD}\Delta x^3 = O(\Delta x^3)$.

As addressed in Section 1.12 and Assumption 2.1.3, well posed problems are given an initial state and velocity, $\left\{F(x,t)\,|_{t=0}, \frac{\partial F(x,t)}{\partial t}\,|_{t=0}\right\}$, and let $\{\theta_{DoD}, K_{DoD}\}$ denote the Hölder piecewise exponent and constant for the initial conditions over $DoD(x,t)$. Thus, $\min\left(\theta_{F_{\delta U}(z,0)}, \theta_{\frac{\partial F(x,t)}{\partial t}|_{t=0}^{x=z}}\right) \geq \theta_{DoD} \geq \frac{1}{2}$ and $K_{DoD} \geq \max\left(K_{F_{\delta U}(z,0)}, K_{\frac{\partial F(x,t)}{\partial t}|_{t=0}^{x=z}}\right)$, where $z \in \{[\xi_{j,k}, \xi_{j,k-2}] \cup [\zeta_{j,k-2}, \zeta_{j,k}]\}$. This information is used to evaluate boundary and adjacent interior points (i.e., the first two rows) of $\mathbb{Z}^2$ in order to implement a FDSc, such as (2.15). A variety of methods can be used to derive $\left\{\widehat{F}_{j,1}, \widehat{F}_{j,0}\right\}$, but in order to ensure that results are applicable to generic initialization schemes, Assumption 2.3.2 is utilised.

Example 2.3.3. $\widehat{F}_{j,1}$ *can be estimated using a multitude of methods such as a Itô-Taylor expansions, integral evaluation, SDE approximations, the PDE schemes of [2], [33], [57], or the HODIE methods of Lynch and Rice. As per Assumption 2.3.2,* $\max_{DoD(x,t)} \left(\mathbb{E}\left(\mathfrak{e}\mathfrak{g}_{j,0}^2\right), \mathbb{E}\left(\mathfrak{e}\mathfrak{g}_{j,1}^2\right)\right) = O(\Delta x^3)$ *results can be derived when the driving functionals are included in the approximation of* $\left[\widehat{F}_{j,1}\right]$.

Often the initial state, $F(x,0)$, *will be given such that* $[F_{j,0}]$ *can be exactly stated; i.e.,* $\mathfrak{e}_{j,0} = 0$ *and the evaluation of* $\widehat{F}_{j,1}$ *is where an error is introduced. Thus, a scheme that can be utilised consists of* $\widehat{F}_{j,1} - \widehat{F}_{j,-1} = 2\Delta t \frac{\partial F(x,t)}{\partial t}\,|_{t=0}^{x=x_j}$

$+\frac{v_{j,0}}{2C}\mathfrak{M}(\mathtt{D})+\frac{\omega_{j,0}}{2C}\mathbb{W}(\mathtt{D}_j)$; *when* $\lambda=1$, $\widehat{F}_{j,-1}$ *can be eliminated to yield* $\widehat{F}_{j,1}=\frac{\widehat{F}_{j-1,0}+\widehat{F}_{j+1,0}}{2}+\frac{\Delta x}{C}\frac{\partial F(x,t)}{\partial t}\Big|_{t=0}^{x=x_j}+\frac{v_{j,0}}{2C}\mathfrak{M}(\mathtt{D})+\frac{\omega_{j,0}}{2C}\mathbb{W}(\mathtt{D}_j)$, *such that* $\mathbb{E}\left(\mathfrak{e}_{j,1}^2\right)=O\left(\Delta x^3\right)$.

2.3.2 Local error

Lemma 2.3.4. $\mathbb{E}\left(\left(f(y,s)+g(y,s)+h(y,s)\right)^2\right)=O(\Delta x)$.

Proof. Using the inequality $(a+b+c)^2\leq 3\left(a^2+b^2+c^2\right)$ gives
$\mathbb{E}\left(\left(f(y,s)+g(y,s)+h(y,s)\right)^2\right)\leq 3\mathbb{E}\left(f(y,s)^2\right)+3\mathbb{E}\left(g(y,s)^2\right)+3\mathbb{E}\left(h(y,s)^2\right)$.
Evaluating terms yields the following results:
•For the initial conditions, expand using Lemma 2.2.15 and the Hölder continuity of Assumption 2.1.3, to give $|f(y,s)|$

$$=\left|-\frac{F(\xi(x_j,t_{k-2}),0)+F(\zeta(x_j,t_{k-2}),0)}{2}+\frac{F(\xi(y,s),0)+F(\zeta(y,s),0)}{2}+\frac{1}{2C}\int\limits_{L_1(y,s)+L_2(y,s)}\frac{\partial F(z,r)}{\partial r}\Big|_{r=0}dz\right|$$

$$\leq\left|-\frac{F(\xi(x_j,t_{k-2}),0)+F(\zeta(x_j,t_{k-2}),0)}{2}+\frac{F(\xi(x_j,t_{k-2}),0)+F(\zeta(x_j,t_{k-2}),0)}{2}+K_{DoD}\sqrt{2}\Delta x^{\frac{1}{2}}\right.$$
$$\left.+\frac{1}{2C}\left(\frac{\partial F(z,r)}{\partial r}\Big|_{z=\xi(x_j,t_{k-2})}^{r=0}2\Delta x+\frac{\partial F(z,r)}{\partial r}\Big|_{z=\zeta(x_j,t_{k-2})}^{r=0}2\Delta x\right)+\frac{K_{DoD}2\sqrt{2}\Delta x^{\frac{3}{2}}}{C}\right|$$

$$=\sqrt{2}\Delta x^{\frac{1}{2}}\left(K_{DoD}\left(1+\frac{2\Delta x}{C}\right)+\frac{\sqrt{2}}{C}\Delta x^{\frac{1}{2}}\max\left(\frac{\partial F(z,r)}{\partial r}\Big|_{z=\xi(x_j,t_{k-2})}^{r=0},\frac{\partial F(z,r)}{\partial r}\Big|_{z=\zeta(x_j,t_{k-2})}^{r=0}\right)\right).$$

Taking the expected value of the square yields $\mathbb{E}\left(f(y,s)^2\right)=2\Delta x(\cdot)^2=O(\Delta x)$.
•The area of $\left(\iint\limits_{DoI(x_j,t_{k-2})}^{DoI(y,s)}dyds\right)=\mathfrak{M}\left(DoI(y,s)-DoI\left(x_j,t_{k-2}\right)\right)$

$$=\frac{(t_{k-2}+\alpha_s)2C(t_{k-2}+\alpha_s)}{2}-\frac{(t_{k-2})2C(t_{k-2})}{2}\leq 4C\Delta t\left(t_{k-2}+\Delta t\right)=O(\Delta x).$$

Thus, $\left(\iint\limits_{DoI(x_j,t_{k-2})}^{DoI(y,s)}Kdyds\right)=K\mathfrak{M}\left(DoI(y,s)-DoI\left(x_j,t_{k-2}\right)\right)=O(\Delta x)$.
•For the $\mathbb{E}\left(g(y,s)^2\right)$ term, expand using the Lipschitz condition of Assumption 2.1.5 and Cauchy-Schwarz Inequality such that,

$$\mathbb{E}\left(g(y,s)^2\right)=\mathbb{E}\left(\left(\frac{1}{2C}\iint\limits_{DoI(x_j,t_{k-2})}^{DoI(y,s)}v\left(F(z,r),z,r\right)dzdr\right)^2\right)$$

$$\leq\mathbb{E}\left(\left(\frac{1}{2C}\iint\limits_{DoI(x_j,t_{k-2})}^{DoI(y,s)}|v(0,z,r)|+K_v|F(z,r)|\,dzdr\right)^2\right)$$

$$\leq 2\mathbb{E}\left(\left(\frac{1}{2C}\iint\limits_{DoI(x_j,t_{k-2})}^{DoI(y,s)}|v(0,z,r)|\,dzdr\right)^2\right)$$
$$+2\mathbb{E}\left(\left(\frac{1}{2C}\iint\limits_{DoI(x_j,t_{k-2})}^{DoI(y,s)}K_v|F(z,r)|\,dzdr\right)^2\right)$$

$$\leq\frac{1}{2C^2}\left(\iint\limits_{DoI(x_j,t_{k-2})}^{DoI(y,s)}K_v\left(1+\|z,r\|_2\right)dzdr\right)^2$$
$$+\frac{1}{2C^2}\mathbb{E}\left(\iint\limits_{DoI(x_j,t_{k-2})}^{DoI(y,s)}K_v^2dzdr\right)\mathbb{E}\left(\iint\limits_{DoI(x_j,t_{k-2})}^{DoI(y,s)}|F(z,r)|^2\,dzdr\right)$$

$\leq \frac{1}{2C^2}\left(K_v\left(1+\|z,r\|_2\right)\right)^2 O\left(\Delta x^2\right)+\frac{K_v^2}{2C^2}O\left(\Delta x\right)\mathbb{E}\left(\iint\limits_{DoI(x_j,t_{k-2})}^{DoI(y,s)}\left|F\left(z,r\right)\right|^2 dzdr\right)$.

From Lemma's 2.1.14 and 2.1.20; $\mathbb{E}\left(\left|F\left(z,r\right)\right|^2\right)$ is bounded since $F\left(x,t\right)_0=\frac{F(\zeta(x,t),0)+F(\xi(x,t),0)}{2}+\frac{1}{2C}\int\limits_{DoD(x,t)}\frac{\partial F(y,s)}{\partial s}\left|_{s=0}\right. dy$ is a $\mathcal{F}_0$-measurable continuous process satisfying: $\iint\limits_{DoI(x,t)}\mathbb{E}\left(\left|F\left(y,s\right)_0\right|^2\right)dyds<\infty$. Thus, taking the expected value of the square yields $\mathbb{E}\left(g\left(y,s\right)^2\right)$

$\leq \frac{1}{2C^2}\left(K_v\left(1+\|z,r\|_2\right)\right)^2 O\left(\Delta x^2\right)+\frac{K_v^2}{2C^2}O\left(\Delta x\right)\iint\limits_{DoI(x_j,t_{k-2})}^{DoI(y,s)}Kdzdr=O\left(\Delta x^2\right)$.

•Using the properties of the Ito integral and Lipschitz condition of Assumption 2.1.5 gives $\mathbb{E}\left(\left(h\left(y,s\right)\right)^2\right)=\mathbb{E}\left(\left(\frac{1}{2C}\iint\limits_{DoI(x_j,t_{k-2})}^{DoI(y,s)}\omega\left(F\left(z,r\right),z,r\right)dW\left(z,r\right)\right)^2\right)$

$=\left(\frac{1}{2C}\right)^2\mathbb{E}\left(\iint\limits_{DoI(x_j,t_{k-2})}^{DoI(y,s)}\left|\omega\left(F\left(z,r\right),z,r\right)\right|^2 dzdr\right)$

$\leq\left(\frac{1}{2C}\right)^2\mathbb{E}\left(\iint\limits_{DoI(x_j,t_{k-2})}^{DoI(y,s)}\left(\left|\omega\left(0,z,r\right)\right|+K_\omega\left|F\left(z,r\right)\right|\right)^2 dzdr\right)$

$\leq\frac{1}{2C^2}\mathbb{E}\left(\iint\limits_{DoI(x_j,t_{k-2})}^{DoI(y,s)}\left|\omega\left(0,z,r\right)\right|^2+\left(K_\omega\left|F\left(z,r\right)\right|\right)^2 dzdr\right)$

$\leq\frac{K_\omega^2}{2C^2}\left(\iint\limits_{DoI(x_j,t_{k-2})}^{DoI(y,s)}\left(1+\|z,r\|_2\right)^2 dzdr+\iint\limits_{DoI(x_j,t_{k-2})}^{DoI(y,s)}F\left(z,r\right)^2 dzdr\right)$.

Using Lemma's 2.1.14 and 2.1.20 to bound the $F\left(z,r\right)^2$ term yields

$\mathbb{E}\left(\left(h\left(y,s\right)\right)^2\right)\leq\frac{K_\omega^2}{2C^2}\left(\iint\limits_{DoI(x_j,t_{k-2})}^{DoI(y,s)}Kdzdr+\iint\limits_{DoI(x_j,t_{k-2})}^{DoI(y,s)}Kdzdr\right)=O\left(\Delta x\right)$.

•Combining these results gives

$\mathbb{E}\left(\left(f\left(y,s\right)+g\left(y,s\right)+h\left(y,s\right)\right)^2\right)\leq 3\mathbb{E}\left(f\left(y,s\right)^2\right)+3\mathbb{E}\left(g\left(y,s\right)^2\right)+3\mathbb{E}\left(h\left(y,s\right)^2\right)$

$\leq O\left(\Delta x\right)+O\left(\Delta x^2\right)+O\left(\Delta x\right)=O\left(\Delta x\right)$. □

Lemma 2.3.5. $\mathbb{E}\left(\left(\iint\limits_{\mathcal{D}_{j,k-1}}\upsilon\left(F\left(y,s\right),y,s\right)dyds-\upsilon\left(F_{j,k-2},x_j,t_{k-2}\right)\mathfrak{M}\left(\mathtt{D}_{j,k-1}\right)\right)^2\right)$

$=O\left(\Delta x^5\right)$.

Proof. Using Lemma 2.2.15 and Assumption 2.1.5, $\upsilon\left(F\left(y,s\right),y,s\right)$

$=\upsilon\left(F_{j,k-2}+f\left(y,s\right)+g\left(y,s\right)+h\left(y,s\right),x_j+\alpha_y,t_{k-2}+\alpha_s\right)$. Hence,

$\left|\upsilon\left(F\left(y,s\right),y,s\right)-\upsilon\left(F_{j,k-2},x_j,t_{k-2}\right)\right|$

$=\left|\upsilon\left(F_{j,k-2}+f\left(y,s\right)+g\left(y,s\right)+h\left(y,s\right),x_j+\alpha_y,t_{k-2}+\alpha_s\right)-\upsilon\left(F_{j,k-2},x_j,t_{k-2}\right)\right|$

$\leq K_\upsilon\left|f\left(y,s\right)+g\left(y,s\right)+h\left(y,s\right)\right|+K_\upsilon\left(\left|\alpha_y\right|+\alpha_s\right)$

$\leq K_\upsilon\left|f\left(y,s\right)+g\left(y,s\right)+h\left(y,s\right)\right|+K_\upsilon\left(1+\frac{2}{C}\right)\Delta x$.

Using the properties of the Lebesgue integral gives

$$\left| \iint_{\mathtt{D}_{j,k-1}} \upsilon\left(F\left(y,s\right),y,s\right) dyds - \mathfrak{M}\left(\mathtt{D}_{j,k-1}\right) \upsilon\left(F_{j,k-1},x_j,t_{k-1}\right) \right|$$
$$= \left| \iint_{\mathtt{D}_{j,k-1}} \left(\upsilon\left(F\left(y,s\right),y,s\right) - \upsilon\left(F_{j,k-1},x_j,t_{k-1}\right)\right) dyds \right|$$
$$\leq \iint_{\mathtt{D}_{j,k-1}} \left|\upsilon\left(F\left(y,s\right),y,s\right) - \upsilon\left(F_{j,k-1},x_j,t_{k-1}\right)\right| dyds$$
and substitution into the integral yields,
$$\left| \iint_{\mathtt{D}_{j,k-1}} \upsilon\left(F\left(y,s\right),y,s\right) dyds - \mathfrak{M}\left(\mathtt{D}_{j,k-1}\right) \upsilon\left(F_{j,k-1},x_j,t_{k-1}\right) \right|$$
$$\leq K_\upsilon \iint_{\mathtt{D}_{j,k-1}} \left(\left|f\left(y,s\right) + g\left(y,s\right) + h\left(y,s\right)\right| + O\left(\Delta x\right)\right) dyds$$
$$\leq K_\upsilon \iint_{\mathtt{D}_{j,k-1}} \left|f\left(y,s\right) + g\left(y,s\right) + h\left(y,s\right)\right| dyds + O\left(\Delta x^3\right).$$
Thus, $\mathbb{E}\left(\left(\iint_{\mathtt{D}_{j,k-1}} \upsilon\left(F\left(y,s\right),y,s\right) dyds - \mathfrak{M}\left(\mathtt{D}_{j,k-1}\right) \upsilon\left(F_{j,k-1},x_j,t_{k-1}\right)\right)^2\right)$
$$\leq \mathbb{E}\left(\left(K_\upsilon \iint_{\mathtt{D}_{j,k-1}} \left|f\left(y,s\right) + g\left(y,s\right) + h\left(y,s\right)\right| dyds + O\left(\Delta x^3\right)\right)^2\right)$$
$$\leq 2K_\upsilon^2 \mathbb{E}\left(\left(\iint_{\mathtt{D}_{j,k-1}} \left|f\left(y,s\right) + g\left(y,s\right) + h\left(y,s\right)\right| dyds\right)^2\right) + 2O\left(\Delta x^6\right).$$
Using Lemma 2.3.4 and Definition 2.2.2 yields
$$\mathbb{E}\left(\left(\iint_{\mathtt{D}_{j,k-1}} \upsilon\left(F\left(y,s\right),y,s\right) dyds - \mathfrak{M}\left(\mathtt{D}_{j,k-1}\right) \upsilon\left(F_{j,k-1},x_j,t_{k-1}\right)\right)^2\right)$$
$$\leq 2K_\upsilon^2 \left(O\left(\Delta x^{\frac{5}{2}}\right)\right)^2 + O\left(\Delta x^6\right) = O\left(\Delta x^5\right). \qquad \square$$

Lemma 2.3.6. $\mathbb{E}\left(\left(\iint_{\mathtt{D}_{j,k-1}} \omega\left(F\left(y,s\right),y,s\right) dW\left(y,s\right) - \omega\left(F_{j,k-2},x_j,t_{k-2}\right) \mathbb{W}\left(\mathtt{D}_{j,k-1}\right)\right)^2\right)$
$= O\left(\Delta x^3\right).$

Proof. Evaluating the expectation yields
$$\mathbb{E}\left(\left(\iint_{\mathtt{D}_{j,k-1}} \omega\left(F\left(y,s\right),y,s\right) dW\left(y,s\right) - \mathbb{W}\left(\mathtt{D}_{j,k-1}\right) \omega\left(F_{j,k-2},x_j,t_{k-2}\right)\right)^2\right)$$
$$= \mathbb{E}\left(\left(\iint_{\mathtt{D}_{j,k-1}} \left(\omega\left(F\left(y,s\right),y,s\right) - \omega\left(F_{j,k-1},x_j,t_{k-1}\right)\right) dW\left(y,s\right)\right)^2\right)$$
$$= \mathbb{E}\left(\iint_{\mathtt{D}_{j,k-1}} \left|\omega\left(F\left(y,s\right),y,s\right) - \omega\left(F_{j,k-1},x_j,t_{k-1}\right)\right|^2 dyds\right)$$
Hence, $\left|\omega\left(F\left(y,s\right),y,s\right) - \omega\left(F_{j,k-2},x_j,t_{k-2}\right)\right|$
$$= \left|\omega\left(F\left(x_j,t_{k-2}\right) + f\left(y,s\right) + g\left(y,s\right) + h\left(y,s\right), x_j + \alpha_y, t_{k-2} + \alpha_s\right) - \omega\left(F_{j,k-2},x_j,t_{k-2}\right)\right|$$
$$\leq K_\omega \left|f\left(y,s\right) + g\left(y,s\right) + h\left(y,s\right)\right| + K_\omega\left(\left|\alpha_y\right| + \alpha_s\right)$$
$$\leq K_\omega \left|f\left(y,s\right) + g\left(y,s\right) + h\left(y,s\right)\right| + K_\omega\left(1 + \tfrac{2}{C}\right) O\left(\Delta x\right).$$

Substitution into the expectation yields

$$\mathbb{E}\left(\left(\iint_{\mathtt{D}_{j,k-1}} \omega\left(F\left(y,s\right),y,s\right)dW\left(y,s\right)-\mathbb{W}\left(\mathtt{D}_{j,k-1}\right)\omega\left(F_{j,k-2},x_j,t_{k-2}\right)\right)^2\right)$$

$$\leq K_\omega^2\mathbb{E}\left(\iint_{\mathtt{D}_{j,k-1}}\left(\left|f\left(y,s\right)+g\left(y,s\right)+h\left(y,s\right)\right|+O\left(\Delta x\right)\right)^2 dyds\right)$$

$$\leq 2K_\omega^2\mathbb{E}\left(\iint_{\mathtt{D}_{j,k-1}}\left|f\left(y,s\right)+g\left(y,s\right)+h\left(y,s\right)\right|^2 dyds\right)+O\left(\Delta x^4\right)$$

and using Lemma 2.3.4 and Definition 2.2.2 gives

$$\mathbb{E}\left(\left(\iint_{\mathtt{D}_{j,k-1}} \omega\left(F\left(y,s\right),y,s\right)dW\left(y,s\right)-\mathbb{W}\left(\mathtt{D}_{j,k-1}\right)\omega\left(F_{j,k-2},x_j,t_{k-2}\right)\right)^2\right)$$

$$\leq 2K_\omega^2 O\left(\Delta x^3\right)+O\left(\Delta x^4\right)=O\left(\Delta x^3\right).$$ □

Remark 2.3.7. *When utilising the additive functionals:* $\{\upsilon\left(x,t\right),\omega\left(x,t\right)\}$, *either a direct evaluation of the integrals or a similar evaluation utilising Taylor expansions gives the following improved bounds:*

$\bullet\mathbb{E}\left(\iint_{\mathtt{D}_{j,k-1}}\omega\left(y,s\right)dW\left(y,s\right)-\omega_{j,k-2}\mathbb{W}\left(\mathtt{D}_{j,k-1}\right)\right)^2=O\left(\Delta x^4\right).$

$\bullet$*If* $\upsilon\left(x,y\right)\in\mathfrak{C}^{(2)}$ *then* $\left(\iint_{\mathtt{D}_{j,k-1}}\upsilon\left(y,s\right)dyds-\mathfrak{M}\left(\mathtt{D}_{j,k-2}\right)\upsilon_{j,k-1}\right)^2=O\left(\Delta x^8\right)$, *otherwise if* $\upsilon\left(x,y\right)$ *is not differentiable and the Lipschitz condition must be utilised, then* $\left(\iint_{\mathtt{D}_{j,k-1}}\upsilon\left(y,s\right)dyds-\mathfrak{M}\left(\mathtt{D}_{j,k-2}\right)\upsilon_{j,k-1}\right)^2=O\left(\Delta x^6\right).$

2.3.3 Convergence

Refer to Section 2.3.4 for numerical rate of convergence results.

Theorem 2.3.8. *A numerical approximation of (2.8) utilising the canonical five point FDSc is mean square convergent, where* $\mathbb{E}\left(\mathfrak{e}_{j,k}^2\right)=O\left(\Delta x\right)$.

Proof. Using (2.15) and Lemma 2.2.6, since $\lambda=1$; $\mathfrak{e}_{j,k}=\left(F\left(x_j,t_k\right)-\widehat{F}\left(x_j,t_k\right)\right)$

$$=F\left(x_{j+1},t_{k-1}\right)+F\left(x_{j-1},t_{k-1}\right)-F\left(x_j,t_{k-2}\right)+\tfrac{1}{2C}\iint_{\mathtt{D}_{j,k-1}}\upsilon\left(F\left(z,r\right),z,r\right)dzdr$$
$$+\tfrac{1}{2C}\iint_{\mathtt{D}_{j,k-1}}\omega\left(F\left(z,r\right),z,r\right)dW\left(z,r\right)-\widehat{F}_{j+1,k-1}-\widehat{F}_{j-1,k-1}+\widehat{F}_{j,k-2}$$
$$-\tfrac{1}{2C}\mathfrak{M}\left(\mathtt{D}_{j,k-1}\right)\upsilon\left(\widehat{F}_{j,k-2},x_j,t_{k-2}\right)-\tfrac{1}{2C}\omega\left(\widehat{F}_{j,k-2},x_j,t_{k-2}\right)\mathbb{W}\left(\mathtt{D}_{j,k-1}\right)$$
$$=\widehat{F}\left(x_{j+1},t_{k-1}\right)+\mathfrak{e}_{j+1,k-1}+\widehat{F}\left(x_{j-1},t_{k-1}\right)+\mathfrak{e}_{j-1,k-1}-\widehat{F}\left(x_j,t_{k-2}\right)$$
$$-\mathfrak{e}_{j,k-2}-\widehat{F}_{j+1,k-1}-\widehat{F}_{j-1,k-1}+\widehat{F}_{j,k-2}$$
$$+\tfrac{1}{2C}\left(\iint_{\mathtt{D}_{j,k-1}}\upsilon\left(F\left(z,r\right),z,r\right)dzdr-\mathfrak{M}\left(\mathtt{D}_{j,k-1}\right)\upsilon\left(\widehat{F}_{j,k-2},x_j,t_{k-2}\right)\right)$$

$$+\tfrac{1}{2C}\left(\iint_{\mathtt{D}_{j,k-1}}\omega\left(F\left(z,r\right),z,r\right)dW\left(z,r\right)-\omega\left(\widehat{F}_{j,k-2},x_j,t_{k-2}\right)\mathbb{W}\left(\mathtt{D}_{j,k-1}\right)\right)$$
$$=\mathtt{e}_{j+1,k-1}+\mathtt{e}_{j-1,k-1}-\mathtt{e}_{j,k-2}$$
$$+\tfrac{1}{2C}\left(\iint_{\mathtt{D}_{j,k-1}}\upsilon\left(F\left(z,r\right),z,r\right)dzdr-\mathfrak{M}\left(\mathtt{D}_{j,k-1}\right)\upsilon\left(F_{j,k-2},x_j,t_{k-2}\right)\right)$$
$$+\tfrac{1}{2C}\mathfrak{M}\left(\mathtt{D}_{j,k-1}\right)\left(\upsilon\left(F_{j,k-2},x_j,t_{k-2}\right)-\upsilon\left(\widehat{F}_{j,k-2},x_j,t_{k-2}\right)\right)$$
$$+\tfrac{1}{2C}\left(\iint_{\mathtt{D}_{j,k-1}}\omega\left(F\left(z,r\right),z,r\right)dW\left(z,r\right)-\omega\left(F_{j,k-2},x_j,t_{k-2}\right)\mathbb{W}\left(\mathtt{D}_{j,k-1}\right)\right)$$
$$+\tfrac{1}{2C}\mathbb{W}\left(\mathtt{D}_{j,k-1}\right)\left(\omega\left(F_{j,k-2},x_j,t_{k-2}\right)-\omega\left(\widehat{F}_{j,k-2},x_j,t_{k-2}\right)\right)$$
$$=\mathtt{e}_{j+1,k-1}+\mathtt{e}_{j-1,k-1}-\mathtt{e}_{j,k-2}+\Upsilon^{\upsilon}_{j,k-2}+\Upsilon^{\omega}_{j,k-2}+\beta^{\upsilon}_{j,k-2}+\beta^{\omega}_{j,k-2},\text{ where:}$$
$$\bullet\Upsilon^{\upsilon}_{j,k-2}=\tfrac{1}{2C}\left(\iint_{\mathtt{D}_{j,k-1}}\upsilon\left(F\left(z,r\right),z,r\right)dzdr-\mathfrak{M}\left(\mathtt{D}\right)\upsilon\left(F_{j,k-2},x_j,t_{k-2}\right)\right)$$
$$\bullet\Upsilon^{\omega}_{j,k-2}=\tfrac{1}{2C}\left(\iint_{\mathtt{D}_{j,k-1}}\omega\left(F\left(z,r\right),z,r\right)dW\left(z,r\right)-\mathbb{W}\left(\mathtt{D}_{j,k-1}\right)\omega\left(F_{j,k-2},x_j,t_{k-2}\right)\right)$$
$$\bullet\beta^{\upsilon}_{j,k-2}=\tfrac{1}{2C}\mathfrak{M}\left(\mathtt{D}_{j,k-1}\right)\left(\upsilon\left(F_{j,k-2},x_j,t_{k-2}\right)-\upsilon\left(\widehat{F}_{j,k-2},x_j,t_{k-2}\right)\right)$$
$$\bullet\beta^{\omega}_{j,k-2}=\tfrac{1}{2C}\mathbb{W}\left(\mathtt{D}_{j,k-1}\right)\left(\omega\left(F_{j,k-2},x_j,t_{k-2}\right)-\omega\left(\widehat{F}_{j,k-2},x_j,t_{k-2}\right)\right).$$

Using Corollary 2.2.20 and Assumption 2.3.2, this yields the recurrence relation

$$\left[\mathtt{e}_{j,k}\right]=\left[\mathtt{e}_{j-1,k-1}+\mathtt{e}_{j+1,k-1}\right]-\left[\mathtt{e}_{j,k-2}\right]+\left[\Upsilon^{\upsilon}_{j,k-2}+\Upsilon^{\omega}_{j,k-2}+\beta^{\upsilon}_{j,k-2}+\beta^{\omega}_{j,k-2}\right]$$
$$=\left[A_n\right]\left[\mathtt{e}_{j,k-1}\right]-\left[I\right]\left[\mathtt{e}_{j,k-2}\right]+\left[I\right]\left[\Upsilon^{\upsilon}_{j,k-2}+\Upsilon^{\omega}_{j,k-2}+\beta^{\upsilon}_{j,k-2}+\beta^{\omega}_{j,k-2}\right]$$
$$=P\left(k,1\right)\left[\mathtt{e}_{j,1}\right]-P\left(k-1,1\right)\left[\mathtt{e}_{j,0}\right]+\sum_{l=1}^{k-1}P\left(l,1\right)\left[\Upsilon^{\upsilon}_{j,k-l-1}+\Upsilon^{\omega}_{j,k-l-1}+\beta^{\upsilon}_{j,k-l-1}\right.$$
$$\left.+\beta^{\omega}_{j,k-l-1}\right]\text{ and using Corollary 2.2.21 to expand }P\left(n,1\right),\text{ this equates to}$$

$$\mathtt{e}_{j,k}=\sum_{l=0}^{k}\mathtt{e}_{j-k+2l,1}-\sum_{l=0}^{k-1}\mathtt{e}_{j-k+2l+1,0}+\sum_{l=1}^{k-1}\sum_{m=0}^{l-1}\left(\Upsilon^{\upsilon}_{j-l+2m+1,k-l-1}\right.$$
$$\left.+\Upsilon^{\omega}_{j-l+2m+1,k-l-1}+\beta^{\upsilon}_{j-l+2m+1,k-l-1}+\beta^{\omega}_{j-l+2m+1,k-l-1}\right).\qquad(2.20)$$

Evaluating the expectations of the square of (2.20) yields,

$$\mathbb{E}\left(\mathtt{e}^2_{j,k}\right)=\mathbb{E}\left(\left(\sum_{l=0}^{k}\mathtt{e}_{j-k+2l,1}-\sum_{l=0}^{k-1}\mathtt{e}_{j-k+2l+1,0}+\sum_{l=1}^{k-1}\sum_{m=0}^{l-1}\left(\Upsilon^{\upsilon}_{j-l+2m+1,k-l-1}\right.\right.\right.$$
$$\left.\left.\left.+\Upsilon^{\omega}_{j-l+2m+1,k-l-1}+\beta^{\upsilon}_{j-l+2m+1,k-l-1}+\beta^{\omega}_{j-l+2m+1,k-l-1}\right)\right)^2\right)$$
$$\leq 3\mathbb{E}\left(\left(\sum_{l=0}^{k}\mathtt{e}_{j-k+2l,1}\right)^2\right)+3\mathbb{E}\left(\left(\sum_{l=0}^{k-1}\mathtt{e}_{j-k+2l+1,0}\right)^2\right)+3\mathbb{E}\left(\left(\sum_{l=1}^{k-1}\sum_{m=0}^{l-1}\left(\Upsilon^{\upsilon}_{j-l+2m+1,k-l-1}\right.\right.\right.$$
$$\left.\left.\left.+\Upsilon^{\omega}_{j-l+2m+1,k-l-1}+\beta^{\upsilon}_{j-l+2m+1,k-l-1}+\beta^{\omega}_{j-l+2m+1,k-l-1}\right)\right)^2\right)$$
$$\leq 3\mathbb{E}\left(\left(\sum_{l=0}^{k}\mathtt{e}_{j-k+2l,1}\right)^2\right)+3\mathbb{E}\left(\left(\sum_{l=0}^{k-1}\mathtt{e}_{j-k+2l+1,0}\right)^2\right)$$
$$+3\mathbb{E}\left(\left(\sum_{l=1}^{k-1}\sum_{m=0}^{l-1}\Upsilon^{\upsilon}_{j-l+2m+1,k-l-1}+\sum_{l=1}^{k-1}\sum_{m=0}^{l-1}\beta^{\upsilon}_{j-l+2m+1,k-l-1}\right)^2\right)$$

$$+3\mathbb{E}\left(\left(\sum_{l=1}^{k-1}\sum_{m=0}^{l-1}\Upsilon^{\omega}_{j-l+2m+1,k-l-1}+\sum_{l=1}^{k-1}\sum_{m=0}^{l-1}\beta^{\omega}_{j-l+2m+1,k-l-1}\right)^2\right),$$

given that the expectation of the $\{v(\cdot),\omega(\cdot)\}$ cross terms are 0 due the inclusion of $\mathbb{W}(\mathtt{D})$ values. Thus, $\mathbb{E}\left(\mathfrak{e}^2_{j,k}\right) \leq 3\mathbb{E}\left(\left(\sum_{l=0}^{k}\mathfrak{e}_{j-k+2l,1}\right)^2\right)+3\mathbb{E}\left(\left(\sum_{l=0}^{k-1}\mathfrak{e}_{j-k+2l+1,0}\right)^2\right)$

$$+6\left(\mathbb{E}\left(\left(\sum_{l=1}^{k-1}\sum_{m=0}^{l-1}\Upsilon^{v}_{j-l+2m+1,k-l-1}\right)^2\right)+\mathbb{E}\left(\left(\sum_{l=1}^{k-1}\sum_{m=0}^{l-1}\beta^{v}_{j-l+2m+1,k-l-1}\right)^2\right)\right)$$

$$+6\left(\mathbb{E}\left(\left(\sum_{l=1}^{k-1}\sum_{m=0}^{l-1}\Upsilon^{\omega}_{j-l+2m+1,k-l-1}\right)^2\right)+\mathbb{E}\left(\left(\sum_{l=1}^{k-1}\sum_{m=0}^{l-1}\beta^{\omega}_{j-l+2m+1,k-l-1}\right)^2\right)\right).$$

•For notational ease, let $\max_j = \max_{j\in[j-k+l+1,j+k-l-1]}$ and use $\sum_{l=1}^{n}\alpha_l = \frac{n}{n}\sum_{l=1}^{n}\alpha_l = n\overline{\alpha}$, where $\overline{\alpha}$ is the average of the α's.

•From Lemma 2.3.5: $\mathbb{E}\left(\left(\Upsilon^{v}_{j,k-2}\right)^2\right) = \frac{1}{4C^2}O\left(\Delta x^5\right) = O\left(\Delta x^5\right)$.

•From Lemma 2.3.6: $\mathbb{E}\left(\left(\Upsilon^{\omega}_{j,k-2}\right)^2\right) = \frac{1}{4C^2}O\left(\Delta x^3\right) = O\left(\Delta x^3\right)$.

•$\mathbb{E}\left(\left(\beta^{v}_{j,k-2}\right)^2\right) = \frac{1}{4C^2}\mathfrak{M}\left(\mathtt{D}_{j,k-1}\right)^2\left|v\left(F_{j,k-2},x_j,t_{k-2}\right)-v\left(\widehat{F}_{j,k-2},x_j,t_{k-2}\right)\right|^2$

$\leq \frac{1}{4C^2}\mathfrak{M}\left(\mathtt{D}_{j,k-1}\right)^2\mathbb{E}\left(\left(v\left(\widehat{F}_{j,k-2},x_j,t_{k-2}\right)+K_v\mathfrak{e}_{j,k-2}-v\left(\widehat{F}_{j,k-2},x_j,t_{k-2}\right)\right)^2\right)$

$= \frac{K_v^2}{4C^2}O\left(\Delta x^4\right)\mathbb{E}\left(\mathfrak{e}^2_{j,k-2}\right) = O\left(\Delta x^4\right)\mathbb{E}\left(\mathfrak{e}^2_{j,k-2}\right)$.

•$\mathbb{E}\left(\left(\beta^{\omega}_{j,k-2}\right)^2\right) = \frac{1}{4C^2}\mathbb{E}\left(\left(\mathbb{W}\left(\mathtt{D}_{j,k-1}\right)\left(\omega\left(\widehat{F}_{j,k-2}+\mathfrak{e}_{j,k-2},x_j,t_{k-2}\right)-\omega\left(\widehat{F}_{j,k-2},x_j,t_{k-2}\right)\right)\right)^2\right)$

$= \frac{K_\omega^2}{2C^3}\mathfrak{M}\left(\mathtt{D}_{j,k-1}\right)\mathbb{E}\left(\mathfrak{e}^2_{j,k-2}\right) = \frac{K_\omega^2}{4C^2}O\left(\Delta x^2\right)\mathbb{E}\left(\mathfrak{e}^2_{j,k-2}\right) = O\left(\Delta x^2\right)\mathbb{E}\left(\mathfrak{e}^2_{j,k-2}\right)$.

Hence $\mathbb{E}\left(\mathfrak{e}^2_{j,k}\right) \leq 3k^2\mathbb{E}\left(\overline{\mathfrak{e}_{j,1}}^2\right)+3\left(k-1\right)^2\mathbb{E}\left(\overline{\mathfrak{e}_{j,0}}^2\right)+6\sum_{l=1}^{k-1}l^2O\left(\Delta x^5\right)$,

$$+6\sum_{l=1}^{k-1}l^2O\left(\Delta x^4\right)\max_j\left(\mathbb{E}\left(\mathfrak{e}^2_{j,k-l-1}\right)\right)+6\sum_{l=1}^{k-1}lO\left(\Delta x^3\right)+6\sum_{l=1}^{k-1}lO\left(\Delta x^2\right)\max_j\left(\mathbb{E}\left(\mathfrak{e}^2_{j,k-l-1}\right)\right)$$

$\leq k^2O\left(\Delta x^3\right)+\left(k-1\right)^2O\left(\Delta x^3\right)+k^3O\left(\Delta x^5\right)+\sum_{l=1}^{k-1}l^2O\left(\Delta x^4\right)\max_j\left(\mathbb{E}\left(\mathfrak{e}^2_{j,k-l-1}\right)\right)$

$+k^2O\left(\Delta x^3\right)+\sum_{l=1}^{k-1}lO\left(\Delta x^2\right)\max_j\left(\mathbb{E}\left(\mathfrak{e}^2_{j,k-l-1}\right)\right)$. Since the domain is bounded and $k = O\left(\Delta x\right)^{-1}$, this yields $\mathbb{E}\left(\mathfrak{e}^2_{j,k}\right) \leq O\left(\Delta x\right)+O\left(\Delta x\right)+O\left(\Delta x^2\right)+O\left(\Delta x\right)$

$$+\sum_{l=1}^{k-1}l^2O\left(\Delta x^4\right)\max_j\left(\mathbb{E}\left(\mathfrak{e}^2_{j,k-l-1}\right)\right)+\sum_{l=1}^{k-1}lO\left(\Delta x^2\right)\max_j\left(\mathbb{E}\left(\mathfrak{e}^2_{j,k-l-1}\right)\right)$$

$\leq O\left(\Delta x\right)+O\left(\Delta x^2\right)\sum_{l=1}^{k-1}\max_j\left(\mathbb{E}\left(\mathfrak{e}^2_{j,k-l-1}\right)\right)+O\left(\Delta x\right)\sum_{l=1}^{k-1}\max_j\left(\mathbb{E}\left(\mathfrak{e}^2_{j,k-l-1}\right)\right)$

$\leq O\left(\Delta x\right)\left(1+\sum_{l=1}^{k-1}\max_j\left(\mathbb{E}\left(\mathfrak{e}^2_{j,k-l-1}\right)\right)\right)$. Given that $\max_{DoD}\left(\mathbb{E}\left(\mathfrak{e}^2_{j,0}\right),\mathbb{E}\left(\mathfrak{e}^2_{j,0}\right)\right)$ $= O\left(\Delta x^3\right)$, then the recurrence relation yields the desired result. □

2.3.4 Numerical rates of convergence

The following tables summarize pathwise numerical global errors and numerical rates of convergence for (2.1) with additive and multiplicative noise where $(x,t) \in \left\{[0,1] \times \left[0,\frac{1}{2}\right]\right\}$ and the $\mathbb{Z}^2_{\Delta x=\frac{1}{1024}}$ domain refinement is the 'numerical solution.' The number of iterations represents the number of Brownian sheets the errors are averaged over and the results support Theorem 2.3.8 yielding $\widehat{\mathrm{RC}}\left(\widehat{F}\left(\frac{1}{2},\frac{1}{2}\right),2\Delta x\right) = \frac{1}{2}$, within statistical sampling error.

Remark 2.3.9. *It is interesting to note that for these examples, virtually equivalent results are achieved when utilising* $\left\{\upsilon\left(\widehat{F}_{j,k-1},x_j,t_{k-1}\right),\omega\left(\widehat{F}_{j,k-1},x_j,t_{k-1}\right)\right\}$ *in place of* $\left\{\upsilon\left(\widehat{F}_{j,k-2},x_j,t_{k-2}\right),\omega\left(\widehat{F}_{j,k-2},x_j,t_{k-2}\right)\right\}$ *when approximating the driving functionals of (2.16). This is due to the initial conditions being bounded between* $[-1,1]$ *and the nature of the Brownian sheets utilised.*

Iterations = $\widehat{\mathfrak{eg}}\left(\widehat{F}\left(\frac{1}{2},\frac{1}{2}\right)\right)$	32	64	128	256	512
(513×257)	0.00981	0.00973	0.01117	0.01035	0.01153
(257×129)	0.01513	0.01642	0.01534	0.01569	0.01649
(129×65)	0.02504	0.02384	0.02683	0.02411	0.02411
(65×33)	0.02886	0.03435	0.03740	0.03665	0.03153
(33×17)	0.04553	0.04456	0.05586	0.04473	0.04761
(17×9)	0.05704	0.07231	0.07469	0.06816	0.06956
(9×5)	0.06986	0.08849	0.10447	0.10360	0.10316
(5×3)	0.16952	0.14281	0.13653	0.14866	0.13300
(3×1)	0.19321	0.20787	0.20491	0.20621	0.18891
$\widehat{\mathrm{RC}}\left(\widehat{F}\left(\frac{1}{2},\frac{1}{2}\right),2\Delta x\right)$					
(257×129)	0.625	0.755	0.458	0.600	0.516
(129×65)	0.727	0.538	0.806	0.620	0.548
(65×33)	0.205	0.527	0.479	0.604	0.387
(33×17)	0.658	0.376	0.579	0.288	0.595
(17×9)	0.325	0.698	0.419	0.608	0.547
(9×5)	0.292	0.291	0.484	0.604	0.569
(5×3)	1.279	0.690	0.386	0.521	0.367
(3×1)	0.189	0.542	0.586	0.472	0.506

Table 2.1: $\mathfrak{H}^2\left(F\left(x,t\right),1\right) = \frac{\partial^2 W(x,t)}{\partial x \partial t}$; $F\left(x,0\right) = \sin\left(x+t\right) = \sin\left(x\right)$; $\widehat{F}_1 = \sin\left(x+\Delta t\right)$

Iterations = $\widehat{\mathfrak{eg}}\left(\widehat{F}\left(\frac{1}{2},\frac{1}{2}\right)\right)$	32	64	128	256	512
(513×257)	0.01168	0.00991	0.01070	0.01539	0.01034
(257×129)	0.01874	0.01639	0.01591	0.01985	0.01698
(129×65)	0.02776	0.02317	0.02669	0.03037	0.02659
(65×33)	0.04214	0.04224	0.04035	0.04446	0.04035
(33×17)	0.08408	0.06108	0.07176	0.06229	0.06494
(17×9)	0.11410	0.11454	0.10741	0.09590	0.11133
(9×5)	0.19857	0.24393	0.18706	0.13760	0.21228
(5×3)	0.41484	0.47062	0.41240	0.21469	0.42335
(3×1)	0.97715	1.03995	0.97580	0.28029	1.00018
$\widehat{\mathrm{RC}}\left(\widehat{F}\left(\frac{1}{2},\frac{1}{2}\right),2\Delta x\right)$					
(257×129)	0.681	0.726	0.573	0.367	0.716
(129×65)	0.567	0.500	0.746	0.614	0.647
(65×33)	0.602	0.866	0.596	0.550	0.602
(33×17)	0.996	0.532	0.831	0.486	0.687
(17×9)	0.440	0.907	0.582	0.623	0.778
(9×5)	0.799	1.091	0.800	0.521	0.931
(5×3)	1.063	0.948	1.141	0.642	0.996
(3×1)	1.236	1.144	1.243	0.385	1.240

Table 2.2: $\mathfrak{H}^2\left(F\left(x,t\right),1\right) = \frac{\partial^2 W(x,t)}{\partial x \partial t}$; $F\left(x,0\right) = \sin\left(x+t\right) = \sin\left(x\right)$; $\widehat{F}_1 = \sin\left(x\right) + \Delta t \cos\left(x\right)$

Iterations = $\widehat{\mathfrak{eg}}\left(\widehat{F}\left(\frac{1}{2},\frac{1}{2}\right)\right)$	32	64	128	256	512
(513×257)	0.01107	0.01137	0.01171	0.01130	0.01099
(257×129)	0.01543	0.01448	0.01597	0.01616	0.01594
(129×65)	0.02430	0.02452	0.02100	0.02590	0.02355
(65×33)	0.03696	0.02974	0.03645	0.03415	0.03368
(33×17)	0.04823	0.05118	0.04775	0.05115	0.04942
(17×9)	0.07039	0.06604	0.07337	0.07541	0.06905
(9×5)	0.08428	0.08773	0.08714	0.09898	0.09591
(5×3)	0.13182	0.13964	0.14763	0.14488	0.14377
(3×1)	0.24744	0.20701	0.21680	0.19671	0.20281
$\widehat{\mathrm{RC}}\left(\widehat{F}\left(\frac{1}{2},\frac{1}{2}\right),2\Delta x\right)$					
(257×129)	0.478	0.348	0.448	0.516	0.537
(129×65)	0.655	0.760	0.395	0.681	0.563
(65×33)	0.605	0.278	0.795	0.399	0.516
(33×17)	0.384	0.783	0.390	0.583	0.553
(17×9)	0.545	0.368	0.620	0.560	0.482
(9×5)	0.260	0.410	0.248	0.392	0.474
(5×3)	0.645	0.670	0.761	0.550	0.584
(3×1)	0.908	0.568	0.554	0.441	0.496

Table 2.3: $\mathfrak{H}^2\left(F\left(x,t\right),1\right)=\frac{\partial^2 W(x,t)}{\partial x \partial t}$; $F\left(x,0\right)=x^2+t^2=x^2$; $\widehat{F}_1=x^2+\Delta t^2$

Iterations = $\widehat{\mathfrak{eg}}\left(\widehat{F}\left(\frac{1}{2},\frac{1}{2}\right)\right)$	32	64	128	256	512
(513×257)	0.01248	0.00905	0.00995	0.01112	0.01052
(257×129)	0.01403	0.01525	0.01536	0.01630	0.01642
(129×65)	0.02356	0.02629	0.02582	0.02645	0.02393
(65×33)	0.02561	0.02859	0.03753	0.03518	0.03494
(33×17)	0.05235	0.05413	0.05118	0.05004	0.04937
(17×9)	0.07485	0.07234	0.07551	0.07625	0.06963
(9×5)	0.10941	0.10575	0.11537	0.11550	0.10835
(5×3)	0.16577	0.17861	0.17955	0.16226	0.18294
(3×1)	0.26059	0.27318	0.31494	0.28895	0.29099
$\widehat{\mathrm{RC}}\left(\widehat{F}\left(\frac{1}{2},\frac{1}{2}\right),2\Delta x\right)$					
(257×129)	0.170	0.754	0.627	0.552	0.642
(129×65)	0.747	0.785	0.749	0.698	0.544
(65×33)	0.120	0.121	0.540	0.412	0.546
(33×17)	1.031	0.921	0.448	0.508	0.499
(17×9)	0.516	0.418	0.561	0.608	0.496
(9×5)	0.548	0.548	0.611	0.599	0.638
(5×3)	0.599	0.756	0.638	0.490	0.756
(3×1)	0.653	0.613	0.811	0.833	0.670

Table 2.4: $\mathfrak{H}^2\left(F\left(x,t\right),1\right)=\frac{\partial^2 W(x,t)}{\partial x \partial t}$; $U\left(x,t\right)=x^2+t^2=x^2$; $\widehat{F}_1=x^2+2\Delta t$

Iterations = $\widehat{\mathfrak{eg}}\left(\widehat{F}\left(\frac{1}{2},\frac{1}{2}\right)\right)$	32	64	128	256	512
(513×257)	0.01592	0.01560	0.01526	0.01443	0.01506
(257×129)	0.01731	0.02193	0.01979	0.02269	0.02153
(129×65)	0.03118	0.03538	0.03164	0.03213	0.03209
(65×33)	0.03895	0.05264	0.04173	0.04594	0.04498
(33×17)	0.07385	0.07405	0.06998	0.06311	0.06331
(17×9)	0.11046	0.09474	0.09341	0.09035	0.08897
(9×5)	0.12074	0.13375	0.12806	0.13616	0.13228
(5×3)	0.18000	0.18114	0.17746	0.18559	0.19975
(3×1)	0.28169	0.26066	0.25507	0.25614	0.27362
$\widehat{\mathrm{RC}}\left(\widehat{F}\left(\frac{1}{2},\frac{1}{2}\right),2\Delta x\right)$					
(257×129)	0.121	0.491	0.374	0.653	0.516
(129×65)	0.849	0.690	0.677	0.502	0.576
(65×33)	0.321	0.573	0.399	0.516	0.487
(33×17)	0.923	0.492	0.746	0.458	0.493
(17×9)	0.581	0.356	0.417	0.518	0.491
(9×5)	0.128	0.497	0.455	0.592	0.572
(5×3)	0.576	0.438	0.471	0.447	0.595
(3×1)	0.646	0.525	0.523	0.465	0.454

Table 2.5: $\mathfrak{H}^2\left(F\left(x,t\right),1\right) = F\left(x,t\right)\frac{\partial^2 W(x,t)}{\partial x \partial t}$; $F\left(x,0\right) = \sin\left(x+t\right) = \sin\left(x\right)$; $\widehat{F}_1 = \sin\left(x+\Delta t\right)$

Iterations = $\widehat{\mathfrak{eg}}\left(\widehat{F}\left(\frac{1}{2},\frac{1}{2}\right)\right)$	32	64	128	256	512
(513×257)	0.01719	0.01395	0.01670	0.01398	0.01573
(257×129)	0.02417	0.02724	0.02282	0.02111	0.02124
(129×65)	0.03355	0.03459	0.03258	0.03109	0.03340
(65×33)	0.05143	0.04454	0.04520	0.04997	0.04829
(33×17)	0.07063	0.07368	0.08744	0.07528	0.07401
(17×9)	0.10214	0.12769	0.13364	0.12769	0.11994
(9×5)	0.24397	0.20316	0.22156	0.22243	0.22025
(5×3)	0.44343	0.40094	0.41627	0.41570	0.40785
(3×1)	1.04837	0.95783	0.94393	0.96733	0.93687
$\widehat{\mathrm{RC}}\left(\widehat{F}\left(\frac{1}{2},\frac{1}{2}\right),2\Delta x\right)$					
(257×129)	0.492	0.965	0.451	0.595	0.434
(129×65)	0.473	0.344	0.514	0.558	0.653
(65×33)	0.617	0.365	0.472	0.685	0.532
(33×17)	0.457	0.726	0.952	0.591	0.616
(17×9)	0.532	0.793	0.612	0.762	0.697
(9×5)	1.256	0.670	0.729	0.801	0.877
(5×3)	0.862	0.981	0.910	0.902	0.889
(3×1)	1.241	1.256	1.181	1.218	1.200

Table 2.6: $\mathfrak{H}^2\left(F\left(x,t\right),1\right) = F\left(x,t\right)\frac{\partial^2 W(x,t)}{\partial x \partial t}$; $U\left(x,0\right) = \sin\left(x+t\right) = \sin\left(x\right)$; $\widehat{F}_1 = \sin\left(x\right) + \Delta t \cos\left(x\right)$

Iterations = $\widehat{\mathfrak{eg}}\left(\widehat{F}\left(\frac{1}{2},\frac{1}{2}\right)\right)$	32	64	128	256	512
(513×257)	0.01898	0.01401	0.01854	0.01891	0.01835
(257×129)	0.01933	0.02296	0.02451	0.02539	0.02651
(129×65)	0.03842	0.03553	0.03695	0.03530	0.03551
(65×33)	0.04501	0.04738	0.05279	0.04971	0.05050
(33×17)	0.08349	0.06763	0.06704	0.06789	0.07058
(17×9)	0.10061	0.09665	0.09651	0.10159	0.09947
(9×5)	0.10522	0.14464	0.12570	0.13177	0.13218
(5×3)	0.13336	0.18610	0.17893	0.20221	0.19011
(3×1)	0.23909	0.19775	0.21050	0.21781	0.20956
$\widehat{\mathrm{RC}}\left(\widehat{F}\left(\frac{1}{2},\frac{1}{2}\right),2\Delta x\right)$					
(257×129)	0.027	0.713	0.402	0.425	0.531
(129×65)	0.991	0.630	0.592	0.475	0.422
(65×33)	0.229	0.415	0.515	0.494	0.508
(33×17)	0.891	0.513	0.345	0.450	0.483
(17×9)	0.269	0.515	0.526	0.582	0.495
(9×5)	0.065	0.582	0.381	0.375	0.410
(5×3)	0.342	0.364	0.510	0.618	0.524
(3×1)	0.842	0.088	0.234	0.107	0.141

Table 2.7: $\mathfrak{H}^2\left(F\left(x,t\right),1\right) = F\left(x,t\right)\frac{\partial^2 W(x,t)}{\partial x \partial t}$; $F\left(x,0\right) = x^2 + t^2 = x^2$; $\widehat{F}_1 = x^2\Delta t^2$

Iterations = $\widehat{\mathfrak{eg}}\left(\widehat{F}\left(\frac{1}{2},\frac{1}{2}\right)\right)$	32	64	128	256	512
(513×257)	0.01712	0.02083	0.01734	0.01851	0.01803
(257×129)	0.03079	0.02682	0.02655	0.02553	0.02735
(129×65)	0.04006	0.03549	0.03831	0.03662	0.03484
(65×33)	0.04676	0.04700	0.05403	0.04978	0.05323
(33×17)	0.07278	0.07085	0.07873	0.07322	0.07250
(17×9)	0.09323	0.09642	0.09076	0.09811	0.10232
(9×5)	0.13752	0.13817	0.12612	0.14147	0.13997
(5×3)	0.22030	0.20724	0.18938	0.20899	0.21281
(3×1)	0.25710	0.29370	0.26297	0.32182	0.30925
$\widehat{\mathrm{RC}}\left(\widehat{F}\left(\frac{1}{2},\frac{1}{2}\right),2\Delta x\right)$					
(257×129)	0.847	0.365	0.615	0.464	0.601
(129×65)	0.380	0.404	0.529	0.520	0.349
(65×33)	0.223	0.405	0.496	0.443	0.611
(33×17)	0.638	0.592	0.543	0.557	0.446
(17×9)	0.357	0.445	0.205	0.422	0.497
(9×5)	0.561	0.519	0.475	0.528	0.452
(5×3)	0.680	0.585	0.586	0.563	0.604
(3×1)	0.223	0.503	0.474	0.623	0.539

Table 2.8: $\mathfrak{H}^2\left(F\left(x,t\right),1\right) = F\left(x,t\right)\frac{\partial^2 W(x,t)}{\partial x \partial t}$; $F\left(x,0\right) = x^2 + t^2 = x^2$; $\widehat{F}_1 = \left(x\right)^2 + 2\Delta t$

Chapter 3

Elliptic processes

3.1 Introduction

Notation 3.1.1. *The second order elliptic operator is denoted by* $\nabla^2 F(X) = \sum_{j=1}^{d} (C_j)^2 \frac{\partial^2 F(X)}{\partial x_j^2}$, *where* $C_1 = C_x = 1$.

This chapter concentrates on quasi-linear second-order elliptic SPDE's in $\mathbb{R}^d$ with additive noise of the canonical form:

$$\nabla^2 F(X) = -\upsilon(F(X), X) - \omega(X)\dot{W}(X) \tag{3.1}$$

with well posed boundary conditions, where $d \leq 3$ and $\upsilon(\cdot)$ is a general function possibly containing functionals of the lower order terms $\{F(X), F'(X)\}$. The multiplicative and general noise cases of (3.1) will be addressed in Section 3.3, but they are of minor concern. $\nabla^2 F(X) = 0$ is the 'Laplace' equation with solutions called 'harmonic functions' and when $\omega(X) = 0$, (3.1) is the deterministic 'Poisson' equation. The $\{d = 1, 2, 3\}$ forms of (3.1) are:

$$\frac{\partial^2 F(x)}{\partial x^2} = -\upsilon(F(x), x) - \omega(x)\frac{\partial W(x)}{\partial x}, \tag{3.2}$$

$$\frac{\partial^2 F(x,y)}{\partial x^2} + C_y^2 \frac{\partial^2 F(x,y)}{\partial y^2} = -\upsilon(F(x,y), x, y) - \omega(x,y)\frac{\partial^2 W(x,y)}{\partial x \partial y}, \tag{3.3}$$

$$\text{and } \frac{\partial^2 F(x,y,z)}{\partial x^2} + C_y^2 \frac{\partial^2 F(x,y,z)}{\partial y^2} + C_z^2 \frac{\partial^2 F(x,y,z)}{\partial z^2} = -\upsilon(F(x,y,z), x, y, z) - \omega(x,y,z)\frac{\partial^3 W(x,y,z)}{\partial x \partial y \partial z}. \tag{3.4}$$

Elliptic equations such as (1.1), where $b \neq 0$, can be transformed into (3.1) via a change of basis; for example, replace the (x, y) coordinates of (1.2) with $(x_\dagger, y_\dagger)$ where $0 = \frac{\partial x_\dagger}{\partial x} - \left(\frac{a}{c}\right)^2 \frac{\partial x_\dagger}{\partial y} = \frac{\partial y_\dagger}{\partial x} + \left(\frac{a}{c}\right)^2 \frac{\partial y_\dagger}{\partial y}$, to yield (3.3).

3.1.1 Summary of results

Similar to the deterministic system, convergence results for the stochastic system are highly reliant upon the geometry of the domain. As expected, higher rates of convergence can be achieved with efficient handling of boundary conditions; refer to the works of Hackbush, Wasow, and [1, page 140].

3.1.2 Elliptic Assumed Initial Conditions (EAIC)

The following initial conditions assure that elliptic processes are well posed.

Assumption 3.1.2. *Only closed and bounded domains will be utilised.*

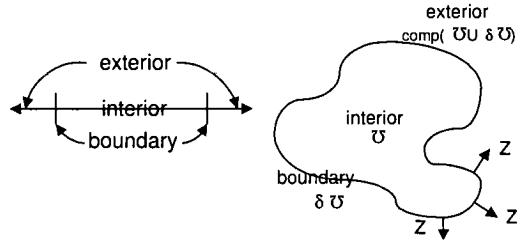

Figure 3.1: Geometric overview

Assumption 3.1.3. *Dirichlet boundary conditions are given, where* $F_{\delta \mho}(X)$ *is a real valued piecewise analytic Hölder continuous function.*

Remark 3.1.4. *As per Remark 1.2.3, Neuman and Robin boundary conditions can be implemented in place of Assumption 3.1.3 with only slight modifications. A heuristic example of these boundary conditions is a heat problem, where the Dirichlet and Neuman conditions represent the actual temperature and heat flux while the Robin condition represents a linear combination of the terms.*

Assumption 3.1.5. $\{v(\cdot), \omega(\cdot)\} \in \mathfrak{C}^{(2)}$ *are real valued functions on* $\mathbb{R}^d$ *and they are globally Lipschitz continuous with coefficients* $\{K_v, K_\omega\}$. *In order to assure uniqueness, assume* $v(\cdot)$ *is an increasing function of* $F(\cdot)$.

Assumption 3.1.6. *A Brownian sheet is utilised.*

3.1.3 The elliptic process

The motivation for solving elliptic processes is to model steady state systems observing inverse-α such as:

•equilibrium states of heat flow, gravitation, or electromagnetic fields.

•processes involving Maxwell's equation or Steady Stokes equations.
•the flow of incompressible viscous fluids.
Since the characteristic equations of (3.1) are conjugate complex, initial conditions and singularities instantaneously propagate in all directions. Thus, elliptic processes are at a 'state of equilibrium' where time is irrelevant and characteristic equations will not be utilised as in Chapter 2.

Notation 3.1.7. *When two position vectors are given, such as $G(X;Y)$, X is the location of a singularity and the operator is with respect to Y.*

$$F(X) = \int_{\delta\upsilon} H(X;Y) F_{\delta\upsilon}(Y)\, dY + \int_{\upsilon} G(X;Y)\, v(F(Y),Y)\, dY + \int_{\upsilon} G(X;Y)\, \omega(Y)\, dW(Y). \tag{3.5}$$

(3.5) is not an explicit formula due to the Green's function dependency upon the domain, but it expresses solutions to (3.1) when the additive functionals $\{v(X), \omega(X)\}$ are utilised and approximations to the solution when $v(\cdot)$ is either a multiplicative or general function.

> One might feel uncomfortable seeing only existence and uniqueness theorems. Indeed, the most important thing in real applications is to find the solution. Of course, we cannot hope to find explicit formulas for solutions for general elliptic operations, by the way, even if one manages to find such a formula for a particular problem, and the formula is complicated, one has to find numerical methods to be able to use the formula for real computations. [40, page 85]

3.1.3.1 The deterministic process

The following Lemma's will be stated for reference and refer to [40] for the definitive text covering this subject. Further theoretical and numerical results can be found in [2], [19], [21], [33], [38], [17, Section 1.3], [46], and virtually any work by Wolfgang Hackbusch.

Lemma 3.1.8. *Given (EAIC), any two solutions of $\{(3.1), \omega(X) = 0\}$ using an equivalent Dirichlet boundary condition must agree or using (Neumann or Robin) boundary conditions must agree or differ by a constant.*

Proof. Refer to [46, page 105]. □

Lemma 3.1.9. *Gauss' Mean Value Theorem: For the Laplace equation where* $F(X)$ *is a harmonic function and* $\delta\mathbb{S} = \delta\mathbb{S}_2(Y, L) \in \mho$*; then* $F(Y)$ *is the average of the solutions over* $\delta\mathbb{S}$ *such that* $F(Y) = \overline{F}(X \mid X \in \delta\mathbb{S}) = \mathfrak{M}(\delta\mathbb{S})^{-1} \int_{\delta\mathbb{S}} F(X)\, dX$.

Proof. Refer to [46, page 105]. □

Lemma 3.1.10. *Maximum Principle: If* $\bigtriangledown^2 F(X) \geq 0$*, then either* $F(X) = C$ *or* $F(X) < \max_{Y \in \delta\mho}(F(Y))$.

Proof. Refer to [40, Sections 2.6 and 2.9], [62, Lemma 1], [49, Theorem 3], or [46, Chapter 4 and Section 8.3] and note that equation (15) should read '$u(\xi) < \sup_{x \in \delta\mho} u(x)$'. □

Corollary 3.1.11. *Minimum Principle: If* $\bigtriangledown^2 F(X) \leq 0$*, then either* $F(X) = C$ *or* $F(X) > \min_{Y \in \delta\mho}(f(Y))$.

Corollary 3.1.12. *Laplacian Maximum - Minimum Principle. For the Laplace Equation;* $\max_{\mho}(F(X)) \leq \max_{\delta\mho}(F_{\delta\mho}(X))$ *and* $\min_{\mho}(F(X)) \geq \min_{\delta\mho}(F_{\delta\mho}(X))$.

Lemma 3.1.13. *Deterministic Existence. Given (EAIC), then a solution to* $\{(3.1), \omega(X) = 0\}$ *exists as defined by (3.5).*

Proof. Refer to Appendix B. □

Lemma 3.1.14. *Deterministic Uniqueness. Given (EAIC), then the solution for* $\{(3.1), \omega(X) = 0\}$*, if it exists, is unique.*

Proof. Refer to Appendix B. □

Lemma 3.1.15. *Let* $f_{\mho}(X) \in \mathfrak{C}^{(2)}$ *and given initial boundary conditions* $f_{\delta\mho}(X) \in \mathfrak{C}^{(1)}$*, then there exists a unique solution to the deterministic Dirichlet problem* $\bigtriangledown^2 F(X) = f_{\mho}(X)$.

Proof. Refer to [40, page 25]. □

Remark 3.1.16. *Given the above results and (EAIC), then a solution to a deterministic Poisson equation is* $\mathfrak{C}^{(2)}$*; refer to [40, pages 18-19] or [46, Section 4.2.a].*

3.1.3.2 Green's function and the Poisson kernel: $\{G(\cdot), H(\cdot)\}$

Due to the extensive coverage of Green's functions in the mathematics and physics literature over the past sixty years, the following will be provided for reference. For a thorough discussion concerning Green's functions and Poisson kernels, refer

to [2], [28, Section 3], [38], [40], [45], [46], [54], and the works of Wasow. Due to complications involving processes with variable coefficients, the Green's function approach has been virtually abandoned in modern theory; but given (1.1) is quasi-linear, this approach will be used in accordance with (1.12), [45], and [63].

Definition 3.1.17. *As defined in [8], let $BM_{\{X,t\}}$ denote a standard Brownian motion starting from X and t is the exit time from the domain under $\mathbb{P}_X$,*

$$\xi(X;Y) = \left\{ \begin{array}{l} -\frac{1}{2}\left\|X-Y\right\|_2 \\ \frac{1}{2\pi}\ln\left(\left\|X-Y\right\|_2\right) - \frac{1}{2\pi}\mathbb{E}\left(\ln\left(\left\|BM_{\{X,t\}}-Y\right\|_2\right)\right) \\ -\frac{\left\|X-Y\right\|_2^{-1}}{4\pi} + \mathbb{E}\left(\frac{\left\|BM_{\{X,t\}}-Y\right\|_2^{-1}}{4\pi}\right) \end{array} \right\}, \text{ where } \{d=1,2,3\}$$

respectively. This is equivalent to [40, page 18], where $\{C_y, C_z\}$ of Notation 3.1.1 have not been normalized.

Definition 3.1.18. *Given a singularity is located at an interior point X, let $\zeta(X;Y) \in \mathfrak{C}^{(2)}$, where $\bigtriangledown^2\zeta(X;\wp_{\mho}) = 0$ and $\zeta(X;Y) = \xi(X;Y)$ when $Y \in \delta\mho$.*

Definition 3.1.19. *The Green's function is $G(X;Y) = \xi(X;Y) - \zeta(X;Y)$ and the Poisson kernel is $H(X;Y) = \frac{\partial G(X;Y)}{\partial Z}$, where Z is the normal vector of a boundary in the exterior of the domain; refer to Figure 3.1.*

Lemma 3.1.20. *For any $g(X) \in \mathfrak{C}^{\infty}$, there exists a function $f(X) \in \mathfrak{C}^{\infty}$, such that $\bigtriangledown^2 f(X) = g(X)$ in $\mathbb{R}^d$.*

Proof. Refer to [40, page 4]. □

Lemma 3.1.21. *If $f(X) \in \mathfrak{C}^{(2)}$, then $g(X) = \int\limits_{\mathbb{R}^d} f(Y)\,\xi(X;Y)\,dy$ defines a bounded continuous function in $\mathbb{R}^d$ which satisfies $\bigtriangledown^2 g(X) = f(X)$ in $\mho$.*

Proof. Refer to [40, page 18]. □

Lemma 3.1.22. *Since the Green's function is a symmetric kernel, a reciprocity relation exits such that $G(X;Y) = G(Y;X)$.*

Proof. Refer to Appendix B. □

From the properties of $\{\xi(\cdot), \zeta(\cdot)\}$, there exists a unique solution to the Green's function; i.e., Laplace function $\bigtriangledown^2 G(X;Y) = 0$. Assuming that $\{f(Y), g(Y)\} \in \mathfrak{C}^{(2)}$ then the following are Green's First and Second Identities, respectively:

$$\int\limits_{\mho} f(Y)\bigtriangledown^2 g(Y)\,dY = \int\limits_{\delta\mho} f(Y)\frac{\partial g(Y)}{\partial Z}dY - \int\limits_{\mho} \mathtt{grad}\left(g(Y)\right)\cdot\mathtt{grad}\left(f(Y)\right)dY \tag{3.6}$$

$$\int_{\mho} f(Y) \bigtriangledown^2 g(Y) dY = \int_{\mho} g(Y) \bigtriangledown^2 f(Y) dY + \int_{\delta\mho} f(Y) \frac{\partial g(Y)}{\partial Z} - g(Y) \frac{\partial f(Y)}{\partial Z} dY \tag{3.7}$$

and when $g(Y) = f(Y)$, this yields the 'Energy Identity'

$$\int_{\mho} |\mathtt{grad}(g(Y))|^2 dY + \int_{\mho} g(Y) \bigtriangledown^2 g(Y) dx = \int_{\delta\mho} g(Y) \frac{\partial g(Y)}{\partial Z} dY. \tag{3.8}$$

This 'conservation of energy' implies that the yield for a Laplace operator is constant, thus the Radiation Principle directly follows.

Lemma 3.1.23. *The Radiation Principle: The fundamental solution to the Laplace equation is a unit source distribution satisfying* $\bigtriangledown^2 F(X) = 1_X$.

Proof. Refer to [46, page 108] where 1_X is a unit source located at X. □

Since $G(X;Y)$ is subject to Lemma 3.1.23, then by definition $\int_{\delta\mho} H(X;Y) dY = 1$. A natural description of this principle is an inverse-d law describing the weakening of a gravitational pull, intensity of light, or strength of an electric field as the distance between objects increases. The radiation principle indicates that the gradient of a field at Y, from a point source X, is indirectly proportional to the surface area of a $\mathbb{R}^d$ sphere; i.e., $\mathfrak{M}(\delta \mathtt{S}_2(X, \|X - Y\|_2))^{-1}$. For an exterior problem where the distance between a boundary and a point is much larger than the interior diameter of the boundary, the geometry of $\{\mho \cup \delta\mho\}$ becomes numerically insignificant and the boundary can be reduced to a point source.

3.1.3.3 The stochastic process

The literature relevant to (3.1) is not as extensive as the hyperbolic or parabolic cases of (1.1), thus relevant articles over the past few years include:

•[1] presents a finite element method for solving elliptic processes using a modified noise that approximates white noise.

•[6] presents a Monte Carlo method for solving elliptic processes.

•[36] discusses Hamilton-Jacobi-Bellman (HBJ) equations experiencing a stochastic 'control' using a scheme related to a method of lines that reduces the dimension of the problem by solving the process in certain directions.

•The existence and uniqueness for the 'token elliptic' case of (3.1) with $\{\upsilon(\cdot) = 0, \omega(X) = 1, F_{\delta\mho}(X) = 0\}$ is presented in [60, Chapter 9]. Also listed is an 'explanation as to how such equations arrive as the limits of parabolic equations.'

•[52] presents the existence and uniqueness results for a modified version of (3.1), where $\bigtriangledown^2 F(X) = -\upsilon(F(X), X) - \dot{W}(X) + 1_{F(X)<0} \Upsilon(X)$, such that white noise

is reflected at 0 and $\Upsilon(X)$ forces $F(X)$ to remain positive over the entire domain; $\Upsilon(X)$ is a random measure satisfying $\int_{\mho} F(X)\, d\Upsilon(X) = 0$.

•[58] discusses the factorization of self-adjoint elliptic FDSy's.

•Although concentrating on deterministic process and systems, the life's work of Dr. Wolfgang Hackbusch is invaluable for the additive stochastic case.

3.1.3.4 Results of [60, Chapter 9]

Assuming a closed and bounded domain with a smooth boundary, consider the Poisson equation where $v(F(Y), Y)$ is bounded and continuous and (3.5) is a weak solution for (3.1). Let M be a l^2 measure on $\mathbb{R}^d$ that is not a $\mathcal{M}$ since there is no time involved with this domain. Set $Q(E_a, E_b) = \mathbb{E}(M(E_a) M(E_b))$ and suppose that there exits a positive definite measure Ω on $\mathbb{R}^d \times \mathbb{R}^d$, such that $|Q(E_a, E_b)| \leq |\Omega(E_a \times E_b)|$ for all Borel spaces $\{E_a, E_b\} \subset \mathbb{R}^d$. Let $M(\delta\mho) = 0$ and $\mathfrak{T}$ be a k^{th} order differential operator on $\mathbb{R}^d$ with smooth coefficients. Consider the SPDE $\left\{\bigtriangledown^2 U(\wp_{\mho}) = \mathfrak{T}\dot{M}, U(\wp_{\delta\mho}) = 0\right\}$; to get the weak form, multiply by a test function $h(X)$ and integrate over $\mathbb{R}^d$, pretending $\dot{M}$ is smooth. Suppose $h(\wp_{\delta\mho}) = 0$ and perform two integrations by parts to get $\int U(X) \bigtriangledown^2 h(X)\, dX - \int_{\mho\cup\delta\mho} \mathfrak{T}\dot{M}(X) h(X)\, dX$. Let $\mathfrak{T}^{\dagger}$ be a formal adjoint of $\mathfrak{T}$ and if $\mathfrak{T}$ is a 0^{th} first order operator or if $h(X)$ has compact support in $\mho$, integrate by parts on the right to get $U(\bigtriangledown^2 h(X)) = \int_{\mho\cup\delta\mho} \mathfrak{T}^{\dagger} h(X) M(dX)$. Since only $\mathbb{R}^d$ is considered, $U(X)$ is a weak solution if $U(X) \in S'(\mathbb{R}^d)$ almost everywhere and holds for all $h(X) \in \left\{S(\mathbb{R}^d) \mid h(Y) = 0; Y \in \delta\mho\right\}$, where S is the Schwartz space of decreasing functions. Refer to [60, Proposition 9.1] for the uniqueness result.

3.1.3.5 Results of [8]

Although the results of Walsh are enlightening, in order to address (3.1), the following results from [8] will be utilised. The case when $v(\cdot) \neq 0$ and $F_{\delta\mho}(X) = 0$ is proven, where (as stated on [8, page 220]) the results can be extended to a more general SPDE with non-zero boundary conditions.

Lemma 3.1.24. *[8, Lemma 2.1]:* $\int_{\mho} G(X;Y)\, \omega(Y)\, dW(Y)$, *where* $X \in \mho$ *posses an almost surely continuous modification.*

Proof. Refer to Appendix B. □

Remark 3.1.25. *It follows that* $\int_{\mho} \ln(\|X - Y\|_2)\, \omega(Y)\, dW(Y)$ *has Lipschitz paths when* $d = 1$, *Hölder continuous with exponent* $1 - \alpha$ *when* $d = 2$, *and Hölder continuous with exponent* $\frac{3}{8} - \alpha$ *when* $d = 3$ *and* $\alpha > 0$.

Lemma 3.1.26. *There exists a constant K such that for any $g(\cdot) \in C^2(\mho)$, $G(X;Y)\, g(Y) \cdot g(X) \geq K \left\| G(X;Y)\, g(Y) \right\|_2$.*

Proof. [8, Lemma 2.4]. □

Lemma 3.1.27. *Let $f(\cdot)$ and $h(\cdot)$ be continuous, non-decreasing on $\mho$, and locally bounded. Moreover, $h(X,r) \leq f(X,r)$ for $X \in \mho, r \in \mathbb{R}$, and $\{u_1(\cdot), u_2(\cdot)\}$ be almost surely continuous random fields on $\mho$; solutions to*

$$u_1(X) = -\int_{\mho} G(X;Y)\, f(F(Y),Y)\, dY + \int_{\mho} G(X;Y)\, v(Y)\, dY + \int_{\mho} G(X;Y)\, dW(Y)$$

$$u_2(X) = -\int_{\mho} G(X;Y)\, h(F(Y),Y)\, dY + \int_{\mho} G(X;Y)\, v(Y)\, dY + \int_{\mho} G(X;Y)\, dW(Y).$$

Then, $u_1(X) \leq u_2(X)$ for $X \in \mho$.

Proof. [8, Lemma 2.6]. □

Lemma 3.1.28. *[8, Lemma 2.5]. Given the (EAIC) then (3.5) is the unique solution to (3.1) which is almost surely continuous on $\mho$.*

Proof. Refer to Appendix B. □

Lemma 3.1.28 is still true if, instead of being non-decreasing, $F(X)$ satisfies $(F(Y_{d-1},r) - F(Y_{d-1},s))(r-s) \geq -\alpha |r-s|^2$ for all $X \in \mho$ and $\{r,s\} \in \mathbb{R}$ provided $\alpha < K$, where K is the constant appearing in Lemma 3.1.26. In other words, $F(X)$ could be the sum of an increasing function that is locally bounded and a Lipschitz function with a constant strictly smaller than K.

3.1.3.6 Results of [1] and [4]

FESy methods to solve $\{(3.2), \omega(x) = 1\}$ are discussed in [1] where

> ... the white noise processes are first approximated by piecewise constant random processes. ... It is shown that the solutions to the new 'simpler' problems converge to the actual solutions of $\{(3.2), \omega(x) = 1\}$ as the white noise approximations become finer. ... Finally, it is proved that the finite element and difference approximations converge to the solutions of the simpler problems and hence to the solutions of the original problems. [1, page 120]

In [4], a general framework to solve (3.3) can be expressed in a variation form, where $\bigtriangledown(u(x,y) \cdot \bigtriangledown F(x,y)) = -\Upsilon(x,y)$ using a FESy. Rate of convergence results for FESy are presented [4, Theorem 3.1] and [4, Theorem 5.1].

3.2 Discretisation of the process

Due to the lack of a time dimension, there is no clear difference between the space dimensions, hence the discretisation will be on the same order of magnitude such that $\Delta y = \lambda_y \Delta x = O(\Delta x)$ and $\Delta z = \lambda_z \Delta x = O(\Delta x)$. Otherwise a FDSy method of lines will be utilised; refer to Section 4.1.0.6.

3.2.1 Discretisation of the boundary

When $\mathfrak{M}(\mathtt{D}) \lll 1$, most often the significant contribution of error is introduced at the boundary; hence a FDSc's handling of errors at the boundary determines the accuracy of the system. [62, Theorem 1] estimates the magnitude of the deterministic errors, but as stated just after the theorem:

> There is not much point in using, as is sometimes proposed, a very accurate approximation in $\mho$ unless it is matched by an equally accurate interpolation scheme near the boundary.
>
> The usefulness of Theorem 1 is limited by the fact that $F(X)$ is not known. ... no really practical appraisal in terms of the data alone seems to exist, except for very special regions. [62, page 88]

When using a uniform $\mathbb{Z}^d_{\Delta x}$ space, unless the $\mathbb{R}^d$ boundary consists of line segments or planes intersecting at appropriate angles, the boundary contains points outside the uniform mesh; refer Figure 3.2-A. Thus, a subset of $\mathbb{Z}^d$ points is redefined as the $\mathbb{Z}^d$ boundary for numerical evaluations, where:

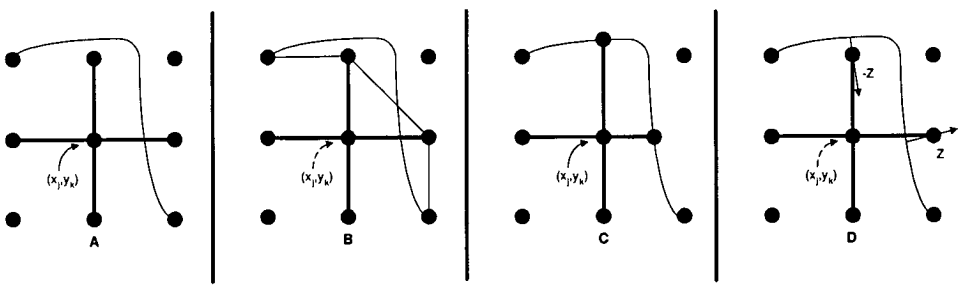

Figure 3.2: Irregular boundary conditions

•Figure 3.2-B. Redefine the discretised boundary such that $\delta\mho_j$ denotes the boundary sub-space assigned to $X_j \in \mathbb{Z}^d$ and adjacent points to the $\mathbb{R}^d$ boundary comprise the new $Y \in \mathbb{Z}^d$ boundary and evaluate $F_{\delta\mho}(Y)$. This method is the preferred approach since a FDSc can be applied without modification.

•Figure 3.2-C. Subtract adjacent points that are required for the FDSc but do

not fall on the boundary and replace them with appropriate points that lie on $\delta\mho$. This method is numerically accurate, but computationally burdensome since the FDSc must be adapted to account for variable Δx's close to the boundary.

•Figure 3.2-D. Select adjacent points and derive their 'boundary value' via a PDE approximation. For example, identifying the boundary and derivatives with respect to $\pm Z$ is trivial, hence $\widehat{F}(Y) = F(X) \pm \frac{\partial F(X)}{\partial Z} \|Y - X\|_2$ approximates adjacent exterior $\{+\}$ and interior $\{-\}$ points using $\mathbb{R}^d$ boundary values.

•Although not utilised in this text, other methods 'solve it locally in neighborhoods of any boundary point by straightening the relevant piece of the boundary' [40, page 79] or '... does not fix the value of $F(\wp_{\delta\mho})$ a priori.' [21, page 200].

3.2.2 Computational molecules

Assumption 3.2.1. *Elliptic computational molecules are weighted averages; thus,* $\lim_{\Delta x \to 0} \mathbb{P}\left(\sum_{X \in \mho} \vartheta(X;Y) = 1 \mid Y \in \mho \right) = 1$, *almost surely.*

Numerous consistent computational molecules have been derived, but due to Assumption 3.2.1, the $FDSc_{\mho}$ matrices are symmetric and irreducible. As alluded to in Section 1.2.2, the 'bench mark' FDSc's for elliptic processes are the explicit three, five, and seven point computational molecules of Figure 3.3. To generate these schemes, expand (3.4) around $F(x_j, y_k, z_l)$ using (1.9) to yield

$$0 = \frac{\partial^2 F(x,y,z)}{\partial x^2} + C_y^2 \frac{\partial^2 F(x,y,z)}{\partial y^2} + C_z^2 \frac{\partial^2 F(x,y,z)}{\partial z^2} + \upsilon(F(x,y,z), x, y, z)$$
$$+\omega(x,y,z) \frac{\partial^2 W(x,y,z)}{\partial x \partial y \partial z} = \frac{\widehat{F}_{j+1,k,l} - 2\widehat{F}_{j,k,l} + \widehat{F}_{j-1,k,l}}{\Delta x^2} + C_y^2 \frac{\widehat{F}_{j,k+1,l} - 2\widehat{F}_{j,k,l} + \widehat{F}_{j,k-1,l}}{\Delta y^2}$$
$$+C_z^2 \frac{\widehat{F}_{j,k,l+1} - 2\widehat{F}_{j,k,l} + \widehat{F}_{j,k,l-1}}{\Delta z^2} + \frac{\Delta x^2}{12} \frac{\partial^4 F(a, y_k, z_l)}{\partial x^4} + \frac{\Delta y^2}{12} \frac{\partial^4 F(x_j, b, z_l)}{\partial y^4}$$
$$+\frac{\Delta z^2}{12} \frac{\partial^4 F(x_j, y_k, c)}{\partial z^4} + \upsilon\left(\widehat{F}(x_j, y_k, z_l), x_j, y_k, z_l\right) + \omega(x_j, y_k, z_l) \frac{\mathbb{W}(\mathtt{D}_{j,k,l})}{\Delta x \Delta y \Delta z}$$
$$+\{\upsilon(\cdot) \text{ and } \omega(\cdot) \text{ truncation errors}\}; \text{ where } a \in [x_{j-1}, x_{j+1}],\ b \in [y_{k-1}, y_{k+1}],$$

and $c \in [z_{l-1}, z_{l+1}]$. This yields the consistent computational molecules:

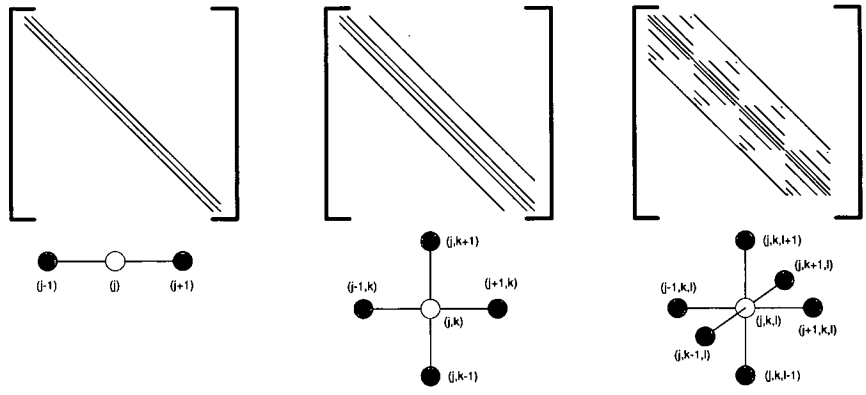

Figure 3.3: $[FDSc_{\mho}]$ matrices for canonical 3, 5, 7 point schemes

$$\widehat{F}_k = \frac{\left(\widehat{F}_{k+1} + \widehat{F}_{k-1}\right)}{2} + \frac{\Delta x^2 \upsilon\left(\widehat{F}_k, y_k\right)}{2} + \frac{\Delta x \omega\left(y_k\right) \mathbb{W}\left(\mathtt{D}_k\right)}{2}, \tag{3.9}$$

$$\begin{aligned}\widehat{F}_{j,k} = & \frac{\left(\widehat{F}_{j+1,k} + \widehat{F}_{j-1,k}\right)}{2\left(1+\lambda_y^2\right)} + \frac{\lambda_y^2\left(\widehat{F}_{j,k+1} + \widehat{F}_{j,k-1}\right)}{2\left(1+\lambda_y^2\right)} \\ & + \frac{\Delta x^2 \upsilon\left(\widehat{F}_{j,k}, x_j, y_k\right)}{2\left(1+\lambda_y^2\right)} + \frac{\lambda_y \omega\left(x_j, y_k\right) \mathbb{W}\left(\mathtt{D}_{j,k}\right)}{2C_y\left(1+\lambda_y^2\right)}, \text{ and}\end{aligned} \tag{3.10}$$

$$\begin{aligned}\widehat{F}_{j,k,l} = & \left(\frac{\widehat{F}_{j+1,k,l} + \widehat{F}_{j-1,k,l}}{2\left(1+\lambda_y^2+\lambda_z^2\right)}\right) + \lambda_y^2\left(\frac{\widehat{F}_{j,k+1,l} + \widehat{F}_{j,k-1,l}}{2\left(1+\lambda_y^2+\lambda_z^2\right)}\right) + \lambda_z^2\left(\frac{\widehat{F}_{j,k,l+1} + \widehat{F}_{j,k,l-1}}{2\left(1+\lambda_y^2+\lambda_z^2\right)}\right) \\ & + \frac{\Delta x^2 \upsilon\left(\widehat{F}_{j,k,l}, x_j, y_k, z_l\right)}{2\left(1+\lambda_y^2+\lambda_z^2\right)} + \frac{\Delta x \omega\left(x_j, y_k, z_l\right) \mathbb{W}\left(\mathtt{D}_{j,k,l}\right)}{2\Delta y \Delta z\left(1+\lambda_y^2+\lambda_z^2\right)}.\end{aligned} \tag{3.11}$$

3.2.2.1 Other computational molecules

Comparing $d = 2$ FDSc computational molecules for the Laplace operator, let $\Delta x = \Delta y$ such that (3.10) yields $\widehat{F}_{j,k} = \frac{1}{4}\left(\widehat{F}_{j,k+1} + \widehat{F}_{j+1,k} + \widehat{F}_{j-1,k} + \widehat{F}_{j,k-1}\right)$.
•Rotated: Apply (1.9) on a space where the coordinates for the basis have been rotated by $\frac{\pi}{4}$ along appropriate axes. For example,

$$\widehat{F}_{j,k} = \frac{1}{4}\left(\widehat{F}_{j-1,k+1} + \widehat{F}_{j+1,k+1} + \widehat{F}_{j-1,k-1} + \widehat{F}_{j+1,k-1}\right). \tag{3.12}$$

•Combination: Weighting the previously mentioned schemes by appropriate factors and adding the results yields further improvements when evaluating the Laplace equation. For example, weighting the molecules by $\frac{4}{5}$ and $\frac{1}{5}$, respectively, yields the canonical nine-point scheme:

$$\begin{aligned}\widehat{F}_{j,k} = & \frac{1}{20}\left(\widehat{F}_{j-1,k+1} + \widehat{F}_{j+1,k+1} + \widehat{F}_{j-1,k-1} + \widehat{F}_{j+1,k-1}\right) \\ & + \frac{1}{5}\left(\widehat{F}_{j+1,k} + \widehat{F}_{j-1,k} + \widehat{F}_{j,k+1} + \widehat{F}_{j,k-1}\right).\end{aligned} \tag{3.13}$$

Remark 3.2.2. *The local error's for harmonic FDSc's where $\Delta x = \Delta y$ are:* $\mathfrak{e}_{(3.10)} = \frac{\Delta x^2}{12}\left(\frac{\partial^4 F(x,y)}{\partial x^4} + \frac{\partial^4 F(x,y)}{\partial y^4}\right)$, $\mathfrak{e}_{(3.12)} = \frac{\Delta x^2}{12}\left(\frac{\partial^4 F(x,y)}{\partial x^4} + 6\frac{\partial^4 F(x,y)}{\partial x^2 \partial y^2} + \frac{\partial^4 F(x,y)}{\partial y^4}\right)$, *and* $\mathfrak{e}_{(3.13)} = \frac{40\Delta x^6}{3 \cdot 8!}\frac{\partial^8 F(x,y)}{\partial x^4 \partial y^4}$. *Unfortunately, when solving (3.1), improvement in the local error of (3.13) are not realized due to truncation errors of* $\{\upsilon(\cdot), \omega(\cdot)\}$.

•Extended: Schemes of higher order for the Laplacian operator can be constructed using more terms from a Taylor expansion. For example:

$\widehat{F}_{j,k} = \frac{4}{15}\left(\widehat{F}_{j+1,k} + \widehat{F}_{j-1,k} + \widehat{F}_{j,k+1} + \widehat{F}_{j,k-1}\right) - \frac{1}{60}\left(\widehat{F}_{j-2,k} + \widehat{F}_{j+2,k} + \widehat{F}_{j,k-2} + \widehat{F}_{j,k+2}\right)$ or the thirteen point scheme: $\widehat{F}_{j,k} = \frac{2}{5}\left(\widehat{F}_{j+1,k} + \widehat{F}_{j-1,k} + \widehat{F}_{j,k+1} + \widehat{F}_{j,k-1}\right) - \frac{1}{20}\left(\widehat{F}_{j-2,k}\right.$
$\left. + \widehat{F}_{j+2,k} + \widehat{F}_{j,k-2} + \widehat{F}_{j,k+2}\right) - \frac{1}{10}\left(\widehat{F}_{j-1,k-1} + \widehat{F}_{j+1,k-1} + \widehat{F}_{j-1,k+1} + \widehat{F}_{j+1,k+1}\right)$.

•Triangular Mesh: FDSc's involving triangles or other bounded polygons have proven popular for filling odd shaped domains. For example, let θ = the angle of rotation from a designated axis, $\mathtt{D}$ = a hexagon, and use six equilateral triangles along with Lemma 3.1.9 to yield $\widehat{F}_{j,k} = \frac{1}{6}\sum_{j=0}^{5} \widehat{F}_{\{\theta=\frac{\pi}{3}j\}}$.

•[62] expands upon the work of Petrowsky and is a general method for evaluating discretisation errors dealing with multiple FDSc using both rectangular, triangular, and hexagonal $\mathtt{D}$.

3.2.3 Green's function approximation

Solving the deterministic Laplace equations using smooth $\mathfrak{C}^{(d+1)}$ functions, such as $G(\cdot)$, was first proved by such authors as Gerschgorin in the early 1930's. The works of McCrea and Whipple, W. Wasow, R. Courant, K.O. Friedrichs, and H. Lewy (CFL condition fame) are invaluable for results concerning discretised Green's functions. As discussed in [21, Section 23.6], [45], and [54], approximating a process with additive noise can be viewed as evaluating a deterministic system with random point sources, as suggested by Lemma 3.2.4. Since the singularities propagate via the deterministic Green's function, approximations are approached by estimating the Laplace operator on a domain with a unit source, this can be heuristically seen as if one were to release one unit of water at X:

•$G(X;Y)$ represents the amount of fluid that visits an interior point Y over an infinite amount of time. This value may of course be greater than 1 since fluid can revisit an interior point more than once, but it is finite as proven in [54]. Thus, $G(X;Y)$ is the expectation that a fluid will visit an interior point Y.

•$H(X;Y)$ represents the amount of fluid that will exit the boundary after an infinite amount of time. Thus, $H(X;Y)$ is the probability of exiting the domain at the boundary point Y.

In approximating this simplified system, one obtains a discretised Green's function, which is sufficient to estimate the 'complicated' problem. Although concentrating on the $d = 2$ case, [63, Section 2] is very robust and results can be easily expanded to $d \in \{1, 3\}$ system.

Lemma 3.2.3. *The approximation to the Poisson kernel where $Y_k \in \delta\mho$ is:*

$$\widehat{H}_{\delta\mho_k}(X;Y_k) = \frac{\widehat{G}(X;Y_k)}{\sum\limits_{X_j \in \delta\mho} \widehat{G}(X;X_j)} \tag{3.14}$$

with errors being proportional to the Green's function approximation error. Thus the Poisson kernel is a PDF, such that the integral of $H(X;Y)$ over $\delta\mho$ is a CDF.

Proof. As per Definitions 3.1.18 and 3.1.19; to fulfill the yield characteristics of a unit source and conserve energy in accordance with (3.8); the Poisson kernel is normalized via the Green's function along the discretised boundary, such that $\int\limits_{\delta\mho} H(X;Y)\,dY = \sum\limits_{Y_k\in\delta\mho}\int\limits_{\delta\mho_k} H(X;Y_k)\,dY = 1 = \sum\limits_{Y_k\in\delta\mho}\widehat{H}_{\delta\mho_k}(X;Y_k)$. For the error, replace $\widehat{G}(\cdot)$ with $G(\cdot)+\mathfrak{e}(G(\cdot))$ such that $\widehat{H}_{\delta\mho_k}(X;Y_k) = (G(X;Y_k))$
$\times\left(\sum\limits_{X_j\in\delta\mho}\widehat{G}(X;X_j)\right)^{-1} + \mathfrak{e}(G(X;X_j))\times\left(\sum\limits_{X_j\in\delta\mho}\widehat{G}(X;X_j)\right)^{-1}$. □

Lemma 3.2.4. *FDSy approximations at a point are derived via:*

$$\widehat{F}(X) = \Delta x^2\sum_{Y_k\in\mho}\widehat{G}(X;Y_k)\,\upsilon\left(\widehat{F}(Y_k),Y_k\right)$$
$$+\Delta x^{2-d}\sum_{Y_k\in\mho}\widehat{G}(X;Y_k)\,\omega(Y_k)\,\mathbb{W}(\mathtt{D}_k) + \sum_{Y_k\in\delta\mho}\widehat{H}_{\delta\mho_k}(X;Y_k)F_{\delta\mho}(Y_k) \tag{3.15}$$

Proof. Using Lemma 3.1.23 and Definition 3.1.19; place a unit source at X and approximate the Laplace function with zero boundary conditions to yield the Green's function estimate $\widehat{G}(X;Y_k)$. Utilise an appropriate weighting of the $\{\mathfrak{M}(\mathtt{D}_k)\,\upsilon(\cdot),\mathbb{W}(\mathtt{D}_k)\,\omega(\cdot)\}$ terms from the FDSc to yield (3.15). □

Corollary 3.2.5. *Using (1.10), FDSy approximations over a domain are derived via:* $\left[\widehat{F}(\wp_{\mho})\right] = O(\Delta x^2)\left[\widehat{G}(\cdot)\right][\upsilon(\cdot)] + O\left(\Delta x^{2-d}\right)\left[\widehat{G}(\cdot)\right][\mathbb{W}(\mathtt{D})][\omega(\cdot)]$
$+\left[\widehat{H}(\cdot)\right][F(\wp_{\delta\mho})]$; *where* $\left[\widehat{G}(\cdot)\right] = \begin{bmatrix} & \widehat{G}(k;k) & \widehat{G}(l;k) & \widehat{G}(m;k) & \\ \cdots & \widehat{G}(k;l) & \widehat{G}(l;l) & \widehat{G}(m;l) & \cdots \\ & \widehat{G}(k;m) & \widehat{G}(l;m) & \widehat{G}(m;m) & \end{bmatrix}$.

Proof. Refer to [49, pages 257-258] □

Corollary 3.2.6. *The Discrete Maximum/Minimum Principle: Given a uniform $\mathbb{Z}^d_{\Delta x}$, consider a solution to the difference equation problem $F_{\Delta x}(X) = \sum\limits_{Y=\wp_{\mathbb{Z}}\in\{\mho-X\}}\vartheta(X;Y)\,F_{\Delta x}(Y)$ with a boundary functional $F_{\delta\mho,\Delta x}(X)$. If the maximum and minimum of $F_{\Delta x}(X)$ in $\mho$ are assumed at points that can be effectively linked to a point in $\delta\mho$, then* $\min(F_{\delta\mho,\Delta x}(X)) \le F_{\Delta x}(X) \le \max(F_{\delta\mho,\Delta x}(X))$.

Proof. Refer to [49, pages 257-258] □

Corollary 3.2.7. *Given $X\in\mho$ and $Y\in\delta\mho$ if $\nabla^2 F(X)\ge 0$, then* $\max(F(X)) = \max(F(Y))$. *Similarly if $\nabla^2 F(X)\le 0$, then* $\min(F(X)) = \min(F(Y))$.

Proof. Using Assumption 3.2.1, an FDS is just a weighted average of its neighbors forced by functions $\{\upsilon(\cdot), \omega(\cdot)\}$. This leads to the conclusion that interior points are weighted averages of the boundary conditions plus a constant sign forcing term. Hence if $\nabla^2 F(X) \leq 0$, then the minimum point is on the boundary and if $\nabla^2 F(X) \geq 0$, then the maximum point is on the boundary. □

Corollary 3.2.8. *For the Laplace Equation, both the maximum and minimum value of (3.1) occur on the boundary.*

Proof. Since $0 = \upsilon(\cdot) = \omega(\cdot)$, interior points are just a weighted average of the boundary points in accordance with Assumption 3.2.1. □

To illustrate the following Lemma's, refer to Section D.2, where:
•Figure D.7, depicts a Kroneker delta function located at $\left(\frac{1}{2}, \frac{1}{2}\right)$. Often called a 'unit point source,' this will be utilised to derive the discretised Green's function.
•Figures D.8 through D.12 represent the growth of a Green's function 'close to the boundary' to show that the function experiences limited growth.
•Figures D.13 through D.17 represent the Green's functions on uniform $\mathbb{Z}^2$ grids. Using a $\mathbb{Z}^2$ unit square grid where $\Delta x = \Delta y$; place a unit source at $\left(\frac{1}{2}, \frac{1}{2}\right)$ and using FDSc = (3.10) to yield the following results.

Theorem 3.2.9. *The discretised Green's function exists and is unique.*

Proof. Refer [45, Section 6]. □

Theorem 3.2.10. *The truncation error* $\mathfrak{eg}\left(\widehat{G}(X_j; Y_k)\,\mathfrak{M}(\mathtt{D}_k)\right)$ *corresponding to the approximate solution of the Green's function in* $d = 2$ *by means of equation (3.10) is of order* $O(\Delta x)$*, provided the following conditions are satisfied:*
•*A closed and bounded domain where the boundary is a simple closed analytic curve with a boundary function,* $F_{\delta\mho}$ *being continuous and piecewise analytic.*
•*The distance from the singularities of the boundary function to the nearest discretised interior point is not less than* $\theta\Delta x$*, where* θ *is independent of* Δx*.*
•*If* $\left\{\widehat{F}_{\delta\mho}(X_j) = F_{\delta\mho}(Y) \mid Y \in \delta\mho\right\}$*, then the distance of the singularities of the boundary from the line segment connecting* X_j *and* Y *is not less than* $\theta\Delta x$*.*
Thus the truncation error is $O(\Delta x)$ *uniformly in every closed sub-domain of* $\mho$*.*

Proof. [63, page 62]. □

Lemma 3.2.11. *Placing a unit source at* $\wp_j$*, the Green's function experiences geometric growth, such that* $\widehat{G}_{N+1}(j;j) = \frac{1}{1-\theta^*_{N+1}}\widehat{G}_N(j;j) > 1$ *or simply* $\widehat{G}_{N+1}(j;j) = \frac{1}{1-\theta_{N+1}} > 1$*, where* θ^*_k *denotes the geometric growth of a Green's function due to the inclusion of* $\wp_k$ *and* θ_k *denotes the growth constant of a Green's function, where* $\mathtt{card}(\mho) = k$*.*

Proof. Refer to Appendix B. □

Remark 3.2.12. *Further bounds on the discretized Green's function errors can be found in [61]. Due to the closed loop feedback phenomena, the influence of unit source will almost surely increase and is dependent upon the location within the domain and the number of interior points.*

Corollary 3.2.13. *Given (EAIC), then* $\widehat{G}(X_j; X_j)$ *is a unique constant.*

Proof. Refer to Appendix B. □

Corollary 3.2.14. *Given (EAIC), then* $\theta_{N+1} < 1$.

Proof. Refer to Appendix B. □

Corollary 3.2.15. *When* $\mathsf{card}(\mho) = N \to \infty$, *then* $\widehat{G}_N(X_j; X_j) \to \infty$ *if* X_j *is 'well within the interior' and a finite constant if* X_j *is 'close to the interior.'*

Proof. Refer to Appendix B. Figures D.8 through D.12 show a graphical representation of this result. □

Lemma 3.2.16. *Given (EAIC) where* $\vartheta(X_j; Y_k) = \vartheta(Y_k; X_j)$ *for all* $\{X_j, Y_k\} \in \mho$, *in accordance with Lemma 3.1.22 then the reciprocity relation is true such that* $\widehat{G}_N(X_j; Y_k) = \widehat{G}_N(Y_k; X_j)$.

Proof. Refer to Appendix B, [45, Section 6], or [63]. □

Corollary 3.2.17. *Given (EAIC), as* $\Delta x \to 0$, *the difference between two Green's function approximations on the same domain that are a* $[V] = [\alpha_j \Delta x]$ *distance apart is a constant such that:* $\lim_{\Delta x \to 0} \left(\widehat{G}_{\Delta x}(X; Y) - \widehat{G}_{\Delta x}([X - V]; Y) \right)$
$= \lim_{\Delta x \to 0} \left(\widehat{G}_{s\Delta x}(X; Y) - \widehat{G}_{s\Delta x}([X - sV]; Y) \right) = K.$

Proof. Refer to Appendix B. The symmetry of differences in $G(x_j, y_k; x_l, y_m) - G(x_j, y_k; x_n, y_o)$ is also shown in [45, Sections 6 - 7]. Extensions to the $\mathbb{Z}^3$ case are given in [45, Sections 11 - 13]. □

3.2.4 Closed loop feedback

To illustrate the effects of closed loop feedback, derive $\widehat{G}_{\Delta x}(\cdot)$ via the Laplace equation with a point source and homogenous boundary conditions. For this section only, denote the 4-tuple $\left\{ \widehat{F}(Y_k), \widehat{F}(\wp_{middle}), \widehat{F}(\wp_{corner,1}), \widehat{F}(\wp_{corner,2}) \right\}$ where $\{\wp_{corner,j}\}$ is a point with j paths of l^1 distance $2\Delta x$ to the unit source; refer to Figures 3.4 and 3.5. Let $\{\mho \cup \delta\mho \mid F(\wp_{\delta\mho}) = 0\}$ equal the:

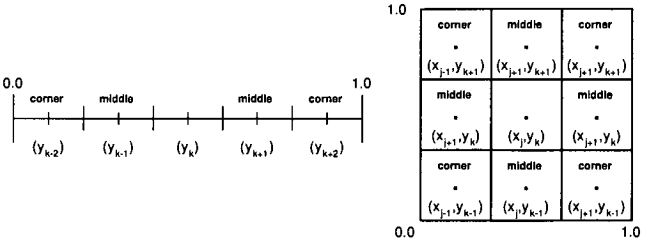

Figure 3.4: Closed and bounded domains for illustrating closed loop feedback

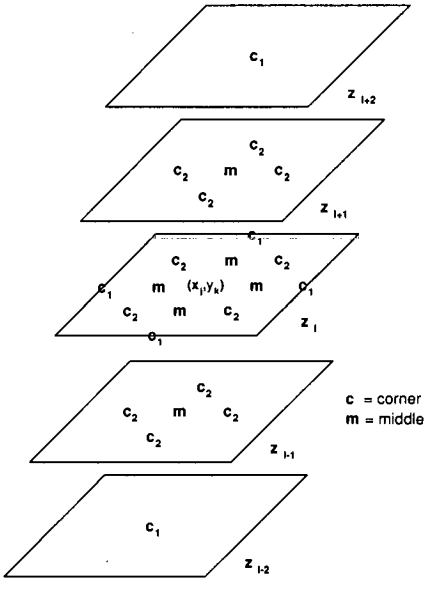

Figure 3.5: Example $\mathtt{S}_1\left((x_j, y_k, z_l); 2\Delta x\right)$ domain

•$\mathbb{Z}^1$ unit length domain of Figure 3.4 such that $\widehat{F}(x_j) = \widehat{G}_{\Delta x}(k; j)$. Let $\Delta y = \frac{1}{5}$ with five interior points, where $\{\wp_{middle}\} = \left\{\frac{3}{10}, \frac{7}{10}\right\}$ and $\{\wp_{corner,1}\} = \left\{\frac{1}{10}, \frac{9}{10}\right\}$.
•$\mathbb{Z}^2$ unit square domain of Figure 3.4; let $\Delta x = \Delta y = \frac{1}{4}$, $(x_j, y_k) = \left(\frac{1}{2}, \frac{1}{2}\right)$, with nine uniform interior points where $\{\wp_{middle}\} = \left\{\left(\frac{1}{2}, \frac{1}{4}\right), \left(\frac{1}{4}, \frac{1}{2}\right), \left(\frac{3}{4}, \frac{1}{2}\right), \left(\frac{1}{2}, \frac{3}{4}\right)\right\}$ and $\{\wp_{corner,2}\} = \left\{\left(\frac{1}{4}, \frac{1}{4}\right), \left(\frac{3}{4}, \frac{1}{4}\right), \left(\frac{1}{4}, \frac{3}{4}\right), \left(\frac{3}{4}, \frac{3}{4}\right)\right\}$.
•$\mathbb{Z}^3$ unit sphere domain of Figure 3.5; let $\Delta x = \Delta y = \Delta z = \frac{1}{6}$ with 25 interior points where: $\{\wp_{middle}\} = \left\{\left(\frac{1}{3}, \frac{1}{2}, \frac{1}{2}\right), \left(\frac{2}{3}, \frac{1}{2}, \frac{1}{2}\right), \left(\frac{1}{2}, \frac{1}{3}, \frac{1}{2}\right), \left(\frac{1}{2}, \frac{2}{3}, \frac{1}{2}\right), \left(\frac{1}{2}, \frac{1}{2}, \frac{1}{3}\right), \left(\frac{1}{2}, \frac{1}{2}, \frac{2}{3}\right)\right\}$, $\{\wp_{corner,1}\} = \left\{\left(\frac{1}{6}, \frac{1}{2}, \frac{1}{2}\right), \left(\frac{1}{2}, \frac{1}{6}, \frac{1}{2}\right), \left(\frac{1}{2}, \frac{1}{2}, \frac{1}{6}\right), \left(\frac{5}{6}, \frac{1}{2}, \frac{1}{2}\right), \left(\frac{1}{2}, \frac{5}{6}, \frac{1}{2}\right), \left(\frac{1}{2}, \frac{1}{2}, \frac{5}{6}\right)\right\}$, and $\{\wp_{corner,2}\} = \left\{\left(\frac{1}{3}, \frac{1}{2}, \frac{1}{3}\right), \left(\frac{1}{2}, \frac{1}{3}, \frac{1}{3}\right), \left(\frac{1}{2}, \frac{2}{3}, \frac{1}{3}\right), \left(\frac{2}{3}, \frac{1}{2}, \frac{1}{3}\right), \left(\frac{1}{3}, \frac{1}{2}, \frac{2}{3}\right), \left(\frac{1}{2}, \frac{1}{3}, \frac{2}{3}\right), \left(\frac{1}{2}, \frac{2}{3}, \frac{2}{3}\right), \left(\frac{2}{3}, \frac{1}{2}, \frac{2}{3}\right), \left(\frac{1}{3}, \frac{1}{3}, \frac{1}{2}\right), \left(\frac{1}{3}, \frac{2}{3}, \frac{1}{2}\right), \left(\frac{2}{3}, \frac{1}{3}, \frac{1}{2}\right), \left(\frac{2}{3}, \frac{2}{3}, \frac{1}{2}\right)\right\}$. To follow the growth of the Green's function approximation and demonstrate closed loop feedback, use the explicit FDSc of (3.9) through (3.11) to derive the FDSy schematic of Figure 3.6. Thus place a unit source at $Y_k =$
•$y_k = \frac{1}{2}$ such that $\{1, 0, 0, 0\}$. Holding the value of $\widehat{F}(y_k)$ constant; applying (3.9)

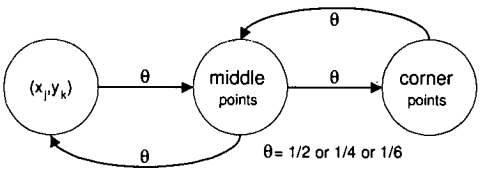

Figure 3.6: Schematic for closed loop feedback

once yields $\left\{1, \frac{1}{2}, 0, 0\right\}$, applying the FDSc a second time yields $\left\{1, \frac{1}{2}, \frac{1}{4}, 0\right\}$, and allowing for closed loop feedback between $\wp_{middle}$ and $\wp_{corner,1}$ yields $\left\{1, \frac{2}{3}, \frac{1}{3}, 0\right\}$. Since $\widehat{F}(y_k)_{n+1}$ is affected by $\widehat{F}(y_k)_n$ and $\widehat{F}(\wp_{middle})$, evaluation gives $\left\{1 + \frac{2}{3}, \frac{2}{3}, \frac{1}{3}, 0\right\}$. Repeating this scheme gives $\widehat{F}(Y_k) = 1 + \frac{2}{3} + \frac{4}{9} + \cdots = \frac{1}{1-\frac{2}{3}} = 3$ and as $N \to \infty$, this yields the relationship, $\widehat{G}_{\Delta x}(k; k-l) = \lfloor \frac{1}{2\Delta x} \rfloor - l$.

$\bullet(x_j, y_k) = \left(\frac{1}{2}, \frac{1}{2}\right)$ such that $\{1, 0, 0, 0\}$. Let $\Delta x = \Delta y$ and holding the value of $\widehat{F}(x_j, y_k)$ constant; applying (3.10) once yields $\left\{1, \frac{1}{4}, 0, 0\right\}$, applying the FDSc a second time yields $\left\{1, \frac{1}{4}, 0, \frac{1}{8}\right\}$, and allowing for closed loop feedback between $\wp_{middle}$ and $\wp_{corner,2}$ yields $\left\{1, \frac{1}{3}, 0, \frac{1}{6}\right\}$. Since $\widehat{F}(x_j, y_k)_{n+1}$ is affected by $\widehat{F}(x_j, y_k)_n$ and $\widehat{F}(\wp_{middle})$, evaluation gives $\left\{1 + \frac{1}{3}, \frac{1}{3}, 0, \frac{1}{6}\right\}$. Repeating this entire scheme with new value of $\widehat{F}(x_j, y_k)$ gives $\widehat{F}(x_j, y_k) = 1 + \frac{1}{3} + \frac{1}{9} + \cdots = \frac{1}{1-\frac{1}{3}} = \frac{3}{2}$. Table 3.1 provides values from $\mathbb{Z}^2$ examples on the unit square, where $\Delta x = \Delta y$ and $\widehat{G}_{\Delta x}(\wp_1, X) = \frac{1}{1-\theta}$. These results are supported by the explicit solutions listed on [45, pages 283-285], where θ is the 'chance of revisiting the point at least once' and truncation errors are listed in [61, Section 2] and [62].

Grid Size	$\widehat{G}_{\Delta x}\left(\lfloor \frac{N}{2} \rfloor, \lfloor \frac{N}{2} \rfloor\right)$	approximate θ	approximate θ
3×3	1	0	0
5×5	$\frac{3}{2}$	$\frac{1}{3}$	0.33333
7×7	1.76923	$\frac{10}{23}$	0.43478
9×9	1.95588	$\frac{21}{43}$	0.48872
17×17	2.40037	$\frac{7}{12}$	0.58340
33×33	2.84243	$\frac{11}{17}$	0.64819
65×65	3.2839	$\frac{32}{46}$	0.69584
129×129	3.72521	$\frac{41}{56}$	0.73156

Table 3.1: Closed loop feedback of $1_{\left(\frac{1}{2}, \frac{1}{2}\right)}$ on a unit square domain using (3.10).

$\bullet(x_j, y_k, z_l) = \left(\frac{1}{2}, \frac{1}{2}, \frac{1}{2}\right)$ such that $\{1, 0, 0, 0\}$. Let $\Delta x = \Delta y = \Delta z$ and holding the value of $\widehat{F}(x_j, y_k, z_l)$ constant; applying (3.11) once yields $\left\{1, \frac{1}{6}, 0, 0\right\}$, applying the FDSc a second time yields $\left\{1, \frac{1}{6}, \frac{1}{36}, \frac{1}{18}\right\}$ and allowing for closed loop feedback as in the previous two examples yields $\widehat{F}(x_j, y_k) = \frac{1}{1-\frac{6}{27}}$, such that $\left\{\frac{27}{21}, \frac{6}{21}, \frac{1}{21}, \frac{2}{21}\right\}$. Similar results hold for the closed loop feedback and differences in the Green's

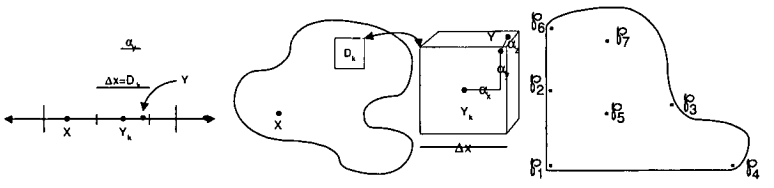

Figure 3.7: Elliptic Problem Set-up

function dependent upon the location within the domain.

Example 3.2.18. *Referring to a uniform* $\mathbb{Z}^1$ *domain and using (3.9),* $\widehat{G}(k;k) - \left(\frac{\widehat{G}(k;k-l)+\widehat{G}(k;k+l)}{2}\right) = l$ *and* $\widehat{G}(\wp_{adjacent};\wp_{adjacent}) \approx 1.9$.
•*Referring to Figure 3.7, on a uniform* $\mathbb{Z}^2$ *domain using a canonical five point FDSc where* $\Delta x = \Delta y$: $\widehat{G}_{\Delta x}(\wp_1;\wp_1) \approx 1.25 \leq \widehat{G}_{\Delta x}(\wp_6;\wp_6) \approx \widehat{G}_{\Delta x}(\wp_4;\wp_4) \leq 1.45 \approx \widehat{G}_{\Delta x}(\wp_2;\wp_2) \leq \widehat{G}_{\Delta x}(\wp_3;\wp_3)$. $\widehat{G}(\wp_5;\wp_{1,2,3,4,6}) \approx 2^{1-\log_2(\max(M,N))}$, $\widehat{G}(\wp_5;\wp_7) = \widehat{G}(\wp_7;\wp_5)$, $\widehat{G}(\wp_7;\wp_7) \leq \widehat{G}(\wp_5;\wp_5) \approx 1-0.44(1-\log_2(\max(M,N)))$, *and* $\widehat{G}(\wp_5;\wp_5) - \widehat{G}\left(\wp_5;\frac{\|\wp_5-[V][\Delta x]\|_1}{\Delta x}\right) \approx K$.
•*Analogous results can be derived for a uniform* $\mathbb{Z}^3$ *domain.*

3.3 Elliptic equations with multiplicative and general noise

Expanding upon (3.1), consider quasi-linear second-order elliptic SPDE's in $\mathbb{R}^d$ with multiplicative and general noise of the canonical form:

$$\nabla^2 F(X) = -\upsilon(F(X),X) - \omega(F(X),X)\dot{W}(X) \tag{3.16}$$

with Dirichlet boundary conditions, where $d \leq 3$ and $\{\upsilon(F(X),X), \omega(F(X),X)\}$ are general functions possibly containing the lower order terms $\{F(X), F'(X)\}$. The $\{d = 1,2,3\}$ respective cases of (3.16) are (3.2) through (3.4) when $w(X)$ of is replaced by $\omega(F(X),X)$ for the general case and $\omega(X)F(X)$ for the multiplicative case. In order for a solution to exist, then $\int_{\mho} \mathbb{E}\left[|\omega(F(X),X)|^2\right] dX < \infty$, but due to singularities introduced via the Brownian sheet and the closed loop feedback of an elliptic system, approximations for (3.16) using white noise and a non-trivial $\omega(F(X),X)$ almost surely do not exist. For example, as $\Delta x \to 0$, $\left|\mathbb{W}(\mathtt{D})\,\mathfrak{M}(\mathtt{D})^{-1}\right|$ is a random variable with a positive probability of being greater than a significant value where singularities of non-zero measure almost surely exist, hence the resulting system is unstable and will almost surely explode from $\omega(X)F(X)$ and $\omega(F(X),X)$ involving functionals of the solution. This fundamental change in the nature of the process explains a lack of literature regarding

existence and uniqueness results, further:

•The Maximum-Minimum Principle and Lemma 3.1.10 are no longer valid.

•Assumption 3.2.1 is invalid, so any FDSc is not symmetric and computational molecules are almost surely not weighted averages.

•The Radiation Principle, Lemma 3.1.23, must be revised due to the functional dependence of the process modifying the Green's function.

•Results are no longer applicable to Neumann and Robin boundary conditions since Neumann boundary conditions yields approximations $\pm K$. Given that $\omega(\cdot)$ is dependent upon $F(\cdot)$ over the entire domain, the K value is no longer arbitrary.

•An iterative FDSc must be relied upon in order to derive approximations.

•The Green's function and Poisson kernel for a multiplicative or general noise system cannot be represented in a closed or functional form.

3.3.1 Finite difference system

The Maximum-Minimum Principle allows one to construct proofs for uniqueness and existence for the deterministic and additive noise processes, but since Lemma 3.1.10 is no longer valid, theoretical results for existence and uniqueness for (3.16) do not exist. Using the canonical elliptic FDSc, (3.11), as a template, refer to Figure 3.3 for a graphical representation of the canonical FDSc2 matrices where computational molecules for (3.16) are expressed as:

$$\widehat{F}_{j,k,l}=\left(\frac{\widehat{F}_{j+1,k,l}+\widehat{F}_{j-1,k,l}}{2\left(1+\lambda_y^2+\lambda_z^2\right)}\right)+\lambda_y^2\left(\frac{\widehat{F}_{j,k+1,l}+\widehat{F}_{j,k-1,l}}{2\left(1+\lambda_y^2+\lambda_z^2\right)}\right)+\lambda_z^2\left(\frac{\widehat{F}_{j,k,l+1}+\widehat{F}_{j,k,l-1}}{2\left(1+\lambda_y^2+\lambda_z^2\right)}\right)$$
$$+\frac{\Delta x^2 v\left(\widehat{F}_{j,k,l},x_j,y_k,z_l\right)}{2\left(1+\lambda_y^2+\lambda_z^2\right)}+\frac{\Delta x\omega\left(\widehat{F}_{j,k,l},x_j,y_k,z_l\right)\mathbb{W}\left(\mathtt{D}_{j,k,l}\right)}{2\left(1+\lambda_y^2+\lambda_z^2\right)\left(1_{d=1}+1_{d=2}\Delta y+1_{d=3}\Delta y\Delta z\right)}. \tag{3.17}$$

Since both $\{v(F(X),X),\omega(F(X),X)\}$ can be functionals of the solution, let $\vartheta 2(j;j)=\vartheta(j;j)+\frac{1}{2\left(1+\lambda_y^2+\lambda_z^2\right)}\left(\Delta x^2\widehat{F}(X_j)^{-1}v\left(\widehat{F}(X_j)_n,X_j\right)\right.$
$\left.+\frac{\Delta x}{\left(1_{d=1}+1_{d=2}\Delta y+1_{d=3}\Delta y\Delta z\right)}\mathbb{W}\left(\mathtt{D}_j\right)\widehat{F}(X_j)^{-1}\omega\left(\widehat{F}(X_j)_n,X_j\right)\right)$ such that

$$[FDSc2]=\begin{bmatrix}\vartheta 2(k;k) & \vartheta(l;k) & \vartheta(m;k) & \\ \vartheta(k;l) & \vartheta 2(l;l) & \vartheta(m;l) & \cdots \\ \vartheta(k;m) & \vartheta(l;m) & \vartheta 2(m;m) & \end{bmatrix}.$$

Notation 3.3.1. *The spectral radius is denoted as* $\mathtt{sr}([FDSc])=\|[|r|]\|_\infty$, *where* $[r]$ *are the eigen values of the matrix* $[FDSc]$.

Remark 3.3.2. *The* $\mathtt{sr}(\cdot)$ *is related to the* l^2 *norm of a matrix such that* $\|[{}_n^nB]\|_2=\sqrt{\mathtt{sr}\left([B^T][B]\right)}$ *and* $\mathtt{sr}([B])\leq\|[B]\|$. *Given a FDSc matrix, the spectral radius*

can be calculated by either direct or numerical methods; for example use [19, Program PWERM91.EXT] for a general matrix and if the matrix is symmetric, use [19, Program SYNPW92.EXT].

The FDSy focus will switch from using the Green's function approximation to an iterative FDSc method involving $\left[\widehat{F}_n\right] = \beth\left(FDSc2, \left[\widehat{F}_{n-1}\right], [F_{\delta\upsilon}]\right)$. The FDSc2 matrix is now a function of Δx, the discretised domain, boundary conditions, driving functionals, and the underlying FDSc; thus numerical approximations may exist and converge iff $\lim_{\Delta x \to 0} \mathtt{sr}\left([FDSc2]\right) < 1$; refer to Proposition 4.1.1. As per Remark 2.1.11 some smoother than white noise stochastic spaces are listed in [35, Chapter 6] and examples of non-pathwise stochastic spaces are found in [39]. If smoother than white noise is utilised, numerical approximations and solutions might exist, but only if singularities are less than a critical value dependent upon the domain, underlying noise, and functionals of the process. Thus, the maximum magnitude of singularities can be bounded such that $\mathtt{sr}\left([FDSc2]\right) < 1$ almost surely. Given that a consistent and stable numerical approximation can be constructed, using refinements of the noise, the limiting case of $\Delta x \to 0$ can be utilised to demonstrate if an approximation is convergent to a finite value which may or may not be the solution.

Often a system will not be applicable without modification, where some author's 'accepted technique' is to subtract a singularity and possibly a neighborhood from the domain, thereby generating a new problem that is numerically well behaved. Otherwise, a local solution can be used if the nature of the singularity is modified or a mesh refinement examining an 'area of infection' can be conducted and used to replace the sub-domain in the original problem. Other methods are applicable, but will not be addressed; refer to [2, pages 414-415].

Chapter 4

Numerical methods for elliptic processes

Refer to Section D.2 for diagrams of numerical approximations to (3.1) and (3.16) with both linear and non-linear boundary conditions.

4.1 Iterative FDSc methods

Since the additive noise FDSc matrices considered are positive definite, this ensures stability with respect to round off errors, thus if a large step size is utilised, where $\mathtt{card}\left(\wp_{\mathbb{Z}^d} \in \mho\right) \leq O\left(100\right)$, use a direct method such as Gaussian elimination to solve the system; refer to [21, page 283]. As the cardinality of the interior points increases, direct methods are often computationally prohibitive due to the sparse FDSc matrices. Thus, iterative methods are 'more efficient' since calculating an inverse of a sparse FDSc matrix often yields a full matrix, which requires substantial computational effort to derive and implement. As depicted in Section 1.2.3 and Figure 1.6, a Picard-Lindelöf iterative method uses the boundary conditions and driving functionals of a process to approximate solutions by repeated 'sweepings' of a FDSc over a discretised domain. When implementing an iterative scheme where $\mathtt{card}\left(\mho\right)$ is large (i.e. $\Delta x \to 0$), it is usually necessary to limit the number of previous approximations stored in memory such that $\mathtt{card}\left(\left\{\left[\widehat{F}\left(X\right)_0\right], \cdots, \left[\widehat{F}\left(X\right)_{j-1}\right]\right\}\right) \leq 3$.

Proposition 4.1.1. *For any* $[A_j]$ *in* $\mathbb{R}^m$, *the sequence* $[A_{n+1}] = [B]\,[A_n] + [K]$ *converges to the unique solution* $[A_\infty] = [B]\,[A_\infty] + [K]$, *when* $\mathtt{sr}\left(B\right) < 1$.

Proof. Refer to [19, page 255]. □

Remark 4.1.2. *As per standard series convergence, the system is absolutely convergent when* $\mathtt{sr}\left(FDSc\right) < 1$; *hence Assumption 3.2.1 for (3.1). The successive approximations can be roughly viewed as a geometric series; refer to [37].*

When implementing an iterative FDSc, one of the most important factors for determining the accuracy of the system is the value of $\mathfrak{es}$ that will be utilised to terminate the iterations. From Notation 1.2.4, an iterative FDSc will discontinue when $\mathfrak{es}(X_j) \geq \left|\widehat{F}_{\Delta x}(X_j)_n - \widehat{F}_{\Delta x}(X_j)_{n-1}\right|$. Hence $\mathfrak{es}$ is directly related to the global error and indirectly proportional to the computational effort required before a Picard-Lindelöf iteration method terminates. Due to the Green's function, the accuracy imparted by a given $\mathfrak{es} \lll 1$ is domain dependent, but as a general rule, $\mathfrak{eg}\left(\widehat{F}(X)\right) \approx O\left(\sqrt{\mathfrak{es}}\right)$; refer to Example 4.1.3. Due to the accuracy of an estimate being dependent upon $\mathfrak{es}$, the domain, Δx, computational molecule utilised, boundary conditions, error along the boundary, and how one measures error (at a point, average over a domain, maximum over a domain), deriving a comprehensive numerical rate of convergence is often an ill defined task.

Example 4.1.3. *Approximate a deterministic Laplace equation on a* 25×25 *unit square using a Jacobi method with FDSc = (3.10),* $F_{\delta\mho}(X) = 1.0$*, and an initial guess of 0 along the interior. Given* $\mathfrak{es} = \frac{1}{10{,}000}$*, the scheme terminates once* $\max_{X \in \mho}\left(\left|\widehat{F}(X)_n - \widehat{F}(X)_{n-1}\right|\right) = 9.84831 \times 10^{-5}$*; yielding Figure 4.1.*

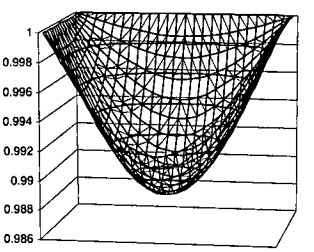

Figure 4.1: Refer to Example 4.1.3: $\sqrt{\mathfrak{es}} = 0.01$

$$\frac{\partial^2 F(x,y)}{\partial x^2} + \frac{\partial^2 F(x,y)}{\partial y^2} = -\frac{\partial^2 W(x,y)}{\partial x \partial y} \tag{4.1}$$

Example 4.1.4. *Approximating (4.1) on a unit square domain where* $\lambda_y = 1$ *and* $F_{\delta\mho}(x,y) = 1$*, let* $\left[\widehat{F}_{\dagger}\right] = \widehat{F}\left((3.10), \Delta x = \frac{1}{513}, \mathfrak{es} = 5 \times 10^{-12}\right)$ *be the 'numerical solution.' The errors listed in the following tables suggest a ratio of* $\sqrt{2}$ *and thus a numerical rate of convergence of* $\widehat{\mathrm{RC}}(\cdot) = \frac{1}{2}$*, similar to the results of Chapter 2. Due to the choice of the domain and boundary conditions, this result is not surprising and represents a 'best case' scenario. As previously mentioned, the error introduced along the boundary plays the significant role in determining the error within the domain, thus this error has been eliminated in this system.*

$\mathbb{Z}^2_{\Delta x}$	Grid mesh $(M \times M)$	$\chi^2(X)$	$\overline{\mathfrak{eg}(X)}$	$\max_{X_j \in \mho} (\mathfrak{eg}(X_j))$
$\Delta x = \frac{1}{128}$	(129×129)	$4.43E-06$	$2.56E-04$	$1.50E-03$
$\Delta x = \frac{1}{64}$	(65×65)	$2.66E-04$	$3.54E-03$	$1.88E-02$
$\Delta x = \frac{1}{32}$	(33×33)	$4.29E-04$	$5.01E-03$	$2.38E-02$
$\Delta x = \frac{1}{16}$	(17×17)	$9.34E-04$	$8.51E-03$	$3.42E-02$
$\Delta x = \frac{1}{8}$	(9×9)	$1.38E-03$	$9.39E-03$	$7.38E-02$
$\Delta x = \frac{1}{4}$	(5×5)	$1.37E-03$	$8.96E-03$	$3.65E-02$
$\Delta x = \frac{1}{2}$	(3×3)	$2.02E-03$	$6.69E-03$	$6.02E-02$

Table 4.1: $\mathfrak{eg} = \left|\widehat{F}\left((3.10), \mathfrak{es} = 1 \times 10^{-10}\right) - \widehat{F}_{\dagger}\right|$

$\mathbb{Z}^2_{\Delta x}$	Grid mesh $(M \times M)$	$\chi^2(X)$	$\overline{\mathfrak{eg}(X)}$	$\max_{X_j \in \mho} (\mathfrak{eg}(X_j))$
$\Delta x = \frac{1}{128}$	(129×129)	$4.71E-07$	$1.25E-04$	$5.64E-03$
$\Delta x = \frac{1}{64}$	(65×65)	$3.14E-04$	$3.65E-03$	$1.93E-02$
$\Delta x = \frac{1}{32}$	(33×33)	$5.04E-04$	$5.29E-03$	$2.65E-02$
$\Delta x = \frac{1}{16}$	(17×17)	$1.13E-03$	$9.31E-03$	$4.58E-02$
$\Delta x = \frac{1}{8}$	(9×9)	$1.83E-03$	$1.02E-02$	$8.78E-02$
$\Delta x = \frac{1}{4}$	(5×5)	$1.84E-03$	$9.73E-03$	$4.60E-02$
$\Delta x = \frac{1}{2}$	(3×3)	$3.55E-03$	$8.88E-03$	$7.99E-02$

Table 4.2: $\left|\widehat{F}\left((3.13), \mathfrak{es} = 1 \times 10^{-10}\right) - \widehat{F}_{\dagger}\right|$

Remark 4.1.5. *For the aforementioned tables, $\chi^2(X)$ is a standard Pearson Chi-square statistic, $\overline{\mathfrak{eg}(X)}$ denotes the average error over the interior, and $\max_{X_j \in \mho}(\mathfrak{eg}(X_j))$ denotes the maximum error over the grid.*

4.1.0.1 Jacobi iterative method

Often called the 'Method of Simultaneous Displacements,' the Jacobi iterative method dates to the late eighteenth century and is applicable to systems involving large sparse matrices. The Jacobi method is the benchmark FDSc by which all other iterative systems are measured and is constructed as follows. Let $[A]$ $= [A_{diag}] - [A_{low}] - [A_{up}]$, where $[A_{diag}] = \begin{bmatrix} a_{1,1} & 0 & \cdots & 0 \\ 0 & a_{2,2} & 0 & \ddots \\ \ddots & 0 & \ddots & 0 \\ 0 & \cdots & 0 & a_{n,n} \end{bmatrix}$,

$[A_{low}] = \begin{bmatrix} 0 & 0 & \cdots & 0 \\ a_{2,1} & 0 & \ddots & 0 \\ \ddots & \ddots & 0 & 0 \\ a_{n,1} & \cdots & a_{n,n-1} & 0 \end{bmatrix}$, and $[A_{up}] = \begin{bmatrix} 0 & a_{1,2} & \cdots & a_{1,n} \\ \ddots & 0 & \ddots & \ddots \\ 0 & \cdots & 0 & a_{n-1,n} \\ 0 & \cdots & 0 & 0 \end{bmatrix}$.

Transform $[A]\left[\widehat{F}(X)\right] = [B]$ into $[A_{diag}]\left[\widehat{F}(X)_n\right] = ([A_{low}] + [A_{up}]) \times \left[\widehat{F}(X)_{n-1}\right]$ $+ [B]$. If $a_{j,j} \neq 0$ for all $j \in [1, n]$ then $\left[A_{diag}^{-1}\right]$ exists and $\left[\widehat{F}(X)_n\right]$ $= \left[A_{diag}^{-1}\right]([A_{low}] + [A_{up}])\left[\widehat{F}(X)_{n-1}\right] + \left[A_{diag}^{-1}\right][B]$ or simply $\left[\widehat{F}(X)_n\right] = [FDSc]$ $\times \left[\widehat{F}(X)_{n-1}\right] + [B_2]$. Approximations using this system are repeatedly cycled until $\mathfrak{es} \geq \max_{X_j \in \{\mho \cap \mathbb{Z}^d\}} \left(\left[\left| \widehat{F}_{\Delta x}(X_j)_n - \widehat{F}_{\Delta x}(X_j)_{n-1} \right| \right] \right)$, yielding an approximation.

4.1.0.2 Gauss-Seidel method

Often called the Liebmann method, improvement can be made to the Jacobi method by utilising current approximations to the grid immediately after they have been calculated. Hence, $\left[\widehat{F}(X)_{n+1}\right] = [FDSc]\left[\widehat{F}(X)_{n+\frac{1}{2}}\right] + [B]$, where $\left[\widehat{F}(X)_{n+\frac{1}{2}}\right]$ is the matrix storing the newly estimated $\widehat{F}(X)_{n+1}$ values and the remaining $\widehat{F}(X)_n$ values. The Gauss-Seidel method not only converges approximately twice as fast as the Jacobi method, but it also requires less storage space since only one approximation grid is retained in memory.

Lemma 4.1.6. *If a FDSc matrix is irreducible; i.e. diagonally dominant with at least one row being strictly diagonally dominant, then the Jacobi and Gauss-Seidel methods are convergent.*

Proof. Refer to [57, pages 299-300]. □

4.1.0.3 Simultaneous Relaxation Methods

Improving on the Jacobi method, use $((1-\alpha)[A_{diag}]+\alpha[A_{up}])\left[\widehat{F}(X)_n\right]+\alpha[B]$ $=([A_{diag}]+\alpha[A_{low}])\left[\widehat{F}(X)_{n+1}\right]$ to produce successive approximations. When $\alpha \in (0,1)$ the FDSy is called an 'successive under-relaxation' method and when $a>1$ the FDSy is called an 'successive over-relaxation' method, otherwise known as a SOR method. Although not often used, successive under-relaxation methods are useful in systems with singularities where other numerical methods do not easily converge or explode. Various authors have derived 'optimal' SOR α values dependent upon the FDSc, the shape of the domain, roughness of the boundary, and internal noise. Values such as $\alpha \approx \frac{2}{1+K\Delta x}$ or $\alpha \approx \frac{2}{1+\frac{r\Delta x}{\sqrt{2}}}$ are often used, where r is the minimum eigen value of the deterministic system.

Example 4.1.7. *When performing an SOR using the Jacobi method matrix on a rectangular domain, then* $\mathtt{sr}\left(\left[A_{diag}^{-1}\right]([A_{low}]+[A_{up}])\right)=\frac{1}{2}\left(\cos\left(\frac{\pi\Delta x}{L_x}\right)+\cos\left(\frac{\pi\Delta y}{L_y}\right)\right)$ *and for optimal SOR results, let* $\alpha=\frac{2}{1+\sqrt{1-\mathtt{sr}(\cdot)^2}}$. *[19, Section 12.2]*

4.1.0.4 Richardson Method

Given that the FDSc is a positive definite matrix, systems can be rewritten in the form $\left[\widehat{F}(X)_{n+1}\right]=\left[\widehat{F}(X)_n\right]+\alpha_n\left([B]-[A_2]\left[\widehat{F}(X)_n\right]\right)$ where α_n is chosen to accelerate the convergence properties of the system. Refer to [62, Section 5] and [21, Section 21.5] for an introduction to this method. Although this method is important, it is rarely utilised in practice.

4.1.0.5 Alternating Direction Iteration (ADI) Method

The Peaceman-Rachford or ADI method involves two implicit variations of the Richardson Method where $[A]=[A_{hor}]+[A_{ver}]$ yields a Predictor-Corrector
$\left[\widehat{F}(X)_{n+\frac{1}{2}}\right]=\left[\widehat{F}(X)_n\right]+\alpha_n\left([A_{hor}]\left[\widehat{F}(X)_{n+\frac{1}{2}}\right]+[A_{ver}]\left[\widehat{F}(X)_n\right]-[B]\right)$
$\left[\widehat{F}(X)_{n+1}\right]=\left[\widehat{F}(X)_{n+\frac{1}{2}}\right]+\beta_n\left([A_{hor}]\left[\widehat{F}(X)_{n+\frac{1}{2}}\right]+[A_{ver}]\left[\widehat{F}(X)_{n+1}\right]-[B]\right)$.
When using a rectangular domain, significant improvements can be realized over the previous methods since the implicit steps are closely related to a direct substitution method and the eigen values of $[A_{hor}]$ and $[A_{ver}]$ are often radically different. Unfortunately the improvement of this method often fails in non-rectangular domains since the scheme is implemented with non-optimal parameters $\{\alpha_n,\beta_n\}$ due to the arbitrary geometry of the domain. Implementations of this scheme on a variety of domains will not be addressed; refer to works by Herbert Stone.

4.1.0.6 Method of Lines

Another method utilised, with various degrees of success, discretises a space dimension using N divisions and leave the other dimensions continuous. When suitable expressions are substituted, the SPDE is converted into a coupled system of SDE's; i.e. difference - differential equations. Using this method on a computer, one also tends to discretise the remaining space dimensions using M discretisations where $M \lll N$. By definition, this will fulfill the requirements for a uniform $\mathbb{Z}^d$ space, but the magnitudes of $\{\Delta x, \Delta y, \Delta z\}$ force $\lim_{\Delta x \to 0} \lambda \to \{0 \text{ or } \infty\}$.

4.1.0.7 Hackbusch Multi-Grid Method

The most computationally efficient methods that exist today involve the multigrid iterations of Dr. Wolfgang Hackbusch. Although the subtleties and mathematics of these methods are quite beautiful, a discussion will be omitted. To implement this system, define several uniform $\mathbb{Z}^d_{j\Delta x}$ spaces where $j \in \{1, 2, \cdots, o\}$. Since numerical methods are fast for domains of small cardinality, initially approximate for a coarse $\mathbb{Z}^d_{o\Delta x}$ grid then repeatedly 'bounce' between refinement levels using predetermined 'jump' criteria to yield a final $\mathbb{Z}^d_{\Delta x}$ approximation. Using these recursive refinements, this method provides a computationally efficient means for deriving an approximation; refer to [26] or [27, Chapter 4].

4.1.0.8 Other methods

Related to the Method of Lines, [5] uses a rather ingenious Stochastic Monte-Carlo method by performing a random walk over a $\mathbb{R}^d$ domain to derive an approximation to a solution at a point. This has the highly desirable effect that the only error introduced to the approximation is a statistical sampling error, which decreases as the number of Monte-Carlo paths increases. By statistically accounting for the propagation of disturbances in all space dimensions, this approach provides a powerful tool for researchers where computational time is of secondary concern to approximation accuracy. Using the results of [5], [6] this method can be expanded to approximate the entire domain where:

> ... the technique may be applied in any separable coordinate system. Thus, the technique can easily be generalized into N dimensions; in general, Monte Carlo methods become more competitive with deterministic methods as the dimension and complexity increase.

If one is modeling a process with complicated boundary conditions this method is in fact more than 'competitive' to other methods, it is often superior.

FESy methods are often more efficient than FDSy methods for their ability to handle errors introduced at the boundary. Thus, refer to [19, Program LINFE125.EXT] for a FESy method approximating the $d = 2$ Poisson elliptic equation and [1] for a discussion of the benefits FESy methods exhibit for some elliptic problems.

4.1.0.9 Symmetry considerations

In order to account for the 'instantaneous propagation' of disturbances in all space dimensions; it is best to 'mix things up' and avoid problems from iterating a domain in only one direction or pattern. For example, let $\mho$ be a $\mathbb{R}^2$ unit square with corner points $(0,0)$ and $(1,1)$; refer to Figures 4.1 and 4.2. Thus, when approximating using an iterative method, one should start at the corner point:

A. $(0,0)$ and proceed in the positive x and positive y direction.

B. $(1,1)$ and proceed in the negative x and negative y direction.

C. $(1,0)$ and proceed in the positive y and negative x direction.

D. $(0,1)$ and proceed in the negative y and positive x direction.

In doing so, initial conditions are allowed to propagate in all space directions without a 'wind effect' being forced on the system. The geometry of the domain is crucial since there often exists a natural symmetry that can be exploited. Thus, only a subset of the domain's discretized points need to be evaluated to approximate the entire domain; i.e. reduce a $\texttt{card}\,(\mho) = N$ system to a $\texttt{card}\,(\mho) = \frac{N}{m}$ system, where m is the number of symmetries inherent in the domain.

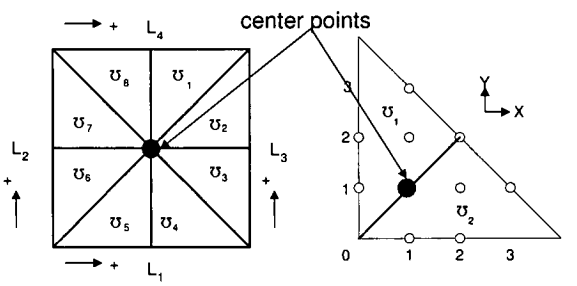

Figure 4.2: A symmetric rectangular domain

Example 4.1.8. *Considering the square domain of Figure 4.2, only the triangular sub-domain $\mho_1$ must be approximated, since the remaining sub-domains are either rotations or reflections of $\mho_1$. Thus, only one eighth of the interior points must be approximated. Estimating the Laplace equation yields:*

$$\left[\widehat{F}\left(\wp_{\mho_1}\right)\right] = \left[\widehat{H}\left(\cdot\right)\right]\times[+L_1 + L_2 + L_3 + L_4],\ \left[\widehat{F}\left(\wp_{\mho_2}\right)\right] = \left[\widehat{H}\left(\cdot\right)\right]\times[+L_2 + L_1 + L_4 + L_3]$$

$$\left[\widehat{F}\left(\wp_{\mho_3}\right)\right] = \left[\widehat{H}\left(\cdot\right)\right]\times[-L_2 + L_4 + L_1 - L_3],\ \left[\widehat{F}\left(\wp_{\mho_4}\right)\right] = \left[\widehat{H}\left(\cdot\right)\right]\times[+L_4 - L_2 - L_3 + L_1]$$

$$\left[\widehat{F}\left(\wp_{\mho_5}\right)\right] = \left[\widehat{H}\left(\cdot\right)\right]\times[-L_4 - L_3 - L_2 - L_1],\ \left[\widehat{F}\left(\wp_{\mho_6}\right)\right] = \left[\widehat{H}\left(\cdot\right)\right]\times[-L_3 - L_4 - L_1 - L_2]$$
$$\left[\widehat{F}\left(\wp_{\mho_7}\right)\right] = \left[\widehat{H}\left(\cdot\right)\right]\times[+L_3 - L_1 - L_4 + L_2],\ \left[\widehat{F}\left(\wp_{\mho_8}\right)\right] = \left[\widehat{H}\left(\cdot\right)\right]\times[-L_1 + L_3 + L_2 - L_4].$$

Similar rotations and reflections apply for the Green's function when estimating the stochastic Poisson equation.

4.2 Numerical examples

To demonstrate how a FDSc matrix is derived and used to formulate a FDSy matrix, consider the following well posed process

$$\frac{\partial^2 F\left(x,y\right)}{\partial x^2} + \frac{\partial^2 F\left(x,y\right)}{\partial y^2} = -\upsilon\left(F\left(x,y\right),x,y\right) - \omega\left(x,y\right)\frac{\partial^2 W\left(x,y\right)}{\partial x \partial y}. \tag{4.2}$$

The domain for this system is depicted in Figures 4.2 and 4.3, where utilising the symmetry of the domain, the Green's function and Poisson kernel values for $\widehat{F}_{1,2}$ also yield $\widehat{F}_{2,1}$. A FDSc is built using $\left\{(3.10), \Delta x = \Delta y, \lambda_y = 1, \vartheta = \frac{1}{4}\right\}$ such that

$$\widehat{F}_{j,k} = \frac{\widehat{F}_{j+1,k} + \widehat{F}_{j-1,k} + \widehat{F}_{j,k+1} + \widehat{F}_{j,k-1}}{4} + \frac{\Delta x^2}{4}\upsilon\left(\widehat{F}_{j,k}, x_j, y_k\right) + \frac{\omega\left(x_j, y_k\right)}{4}\mathbb{W}\left(\mathtt{D}_{j,k}\right). \tag{4.3}$$

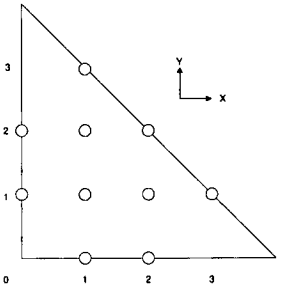

Figure 4.3: Triangular domain for example

4.2.1 FDSc matix

In order to construct the FDSc matrix, utilise (1.10) and (4.3) to yield:

$$\begin{bmatrix} \widehat{F}\left(\wp_{\mho}\right)_n \\ F\left(\wp_{\delta\mho}\right) \end{bmatrix} = \begin{bmatrix} FDSc_{\mho} & FDSc_{\delta\mho} \\ 0 & I \end{bmatrix}\begin{bmatrix} \widehat{F}\left(\wp_{\mho}\right)_{n-1} \\ F\left(\wp_{\delta\mho}\right) \end{bmatrix} + \tfrac{1}{4}\left(\Delta x^2\left[\upsilon\left(\cdot\right)\right] + \left[\mathbb{W}\left(\cdot\right)\right]\left[\omega\left(\cdot\right)\right]\right).$$

Thus, the canonical five point FDSc of (4.3) will be of the form,

$$
\begin{bmatrix} \widehat{F}_{1,2} \\ \widehat{F}_{1,1} \\ \widehat{F}_{2,1} \\ F_{1,0} \\ F_{2,0} \\ F_{3,1} \\ F_{2,2} \\ F_{1,3} \\ F_{0,2} \\ F_{0,1} \end{bmatrix}
= \tfrac{1}{4}
\left[\begin{array}{ccc|ccccccc}
0 & 1 & 0 & 0 & 0 & 0 & 1 & 1 & 1 & 0 \\
1 & 0 & 1 & 1 & 0 & 0 & 0 & 0 & 0 & 1 \\
0 & 1 & 0 & 0 & 1 & 1 & 1 & 0 & 0 & 0 \\
\hline
0 & 0 & 0 & 4 & 0 & 0 & 0 & 0 & 0 & 0 \\
0 & 0 & 0 & 0 & 4 & 0 & 0 & 0 & 0 & 0 \\
0 & 0 & 0 & 0 & 0 & 4 & 0 & 0 & 0 & 0 \\
0 & 0 & 0 & 0 & 0 & 0 & 4 & 0 & 0 & 0 \\
0 & 0 & 0 & 0 & 0 & 0 & 0 & 4 & 0 & 0 \\
0 & 0 & 0 & 0 & 0 & 0 & 0 & 0 & 4 & 0 \\
0 & 0 & 0 & 0 & 0 & 0 & 0 & 0 & 0 & 4
\end{array}\right]
\begin{bmatrix} \widehat{F}_{1,2} \\ \widehat{F}_{1,1} \\ \widehat{F}_{2,1} \\ F_{1,0} \\ F_{2,0} \\ F_{3,1} \\ F_{2,2} \\ F_{1,3} \\ F_{0,2} \\ F_{0,1} \end{bmatrix}
$$

$$
+\tfrac{1}{4}\Delta x^2
\begin{bmatrix}
\upsilon\left(\widehat{F}_{1,2}, \Delta x, 2\Delta y\right) \\
\upsilon\left(\widehat{F}_{1,1}, \Delta x, \Delta y\right) \\
\upsilon\left(\widehat{F}_{2,1}, 2\Delta x, \Delta y\right) \\
0 \\
\ddots \\
0
\end{bmatrix}
$$

$$
+\tfrac{1}{4}
\begin{bmatrix}
\mathbb{W}(\mathtt{D}_{1,2}) & 0 & 0 & 0 & 0 & 0 & 0 & 0 & 0 & 0 \\
0 & \mathbb{W}(\mathtt{D}_{1,1}) & 0 & 0 & 0 & 0 & 0 & 0 & 0 & 0 \\
0 & 0 & \mathbb{W}(\mathtt{D}_{2,1}) & 0 & 0 & 0 & 0 & 0 & 0 & 0 \\
 & \ddots & & & & & \ddots & & & \\
 & 0 & & & & & 0 & & &
\end{bmatrix}
\begin{bmatrix}
\omega\left(\Delta x, 2\Delta y\right) \\
\omega\left(\Delta x, \Delta y\right) \\
\omega\left(2\Delta x, \Delta y\right) \\
0 \\
\ddots \\
0
\end{bmatrix}
$$

which is often stated as

$$
\begin{bmatrix} \widehat{F}_{1,2} \\ \widehat{F}_{1,1} \\ \widehat{F}_{2,1} \end{bmatrix}
= \tfrac{1}{4}
\begin{bmatrix}
0 & 1 & 0 & 0 & 0 & 0 & 1 & 1 & 1 & 0 \\
1 & 0 & 1 & 1 & 0 & 0 & 0 & 0 & 0 & 1 \\
0 & 1 & 0 & 0 & 1 & 1 & 1 & 0 & 0 & 0
\end{bmatrix}
\begin{bmatrix} \widehat{F}_{1,2} \\ \widehat{F}_{1,1} \\ \widehat{F}_{2,1} \\ F_{1,0} \\ F_{2,0} \\ F_{3,1} \\ F_{2,2} \\ F_{1,3} \\ F_{0,2} \\ F_{0,1} \end{bmatrix}
$$

$$
+\tfrac{1}{4}
\begin{bmatrix}
\Delta x^2 \upsilon\left(\widehat{F}_{1,2}, \Delta x, 2\Delta y\right) + \mathbb{W}(\mathtt{D}_{1,2})\, \omega\left(\Delta x, 2\Delta y\right) \\
\Delta x^2 \upsilon\left(\widehat{F}_{1,1}, \Delta x, \Delta y\right) + \mathbb{W}(\mathtt{D}_{1,1})\, \omega\left(\Delta x, \Delta y\right) \\
\Delta x^2 \upsilon\left(\widehat{F}_{2,1}, 2\Delta x, \Delta y\right) + \mathbb{W}(\mathtt{D}_{2,1})\, \omega\left(2\Delta x, \Delta y\right)
\end{bmatrix}.
$$

4.2.1.1 FDSc → FDSy

Subtract $\begin{bmatrix} \widehat{F}\left(\wp_{\mho}\right)_n \\ F\left(\wp_{\delta\mho}\right) \end{bmatrix}$ from both sides of the FDSc matrix to yield:

$$[0] = \tfrac{1}{4}\begin{bmatrix} -4 & 1 & 0 & 0 & 0 & 0 & 1 & 1 & 1 & 0 \\ 1 & -4 & 1 & 1 & 0 & 0 & 0 & 0 & 0 & 1 \\ 0 & 1 & -4 & 0 & 1 & 1 & 1 & 0 & 0 & 0 \\ 0 & 0 & 0 & 4-4 & 0 & 0 & 0 & 0 & 0 & 0 \\ 0 & 0 & 0 & 0 & 4-4 & 0 & 0 & 0 & 0 & 0 \\ 0 & 0 & 0 & 0 & 0 & 4-4 & 0 & 0 & 0 & 0 \\ 0 & 0 & 0 & 0 & 0 & 0 & 4-4 & 0 & 0 & 0 \\ 0 & 0 & 0 & 0 & 0 & 0 & 0 & 4-4 & 0 & 0 \\ 0 & 0 & 0 & 0 & 0 & 0 & 0 & 0 & 4-4 & 0 \\ 0 & 0 & 0 & 0 & 0 & 0 & 0 & 0 & 0 & 4-4 \end{bmatrix}\begin{bmatrix} \widehat{F}_{1,2} \\ \widehat{F}_{1,1} \\ \widehat{F}_{2,1} \\ F_{1,0} \\ F_{2,0} \\ F_{3,1} \\ F_{2,2} \\ F_{1,3} \\ F_{0,2} \\ F_{0,1} \end{bmatrix}$$

$$+\tfrac{1}{4}\begin{bmatrix} \Delta x^2 \upsilon\left(\widehat{F}_{1,2}, \Delta x, 2\Delta y\right) + \mathbb{W}\left(\mathtt{D}_{1,2}\right)\omega\left(\Delta x, 2\Delta y\right) \\ \Delta x^2 \upsilon\left(\widehat{F}_{1,1}, \Delta x, \Delta y\right) + \mathbb{W}\left(\mathtt{D}_{1,1}\right)\omega\left(\Delta x, \Delta y\right) \\ \Delta x^2 \upsilon\left(\widehat{F}_{2,1}, 2\Delta x, \Delta y\right) + \mathbb{W}\left(\mathtt{D}_{2,1}\right)\omega\left(2\Delta x, \Delta y\right) \end{bmatrix}.$$

Given the small size of the domain, reduction via the direct method of Gaussian elimination yields:

$$[0] = \tfrac{1}{56}\begin{bmatrix} -56 & 0 & 0 & 4 & 1 & 1 & 16 & 15 & 15 & 4 \\ 0 & -56 & 0 & 16 & 4 & 4 & 8 & 4 & 4 & 16 \\ 0 & 0 & -56 & 4 & 15 & 15 & 16 & 1 & 1 & 4 \end{bmatrix}\begin{bmatrix} \widehat{F}_{1,2} \\ \widehat{F}_{2,1} \\ \widehat{F}_{1,1} \\ F_{1,0} \\ F_{2,0} \\ F_{3,1} \\ F_{2,2} \\ F_{1,3} \\ F_{0,2} \\ F_{0,1} \end{bmatrix}$$

$$+\tfrac{1}{56}\begin{bmatrix} 60 & 16 & 4 \\ 16 & 64 & 16 \\ 4 & 16 & 60 \end{bmatrix}\begin{bmatrix} \Delta x^2 \upsilon\left(\widehat{F}_{1,2}, \Delta x, 2\Delta y\right) + \omega\left(\Delta x, 2\Delta y\right)\mathbb{W}\left(\mathtt{D}_{1,2}\right) \\ \Delta x^2 \upsilon\left(\widehat{F}_{1,1}, \Delta x, \Delta y\right) + \omega\left(\Delta x, \Delta y\right)\mathbb{W}\left(\mathtt{D}_{1,1}\right) \\ \Delta x^2 \upsilon\left(\widehat{F}_{2,1}, 2\Delta x, \Delta y\right) + \omega\left(2\Delta x, \Delta y\right)\mathbb{W}\left(\mathtt{D}_{2,1}\right) \end{bmatrix}$$

or simply $\begin{bmatrix} \widehat{F}_{1,2} \\ \widehat{F}_{1,1} \\ \widehat{F}_{2,1} \end{bmatrix} = \tfrac{1}{56}\begin{bmatrix} 4 & 1 & 1 & 16 & 15 & 15 & 4 \\ 16 & 4 & 4 & 8 & 4 & 4 & 16 \\ 4 & 15 & 15 & 16 & 1 & 1 & 4 \end{bmatrix}\begin{bmatrix} F_{1,0} \\ F_{2,0} \\ F_{3,1} \\ F_{2,2} \\ F_{1,3} \\ F_{0,2} \\ F_{0,1} \end{bmatrix}$

$$+\tfrac{1}{56}\begin{bmatrix} 60 & 16 & 4 \\ 16 & 64 & 16 \\ 4 & 16 & 60 \end{bmatrix}\begin{bmatrix} \Delta x^2 \upsilon\left(\widehat{F}_{1,2}, \Delta x, 2\Delta y\right) + \omega\left(\Delta x, 2\Delta y\right)\mathbb{W}\left(\mathtt{D}_{1,2}\right) \\ \Delta x^2 \upsilon\left(\widehat{F}_{1,1}, \Delta x, \Delta y\right) + \omega\left(\Delta x, \Delta y\right)\mathbb{W}\left(\mathtt{D}_{1,1}\right) \\ \Delta x^2 \upsilon\left(\widehat{F}_{2,1}, 2\Delta x, \Delta y\right) + \omega\left(2\Delta x, \Delta y\right)\mathbb{W}\left(\mathtt{D}_{2,1}\right) \end{bmatrix}$$ it is eas-

ily verified that the above FDSy can also derived by iterating the FDSc matrix.

4.2.2 Green's Function

The discretised Green's function is $\left[\widehat{G}(\cdot)\right] = \frac{1}{56}\begin{bmatrix} 60 & 16 & 4 \\ 16 & 64 & 16 \\ 4 & 16 & 60 \end{bmatrix}$. As expected from Lemma 3.1.23, these values can also be generated by placing a unit source at the respective interior points and estimate the Laplace equation $\{\upsilon(\cdot) = 0, \omega(\cdot) = 0\}$ with $F_{\delta\upsilon}(X) = 0$ boundary conditions. Thus, approximating the simplified system yields:

$$\begin{bmatrix} \widehat{F}_{1,2} \\ \widehat{F}_{1,1} \\ \widehat{F}_{2,1} \end{bmatrix}_n = \frac{1}{4}\begin{bmatrix} 0 & 1 & 0 & 0 & 0 & 0 & 1 & 1 & 1 & 0 \\ 1 & 0 & 1 & 1 & 0 & 0 & 0 & 0 & 0 & 1 \\ 0 & 1 & 0 & 0 & 1 & 1 & 1 & 0 & 0 & 0 \end{bmatrix} \begin{bmatrix} \widehat{F}_{1,2} \\ \widehat{F}_{1,1} \\ \widehat{F}_{2,1} \\ 0 \\ \ddots \\ 0 \end{bmatrix}_{n-1} + [0].$$

Thus, $\begin{bmatrix} \widehat{F}_{1,2} \\ \widehat{F}_{1,1} \\ \widehat{F}_{2,1} \end{bmatrix}_n = \frac{1}{4}\begin{bmatrix} 0 & 1 & 0 \\ 1 & 0 & 1 \\ 0 & 1 & 0 \end{bmatrix} \begin{bmatrix} \widehat{F}_{1,2} \\ \widehat{F}_{1,1} \\ \widehat{F}_{2,1} \end{bmatrix}_{n-1}$ which implies $\left[\widehat{F}_n\right] = [FDSc]\left[\widehat{F}_{n-1}\right]$ or simply $\left[\widehat{G}(\cdot)_{n+1}\right] = [FDSc_{\mho}]\left[\widehat{G}(\cdot)_n\right]$. To derive the $\left[\widehat{G}(1,1;j,k)\right]$ vector, place a unit source at $(\Delta x, \Delta y)$ and iterate the scheme

$$\begin{bmatrix} \widehat{G}(1,1;1,2)_{n+1} \\ \widehat{G}(1,1;1,1)_{n+1} + 1 \\ \widehat{G}(1,1;2,1)_{n+1} \end{bmatrix} = \frac{1}{4}\begin{bmatrix} 0 & 1 & 0 \\ 1 & 0 & 1 \\ 0 & 1 & 0 \end{bmatrix} \begin{bmatrix} \widehat{G}(1,1;1,2)_n \\ \widehat{G}(1,1;1,1)_n + 1 \\ \widehat{G}(1,1;2,1)_n \end{bmatrix} \text{ such that}$$

$$\frac{1}{4}\begin{bmatrix} 0 & 1 & 0 \\ 1 & 0 & 1 \\ 0 & 1 & 0 \end{bmatrix} \begin{bmatrix} 0 \\ 0+1 \\ 0 \end{bmatrix} = \begin{bmatrix} \frac{1}{4} \\ 1 \\ \frac{1}{4} \end{bmatrix} \rightarrow \frac{1}{4}\begin{bmatrix} 0 & 1 & 0 \\ 1 & 0 & 1 \\ 0 & 1 & 0 \end{bmatrix} \begin{bmatrix} \frac{1}{4} \\ 1 \\ \frac{1}{4} \end{bmatrix} = \begin{bmatrix} \frac{1}{4} \\ \frac{1}{8}+1 \\ \frac{1}{4} \end{bmatrix},$$

which eventually yields the middle row of the Green's function matrix $\begin{bmatrix} \frac{16}{56} \\ \frac{8}{56}+1 \\ \frac{16}{56} \end{bmatrix} = \begin{bmatrix} \frac{16}{56} \\ \frac{64}{56} \\ \frac{16}{56} \end{bmatrix}$. The other Green's function matrix rows can be derived by placing a unit source at $(1,2)$ and $(2,1)$.

4.2.2.1 Discretised Poisson kernel

The discretised Poisson kernel is: $\left[\widehat{H}(\cdot)\right] = \frac{1}{56}\begin{bmatrix} 4 & 1 & 1 & 16 & 15 & 15 & 4 \\ 16 & 4 & 4 & 8 & 4 & 4 & 16 \\ 4 & 15 & 15 & 16 & 1 & 1 & 4 \end{bmatrix}$. Once the discretised Green's function is established, the discretised Poisson kernel is a direct consequence of the $\widehat{G}(\cdot)$ values along the adjacent points of the domain. By definition, $[G(\wp_{\delta\mho})] = 0$, thus adjacent points must be utilised to normalize the boundary conditions. From (4.3), $\vartheta(\cdot) = \vartheta = \frac{1}{4}$ and $\Upsilon(1,1)$
$= \sum \widehat{G}(\wp_{(1,1)}; \wp_j) = \widehat{G}_{1,0} + \widehat{G}_{2,0} + \widehat{G}_{3,1} + \widehat{G}_{2,2} + \widehat{G}_{1,3} + \widehat{G}_{0,2} + \widehat{G}_{0,1}$

$= \vartheta\widehat{G}_{1,1} + \vartheta\widehat{G}_{2,1} + \vartheta\widehat{G}_{2,1} + \left(\vartheta\widehat{G}_{2,1} + \vartheta\widehat{G}_{1,2}\right) + \vartheta\widehat{G}_{1,2} + \vartheta\widehat{G}_{1,2} + \vartheta\widehat{G}_{1,1}$
$= \frac{1}{4}\frac{64}{56} + \frac{1}{4}\frac{16}{56} + \frac{1}{4}\frac{16}{56} + \frac{1}{4}\left(\frac{16}{56} + \frac{16}{56}\right) + \frac{1}{4}\frac{16}{56} + \frac{1}{4}\frac{16}{56} + \frac{1}{4}\frac{64}{56} = 1$, which is expected from the Radiation Principle and Conservation of Energy. To derive the middle row of the Poisson kernel which is the $\left[\widehat{H}\left(\wp_{1,1} : \cdot\right)\right]$ vector:

$\bullet \widehat{H}\left(1,1;1,0\right) = \frac{\widehat{G}_{1,0}}{\Upsilon(1,1)} = \frac{\vartheta\widehat{G}_{1,0}}{\Upsilon(1,1)} = \frac{1}{4}\frac{64}{56}\frac{1}{\Upsilon(1,1)} = \frac{16}{56} = \widehat{H}\left(1,1;0,1\right)$.

$\bullet \widehat{H}\left(1,1;2,2\right) = \frac{\widehat{G}_{1,1}}{\Upsilon(1,1)} = \frac{\vartheta\widehat{G}_{1,2}+\vartheta\widehat{G}_{1,2}}{\Upsilon(1,1)} = \left(\frac{1}{4}\frac{16}{56} + \frac{1}{4}\frac{16}{56}\right)\frac{1}{\Upsilon(1,1)} = \frac{8}{56}$.

$\bullet \widehat{H}\left(1,1;1,3\right) = \frac{\widehat{G}_{1,3}}{\Upsilon(1,1)} = \frac{\vartheta\widehat{G}_{1,2}}{\Upsilon(1,1)} = \frac{1}{4}\frac{16}{56}\frac{1}{\Upsilon(1,1)} = \frac{4}{56} = \widehat{H}\left(1,1;3,1\right) = \widehat{H}\left(1,1;2,0\right) = \widehat{H}\left(1,1;0,2\right)$.

When constructing the discretised Poisson kernel values as functionals of the number of discretised paths, let $\wp_{\cdot} \in \{\wp_{2,0}, \wp_{3,1}, \wp_{2,2}\}$ where:

$\bullet \Delta x = \|\wp_{2,1}, \wp_{\cdot}\|_1 = \|\wp_{2,1}, \wp_{\cdot}\|_2$, the respective Poisson kernel approximation values are $\left\{\frac{15}{56}, \frac{15}{56}, \frac{16}{56}\right\}$. This is due to the fact that there are two discretised paths between $\wp_{2,2}$ and $\wp_{2,1}$ via $\left\{\{\wp_{2,2} \to \wp_{1,2} \to \wp_{1,1} \to \wp_{2,1}\}, \{\wp_{2,2} \to \wp_{2,1}\}\right\}$ and only one path for the other boundary points.

$\bullet 2\Delta x = \|\wp_{1,1}, \wp_{\cdot}\|_1$, the respective Poisson kernel approximation values are $\left\{\frac{4}{56}, \frac{4}{56}, \frac{8}{56}\right\}$. This is due to the fact that there are two discretised paths between $\wp_{2,2}$ and $\wp_{1,1}$ via $\left\{\{\wp_{2,2} \to \wp_{1,2} \to \wp_{1,1}\}, \{\wp_{2,2} \to \wp_{2,1} \to \wp_{1,1}\}\right\}$ and only one path for the other boundary points.

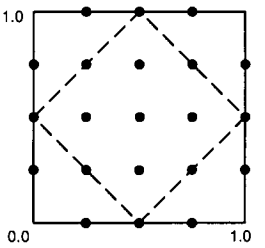

Figure 4.4: Discretised $d = 2$ domains for examples

Example 4.2.1. *Utilising the diamond and square domains depicted in Figure 4.4, evaluation of the d=2 Laplace system using* $\left[\widehat{F}_{n+1}\right] = \beth\left((3.10), \left[\widehat{F}_n\right], \left[\widehat{F}_{\delta\mho}\right]\right)$, *where* $\Delta x = \Delta y = \frac{1}{4}$ *yields the following:*

$\bullet$*For the diamond* $\mathtt{S}_1\left(\left(2\Delta x, 2\Delta y\right), 2\Delta x\right)$ *domain denoted by the dotted line of Figure 4.4, the FDSc matrix is*

$$\begin{bmatrix} \widehat{F}_{2,3} \\ \widehat{F}_{1,2} \\ \widehat{F}_{2,2} \\ \widehat{F}_{3,2} \\ \widehat{F}_{2,1} \\ F_{2,4} \\ F_{3,3} \\ F_{4,2} \\ F_{3,1} \\ F_{2,0} \\ F_{1,1} \\ F_{0,2} \end{bmatrix} = \frac{1}{4} \left[\begin{array}{ccccc|cccccccc} 0 & 0 & 1 & 0 & 0 & 1 & 1 & 0 & 0 & 0 & 0 & 0 & 1 \\ 0 & 0 & 1 & 0 & 0 & 0 & 0 & 0 & 0 & 0 & 1 & 1 & 1 \\ 1 & 1 & 0 & 1 & 1 & 0 & 0 & 0 & 0 & 0 & 0 & 0 & 0 \\ 0 & 0 & 1 & 0 & 0 & 0 & 1 & 1 & 1 & 0 & 0 & 0 & 0 \\ 0 & 0 & 1 & 0 & 0 & 0 & 0 & 0 & 1 & 1 & 1 & 0 & 0 \\ \hline 0 & 0 & 0 & 0 & 0 & 4 & 0 & 0 & 0 & 0 & 0 & 0 & 0 \\ 0 & 0 & 0 & 0 & 0 & 0 & 4 & 0 & 0 & 0 & 0 & 0 & 0 \\ 0 & 0 & 0 & 0 & 0 & 0 & 0 & 4 & 0 & 0 & 0 & 0 & 0 \\ 0 & 0 & 0 & 0 & 0 & 0 & 0 & 0 & 4 & 0 & 0 & 0 & 0 \\ 0 & 0 & 0 & 0 & 0 & 0 & 0 & 0 & 0 & 4 & 0 & 0 & 0 \\ 0 & 0 & 0 & 0 & 0 & 0 & 0 & 0 & 0 & 0 & 4 & 0 & 0 \\ 0 & 0 & 0 & 0 & 0 & 0 & 0 & 0 & 0 & 0 & 0 & 4 & 0 \\ 0 & 0 & 0 & 0 & 0 & 0 & 0 & 0 & 0 & 0 & 0 & 0 & 4 \end{array}\right] \begin{bmatrix} \widehat{F}_{2,3} \\ \widehat{F}_{1,2} \\ \widehat{F}_{2,2} \\ \widehat{F}_{3,2} \\ \widehat{F}_{2,1} \\ F_{2,4} \\ F_{3,3} \\ F_{4,2} \\ F_{3,1} \\ F_{2,0} \\ F_{1,1} \\ F_{0,2} \\ F_{1,4} \end{bmatrix}$$

which yields a Poisson kernel of

$$\begin{bmatrix} \widehat{F}_{2,3} \\ \widehat{F}_{1,2} \\ \widehat{F}_{2,2} \\ \widehat{F}_{3,2} \\ \widehat{F}_{2,1} \end{bmatrix} = \frac{1}{48} \begin{bmatrix} 13 & 14 & 1 & 2 & 1 & 2 & 1 & 14 \\ 1 & 2 & 1 & 2 & 1 & 14 & 13 & 14 \\ 4 & 8 & 4 & 8 & 4 & 8 & 4 & 8 \\ 1 & 14 & 13 & 14 & 1 & 2 & 1 & 2 \\ 1 & 2 & 1 & 14 & 13 & 14 & 1 & 2 \end{bmatrix} \begin{bmatrix} F_{2,4} \\ F_{3,3} \\ F_{4,2} \\ F_{3,1} \\ F_{2,0} \\ F_{1,1} \\ F_{0,2} \\ F_{1,3} \end{bmatrix}.$$

•*For the solid line square domain of Figure 4.4, the FDSc is omitted due to a lack of space, but the resulting system yields a Poisson kernel of*

$$\begin{bmatrix} \widehat{F}_{1,3} \\ \widehat{F}_{2,3} \\ \widehat{F}_{3,3} \\ \widehat{F}_{1,2} \\ \widehat{F}_{2,2} \\ \widehat{F}_{3,2} \\ \widehat{F}_{1,1} \\ \widehat{F}_{2,1} \\ \widehat{F}_{3,1} \end{bmatrix} = \frac{1}{224} \begin{bmatrix} 67 & 22 & 7 & 7 & 6 & 3 & 3 & 6 & 7 & 7 & 22 & 67 \\ 22 & 74 & 22 & 22 & 14 & 6 & 6 & 10 & 6 & 6 & 14 & 22 \\ 7 & 22 & 67 & 67 & 22 & 7 & 7 & 6 & 3 & 3 & 6 & 7 \\ 22 & 14 & 6 & 6 & 10 & 6 & 6 & 14 & 22 & 22 & 74 & 22 \\ 14 & 28 & 14 & 14 & 28 & 14 & 14 & 28 & 14 & 14 & 28 & 14 \\ 6 & 14 & 22 & 22 & 74 & 22 & 22 & 14 & 6 & 6 & 10 & 6 \\ 7 & 6 & 3 & 3 & 6 & 7 & 7 & 22 & 67 & 67 & 22 & 7 \\ 6 & 10 & 6 & 6 & 14 & 22 & 22 & 74 & 22 & 22 & 14 & 6 \\ 3 & 6 & 7 & 7 & 22 & 67 & 67 & 22 & 7 & 7 & 6 & 3 \end{bmatrix} \begin{bmatrix} F_{1,4} \\ F_{2,4} \\ F_{3,4} \\ F_{4,3} \\ F_{4,2} \\ F_{4,1} \\ F_{3,0} \\ F_{2,0} \\ F_{1,0} \\ F_{0,1} \\ F_{0,2} \\ F_{0,3} \end{bmatrix}.$$

It is important to note that the FDSc are small matrices with relatively few non-zero entries. As the size of the domain increases, evaluating the inverse of the sparse FDSc matrix is prohibitive; hence, the need for iterative methods to derive approximations.

4.2.3 Non-additive noise processes

To demonstrate how the non-additive noise fundamentally changes the system, consider the iterative FDSc

$$\begin{bmatrix} \widehat{F}_{1,2} \\ \widehat{F}_{1,1} \\ \widehat{F}_{2,1} \end{bmatrix}_{n+1} = \tfrac{1}{4}\begin{bmatrix} \vartheta 2\left(1,2\right) & 1 & 0 & 0 & 0 & 0 & 1 & 1 & 1 & 0 \\ 1 & \vartheta 2\left(1,1\right) & 1 & 1 & 0 & 0 & 0 & 0 & 0 & 1 \\ 0 & 1 & \vartheta 2\left(2,1\right) & 0 & 1 & 1 & 1 & 0 & 0 & 0 \end{bmatrix}\begin{bmatrix} \widehat{F}_{1,2} \\ \widehat{F}_{1,1} \\ \widehat{F}_{2,1} \\ F_{1,0} \\ F_{2,0} \\ F_{3,1} \\ F_{2,2} \\ F_{1,3} \\ F_{0,2} \\ F_{0,1} \end{bmatrix}_{n}$$

where $\vartheta 2\left(j,k\right) = \omega_{j,k}\mathbb{W}\left(\mathtt{D}_{j,k}\right) + \Delta x^2 \upsilon\left(\widehat{F}_{j,k}, j\Delta x, k\Delta y\right)\widehat{F}_{j,k}^{-1}$ if the noise is multiplicative and $\left(\Delta x^2 \upsilon\left(\widehat{F}_{j,k}, j\Delta x, k\Delta y\right) + \omega\left(\widehat{F}_{j,k}, j\Delta x, k\Delta y\right)\mathbb{W}\left(\mathtt{D}_{j,k}\right)\right)\widehat{F}_{j,k}^{-1}$ if the noise is general. The inclusion of the $\{\upsilon\left(\cdot\right), \omega\left(\cdot\right)\}$ terms in the FDSc2 matrix force the Green's function to be dependent upon the Brownian sheet, numerical approximation over the grid, and driving functionals; hence the spectral radius of FDSc2 is a random variable possibly greater than one.

Example 4.2.2. *For the multiplicative process,* $\frac{\partial^2 F(x,y)}{\partial x^2} + \frac{\partial^2 F(x,y)}{\partial y^2} = -\widehat{F}\left(x,y\right)\frac{\partial^2 W(x,y)}{\partial x \partial y}$, *assume* $F_{\delta\upsilon}\left(x,y\right) = 0$ *to yield*

$$\begin{bmatrix} \widehat{F}_{1,2} \\ \widehat{F}_{1,1} \\ \widehat{F}_{2,1} \end{bmatrix}_{n+1} = \tfrac{1}{4}\begin{bmatrix} \omega_{j,k}\mathbb{W}\left(\mathtt{D}_{1,2}\right) & 1 & 0 \\ 1 & \omega_{j,k}\mathbb{W}\left(\mathtt{D}_{1,1}\right) & 1 \\ 0 & 1 & \omega_{j,k}\mathbb{W}\left(\mathtt{D}_{2,1}\right) \end{bmatrix}\begin{bmatrix} \widehat{F}_{1,2} \\ \widehat{F}_{1,1} \\ \widehat{F}_{2,1} \end{bmatrix}_{n}.$$

Define the stochastic space to be a weighted singularity such that

$$\begin{bmatrix} \widehat{F}_{1,2} \\ \widehat{F}_{1,1} \\ \widehat{F}_{2,1} \end{bmatrix}_{n+1} = \tfrac{1}{4}\begin{bmatrix} 0 & 1 & 0 \\ 1 & \sqrt{\aleph} & 1 \\ 0 & 1 & 0 \end{bmatrix}\begin{bmatrix} \widehat{F}_{1,2} \\ \widehat{F}_{1,1} \\ \widehat{F}_{2,1} \end{bmatrix}_{n}; \text{ i.e. } \left[\widehat{F}_{n+1}\right] = \beth\left(\left[FDSc2_{\upsilon}\right], \left[\widehat{F}\left(x,y\right)_n\right]\right).$$

Placing a unit source at $1_{1,1}$ *and using the transpose* $\left[\widehat{F}_{1,2}, \widehat{F}_{1,1}, \widehat{F}_{2,1}\right]_n$, *if*

- $\aleph = 0$ *yields the deterministic Green's function growth* $[0,1,0] \to \left[\frac{1}{4}, 1, \frac{1}{4}\right] \to \left[\frac{1}{4}, \frac{18}{16}, \frac{1}{4}\right] \to \left[\frac{9}{32}, \frac{18}{16}, \frac{9}{32}\right]$ *which eventually converges to* $\left[\frac{2}{7}, \frac{8}{7}, \frac{2}{7}\right]$. *Thus,* $\theta_3 = \frac{1}{8}$ *such that* $\left(1-\theta_3\right)^{-1} = \frac{8}{7}$.
- $\frac{\sqrt{\aleph}}{4} = 0.5$ *yields the Green's function growth* $[0,1,0]_0 \to \left[\frac{1}{4}, \frac{3}{2}, \frac{1}{4}\right]_1 \to \left[\frac{3}{8}, \frac{15}{8}, \frac{3}{8}\right]_2 \to \left[\frac{15}{32}, \frac{17}{8}, \frac{15}{32}\right]_3$ *which eventually converges to* $\left[\frac{2}{3}, \frac{8}{3}, \frac{2}{3}\right]_{\infty}$.
- $\frac{\sqrt{\aleph}}{4} = \frac{2}{3}$ *yields the Green's function growth* $[0,1,0]_0 \to \left[\frac{1}{4}, \frac{5}{3}, \frac{1}{4}\right]_1 \to \left[\frac{5}{12}, \frac{161}{72}, \frac{5}{12}\right]_2 \to \left[\frac{483}{864}, \frac{2332}{864}, \frac{483}{864}\right]_3$ *which eventually converges to* $\left[\frac{6}{5}, \frac{24}{5}, \frac{6}{5}\right]_{\infty}$.
- $\frac{\sqrt{\aleph}}{4} = 1$ *yields the Green's function growth* $[0,1,0]_0 \to \left[\frac{1}{4}, 2, \frac{1}{4}\right]_1 \to \left[\frac{1}{2}, \frac{25}{8}, \frac{1}{2}\right]_2 \to \left[\frac{25}{32}, \frac{140}{32}, \frac{25}{32}\right]_3$ *which eventually explodes.*

Reduction shows that the limiting value of $\widehat{F}\left(\wp_{1,2}\right) = \widehat{F}\left(\wp_{2,1}\right) = \frac{1}{4}\widehat{F}\left(\wp_{1,1}\right)$ *with* $\lim_{n\to\infty}\widehat{F}\left(\wp_{1,1}\right)_n = \left(1 - \frac{1}{8} - \frac{\sqrt{\aleph}}{4}\mathbb{W}\left(\mathtt{D}_{1,1}\right)\right)^{-1}$, *which explodes when* $\frac{\sqrt{\aleph}}{4}\mathbb{W}\left(\mathtt{D}_{1,1}\right) \geq \frac{7}{8}$. *Explosion is even more prolific when* $\upsilon\left(\cdot\right) \neq 0$ *and non-homogenous boundary conditions are utilised.*

Example 4.2.3. *Consider the multiplicative and general noises on the* $\mathbb{R}^1$ *unit line segment domain using* $\frac{\partial^2 F(x)}{\partial x^2} = -F(x)\sin(2\pi x) - F(x)\cos(2\pi x)\frac{\partial W(x)}{\partial x}$ *and* $\frac{\partial^2 F(x)}{\partial x^2} = -F(x)\sin(2\pi x) - F(x)^2\cos(2\pi x)\frac{\partial W(x)}{\partial x}$. *Thus,* $\vartheta 2_{\times}(x_j) = \frac{1}{2(1-\sin(2\pi x_j)\Delta x^2 - \cos(2\pi x_j)\Delta x \mathbb{W}(\mathtt{D}_j))}$ *and* $\vartheta 2_{\dagger}(x_j) = \frac{1}{2(1-\sin(2\pi x_j)\Delta x^2 - F(x)\cos(2\pi x_j)\Delta x \mathbb{W}(\mathtt{D}_j))}$, *respectively. Utilise a* $\mathbb{Z}^1_{\frac{1}{36}}$ *with a canonical 3 point FDSc driven by the noise depicted in Figure 4.5 to yield the approximations depicted in the Figures 4.6 through 4.10. Due to the fact that approximations exist, this demonstrates that* $\mathtt{sr}(FDSc2) < 1$. *As expected, explosion occurs soon after* $\aleph \geq 1$ *(refer to Figure 4.10) and if the nature of the driving functionals is ill behaved, then even if* $\aleph \lll 1$ *the system might explode.*

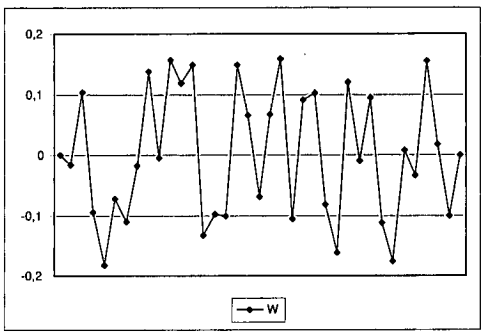

Figure 4.5: Stochastic path where $\aleph = 1$, $x \in [0,1]$, and $\Delta x = \frac{1}{36}$

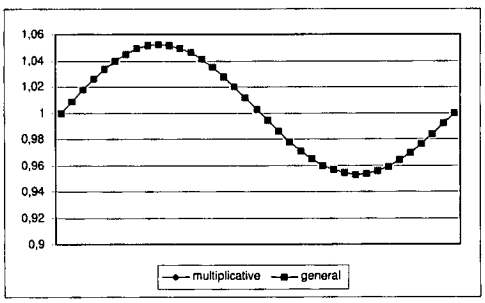

Figure 4.6: Deterministic solution with $\widehat{F}_{\delta\mho}(0) = 1$, $\widehat{F}_{\delta\mho}(1) = 1$, and $\aleph = 0$.

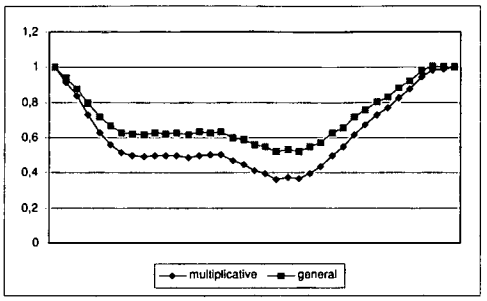

Figure 4.7: Convergence with $\widehat{F}_{\delta\mho}(0) = 1$, $\widehat{F}_{\delta\mho}(1) = 1$, and $\aleph = 1$.

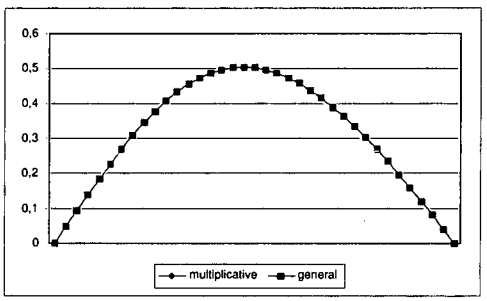

Figure 4.8: Deterministic solution with $\widehat{F}_{\delta\mho}(0) = 0$, $\widehat{F}_{\delta\mho}(1) = 0$, and $\aleph = 0$.

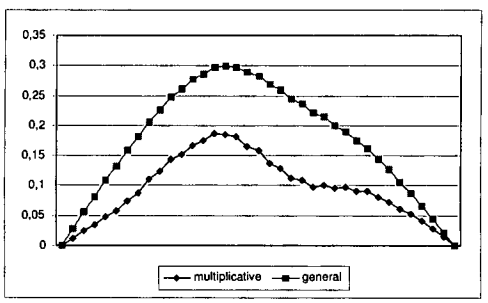

Figure 4.9: Convergence with $\widehat{F}_{\delta\mho}(0) = 0$, $\widehat{F}_{\delta\mho}(1) = 0$, and $\aleph = 1$

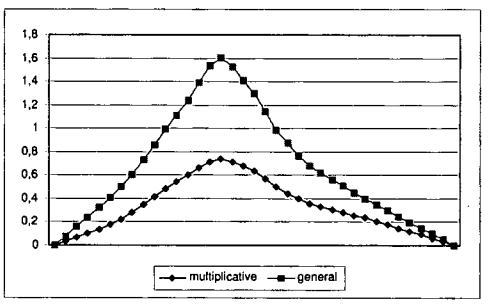

Figure 4.10: Convergence with $\widehat{F}_{\delta\mho}(0) = 0$, $\widehat{F}_{\delta\mho}(1) = 0$, and $\aleph = 1.03$

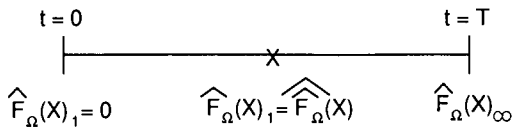

Figure 4.11: Reduction in time using an a priori estimate

4.3 A priori initialization methods

Due to the time consuming iterations of a FDSc to derive an approximation, a significant amount of effort can be eliminated if one chooses values for an initial grid that resemble the final approximation. When estimating a system, one often utilizes zero, homogenous values, or a deterministic solution to begin the iterative process and although each initialization will yield similar estimates, often errors can be eliminated and effort be reduced if one utilises a more 'appropriate' initialization; refer to Example 4.1.3. The objective is not to 'solve' the system, but to derive an a priori 'best guess' for $\widehat{F}(X)_1$ which will reduce the computational effort for an iterative FDSc to derive an approximation; refer to Figure 4.11. Utilising information about the domain and computational molecule, construct an a priori Green's function and Poisson kernel, $\left\{\widehat{\left[\widehat{G}\right]}, \widehat{\left[\widehat{H}\right]}\right\}$, such that

$$\widehat{\left[\widehat{F}(\wp_{\mho})\right]} = O\left(\Delta x^2\right)\widehat{\left[\widehat{G}\right]}\left[\upsilon(\cdot)\right] + O\left(\Delta x^{2-d}\right)\widehat{\left[\widehat{G}\right]}\left[\mathbb{W}(\mathtt{D})\right]\left[\omega(\cdot)\right] + \widehat{\left[\widehat{H}\right]}\left[F(\wp_{\delta\mho})\right]. \tag{4.4}$$

Using this initial guess as a starting point, an iterative FDSc can be implemented to derive an initial numerical approximation

$$\begin{bmatrix} \widehat{F}(\wp_{\mho})_2 \\ F(\wp_{\delta\mho}) \end{bmatrix} = \begin{bmatrix} FDSc_{\mho} & FDSc_{\delta\mho} \\ 0 & I \end{bmatrix} \begin{bmatrix} \widehat{\widehat{F}(\wp_{\mho})} \\ F(\wp_{\delta\mho}) \end{bmatrix} + \left[\Upsilon\left(\widehat{\widehat{F}}, \upsilon(\cdot), \mathbb{W}(\mathtt{D})\,\omega(\cdot)\right)\right]$$

which is utilised in place of

$$\begin{bmatrix} \widehat{F}(\wp_{\mho})_2 \\ F(\wp_{\delta\mho}) \end{bmatrix} = \begin{bmatrix} FDSc_{\mho} & FDSc_{\delta\mho} \\ 0 & I \end{bmatrix} \begin{bmatrix} \widehat{F}(\wp_{\mho})_1 \\ F(\wp_{\delta\mho}) \end{bmatrix} + \left[\Upsilon\left(\widehat{F}_1, \upsilon(\cdot), \mathbb{W}(\mathtt{D})\,\omega(\cdot)\right)\right]$$

where $\widehat{F}(\wp_{\mho})_1$ is often a 0 matrix or a deterministic approximation.

A priori methods are most effective when deriving non-pathwise approximations or one is forced derive approximations for a given domain utilising different stochastic noises; refer to Chapter 5. Although the following methods will be presented as separate entities, the most efficient implementation is utilising a combination of methods dependent upon the size of the domain, Δx, nature of the driving functionals, roughness of the stochastic space, and boundary conditions. Often more difficult to implement than a homogeneous initialization,

the savings in computational effort are worth the trouble; refer to the numerical results of Section 4.3.5.

Example 4.3.1. *Returning to the triangular domain of Section 4.2, Table 4.3 provides a comparison between the discretised Green's function and Poisson kernel and a few a priori estimates. Although it is clear that the a priori matrices are not the true values of* $\left\{\left[\widehat{G}\right], \left[\widehat{H}\right]\right\}$*, they are good estimates to start from. Refer to Section C.3 for a pseudo-code description of the following methods.*

Method	$\left[\widehat{G}_{\Delta x}\left(\wp_{\mho};\wp_{\mho}\right)\right]$	$\left[\widehat{H}_{\Delta x}\left(\wp_{\delta\mho};\wp_{\mho}\right)\right]$
$\left\{\widehat{G},\widehat{H}\right\}$ values	$\frac{1}{56}\begin{bmatrix} 60 & 16 & 4 \\ 16 & 64 & 16 \\ 4 & 16 & 60 \end{bmatrix}$	$\frac{1}{56}\begin{bmatrix} 4 & 1 & 1 & 16 & 15 & 15 & 4 \\ 16 & 4 & 4 & 8 & 4 & 4 & 16 \\ 4 & 15 & 15 & 16 & 1 & 1 & 4 \end{bmatrix}$
Blow-up method	$\frac{1}{2}\begin{bmatrix} 3 & 1 & \frac{5}{8} \\ 1 & 3 & 1 \\ \frac{5}{8} & 1 & 3 \end{bmatrix}$	$\begin{bmatrix} \frac{24}{309} & \frac{15}{309} & \frac{15}{309} & \frac{87}{309} & \frac{72}{309} & \frac{72}{309} & \frac{24}{309} \\ \frac{3}{12} & \frac{1}{12} & \frac{1}{12} & \frac{2}{12} & \frac{1}{12} & \frac{1}{12} & \frac{3}{12} \\ \frac{24}{309} & \frac{72}{309} & \frac{72}{309} & \frac{87}{309} & \frac{15}{309} & \frac{15}{309} & \frac{24}{309} \end{bmatrix}$
$\widehat{G\mathbb{Q}}$ method	$\frac{3}{2}\begin{bmatrix} 1 & \frac{1}{4} & \frac{1}{16} \\ \frac{1}{4} & 1 & \frac{1}{4} \\ \frac{1}{16} & \frac{1}{4} & 1 \end{bmatrix}$	$\begin{bmatrix} \frac{4}{60} & \frac{2}{60} & \frac{2}{60} & \frac{16}{60} & \frac{16}{60} & \frac{16}{60} & \frac{4}{60} \\ \frac{16}{56} & \frac{4}{56} & \frac{4}{56} & \frac{8}{56} & \frac{4}{56} & \frac{4}{56} & \frac{16}{56} \\ \frac{4}{60} & \frac{16}{60} & \frac{16}{60} & \frac{16}{60} & \frac{2}{60} & \frac{2}{60} & \frac{4}{60} \end{bmatrix}$
$\|X,Y\|_2^{-d}$ method	$\frac{1}{2}\begin{bmatrix} 3 & 1 & \frac{1}{2} \\ 1 & 3 & 1 \\ \frac{1}{2} & 1 & 3 \end{bmatrix}$	$\begin{bmatrix} \frac{5}{83} & \frac{4}{83} & \frac{4}{83} & \frac{20}{83} & \frac{20}{83} & \frac{20}{83} & \frac{10}{83} \\ \frac{4}{16} & \frac{2}{16} & \frac{1}{16} & \frac{2}{16} & \frac{1}{16} & \frac{2}{16} & \frac{4}{16} \\ \frac{10}{83} & \frac{20}{83} & \frac{20}{83} & \frac{20}{83} & \frac{4}{83} & \frac{4}{83} & \frac{5}{83} \end{bmatrix}$

Table 4.3: Comparison of a priori methods

4.3.1 Blow-up method

This method will focus on the Green's function and should be used to account for the influence the driving functionals have upon an approximation; i.e. a numerical 'cookie cutter' for $\widehat{G}(\cdot)$. It should not be utilised in deriving a Poisson kernel for domains with a large number of interior points, since only neighborhoods of internal points are considered. Regardless of the domain, given a symmetric computational molecule, the following assumptions can be made about the structure of the discretised Green's function:

•From Lemma 3.2.11, when X is well within the interior, the closed loop feedback of a Green's function approximation will be a function of Δx.

•From Corollary's 3.2.13 through 3.2.15, when X is either an adjacent point or close to the boundary, a Green's function approximation will have a limiting case of $\widehat{G}_{\Delta x}(X;X) \leq \alpha$, where α is usually less than 2.

•From Lemma 3.2.16, $\widehat{G}(X;Y) = \widehat{G}(Y;X)$; i.e. the reciprocity relation is valid.

•From Corollary 3.2.17, the difference between two discretised Green's functions an l^2 distance $n\Delta x$ apart is a constant.

4.3.1.1 Procedure

In order to implement this method, utilise the following steps:
(1) Given a computational molecule, Δx, and the closed loop feedback properties of the FDSc, make a best guess at $\widehat{G}(\wp_{\mho};\wp_{\mho})$ for a point well within the interior. For example, when using the computational molecule (3.10), then $\widehat{G}(X;X) \approx (1.5 + 0.45(log_2(M_x) - 2))$; refer to Program C.3.2.
(2) Copy the stochastic noise matrix and for points well within the interior, multiply the associated $\mathbb{W}(\mathtt{D}_j)$ random values by $\widehat{G}_{\Delta x}(\wp_{\mho};\wp_{\mho})\Delta x^{d-2}\omega(X_j)$ and add $\widehat{G}_{\Delta x}(\wp_{\mho};\wp_{\mho})\upsilon(F(X_j),x_j)\Delta x^2$. For points close to the boundary, utilise the associated limiting value for adjacent discretised Green's functions. For example, when $d = 1$ multiply adjacent points by 1.9 and when $d = 2$ multiply adjacent points by 1.45 and 1.25 for adjacent corner points; refer to Remark 3.2.18.
(3) In accordance with Corollary 3.2.17, calculate a generic Green's function difference for points well within the interior. Use $\widehat{G}_{\Delta x}(Y_k;Y_k)$ and the fact that each l^1 jump of Δx is a constant; refer to Programs C.3.2 and C.3.3.

The difference vector does not have to be very large due to the radiation principle mandating that there is a limited region of significant numerical influence. Often points within a $\mathtt{S}_2(X, 25\Delta x)$ neighborhood are more than adequate.
(4) Divide the difference vector by $\widehat{G}_{\Delta x}(Y_k;Y_k)$ and remove any negative values such that the vector represents influence values between 0 and 1.
(5) Starting from the boundary and progressing towards the interior, multiply the modified functional values by the influence vector and then add the results to the deterministic 'best guess.' Values for the influence vector can be interpolated using linear, trapezoidal, or spline functions.
(6) Utilise the symmetric properties of a domain to minimize the computational effort.
(7) Delete the manipulated functionals and begin the iterative method utilising the a priori approximation as the $\widehat{\widehat{F}}$ estimate.

4.3.2 $\widehat{G\mathtt{Q}}$ method

Notation 4.3.2. *Let a numeric 'center point' denote a point in $\mathbb{Z}^d$ where the weighting of the minimal l^1 distance to the boundary points is equivalent to the total weighting of all paths to the boundary points. For example, refer to Figure 4.2 or consider the geometric center of a sphere, rhombus, or square.*

Given a computational molecule, the assumption that every l^1 jump of Δx implies a Green's function must be multiplied by an appropriate $\widehat{\vartheta}$ factor will be made. Thus, the influence between two points will be approximately $\mathtt{Q}(X;Y) = \widehat{\vartheta}^{\alpha}\mathtt{Qpath}(X,Y)$; where $\alpha = \frac{\|X,Y\|_1}{\Delta x}$, $\mathtt{Q}(X;Y) = \mathtt{Q}(Y;X)$, and $\mathtt{Qpath}(X,Y)$ is the number of paths between two $\mathbb{Z}^d$ points of length $\|X,Y\|_1$; refer to Program C.3.6.

Since it is numerically impossible to cover all paths over all distances, the assumption that all points well within the interior are numeric center points will be made. Despite the obvious fact that this is not true, the radiation principle numerically ignores paths of excessive length so the weighting of minimal paths is assumed to be the same as the total number of paths. This method will evaluate 'exact' approximations for center points regardless of the domain, boundary conditions, and Δx; thus, if one is interested in evaluating a system only at specific points, then this method could be utilised in place of an iterative method. Due to this method being tied to individual Δx jumps, this system will experience the following numerical complications:

•It is difficult to distinguish between l^1 paths of $\{n\Delta x, (n+1)\Delta x, (n+2)\Delta x, ...\}$. Thus this method is most efficient when Δx is a numerically significant (large) value, such that $n\Delta x$ is numerically distinguishable from $(n+1)\Delta x$. For example 0.00001 is distinguishable from 0.00002, while 100.00001 is difficult to distinguish from 100.00002.

•Most boundary points will have only one interior adjacent point, thus corrections will be made for $d \geq 2$ boundary points with more than one adjacent point. In having more than one interior adjacent point, the influence of that boundary point would be understated if only one adjacent point is considered.

•Since $0 \leq \widehat{\vartheta} \leq 1$ and the number of l^1 paths of given length grows exponentially as the distance increases; $\mathtt{Q}(X;Y)$ involves a very small $\widehat{\vartheta}^{\alpha}$ value times a very large $\mathtt{Qpath}(X;Y)$ value. Accurately evaluating $\mathtt{Q}(X;Y)$ is not a trivial exercise.

4.3.2.1 Procedure

In order to implement this method, utilise the following steps:

(1) Given a computational molecule, derive the $\widehat{\vartheta}$ value from the associated $\vartheta(\cdot)$ terms. For example, when $\Delta x = \Delta y = \Delta z$, then $\widehat{\vartheta}_{(3.9)} = \frac{1}{2}$, $\widehat{\vartheta}_{(3.10)} = \frac{1}{4}$, $\widehat{\vartheta}_{(3.11)} = \frac{1}{6}$, and $\widehat{\vartheta}_{(3.13)} \approx 0.3924$.

(2) Assuming $X = (x_j, y_k, z_l)$ and $Y = (x_{j+m}, y_{k+n}, z_{l+a})$, where a is an integer; let $\mathtt{Q}(X;Y) = \mathtt{Qpath}(m,n,a,0,0) \times \widehat{\vartheta}^{(m+n+a)}$ and use this relation to derive $\widehat{G}(X;Y) = \widehat{G\mathtt{Q}}(X;Y) = \mathtt{Q}(X;Y)\left(\sum_{Y_2 \in \{\mho \cup \delta\mho\}} \mathtt{Q}(X;Y_2)\right)^{-1}$ and $\widehat{H}(X;Y_{\delta\mho})$

$= \widehat{GQ}(X;Y_{\delta\mho}) \left(\sum_{Y_2 \in \delta\mho} \widehat{GQ}(X;Y_2) \right)^{-1}$.

(3) Evaluate other interior points in the domain utilising the reciprocity relation and previously calculated values for $\mathtt{Q}(X;Y_2)$.

Example 4.3.3. *Let* $N = \frac{\|X,Y\|_1}{\Delta x} - 1$ *and using (3.10) on* $\mathbb{Z}^2_{\Delta x}$ *to yield* $\widehat{GQ}(X;Y) = \sum_{j=0}^{N} \frac{2^j}{4^N} = \theta^N \sum_{j=0}^{N} 2^j$ *or simply* $\frac{2^{N+1}}{2^{2N}}$. *Evaluation yields,* $\widehat{GQ}(X;\{X \pm \Delta x\}) = 1 - \frac{1}{4} = \frac{3}{4}$, $\widehat{GQ}(X;\{X \pm 2\Delta x\}) = 1 - \frac{1}{4} - \frac{20}{64} = \frac{7}{16}$, $\widehat{GQ}(X;\{X \pm 3\Delta x\}) = 1 - \frac{1}{4} - \frac{20}{64} - \frac{52}{256} = \frac{15}{64}$, $\widehat{GQ}(X;\{X \pm 4\Delta x\}) = 1 - \frac{1}{4} - \frac{20}{64} - \frac{52}{256} - \frac{116}{1024} = \frac{31}{256}$, *and* $\widehat{GQ}(X;\{X \pm 6\Delta x\}) = 1 - \frac{1}{4} - \frac{20}{64} - \frac{52}{256} - \frac{116}{1024} - \frac{244}{4096} = \frac{63}{1024}$. *Hence. the recurrence relation* $\widehat{GQ}_m = \frac{1}{2}\widehat{GQ}_{m-1} + \frac{1}{4^m}$, *where* $m \geq 1$ *and* $\widehat{GQ}_1 = \frac{3}{4}$ *can be utilised to calculate the required* $\widehat{GQ}(\cdot)$ *values.*

4.3.3 $\|X,Y\|_2^{-d}$ method

In order to deal with general domains and evaluate systems where Δx is too small to eliminate paths of excessive length, repeat the $\widehat{GQ}$ method such that $\|X,Y\|_2^{-d}$ is used in place of $\mathtt{Q}(X;Y)$. Thus, the l^2 norm raised to the -d power will be the influence measure between two distinct points.

4.3.3.1 Procedure

In order to implement this method, utilise the following steps:

(1) Evaluate $\|X,Y\|_2^{-d}$ and use this value to derive $\widehat{G}(X;Y) = \|X,Y\|_2^{-d} \times \left(\sum_{Y_2 \in \{\mho \cup \delta\mho\}} \|X,Y_2\|_2^{-d} \right)^{-1}$ and $\widehat{H}(X;Y_{\delta\mho}) = \widehat{G}(X;Y_{\delta\mho}) \left(\sum_{Y_2 \in \delta\mho} \widehat{G}(X;Y_2) \right)^{-1}$.

(2) Evaluate other interior points in the domain utilising previously calculated values for $\widehat{G}(X;Y)$.

4.3.4 GPS method

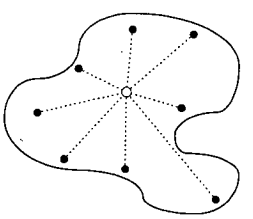

Figure 4.12: GPS average where $\{\wp_E\}$ are the blackened dots

As depicted in Figure 4.12, derive reasonable estimates to a finite set of interior points $\{\wp_E\}$; i.e., derive $\left\{\widehat{F}(\wp_E)\right\}$. From Lemma 3.1.9 and the reciprocity rela-

tion, utilise values of the Green's function calculated when evaluating $\left\{\widehat{F}\left(\wp_E\right)\right\}$ to derive approximations for the remaining interior points. This method is most effective when used on domains with complicated boundaries or the cardinality of the interior points is very large.

$\wp_0 = \left(\frac{M_x}{3}, \frac{N_y}{5}\right)$	$\wp_4 = \left(\frac{2M_x}{3}, \frac{N_y}{5}\right)$
$\wp_1 = \left(\frac{N_y}{5}, \frac{2M_x}{3}\right)$	$\wp_5 = \left(\frac{N_y}{5}, \frac{M_x}{3}\right)$
$\wp_2 = \left(\frac{2(M_x-1)}{3}, \frac{4N_y}{5}\right)$	$\wp_6 = \left(\frac{M_x}{3}, \frac{4N_y}{5}\right)$
$\wp_3 = \left(\frac{4N_y}{5}, \frac{M_x}{3}\right)$	$\wp_7 = \left(\frac{4N_y}{5}, \frac{2(M_x-1)}{3}\right)$

Table 4.4: 8 example GPS points for a square domain

4.3.4.1 Procedure

An approximation will be derived using a limited subset of interior points. Given an a priori discretised Green's function or a Green's function calculated using the Laplace operator on the domain:

(1) Use a rough grid, symmetric conditions, Laplace operator estimates, or numerical center points to estimate $\left\{\widehat{F}\left(\wp_E\right)\right\}$.

(2) Rely upon the reciprocity relation of the $\left[\widehat{G}\left(\cdot;\wp_E\right)\right]$ matrices to build $\left[\widehat{G}\left(\wp_E;\cdot\right)\right]$ and estimate the remaining interior points by ignoring the boundary conditions and only utilising $\left\{\widehat{F}\left(\wp_E\right)\right\}$ and noise within a small neighborhood.

4.3.5 Numerical results

$$\frac{\partial^2 F\left(x,y\right)}{\partial x^2} + \frac{\partial^2 F\left(x,y\right)}{\partial y^2} = -\frac{\partial^2 W\left(x,y\right)}{\partial x \partial y} \tag{4.5}$$

Consider (4.5) on a unit square domain with $\lambda_y = 1$, $F_{\delta\upsilon}\left(x,y\right) = 1$, and $\widehat{F}\left(\left(3.10\right), \mathfrak{es} = 5 \times 10^{-12}\right)$; refer to Figure 4.1. Tables 4.5 through 4.8 list the computational savings realised when using the aforementioned a priori methods with an iterative scheme.

Grid Size	7×7	11×11	19×19	35×35	67×67
0 Fill	0	0	0	0	0
Det. $\widehat{F}(\cdot)$	8.3	48.8	7.2	9.1	10.4
Blow up	16.7	53.3	11.4	13.0	13.5
$\widehat{GQ}$	16.7	50.5	21.1	3.3	2.2
5 $\wp$ GPS	8.3	52.4	11.4	13.0	16.6
8 $\wp$ GPS	8.3	52.4	11.4	14.5	16.6

Table 4.5: Percent savings in computational effort for a Hackbush multigrid method

Grid Size	7×7	11×11	19×19	35×35	67×67
0 Fill	0	0	0	0	0
Det. $\widehat{F}(\cdot)$	4.5	3.3	18.4	9.8	9.4
Blow up	18.2	5.4	12.3	12.4	11.8
$\widehat{GQ}$	9.1	7.6	20.9	3.1	-0.3
5 $\wp$ GPS	9.1	5.4	20.3	16.4	16.8
8 $\wp$ GPS	9.1	4.3	19.3	16.0	15.6

Table 4.6: Percent savings in computational effort for a SOR method

Grid Size	7×7	11×11	19×19	35×35	67×67
0 Fill	0	0	0	0	0
Det. $\widehat{F}(\cdot)$	11.5	19.0	7.7	11.6	12.5
Blow up	19.2	21.3	14.0	14.5	15.5
$\widehat{GQ}$	15.4	34.4	29.6	4.1	2.6
5 $\wp$ GPS	11.5	13.0	15.3	16.7	19.2
8 $\wp$ GPS	11.5	20.2	15.1	18.5	20.4

Table 4.7: Percent savings in computational effort for a Jacobi method using (3.10)

Grid Size	7×7	11×11	19×19	35×35	67×67
0 Fill	0	0	0	0	0
Det. $\widehat{F}(\cdot)$	9.1	24.8	13.0	11.4	12.3
Blow up	18.2	17.5	15.4	14.7	15.3
$\widehat{GQ}$	13.6	47.8	32.6	4.0	1.2
5 $\wp$ GPS	9.1	16.2	18.6	16.8	19.2
8 $\wp$ GPS	9.1	16.2	17.0	19.1	19.8

Table 4.8: Percent savings in computational effort for a Jacobi method using (3.13)

Chapter 5

Quasi-Geostrophic processes with additive noise

> The principles to be derived are largely theoretical concepts that can be applied to an understanding of the natural phenomena. Such principles spring most naturally from the study of model problems whose goal is the development of conceptual comprehension rather than detailed simulation of the complete geophysical phenomenon. Geophysical fluid dynamics has historically progressed by the consideration of a study sequence within a hierarchy of increasingly complex models where each stage builds on the intuition developed by the precise analysis of simpler models. [53, page 2]

Section 5.2 will address the discretisation of the QG processes of interest to this text and highlight the similarities of QG systems with the FDSc's of Chapters 2 - 4. Given that the derivation of the QG process is not intuitive, refer to Section B.3 for an introduction to thin fluids and [53] as to how QG processes arise from a series of assumptions about the nature of a rotating fluid phenomena.

5.1 Introduction

Quasi-Geostrophic (QG) processes can be expressed as

$$\begin{aligned}\frac{\partial \mathcal{Q}(x,y,z,t)}{\partial t} + \mathrm{J}\left(F(x,y,z,t), \mathcal{Q}(x,y,z,t)\right) &= \omega(x,y,z,t)\frac{\partial^3 W(x,y,z,t)}{\partial x \partial y \partial t} \\ &+ v\left(\mathcal{Q}(x,y,z,t), F'(x,y,z,t), F(x,y,z,t), x, y, z, t\right)\end{aligned} \tag{5.1}$$

where $F(\cdot)$ is a stream function and $\mathcal{Q}$ is the potential vorticity of the form

$$\mathcal{Q}(x,y,z,t) = \nabla^2 F(x,y,z,t) + g\left(F(x,y,z,t), x, y, z, t\right). \tag{5.2}$$

Notation 5.1.1. *Due to the thin layered approach of a QG process, the Laplacian and Jacobian operators are with respect to* $\{x, y\}$ *only. Thus, the Jacobian of* $f(x, y, z, t)$ *and* $g(x, y, z, t)$ *is* $\mathrm{J}(f(x, y, z, t), g(x, y, z, t))$ $= \frac{\partial f(x,y,z,t)}{\partial x}\frac{\partial g(x,y,z,t)}{\partial y} - \frac{\partial g(x,y,z,t)}{\partial x}\frac{\partial f(x,y,z,t)}{\partial y}$*; refer to [38, Section 2.7].*

QG processes are a simplification of Navier-Stokes equations used in geophysical processes when modeling zonal flow with sinusoidal shear and baroclinic-barotropic instability. Although deceptively simple, these models are:
•quite robust in describing the transfer energy in thin rotating fluids, thus they provide a basis for depicting large-scale geophysical motions.
•'easier' to implement and derive a theoretical understanding of fluid flows.
•computationally inexpensive compared to more complete processes.
There are a number of other benefits to these QG models, but the major motivation stems from the elimination of: certain aspects of the law's of thermodynamics, the curvature of the manifold, and geostrophic degeneracy via a 'reduction' to planar surfaces. It is desirable that QG systems restrict non-linear interactions to a few wave triads; hence, simplifying oceanography and meteorological concepts for theoretical study. Since waves on a rotating planet can be atmospheric, gravitational, or sound; one must filter out the sound and gravity waves, but if these wavelengths are eliminated from the system, it is impossible to 'accurately solve' a process. If 'long time period' experiments must be conducted and/or solutions are required, the simplified nature of a QG process is inappropriate to attempt detailed quantitative comparisons with laboratory experiments; i.e. complete Navier-Stokes equations should be utilised.

5.1.1 Summary of results

Assuming the following initial conditions are fulfilled, then the FDSc built using the consistent components of Section 5.2.2 ensure that a QG process behaves as an additive elliptic system with a pseudo-deterministic hyperbolic influence. The QG processes outlined in this chapter are the foundation for future applied work in thin fluid lubrication processes, macro-computer network modeling, and possible methods in robotic communications.

5.1.2 Assumed Initial Conditions (QGAIC)

The following initial conditions assure that QG processes are well posed:

Assumption 5.1.2. *A solution exists and is unique in accordance with (5.15).*

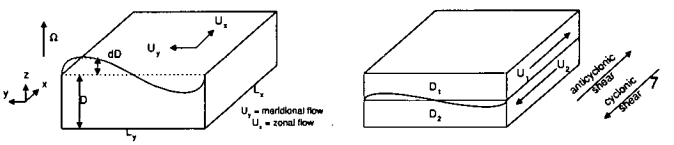

Figure 5.1: Construction of QG layers

Assumption 5.1.3. *Only closed and bounded domains on $\mathbb{R}^4_{+t}$ are utilised. One dimension of space will be used as time and the z dimension will be omitted in place of a counter for the stratification levels.*

Assumption 5.1.4. *A process is bounded from above and below by pressure surfaces and assumes that flow is linear with regards to pressure.*

Assumption 5.1.5. *Dirichlet boundary conditions are given where $\{F_{\delta\mho}(x,y,t), \mathcal{Q}_{\delta\mho}(x,y,t)\}|_{t>0}$ are homogeneous and the initial states $\{F_{\delta\mho}(x,y,t), \mathcal{Q}_{\delta\mho}(x,y,t)\}|_{t=0}$ are Lipschitz continuous with $K_{t=0}$.*

Assumption 5.1.6. *A Brownian sheet is utilised.*

Assumption 5.1.7. *$\upsilon(\cdot)$ and $\omega(\cdot)$ are real valued measurable functions on $\mathbb{R}^4_{+t}$ and they are globally Lipschitz continuous with coefficients K_υ and K_ω.*

Assumption 5.1.8. *Incompressible and inviscid fluids will be assumed where the laws of thermodynamics (entropy), conservation of mass, and conservation of momentum are strictly observed.*

Remark 5.1.9. *When the fluid is irrotational and incompressible, then the potential velocity is harmonic and the divergence of the gradient is uniquely 0. Due to the inclusion of a second order elliptic operator, this chapter will concentrate on additive noise to *hopefully* avoid the complications of non-additive noise.*

5.1.2.1 Domains

Only two-layered closed and bounded domains are considered, where boundary conditions involve 'hard' surfaces above and below with 'walls' and 'wrapping' along the side boundaries. Often the boundary pressure surfaces will be the stochastic shape of the earth's surface and some statement about the 'top' of the fluid. Since, $\mathcal{D}(x,y,z,t)$ is the depth of a layer and the aspect ratio, $\theta_{\mathcal{D}} = \frac{\mathcal{D}}{L} \lll 1$, this thin nature of the domain and internal stratification will allow each layer to be considered two dimensional, such that $\mathcal{U}_z \equiv 0$, and the curvature of the manifold will be ignored. Due to stratification, the thin fluid domains will be 'divided and flattened' into parallel planes perpendicular to $Z^T = [0,0,1]$, where the notation

of Chapter's 2 and 3 will be utilised with respect to $d = 2$ planes. Let l be an integer valued counter that starts at the top of a fluid and proceeds in a $-Z$ direction and since a Pedlosky two-layered model is utilised:

•if $l = 1$ denotes layer one then $\neq l$ denotes layer two.

•if $l = 2$ denotes layer two then $\neq l$ denotes layer one.

•$\Delta F(x_j, y_k, z_l, t_m) = F(x_j, y_k, z_l, t_m) - F(x_j, y_k, z_{\neq l}, t_m)$.

5.1.3 Processes of interest

$\mathcal{B}_{fruh} = 0.1$	$\mathcal{B}_{hh} = 1.6e-11$	$\mathcal{B}_{lee} = 0.25$
$r_{fruh} = 0.2$	$\alpha_{hh} = 4e5$	$\alpha_{lee} = 0.1$
$\mathtt{f}_{fruh} = 90.0$	$\mathtt{f}_{hh} = 7.844e-13$	$\tau_{lee} = 0.1$
$\varkappa_{fruh} = \left(0.8r_{fruh}^2\right)^{-1}$	$b_{hh} = 1.92e-7$	$K_{lee} = 0.1$

Table 5.1: QG constants

The following QG processes will be utilised for the numerical work of this chapter.

5.1.3.1 Früh Process [22]

$$\begin{aligned} &\frac{\partial \mathcal{Q}(x,y,z,t)}{\partial t} + \mathtt{J}\left(F(x,y,z,t), \mathcal{Q}(x,y,z,t)\right) \\ &= -\frac{\sqrt{\mathcal{E}}}{2\theta_{\mathcal{A}}} \nabla^2 F(x,y,z,t) + \frac{1}{\varkappa} \nabla^2 \mathcal{Q}(x,y,z,t) + \omega(x,y,z,t) \frac{\partial^3 W(x,y,z,t)}{\partial x \partial y \partial t} \end{aligned} \tag{5.3}$$

$$\mathcal{Q}(x,y,z,t) = \nabla^2 F(x,y,z,t) + \mathcal{B}y - \mathtt{f}\Delta F(x,y,z,t). \tag{5.4}$$

This model attempts to describe the chaotic weather systems that appear over the middle latitudes of the northern hemisphere; geographical regions such as the United Kingdom and Northern Europe where the 'warm' y=0 boundary represents the Mediterranean and the 'cold' y=1 boundary represents the Arctic Circle. This model integrates the QG process on a $\mathcal{B}$ plane in a zonal periodic channel contained between thin but impermeable ageostrophic boundaries, where discontinuous flow with bifurcation results from steady waves with resonant triads and zonal flow-wave interacting with a strong $\mathcal{B}$ effect. This model also studies nonlinear wave-wave interactions via wave triads, zonal flow-wave interactions, bifurcation, strongly modulated amplitude vacillation, and intermittent weaker wave modes. For the domain, assume Ekman layers at the lid and base with parameters $\left\{\mathcal{E} = \frac{\nu}{(f_0 D^2)}, \varkappa = \frac{UL}{\nu} = \frac{1}{r^2 R_0}, \theta_{\mathcal{A}} \leq 0.1, \frac{\sqrt{\mathcal{E}}}{\theta_{\mathcal{A}}} = 0.3\right\}$ and a unit

Prandtl number. Reducing the deterministic version of (5.3) into its baroclinic and barotropic components yields:

$$\frac{\partial \bigtriangledown^2 \Upsilon \mathtt{t}\left(x,y,z,t\right)}{\partial t}+\mathcal{B}\frac{\partial \Upsilon \mathtt{t}\left(x,y,z,t\right)}{\partial x}+\mathcal{U}_{\Upsilon \mathtt{t}}\left(x,y,z,t\right)\frac{\partial \bigtriangledown^2 \Upsilon \mathtt{t}\left(x,y,z\right)}{\partial x}$$
$$+\mathcal{U}_{\Upsilon \mathtt{c}}\left(x,y,z,t\right)\frac{\partial \bigtriangledown^2 \Upsilon \mathtt{c}\left(x,y,z,t\right)}{\partial x}+\mathtt{J}\left(\Upsilon \mathtt{t}\left(x,y,z,t\right),\bigtriangledown^2\Upsilon \mathtt{t}\left(x,y,z,t\right)\right)$$
$$+\mathtt{J}\left(\Upsilon \mathtt{c}\left(x,y,z,t\right),\bigtriangledown^2\Upsilon \mathtt{c}\left(x,y,z,t\right)\right)=-\frac{\sqrt{\mathcal{E}}}{\theta_{\mathcal{A}}}\bigtriangledown^2\Upsilon \mathtt{t}\left(x,y,z,t\right)+\frac{\bigtriangledown^4\Upsilon \mathtt{t}\left(x,y,z,t\right)}{\varkappa} \tag{5.5}$$

$$\frac{\partial \bigtriangledown^2 \Upsilon \mathtt{c}\left(x,y,z,t\right)-2\mathtt{f}\Upsilon \mathtt{c}\left(x,y,z,t\right)}{\partial t}+\mathcal{B}\frac{\partial \Upsilon \mathtt{c}\left(x,y,z,t\right)}{\partial x}$$
$$+\mathcal{U}_{\Upsilon \mathtt{t}}\left(x,y,z,t\right)\frac{\partial \bigtriangledown^2 \Upsilon \mathtt{c}\left(x,y,z,t\right)}{\partial x}+\mathcal{U}_{\Upsilon \mathtt{c}}\left(x,y,z,t\right)\frac{\partial \bigtriangledown^2 \Upsilon \mathtt{t}\left(x,y,z,t\right)}{\partial x}$$
$$+2\mathtt{f}\mathcal{U}_{\Upsilon \mathtt{c}}\left(x,y,z,t\right)\frac{\partial \Upsilon \mathtt{t}\left(x,y,z,t\right)}{\partial x}+\mathtt{J}\left(\Upsilon \mathtt{t}\left(x,y,z,t\right),\bigtriangledown^2\Upsilon \mathtt{c}\left(x,y,z,t\right)\right)$$
$$+\mathtt{J}\left(\Upsilon \mathtt{c}\left(x,y,z,t\right),\bigtriangledown^2\Upsilon \mathtt{t}\left(x,y,z,t\right)\right)-2\mathtt{f}\mathtt{J}\left(\Upsilon \mathtt{t}\left(x,y,z,t\right),\Upsilon \mathtt{c}\left(x,y,z,t\right)\right)$$
$$=-\frac{\sqrt{\mathcal{E}}}{\theta_{\mathcal{A}}}\bigtriangledown^2\Upsilon \mathtt{c}\left(x,y,z,t\right)+\frac{\bigtriangledown^4\Upsilon \mathtt{c}\left(x,y,z,t\right)-2\mathtt{f}\bigtriangledown^2\Upsilon \mathtt{c}\left(x,y,z,t\right)}{\varkappa} \tag{5.6}$$

with a spectral representations for orthogonal functions (5.5) and (5.6) similar to Chapter 2 such that:

$$\Upsilon\frac{\mathtt{c}}{\mathtt{t}}\left(x,y,z,t\right)=\sum_{n=1}^{N}\varphi_{\left\{n,\Upsilon\frac{\mathtt{c}}{\mathtt{t}}\right\}}\left(t\right)\cos\left(n\pi y\right)+\sum_{n=1}^{N}\sum_{m=1}^{M}\sin\left(n\pi y\right)$$
$$\times\left(\varphi_{\left\{m,n,\Upsilon\frac{\mathtt{c}}{\mathtt{t}}\right\}}\left(t\right)\cos\left(\frac{2m\pi x}{\alpha}\right)+\phi_{\left\{m,n,\Upsilon\frac{\mathtt{c}}{\mathtt{t}}\right\}}\left(t\right)\sin\left(\frac{2m\pi x}{\alpha}\right)\right) \tag{5.7}$$

5.1.3.2 Haines and Holland process [29]

$$\frac{\partial Q\left(x,y,z,t\right)}{\partial t}+\mathtt{J}\left(F\left(x,y,z,t\right),\mathcal{Q}\left(x,y,z,t\right)\right)=1_{l=1}u\left(x,y,t\right)+\omega\left(x,y,z,t\right)\frac{\partial^3 W\left(x,y,z,t\right)}{\partial x\partial y\partial t}$$
$$-\left(b+S\left(x\right)\right)\bigtriangledown^2\left(F\left(x,y,z,t\right)-F^I\left(x,y,z,t\right)\right)+\alpha\bigtriangledown^4\left(F\left(x,y,z,t\right)-F^I\left(x,y,z,t\right)\right) \tag{5.8}$$

$$\mathcal{Q}\left(x,y,z,t\right)=\bigtriangledown^2F\left(x,y,z,t\right)+\mathcal{B}y-\mathtt{f}\Delta F\left(x,y,z,t\right) \tag{5.9}$$

Let $\mathcal{B}=1.6\times10^{-11}\left(ms\right)^{-1}$, $\mathtt{f}=7.844\times10^{-13}\left(m\right)^{-2}$, $\Delta x=\Delta y=\frac{200km}{6{,}000km}$, $b=1.92\times10^{-7}\left(s\right)^{-1}$, $\alpha=4\times10^5\frac{m^2}{s}$, $u\left(x,y,t\right)=u\left(x,y\right)\cos\left(\frac{2\pi}{4{,}000km}x-ct\right)$ such that the period of the wave-maker corresponds to 4.5 days, $v\left(x,y\right)=A\sin\left(\frac{\left(x-x_0\right)\pi}{6{,}000km}\right)\sin\left(\frac{\left(y-y_0\right)\pi}{3{,}600km}\right)$ when $x\in\left[0,6000km\right]$ and $y\in\left[0,3600km\right]$. Further, $F^I\left(x,y,z_1,t\right)=0$, $F^I\left(x,y,z_2,t\right)=-\overline{\left\|\mathcal{U}_{l=1}\right\|_2}y$, $\mathcal{Q}^I\left(x,y,z_1,t\right)=\left(\mathcal{B}-\overline{\left\|\mathcal{U}_{l=1}\right\|_2}\nu^2\right)y$,

$\mathcal{Q}^I(x,y,z_2,t) = \left(\mathcal{B} + \overline{\|\mathcal{U}_{l=1}\|_2}\nu^2\right) y$, and $S(x)$ is the vorticity dissipation term which increases b of (5.8) 'by a factor of 1,000 in the last fifth of the channel to provide a sponge to prevent the re-circulation of the wave maker eddies.'

This model attempts to describe how geographically stable weather fronts are created and maintained for seemingly long periods of time. Known as blocking, these stable weather fronts are important to weather prediction since they cause relatively large changes in the flow of major weather patterns due to their resistance to movement. Regarding the physical model, instead of using a temperature difference to drive wave patterns in the water, this model propagates waves with a physical wave maker to examine baroclinic instability that excites blocking. By altering the meridianal shear in the upper layer, blocking can be excited and maintained from high-frequency eddy activity originating from below.

5.1.3.3 Lee process [42]

$$\frac{\partial Q(x,y,z,t)}{\partial t} + \mathrm{J}\left(F(x,y,z,t), \mathcal{Q}(x,y,z,t)\right) = \frac{(-1)^l}{30}\left(\frac{\Delta F(x,y,z_1,t)}{2} - f(y)\right)$$
$$-1_{l=2}a_m \bigtriangledown^2 F(x,y,z_2,t) - 0.006 \bigtriangledown^6 F(x,y,z,t)\,\omega(x,y,z,t)\,\frac{\partial^3 W(x,y,z,t)}{\partial x \partial y \partial t} \tag{5.10}$$

$$\mathcal{Q}(x,y,z,t) = \bigtriangledown^2 F(x,y,z,t) + \mathcal{B}y + \frac{(-1)^l}{2}\Delta F(x,y,z_1,t) \tag{5.11}$$

where $f(y)$ is the radiative equilibrium temperature and $\mathcal{U} = -2\frac{\partial f(x,y,t)}{\partial y} = 1$ if $|y-45| \leq \alpha$ or $e^{-\frac{(y-45)^2}{}}$ if $|y-45| \geq \alpha$. This model attempts to describe aspects of eddy fluxes and eddy energy that are associated with multiple zonal jets focusing on the transition from a singe get to a double jet state.

5.1.4 Other papers and processes

The literature over the past half-century in this field has been quite extensive, hence, some articles of interest include:

•[11] proves results for nonlinear stochastic evolution equations such as the stochastic Navier-Stokes equation in any dimension with general noise.

•[14] proves global existence and uniqueness for $\frac{\partial \mathcal{Q}(X)}{\partial t} + \mathcal{U}\cdot\bigtriangledown\mathcal{Q}(X) + K\left(-\bigtriangledown^2 \mathcal{Q}(X)\right)^\theta = f(X)$ when $\theta \in \left(\frac{1}{2}, 1\right]$. They further show that weak solutions also exist globally, but uniqueness is only shown for the class of strong solutions.

•[16] shows temporally almost periodic solution exists to the deterministic case of (5.1) and this solution is dependent upon the square integral of the wind.

•C. Basdevant and R. Sadourny wrote 'Ergodic properties of inviscid truncated models of two-dimensional incompressible flows,' Journal of Fluid Mechanic 1975, Volume 6. This is an excellent introduction to systems constrained to a finite number of degrees of freedom.

•Jiménez, Moffatt, and Vasco discuss the elliptic nature of the vorticity distribution in 'The structure of the vortices in freely decaying two-dimensional turbulence,' Journal of Fluid Mechanic 1996, Volume 313.

•Merryfield and Holloway wrote 'Inviscid quasi-geostrophic flow over topography: testing statistical mechanical theory,' Journal of Fluid Mechanic 1996, Volume 309. Their simulations for barotropic QG flow provided a basis for this chapter.

•Almgren, Bell, Colella, and Marthaler's wrote 'A Cartesian grid projection method for the incompressible Euler equations in complex geometries,' SIAM Journal of Scientific Computing, Volume 18, Number 5, 1997. They demonstrated a strong connection between the Euler equations on a uniform $\mathbb{Z}^d$ and the methods used to solve elliptic and hyperbolic PDE's; hence it is the errors at the boundary that cause significant numerical problems in any FDSy or FESy.

•Ramírez-Piscina, Sancho, and Hernández-Machado consider equations of the canonical form $\frac{\partial F(X)}{\partial t} = f\left(F\left(X\right), \bigtriangledown F\left(X\right)\right) + g\left(F\left(X\right), \bigtriangledown F\left(X\right)\right) \frac{\partial W(X)}{\partial X}$ where $\left\{f\left(\cdot\right), g\left(\cdot\right)\right\}$ are nonlinear functions in 'Numerical algorithm for the Ginzburg-Landau equations with multiplicative noise: Application to domain growth,' Physical Review B, Volume 48, Number 1, July, 1993. Further insight is gained in the multiplicative noise on a $\mathbb{R}^2_{+t}$ domain in Ramírez-Piscina, Sancho, et all; 'External Fluctuations in Front Propagation,' Physical Review Letters, Volume 76, Number 17, 22 April 1996.

•Yavneh, Shchepetkin, McWilliams, and Graves wrote 'Multigrid Solution of Rotating, Stably Stratified Flows,' Journal of Computational Physics, volume 136, pages 245-262, 1997. They use balance equations to describe turbulent fluid dynamics, which is similar to elliptic processes.

•Duan and Kloeden wrote 'Dissipative Quasi-Geostrophic Motion under Temporally Almost Periodic Forcing,' Journal of Mathematical Analysis and Applications, Number 236, pages 74-85, 1999. They discus barotropic QG flow model $\frac{\partial \bigtriangledown^2 F(x,y,t)}{\partial t} + \mathrm{J}\left(F\left(x,y,t\right), \bigtriangledown^2 F\left(x,y,t\right)\right) + \mathcal{B}\frac{\partial F(x,y,t)}{\partial x} = \nu \bigtriangledown^4 F\left(x,y,t\right)$
$-\mathcal{E} \bigtriangledown^2 F\left(x,y,t\right) + f\left(x,y,t\right).$

•Timothy DelSole and Brian F. Farrell wrote 'A Stochastically Excited Linear System as a Model for Quasi-Geostrophic Turbulence: Analytic Results for One- and Two-Layer Fluids,' American Meteorological Society, 15 July 1995, pages 2531-2547. They explore the hypothesis that nonlinear eddy interactions in QG turbulence can be parameterized as a stochastic excitation plus an augmented

dissipation in a statistically stationary equilibrium.

•Brian F. Farrell and Petros J. Ioannou wrote 'Stochastic Dynamics of Baroclinic Waves,' Journal of the Atmospheric Sciences, Volume 50, Number 24, 1993, pages 4044-4057. They explore dissipative baroclinic shear flows subject to additive stochastic excitation.

•Victor I. Shrira wrote 'Surface waves on shear currents: solution of the boundary-value problem,' Journal of Fluid Mechanics, Volume 252, 1993, pages 265-584. The author discusses gravity-capillary waves and uses a closed loop feedback technique to show existence and convergence.

•Basdevant and Sadourny wrote 'Ergodic properties of inviscid truncated models of two-dimensional incompressible flows,' Journal of Fluid Mechanics, Volume 69, 1975, pages 673-688. This paper deals with the numerical approximation of Navier-Stokes equations.

•Pratt and Pedlosky wrote 'Linear and nonlinear barotropic instability of geostrophic shear layers,' Journal of Fluid Mechanics, Volume 224, 1991, pages 49-76. The authors discuss evolution of unstable waves from initially small amplitude waves.

•James, Jonas, and Farnell wrote 'A combined laboratory and numerical study of fully developed steady baroclinic waves in a cylindrical annulus,' Quart. J. R. Met. Soc., Volume 107, 1981, pages 51-78. The authors explore how to construct numerical QG systems.

•Brian R. Wetton wrote 'Analysis of the spatial error for a class of finite difference methods for viscous incompressible flow,' SIAM Journal of Numerical Analysis, Volume 34, Number 2, April 1997, pages 723-755. This paper explores several first and second order FDSy's for incompressible flow and derives rates of convergence using a 'careful numerical study.'

•Galves, Olivieri and Vares wrote 'Metastability for a class of dynamical systems subject to small random perturbations,' The Annals of Probability, Volume 15, Number 4, April 1987, pages 1288-1305. This paper considers dynamical systems in $\mathbb{R}^d$ subject to small random disturbances and proves convergence in law when properly normalized to a Markov process.

5.1.4.1 Lewis process [43]

Baroclinic Equation:

$$\frac{\partial \bigtriangledown^2 \Upsilon c - 2f\Upsilon c}{\partial t} + \mathcal{B}\frac{\partial \Upsilon c}{\partial x} + J\left(\Upsilon t, \bigtriangledown^2 \Upsilon c\right) + J\left(\Upsilon c, \bigtriangledown^2 \Upsilon t\right)$$
$$+2fJ\left(\Upsilon c, \Upsilon t\right) = -\frac{\bigtriangledown^2 \Upsilon c}{\mathcal{E}} + \frac{\bigtriangledown^2\left(\bigtriangledown^2 \Upsilon c - 2f\Upsilon c\right)}{\varkappa} - H \qquad (5.12)$$

Barotropic Equation:

$$\frac{\partial \bigtriangledown^2 \Upsilon \mathtt{t}}{\partial t} + \mathcal{B}\frac{\partial \Upsilon \mathtt{t}}{\partial x} + \mathtt{J}\left(\Upsilon \mathtt{c}, \bigtriangledown^2 \Upsilon \mathtt{c}\right) + \mathtt{J}\left(\Upsilon \mathtt{c}, \bigtriangledown^2 \Upsilon \mathtt{c}\right) = -\frac{\bigtriangledown^2 \Upsilon \mathtt{t}}{\mathcal{E}} + \frac{\bigtriangledown^4 \Upsilon \mathtt{t}}{\varkappa} \quad (5.13)$$

where $H = -4\pi^2\left[\frac{1}{r} + \frac{4\pi^2+2F}{Re}\right]\cos(2\pi y)$ represents forced internal heating with wrapping boundary conditions in the x dimension and walls at $y = \{0, 1\}$, $\mathcal{A} = 1s^{-1}$, $\nu = 2 \times 10^{-6}\frac{m^2}{s}$, $\theta_{\mathcal{A}} = 0.067$, $\mathtt{f} = 15$, $\mathcal{E} = 7.5$, $\varkappa = 240$, and $\mathcal{B} = 0.5$.

This model represents a convectional two-layered QG formulation subject to internal diabatic heating resulting in a non-monotonic horizontal temperature gradient on a $\mathcal{B}$ plane in a zonal periodic channel contained between solid ageostrophic boundaries and Ekman layers at the lid and base. This is a harder model to analyze due to the internal heating of the fluid vice boundary heating. Since both vertical and horizontal shear compound the nonlinear interactions of the waves, non-dimensional variables are used with a unit Prandtl number and a spectral representation of orthogonal functions, where:

$$\Upsilon^{\mathtt{c}}_{\mathtt{t}} = \sum_{n=1}^{N} \varphi_{\Upsilon^{\mathtt{c}}_{\mathtt{t}}}(t)\cos(n\pi y) + \sum_{n=1}^{N}\sum_{m=1}^{M}\left(\phi_{\Upsilon^{\mathtt{c}}_{\mathtt{t}}}(t)\cos\left(\tfrac{2m\pi x}{\lambda}\right) + \phi_{\Upsilon^{\mathtt{c}}_{\mathtt{t}}}(t)\sin\left(\tfrac{2m\pi x}{\lambda}\right)\right)\sin(n\pi y)$$

The dominant dissipative term in the model is the Ekman layer and to remove small scale enstrophy, internal viscosity is parameterized as horizontal potential vorticity diffusion which assumes a unit Prandtl number.

5.1.4.2 Spectral process and FESy

Spectral methods for a barotropic vorticity equation with Fourier basis functions are addressed in [32, Section 6-4] and for a description of FESy methods refer to [10] and the early work by Orzag. The spectral representations are similar to the example in Chapter 2 and are more instructive for wave-wave interactions and energy flow, since waves can be decoupled to identify significant wave patterns in the process and by removing a wave, other wave triads distribute the energy. There are some numerical difficulties in the stochastic setting due to the roughness of the driving noise, thus these methods will not be discussed in this text.

5.1.4.3 Assumed solution

Existence and uniqueness results for the deterministic form of (5.1) and

$$\frac{\partial \mathcal{Q}(x,y,z,t)}{\partial t} + \mathtt{J}\left(F(x,y,z,t), \mathcal{Q}(x,y,z,t)\right) + \mathcal{B}\frac{\partial F(x,y,z,t)}{\partial x} = \nu \bigtriangledown^4 F(x,y,z,t) - \mathcal{E}\mathcal{Q}(x,y,z,t) + \frac{\partial W(t)}{\partial t} \quad (5.14)$$

exist, but the inclusion of $d \geq 2$ additive white noise or $d \geq 1$ multiplicative - general white noise remain open problems.

Theorem 5.1.10. *[7, Theorem 1]: Using (QGAIC), there exists a unique global solution $F(X)$ to (5.14).*

Proof. Refer to Appendix B □

As with the elliptic case, a closed form solution cannot be expressed. Given the results of Chapter 3, assume that a Green's function and a Poisson kernel exist and the solution is expressed in an integral form:

$$F(X) = \int_{\delta\mho} H(X;Y) F_{\mho}(Y)\, dY + \int_{\mho} G(X;Y)\, v(F(Y),Y)\, dY + \int_{\mho} G(X;Y)\, \omega(Y)\, dW(Y) \tag{5.15}$$

where $\int_{\mathrm{D}_{j,k,l,m}} g(\cdot)\, df(\cdot) = \int_{t_{m-1}}^{t_m} \int_{x_j-\frac{\Delta x}{2}}^{x_j+\frac{\Delta x}{2}} \int_{y_k-\frac{\Delta y}{2}}^{y_k+\frac{\Delta y}{2}} g(\cdot)\, df(\cdot,l)$,

$\int_{\delta\mho} g(\cdot)\, df(\cdot) = \sum_{o=1}^{l} \int_0^{t_m} \int_{\min(x)}^{\max(x)} \int_{\min(y)}^{\max(y)} 1_{\wp\delta\mho} g(\cdot)\, df(\cdot)$, and

$\int_{\mho} g(\cdot)\, df(\cdot) = \sum_{o=1}^{l} \int_0^{t_m} \int_{\min(x)}^{\max(x)} \int_{\min(y)}^{\max(y)} 1_{\wp\mho} g(\cdot)\, df(\cdot)$. Since the process is both hyperbolic and elliptic, the system must be driven by an additional energy source such as heated walls, added small eddy energy, wave maker, or internal heating; otherwise a state of equilibrium will be reached. The iteration of hyperbolic and elliptic elements accounts for the statement in many QG papers, where a computer model has to 'settle down' or 'overcome errors in the initial conditions' by setting t= 0 after the model has 'run for a while.' One is waiting for the dominant elliptic terms to reach a 'realistic' system.

5.2 Discretisation of the process

Assumption 5.2.1. *A uniform $\mathbb{Z}^d$ is utilised where $\lambda_t = \frac{\Delta t}{\Delta x} \leq O\left(\frac{1}{1000}\right)$.*

Due to the scales involved, it is not unreasonable to expect $\Delta x \leq 200km$ and $\Delta t \leq 10min$, such that the system's FDSc 'characteristic equations' adequately map the $\mathbb{R}^d$ characteristics; similar Assumption 2.3.1 where $\lambda_t \leq 1$. The relevance of adding random noise to a QG process comes from:

•The elimination of the sound and gravity waves from the process.

•The inability to evaluate important characteristics deviations on a much finer scale than can be modeled with a 'reasonable' Δx, hence these variations appear as random perturbations on the meteorological waves. Δx denotes the smallest

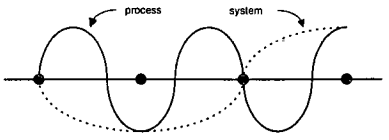

Figure 5.2: Aliasing of waves for a given Δx - [32, Figure 5.9]

'wavelength' that can be represented using the uniform $\mathbb{Z}^d$ space.

•Closed loop feedback and aliasing create nonlinear instability which develops if energy is falsely generated and persistently channeled towards the short resolvable wavelengths of $2\Delta x$ through $4\Delta x$. The Jacobian helps prevent the continued growth of very short waves but as $\Delta x \to 0$, this problem does not subside. Thus truncation and aliasing errors due to harmonic waves often appear as random perturbations.

•The discussions of [21, Section 28] point out that four dimensional models allow both elliptic and hyperbolic behavior in the same domain, thus possibly exhibiting inconsistent FDSc's with determinants equal to zero.

5.2.1 Expansion of terms

The z dimension is a counter for levels 1 and 2, hence, $l \in \{1, 2\}$ and a Brownian sheet is generated for each (x, y, t) level.

Lemma 5.2.2. *When using a uniform $\mathbb{Z}^4$ space:*

$\bullet \mathcal{B}y_k = \mathcal{B}(y_0 + k\Delta y) = \mathcal{B}(y_0 + k\lambda_y \Delta x)$

$\bullet \int_{\mathtt{D}_{j,k,l,m}} \omega(x,y,z,t) \frac{W(x,y,z_l,t)}{\partial x \partial y \partial t} dxdydt = \omega_{j,k,l,m} \frac{\mathbb{W}(\mathtt{D}_{j,k,l,m})}{\Delta x \Delta y \Delta t} + K_\omega \max(1, \lambda_y, \lambda_t) \frac{\mathbb{W}(\mathtt{D}_{j,k,l,m})}{\lambda_y \lambda_t \Delta x^2}$

$\bullet a\Delta F(x_j, y_k, z_l, t_m) = a\left(\widehat{F}_{j,k,l,m} - \widehat{F}_{j,k,\neq l,m}\right) + a\left(\mathfrak{e}\left(\widehat{F}_{j,k,l,m}\right) - \mathfrak{e}\left(\widehat{F}_{j,k,\neq l,m}\right)\right)$

$\bullet a\frac{\partial F(x_j,y_k,z_l,t_m)}{\partial t} = \frac{a}{\lambda_t \Delta x}\left(\widehat{F}_{j,k,l,m+1} - \widehat{F}_{j,k,l,m}\right) + \frac{a}{\lambda_t \Delta x}\left(\mathfrak{e}\left(\widehat{F}_{j,k,l,m+1}\right) + \mathfrak{e}\left(\widehat{F}_{j,k,l,m}\right)\right)$
$+ \frac{a\Delta t}{2}\frac{\partial^2 F(\cdot)}{\partial t^2}$

$\bullet a\frac{\partial F(x_j,y_k,z_l,t_m)}{\partial x} = \frac{a}{\Delta x}\left(\widehat{F}_{j+1,k,l,m} - \widehat{F}_{j,k,l,m}\right) + \frac{a}{\Delta x}\left(\mathfrak{e}\left(\widehat{F}_{j+1,k,l,m}\right) - \mathfrak{e}\left(\widehat{F}_{j,k,l,m}\right)\right)$
$+ \frac{a\Delta x}{2}\frac{\partial^2 F(\cdot)}{\partial x^2}$

$\bullet a\frac{\partial F(x_j,y_k,z_l,t_m)}{\partial y} = \frac{a}{\lambda_y \Delta x}\left(\widehat{F}_{j,k+1,l,m} - \widehat{F}_{j,k,l,m}\right) + \frac{a}{\lambda_y \Delta x}\left(\mathfrak{e}\left(\widehat{F}_{j,k+1,l,m}\right) - \mathfrak{e}\left(\widehat{F}_{j,k,l,m}\right)\right)$
$+ \frac{a\Delta x}{2}\frac{\partial^2 F(\cdot)}{\partial y^2}$

Proof. The first term is trivial and use either Assumption 5.1.7 or a Taylor expansion to yield the second term. For the remaining terms, multiply by a constant a, and substitute $F(\cdot) = \widehat{F}(\cdot) + \mathfrak{e}\left(\widehat{F}(\cdot)\right)$ to yield the desired results. □

Lemma 5.2.3. $a \bigtriangledown^2 F(x_j, y_k, z_l, t_m) = -\frac{2a}{\Delta x^2}\left(1 + \frac{1}{\lambda_y^2}\right)\widehat{F}_{j,k,l,m}$

$$+\frac{a}{\Delta x^2}\left(\widehat{F}_{j+1,k,l,m}+\widehat{F}_{j-1,k,l,m}+\frac{1}{\lambda_y^2}\left(\widehat{F}_{j,k+1,l,m}+\widehat{F}_{j,k-1,l,m}\right)\right)$$
$$+\frac{a}{\Delta x^2}\left(\mathfrak{e}\left(\widehat{F}_{j+1,k,l,m}\right)+\mathfrak{e}\left(\widehat{F}_{j-1,k,l,m}\right)+\frac{1}{\lambda_y^2}\left(\mathfrak{e}\left(\widehat{F}_{j,k+1,l,m}\right)+\mathfrak{e}\left(\widehat{F}_{j,k-1,l,m}\right)\right)\right)$$
$$-\frac{2a}{\Delta x^2}\left(1+\frac{1}{\lambda_y^2}\right)\mathfrak{e}\left(\widehat{F}_{j,k,l,m}\right)+a\frac{\Delta x^2}{12}\frac{\partial^4 F(\cdot)}{\partial x^4}+a\frac{\Delta y^2}{12}\frac{\partial^4 F(\cdot)}{\partial y^4}.$$

Proof. Using (1.9), $\nabla^2 F\left(x_j,y_k,z_l,t_m\right)=\frac{\partial^2 F(x_j,y_k,z_l,t_m)}{\partial x^2}+\frac{\partial^2 F(x_j,y_k,z_l,t_m)}{\partial y^2}$
$=\frac{\Delta_c^2 F(x_j,y_k,z_l,t_m)}{\Delta^2 x}+\frac{\Delta_c^2 F(x_j,y_k,z_l,t_m)}{\Delta^2 y}+\frac{\Delta x^2}{12}\frac{\partial^4 F(\cdot)}{\partial x^4}+\frac{\Delta y^2}{12}\frac{\partial^4 F(\cdot)}{\partial x^4}$
$=\frac{1}{\Delta x^2}\left(F_{j+1,k,l,m}+F_{j-1,k,l,m}\right)+\frac{1}{\Delta y^2}\left(F_{j,k+1,l,m}+F_{j,k-1,l,m}\right)-\frac{2}{\Delta x^2}\left(1+\frac{1}{\lambda_y^2}\right)F_{j,k,l,m}$
$+\frac{\Delta x^2}{12}\frac{\partial^4 F(\cdot)}{\partial x^4}+\frac{\Delta y^2}{12}\frac{\partial^4 F(\cdot)}{\partial y^4}$. Substituting approximations and errors yields the desired results. □

Lemma 5.2.4. *a* $\nabla^4 F\left(x_j,y_k,z_l,t_m\right)=\frac{6a}{\Delta x^4}\left(1+\frac{1}{\lambda_y^4}\right)\widehat{F}_{j,k,l,m}$
$$+\frac{a}{\Delta x^4}\left(\widehat{F}_{j+2,k,l,m}-4\widehat{F}_{j+1,k,l,m}-4\widehat{F}_{j-1,k,l,m}+\widehat{F}_{j-2,k,l,m}\right.$$
$$\left.+\frac{1}{\lambda_y^4}\left(\widehat{F}_{j,k+2,l,m}-4\widehat{F}_{j,k+1,l,m}-4\widehat{F}_{j,k-1,l,m}+\widehat{F}_{j,k-2,l,m}\right)\right)$$
$$+\frac{6a}{\Delta x^4}\left(1+\frac{1}{\lambda_y^4}\right)\mathfrak{e}\left(\widehat{F}_{j,k,l,m}\right)+O\left(\Delta x^4\right)$$
$$+\frac{a}{\Delta x^4}\left(\mathfrak{e}\left(\widehat{F}_{j+2,k,l,m}\right)-4\mathfrak{e}\left(\widehat{F}_{j+1,k,l,m}\right)-4\mathfrak{e}\left(\widehat{F}_{j-1,k,l,m}\right)+\mathfrak{e}\left(\widehat{F}_{j-2,k,l,m}\right)\right.$$
$$\left.+\frac{1}{\lambda_y^4}\left(\mathfrak{e}\left(\widehat{F}_{j,k+2,l,m}\right)-4\mathfrak{e}\left(\widehat{F}_{j,k+1,l,m}\right)-4\mathfrak{e}\left(\widehat{F}_{j,k-1,l,m}\right)+\mathfrak{e}\left(\widehat{F}_{j,k-2,l,m}\right)\right)\right)$$
and $a\ \nabla^6 F\left(x,y,z_l,t\right)=-\frac{20a}{\Delta x^6}\left(1+\frac{1}{\lambda_y^6}\right)\widehat{F}_{j,k,l,m}$
$$+\frac{a}{\Delta x^6}\left(\widehat{F}_{j+3,k,l,m}-6\widehat{F}_{j+2,k,l,m}+15\widehat{F}_{j+1,k,l,m}+15\widehat{F}_{j-1,k,l,m}-6\widehat{F}_{j-2,k,l,m}+\widehat{F}_{j-3,k,l,m}\right.$$
$$\left.+\frac{1}{\lambda_y^6}\left(\widehat{F}_{j,k+3,l,m}-6\widehat{F}_{j,k+2,l,m}+15\widehat{F}_{j,k+1,l,m}+15\widehat{F}_{j,k-1,l,m}-6\widehat{F}_{j,k-2,l,m}+\widehat{F}_{j,k-3,l,m}\right)\right)$$
$$-\frac{20a}{\Delta x^6}\left(1+\frac{1}{\lambda_y^6}\right)\mathfrak{e}\left(\widehat{F}_{j,k,l,m}\right)+O\left(\Delta x^6\right)$$
$$+\frac{a}{\Delta x^6}\left(\mathfrak{e}\left(\widehat{F}_{j+3,k,l,m}\right)-6\mathfrak{e}\left(\widehat{F}_{j+2,k,l,m}\right)+15\mathfrak{e}\left(\widehat{F}_{j+1,k,l,m}\right)+15\mathfrak{e}\left(\widehat{F}_{j-1,k,l,m}\right)\right.$$
$$-6\mathfrak{e}\left(\widehat{F}_{j-2,k,l,m}\right)+\mathfrak{e}\left(\widehat{F}_{j-3,k,l,m}\right)+\frac{1}{\lambda_y^6}\left(\mathfrak{e}\left(\widehat{F}_{j,k+3,l,m}\right)-6\mathfrak{e}\left(\widehat{F}_{j,k+2,l,m}\right)\right.$$
$$\left.\left.\left.+15\mathfrak{e}\left(\widehat{F}_{j,k+1,l,m}\right)+15\mathfrak{e}\left(\widehat{F}_{j,k-1,l,m}\right)-6\mathfrak{e}\left(\widehat{F}_{j,k-2,l,m}\right)+\mathfrak{e}\left(\widehat{F}_{j,k-3,l,m}\right)\right)\right).$$

Proof. Using the $[MPR]$ notation of Chapter 2,
$\nabla^4 F\left(x_j,y_k,z_l,t_m\right)=\frac{\partial^4 F(x_j,y_k,z_l,t_m)}{\partial x^4}+\frac{\partial^4 F(x_j,y_k,z_l,t_m)}{\partial y^4}$
$=\frac{\Delta_c^4 F(x_j,y_k,z_l,t_m)}{\Delta^4 x}+\frac{\Delta_c^4 F(x_j,y_k,z_l,t_m)}{\Delta^4 y}+\frac{\Delta x^4}{360}\frac{\partial^6 F(\cdot)}{\partial^6 x}+\frac{\Delta y^4}{360}\frac{\partial^6 F(\cdot)}{\partial^6 y}$
$=\frac{1}{\Delta x^4}\left(F_{j+2,k,l,m}-4F_{j+1,k,l,m}+6F_{j,k,l,m}-4F_{j-1,k,l,m}+F_{j-2,k,l,m}\right)$
$+\frac{1}{\Delta y^4}\left(F_{j,k+2,l,m}-4F_{j,k+1,l,m}+6F_{j,k,l,m}-4F_{j,k-1,l,m}+F_{j,k-2,l,m}\right)+O\left(\Delta x^4\right)$
$=\frac{1}{\Delta x^4}\left(F_{j+2,k,l,m}-4F_{j+1,k,l,m}-4F_{j-1,k,l,m}+F_{j-2,k,l,m}\right)+\frac{6}{\Delta x^4}\left(1+\frac{1}{\lambda_y^4}\right)F_{j,k,l,m}$
$+\frac{1}{\Delta y^4}\left(F_{j,k+2,l,m}-4F_{j,k+1,l,m}-4F_{j,k-1,l,m}+F_{j,k-2,l,m}\right)+O\left(\Delta x^4\right)$
$=\frac{6}{\Delta x^4}\left(1+\frac{1}{\lambda_y^4}\right)\widehat{F}_{j,k,l,m}+\frac{1}{\Delta x^4}\left(\widehat{F}_{j+2,k,l,m}-4\widehat{F}_{j+1,k,l,m}-4\widehat{F}_{j-1,k,l,m}+\widehat{F}_{j-2,k,l,m}\right.$
$\left.+\frac{1}{\lambda_y^4}\left(\widehat{F}_{j,k+2,l,m}-4\widehat{F}_{j,k+1,l,m}-4\widehat{F}_{j,k-1,l,m}+\widehat{F}_{j,k-2,l,m}\right)\right)+O\left(\Delta x^4\right).$
Repeating this process for the $\nabla^6 F\left(x,y,z_l,t\right)$ term gives
$\nabla^6 F\left(x_j,y_k,z_l,t_m\right)=\frac{\partial^6 F(x_j,y_k,z_l,t_m)}{\partial x^6}+\frac{\partial^6 F(x_j,y_k,z_l,t_m)}{\partial y^6}$

$= \frac{\Delta_c^6 F(x_j,y_k,z_l,t_m)}{\Delta^6 x} + \frac{\Delta_c^6 F(x_j,y_k,z_l,t_m)}{\Delta^6 y} + O\left(\Delta x^6\right)$
$= \frac{1}{\Delta x^6}\left(F_{j+3,k,l,m} - 6F_{j+2,k,l,m} + 15F_{j+1,k,l,m} + 15F_{j-1,k,l,m} - 6F_{j-2,k,l,m} + F_{j-3,k,l,m}\right.$
$+\frac{1}{\lambda_y^6}\left(F_{j,k+3,l,m} - 6F_{j,k+2,l,m} + 15F_{j,k+1,l,m} + 15F_{j,k-1,l,m} - 6F_{j,k-2,l,m} + F_{j,k-3,l,m}\right)\Big)$
$-\frac{20}{\Delta x^6}\left(1+\frac{1}{\lambda_y^6}\right)F_{j,k,l,m} + O\left(\Delta x^6\right)$. Multiplying both expansions by a constant and replacing terms with their approximation and error yields the desired results.

□

Lemma 5.2.5. $S\left(x_j\right)\bigtriangledown^2\left(F\left(x_j,y_k,z_l,t_m\right) - F^I\left(x_j,y_k,z_l,t_m\right)\right)$
$= -S\left(x_j\right)\frac{2a}{\Delta x^2}\left(1+\frac{1}{\lambda_y^2}\right)\widehat{F}_{j,k,l,m} - S\left(x\right)\frac{2a}{\Delta x^2}\left(1+\frac{1}{\lambda_y^2}\right)\mathfrak{e}\left(\widehat{F}_{j,k,l,m}\right) + O\left(\Delta x^2\right)$
$+S\left(x_j\right)\frac{a}{\Delta x^2}\left(\widehat{F}_{j+1,k,l,m} + \widehat{F}_{j-1,k,l,m} + \frac{1}{\lambda_y^2}\left(\widehat{F}_{j,k+1,l,m} + \widehat{F}_{j,k-1,l,m}\right)\right)$
$+S\left(x_j\right)\frac{a}{\Delta x^2}\left(\mathfrak{e}\left(\widehat{F}_{j+1,k,l,m}\right) + \mathfrak{e}\left(\widehat{F}_{j-1,k,l,m}\right) + \frac{1}{\lambda_y^2}\left(\mathfrak{e}\left(\widehat{F}_{j,k+1,l,m}\right) + \mathfrak{e}\left(\widehat{F}_{j,k-1,l,m}\right)\right)\right)$
and $a\bigtriangledown^4\left(F\left(x_j,y_k,z_l,t_m\right) - F^I\left(x_j,y_k,z_l,t_m\right)\right) = S\left(x_j\right)\frac{6a}{\Delta x^4}\left(1+\frac{1}{\lambda_y^4}\right)\widehat{F}_{j,k,l,m}$
$+S\left(x_j\right)\frac{a}{\Delta x^4}\left(\widehat{F}_{j+2,k,l,m} - 4\widehat{F}_{j+1,k,l,m} - 4\widehat{F}_{j-1,k,l,m} + \widehat{F}_{j-2,k,l,m}\right.$
$\left.+\frac{1}{\lambda_y^4}\left(\widehat{F}_{j,k+2,l,m} - 4\widehat{F}_{j,k+1,l,m} - 4\widehat{F}_{j,k-1,l,m} + \widehat{F}_{j,k-2,l,m}\right)\right)$
$+S\left(x_j\right)\frac{6a}{\Delta x^4}\left(1+\frac{1}{\lambda_y^4}\right)\mathfrak{e}\left(\widehat{F}_{j,k,l,m}\right)O\left(\Delta x^4\right)$
$+S\left(x_j\right)\frac{a}{\Delta x^4}\left(\mathfrak{e}\left(\widehat{F}_{j+2,k,l,m}\right) - 4\mathfrak{e}\left(\widehat{F}_{j+1,k,l,m}\right) - 4\mathfrak{e}\left(\widehat{F}_{j-1,k,l,m}\right) + \mathfrak{e}\left(\widehat{F}_{j-2,k,l,m}\right)\right.$
$\left.+\frac{1}{\lambda_y^4}\left(\mathfrak{e}\left(\widehat{F}_{j,k+2,l,m}\right) - 4\mathfrak{e}\left(\widehat{F}_{j,k+1,l,m}\right) - 4\mathfrak{e}\left(\widehat{F}_{j,k-1,l,m}\right) + \mathfrak{e}\left(\widehat{F}_{j,k-2,l,m}\right)\right)\right)$.

Proof. Using Proposition 5.2.3 and (1.9) yields
$S\left(x_j\right)\bigtriangledown^2\left(F\left(x_j,y_k,z_l,t_m\right) - F^I\left(x_j,y_k,z_l,t_m\right)\right)$
$= S\left(x_j\right)\left(\frac{\partial^2\left(F(x_j,y_k,z_l,t_m) - F^I(x_j,y_k,z_l,t_m)\right)}{\partial x^2} + \frac{\partial^2\left(F(x,y,z_l,t) - F^I(x,y,z_l,t)\right)}{\partial y^2}\right)$
$= S\left(x_j\right)\left(\frac{\Delta_c^2\left(F(x_j,y_k,z_l,t_m) - F^I(x_j,y_k,z_l,t_m)\right)}{\Delta x^2} + \frac{\Delta_c^2\left(F(x,y,z_l,t) - F^I(x,y,z_l,t)\right)}{\Delta y^2}\right) + O\left(\Delta x^2\right)$
$= S\left(x_j\right)\left(-\frac{2a}{\Delta x^2}\left(1+\frac{1}{\lambda_y^2}\right)\left(F_{j,k,l,m} - F^I_{j,k,l,m}\right) + \frac{a}{\Delta x^2}\left(F_{j+1,k,l,m} - F^I_{j+1,k,l,m} + F_{j-1,k,l,m}\right.\right.$
$\left.\left.-F^I_{j-1,k,l,m} + \frac{1}{\lambda_y^2}\left(F_{j,k+1,l,m} - F^I_{j,k+1,l,m} + \widehat{F}_{j,k-1,l,m} - F^I_{j,k-1,l,m}\right)\right)\right) + O\left(\Delta x^2\right)$.
From [29, (5)], $F^I_{l=1}\left(\cdot\right) = 0$, $F^I_{l=2}\left(x,y,t\right) = -\overline{\|\mathcal{U}_1\|_2}y$, so canceling $F^I\left(\cdot\right)$ terms since $\widehat{F}^I_{\cdot,k,\cdot} - \widehat{F}^I_{\cdot,k,\cdot} = 0$ and $\widehat{F}^I_{\cdot,k+1,\cdot} - \widehat{F}^I_{\cdot,k,\cdot} - \widehat{F}^I_{\cdot,k,\cdot} + \widehat{F}^I_{\cdot,k-1,\cdot} = 0$ gives
$\bigtriangledown^2\left(F\left(x_j,y_k,z_l,t_m\right) - F^I\left(x_j,y_k,z_l,t_m\right)\right) = -S\left(x\right)\frac{2a}{\Delta x^2}\left(1+\frac{1}{\lambda_y^2}\right)F_{j,k,l,m}$
$+S\left(x\right)\frac{a}{\Delta x^2}\left(F_{j+1,k,l,m} + F_{j-1,k,l,m} + \frac{1}{\lambda_y^2}\left(F_{j,k+1,l,m} + F_{j,k-1,l,m}\right)\right)$.
For the fourth order term, use Proposition 5.2.4 to yield
$a\bigtriangledown^4\left(F\left(x_j,y_k,z_l,t_m\right) - F^I\left(x_j,y_k,z_l,t_m\right)\right)$
$= S\left(x\right)\left(\frac{\partial^4\left(F(x_j,y_k,z_l,t_m) - F^I(x_j,y_k,z_l,t_m)\right)}{\partial x^4} + \frac{\partial^4\left(F(x_j,y_k,z_l,t_m) - Fh^I(x_j,y_k,z_l,t_m)\right)}{\partial y^4}\right)$
$= S\left(x\right)\left(\frac{\Delta_c^4\left(F(x_j,y_k,z_l,t_m) - F^I(x_j,y_k,z_l,t_m)\right)}{\Delta x^4} + \frac{\Delta_c^4\left(F(x_j,y_k,z_l,t_m) - Fh^I(x_j,y_k,z_l,t_m)\right)}{\Delta y^4}\right) + O\left(\Delta x^4\right)$
$= S\left(x\right)\frac{6a}{\Delta x^4}\left(1+\frac{1}{\lambda_y^4}\right)\left(F_{j,k,l,m} - F^I_{j,k,l,m}\right) + S\left(x\right)\frac{a}{\Delta x^4}\left(\left(F_{j+2,k,l,m} - F^I_{j+2,k,l,m}\right)\right.$

$-4\left(F_{j+1,k,l,m}-F^I_{j+1,k,l,m}\right)-4\left(F_{j-1,k,l,m}-F^I_{j-1,k,l,m}\right)+\left(F_{j-2,k,l,m}-F^I_{j-2,k,l,m}\right)$
$+\frac{1}{\lambda_y^4}\left(\left(F_{j,k+2,l,m}-F^I_{j,k+2,l,m}\right)-4\left(F_{j,k+1,l,m}-F^I_{j,k+1,l,m}\right)-4\left(F_{j,k-1,l,m}-F^I_{j,k-1,l,m}\right)\right.$
$\left.+\left(F_{j,k-2,l,m}-F^I_{j,k-2,l,m}\right)\right))+O\left(\Delta x^4\right)$. Canceling $F^I(\cdot)$ terms and replacing terms with their approximation and error yields the desired results. □

Notation 5.2.6. *Let* $\mathfrak{e}\left(\widehat{\mathcal{Q}}_{j,k,l,m}\right)=-\frac{2a}{\Delta x^2}\left(1+\frac{1}{\lambda_y^2}\right)\mathfrak{e}\left(\widehat{F}_{j,k,l,m}\right)$
$+\frac{a}{\Delta x^2}\left(\mathfrak{e}\left(\widehat{F}_{j+1,k,l,m}\right)+\mathfrak{e}\left(\widehat{F}_{j-1,k,l,m}\right)+\frac{1}{\lambda_y^2}\left(\mathfrak{e}\left(\widehat{F}_{j,k+1,l,m}\right)+\mathfrak{e}\left(\widehat{F}_{j,k-1,l,m}\right)\right)\right)$
$-\alpha\left(\mathfrak{e}\left(\widehat{F}_{j,k,l,m}\right)-\mathfrak{e}\left(\widehat{F}_{j,k,\neq l,m}\right)\right)+\frac{\Delta x^2}{12}\frac{\partial^4 F(\cdot)}{\partial x^4}+\frac{\Delta y^2}{12}\frac{\partial^4 F(\cdot)}{\partial x^4}$.

Lemma 5.2.7. *The general format of the potential vorticity is* $\mathcal{Q}(x,y,z_l,t)=\nabla^2F(x,y,z_l,t)+f(x_j,y_k,z_l,t_m)$. *For the numerical examples, let* $\widehat{\mathcal{Q}}_{j,k,l,m}=\nabla^2F(x,y,z_l,t)+\mathcal{B}y-\alpha\Delta F(x,y,z_l,t)$, *where:*
• $\mathcal{Q}(x,y,z_l,t)=\nabla^2F(x,y,z_l,t)+\mathcal{B}y-\mathfrak{f}\Delta F(x,y,z_l,t)$ *for (5.4) and (5.9).*
• $\mathcal{Q}(x,y,z_l,t)=\nabla^2F(x,y,z_l,t)+\mathcal{B}y=\frac{(-1)^{l+1}}{2}\Delta F(x,y,z_1,t)$ *for (5.11).*
Thus, $\mathcal{Q}_{j,k,l,m}=\widehat{\mathcal{Q}}_{j,k,l,m}+\mathfrak{e}\left(\widehat{\mathcal{Q}}_{j,k,l,m}\right)=\nabla^2\widehat{F}_{j,k,l,m}+\mathcal{B}y_k-\alpha\Delta F_{j,k,l,m}+\mathfrak{e}\left(\widehat{\mathcal{Q}}_{j,k,l,m}\right)$
$=-\frac{2}{\Delta x^2}\left(1+\frac{1}{\lambda_y^2}\right)\widehat{F}_{j,k,l,m}+\mathcal{B}k\Delta y-\alpha\Delta\widehat{F}_{j,k,l,m}+\mathfrak{e}\left(\widehat{\mathcal{Q}}_{j,k,l,m}\right)$
$+\frac{1}{\Delta x^2}\left(\widehat{F}_{j+1,k,l,m}+\widehat{F}_{j-1,k,l,m}+\frac{1}{\lambda_y^2}\left(\widehat{F}_{j,k+1,l,m}+\widehat{F}_{j,k-1,l,m}\right)\right)$.

Proof. $\mathcal{Q}(x,y,z_l,t)=\nabla^2F(x,y,z_l,t)+\mathcal{B}y-\alpha\Delta F_{j,k,l,m}=\frac{\partial^2\widehat{F}(x_j,y_k,z_l,t_m)}{\partial x^2}$
$+\frac{\partial^2\widehat{F}(x_j,y_k,z_l,t_m)}{\partial y^2}+\mathcal{B}y_k-\alpha\Delta\widehat{F}(x_j,y_k,z_l,t_m)$. Using Proposition 5.2.3 and expanding yields $\widehat{\mathcal{Q}}_{j,k,l,m}=\nabla^2\widehat{F}_{j,k,l,m}+\mathcal{B}y_k-\alpha\Delta\widehat{F}_{j,k,l,m}$
$=-\frac{2}{\Delta x^2}\left(1+\frac{1}{\lambda_y^2}\right)\widehat{F}_{j,k,l,m}-\frac{2}{\Delta x^2}\left(1+\frac{1}{\lambda_y^2}\right)\mathfrak{e}\left(\widehat{F}_{j,k,l,m}\right)+\mathcal{B}k\Delta y-\alpha\Delta F_{j,k,l,m}$
$+\frac{1}{\Delta x^2}\left(\widehat{F}_{j+1,k,l,m}+\widehat{F}_{j-1,k,l,m}+\frac{1}{\lambda_y^2}\left(\widehat{F}_{j,k+1,l,m}+\widehat{F}_{j,k-1,l,m}\right)\right)$
$+\frac{1}{\Delta x^2}\left(\mathfrak{e}\left(\widehat{F}_{j+1,k,l,m}\right)+\mathfrak{e}\left(\widehat{F}_{j-1,k,l,m}\right)+\frac{1}{\lambda_y^2}\left(\mathfrak{e}\left(\widehat{F}_{j,k+1,l,m}\right)+\mathfrak{e}\left(\widehat{F}_{j,k-1,l,m}\right)\right)\right)$
$+\frac{\Delta x^2}{12}\frac{\partial^4F(\cdot)}{\partial x^4}+\frac{\Delta y^2}{12}\frac{\partial^4F(\cdot)}{\partial x^4}$. Reduction yields the desired results. □

Lemma 5.2.8. $a\frac{\partial\mathcal{Q}(x_j,y_k,z_l,t_m)}{\partial t}=\frac{a}{\Delta t}\left(-\frac{2}{\Delta x^2}\left(1+\frac{1}{\lambda_y^2}\right)\left(\widehat{F}_{j,k,l,m+1}-\widehat{F}_{j,k,l,m}\right)\right.$
$+\frac{a}{\Delta x^2}\left(\left(\widehat{F}_{j+1,k,l,m+1}-\widehat{F}_{j+1,k,l,m}\right)+\left(\widehat{F}_{j-1,k,l,m+1}-\widehat{F}_{j-1,k,l,m}\right)\right.$
$\left.+\frac{1}{\lambda_y^2}\left(\left(\widehat{F}_{j,k+1,l,m+1}-\widehat{F}_{j,k+1,l,m}\right)+\left(\widehat{F}_{j,k-1,l,m+1}-\widehat{F}_{j,k-1,l,m}\right)\right)\right)$
$\left.-\alpha\Delta\widehat{F}_{j,k,l,m+1}+\alpha\Delta\widehat{F}_{j,k,l,m}+\mathfrak{e}\left(\widehat{\mathcal{Q}}_{j,k,l,m+1}\right)-\mathfrak{e}\left(\widehat{\mathcal{Q}}_{j,k,l,m}\right)+\frac{\lambda_t\Delta x}{2}\frac{\partial^2\mathcal{Q}_{j,k,l,m}}{\partial t^2}\right)$.

Proof. Using (1.8) and substitution from Proposition 5.2.7 yields
$\frac{\partial\mathcal{Q}(x_j,y_k,z_l,t_m)}{\partial t}=\frac{\Delta_f\mathcal{Q}(x_j,y_k,z_l,t_m)}{\Delta t}+\frac{\Delta t}{2}\frac{\partial^2\mathcal{Q}(\cdot)}{\partial t^2}$
$=\frac{1}{\Delta t}\left(\widehat{\mathcal{Q}}_{j,k,l,m+1}+\mathfrak{e}\left(\widehat{\mathcal{Q}}_{j,k,l,m+1}\right)-\widehat{\mathcal{Q}}_{j,k,l,m}-\mathfrak{e}\left(\widehat{\mathcal{Q}}_{j,k,l,m}\right)\right)+\frac{\Delta t}{2}\frac{\partial^2\mathcal{Q}_{j,k,l,m}}{\partial t^2}$. Substitution and multiplying by a constant yields the desired results. □

Lemma 5.2.9. $a\frac{\partial\mathcal{Q}(x_j,y_k,z_l,t_m)}{\partial x}=\frac{a}{2\Delta x}\left(-\frac{2}{\Delta x^2}\left(1+\frac{1}{\lambda_y^2}\right)\left(\widehat{F}_{j+1,k,l,m}-\widehat{F}_{j-1,k,l,m}\right)\right.$
$\left.+\frac{1}{\Delta x^2}\left(\left(\widehat{F}_{j+2,k,l,m}-\widehat{F}_{j,k,l,m}\right)+\left(\widehat{F}_{j,k,l,m}-\widehat{F}_{j-2,k,l,m}\right)\right.\right.$

$$+\frac{1}{\lambda_y^2}\left(\left(\widehat{F}_{j+1,k+1,l,m}-\widehat{F}_{j-1,k+1,l,m}\right)+\left(\widehat{F}_{j+1,k-1,l,m}-\widehat{F}_{j-1,k-1,l,m}\right)\right)\right)$$
$$-\alpha\Delta\widehat{F}_{j+1,k,l,m}+\alpha\Delta\widehat{F}_{j-1,k,l,m}+\mathfrak{e}\left(\widehat{\mathcal{Q}}_{j+1,k,l,m}\right)-\mathfrak{e}\left(\widehat{\mathcal{Q}}_{j-1,k,l,m}\right)+\Delta x\frac{\partial^2\mathcal{Q}_{j,k,l,m}}{\partial x^2}\Big).$$

Proof. Repeat Proposition 5.2.8 with respect x and $2\Delta x$ for a central difference to yield $\frac{\partial\mathcal{Q}(x_j,y_k,z_l,t_m)}{\partial x}=\frac{\Delta_f\widehat{\mathcal{Q}}(x_j,y_k,z_l,t_m)+\Delta_b\widehat{\mathcal{Q}}(x_j,y_k,z_l,t_m)}{2\Delta x}$. Substitution yields the desired results. □

Lemma 5.2.10. $a\frac{\partial\mathcal{Q}(x_j,y_k,z_l,t_m)}{\partial y}=\frac{a}{2\lambda_y\Delta x}\frac{1}{\Delta t}\Big(-\frac{2}{\Delta x^2}\left(1+\frac{1}{\lambda_y^2}\right)\left(\widehat{F}_{j,k+1,l,m}-\widehat{F}_{j,k-1,l,m}\right)$
$$+\frac{1}{\Delta x^2}\left(\left(\widehat{F}_{j+1,k+1,l,m}-\widehat{F}_{j+1,k-1,l,m}\right)+\left(\widehat{F}_{j-1,k+1,l,m}-\widehat{F}_{j-1,k-1,l,m}\right)\right.$$
$$\left.+\frac{1}{\lambda_y^2}\left(\left(\widehat{F}_{j,k+2,l,m}-\widehat{F}_{j,k,l,m}\right)+\left(\widehat{F}_{j,k-1,l,m}-\widehat{F}_{j,k-2,l,m}\right)\right)\right)+\alpha\Delta\widehat{F}_{j,k-1,l,m}$$
$$-\alpha\Delta\widehat{F}_{j,k+1,l,m}+2\mathcal{B}k\Delta y+\left(\mathfrak{e}\left(\widehat{\mathcal{Q}}_{j,k+1,l,m}\right)-\mathfrak{e}\left(\widehat{\mathcal{Q}}_{j,k-1,l,m}\right)\right)+\lambda_y\Delta x\frac{\partial^2\mathcal{Q}_{j,k,l,m}}{\partial y^2}\Big).$$

Proof. Repeat Proposition 5.2.8 with respect y and $2\Delta y$ for a central difference to yield $\frac{\partial\mathcal{Q}(x_j,y_k,z_l,t_m)}{\partial y}=\frac{\Delta_f\widehat{\mathcal{Q}}(x_j,y_k,z_l,t_m)+\Delta_b\widehat{\mathcal{Q}}(x_j,y_k,z_l,t_m)}{2\Delta y}$. Substitution yields the desired results. □

Lemma 5.2.11. $a\bigtriangledown^2\mathcal{Q}(x_j,y_k,z_l,t_m)=-\frac{2a}{\Delta x^2}\left(1+\frac{1}{\lambda_y^2}\right)\widehat{\mathcal{Q}}_{j,k,l,m}$
$$+\frac{a}{\Delta x^2}\left(\widehat{\mathcal{Q}}_{j+1,k,l,m}+\widehat{\mathcal{Q}}_{j-1,k,l,m}+\frac{1}{\lambda_y^2}\left(\widehat{\mathcal{Q}}_{j,k+1,l,m}+\widehat{\mathcal{Q}}_{j,k-1,l,m}\right)\right)$$
$$-\frac{2a}{\Delta x^2}\left(1+\frac{1}{\lambda_y^2}\right)\mathfrak{e}\left(\widehat{\mathcal{Q}}_{j,k,l,m}\right)+\frac{\Delta x^2}{12}\frac{\partial^4\mathcal{Q}_{j,k,l,m}}{\partial x^4}+\frac{\Delta y^2}{12}\frac{\partial^4\mathcal{Q}_{j,k,l,m}}{\partial y^4}$$
$$+\frac{a}{\Delta x^2}\left(\mathfrak{e}\left(\widehat{\mathcal{Q}}_{j+1,k,l,m}\right)+\mathfrak{e}\left(\widehat{\mathcal{Q}}_{j-1,k,l,m}\right)+\frac{1}{\lambda_y^2}\left(\mathfrak{e}\left(\widehat{\mathcal{Q}}_{j,k+1,l,m}\right)+\mathfrak{e}\left(\widehat{\mathcal{Q}}_{j,k-1,l,m}\right)\right)\right).$$

Proof. $\bigtriangledown^2\mathcal{Q}(x_j,y_k,z_l,t_m)=\frac{\partial^2\mathcal{Q}(x_j,y_k,z_l,t_m)}{\partial x^2}+\frac{\partial^2\mathcal{Q}(x_j,y_k,z_l,t_m)}{\partial y^2}$
$=\frac{\Delta_c^2\mathcal{Q}(x_j,y_k,z_l,t_m)}{\Delta^2x}+\frac{\Delta_c^2\mathcal{Q}(x_j,y_k,z_l,t_m)}{\Delta^2y}+\frac{\Delta x^2}{12}\frac{\partial^4\mathcal{Q}(\cdot)}{\partial x^4}+\frac{\Delta y^2}{12}\frac{\partial^4\mathcal{Q}(\cdot)}{\partial x^4}$. Use the same reduction of Proposition 5.2.3 where substitution yields the desired results. □

Lemma 5.2.12. $\mathtt{J}\left(F\left(x_j,y_k,z_l,t_m\right),\mathcal{Q}\left(x_j,y_k,z_l,t_m\right)\right)=$
$$\frac{1}{12\lambda_y\Delta x^2}\Big(\left(\widehat{F}_{j+1,k,l,m}-\widehat{F}_{j-1,k,l,m}\right)\left(\widehat{\mathcal{Q}}_{j,k+1,l,m}-\widehat{\mathcal{Q}}_{j,k-1,l,m}\right)$$
$$-\left(\widehat{\mathcal{Q}}_{j+1,k,l,m}-\widehat{\mathcal{Q}}_{j-1,k,l,m}\right)\left(\widehat{F}_{j,k+1,l,m}-\widehat{F}_{j,k-1,l,m}\right)$$
$$+\widehat{F}_{j+1,k,l,m}\left(\widehat{\mathcal{Q}}_{j+1,k+1,l,m}-\widehat{\mathcal{Q}}_{j+1,k-1,l,m}\right)-\widehat{F}_{j-1,k,l,m}\left(\widehat{\mathcal{Q}}_{j-1,k+1,l,m}-\widehat{\mathcal{Q}}_{j-1,k-1,l,m}\right)$$
$$-\widehat{F}_{j,k+1,l,m}\left(\widehat{\mathcal{Q}}_{j+1,k+1,l,m}-\widehat{\mathcal{Q}}_{j-1,k+1,l,m}\right)+\widehat{F}_{j,k-1,l,m}\left(\widehat{\mathcal{Q}}_{j+1,k-1,l,m}-\widehat{\mathcal{Q}}_{j-1,k-1,l,m}\right)$$
$$+\widehat{\mathcal{Q}}_{j,k+1,l,m}\left(\widehat{F}_{j+1,k+1,l,m}-\widehat{F}_{j-1,k+1,l,m}\right)-\widehat{\mathcal{Q}}_{j,k-1,l,m}\left(\widehat{F}_{j+1,k-1,l,m}-\widehat{F}_{j-1,k-1,l,m}\right)$$
$$-\widehat{\mathcal{Q}}_{j+1,k,l,m}\left(\widehat{F}_{j+1,k+1,l,m}-\widehat{F}_{j+1,k-1,l,m}\right)+\widehat{\mathcal{Q}}_{j-1,k,l,m}\left(\widehat{F}_{j-1,k+1,l,m}-\widehat{F}_{j-1,k-1,l,m}\right)\Big)$$
$$+\max\left(\left|\widehat{\mathcal{Q}}(Y)\right|\mathfrak{eg}\left(\widehat{F}(X)\right),\left|\widehat{F}(Y)\right|\mathfrak{eg}\left(\widehat{\mathcal{Q}}(X)\right)\right)+O(\Delta x),\ \textit{where}$$
$\|X-(x_j,y_k,z_l,t_m)\|_1\leq 2\Delta x$ *and* $\|Y-(x_j,y_k,z_l,t_m)\|_1\leq 2\lambda_y\Delta x$.

Proof. The analytic Jacobian of Definition 5.1.1 can be expressed as
$\mathtt{J}\left(f(x,y),g(x,y)\right)=\frac{\partial f(x,y)}{\partial x}\frac{\partial g(x,y)}{\partial y}-\frac{\partial g(x,y)}{\partial x}\frac{\partial f(x,y)}{\partial y}$
$=\frac{\partial}{\partial x}\left(f(x,y)\frac{\partial g(x,y)}{\partial y}\right)-\frac{\partial}{\partial y}\left(f(x,y)\frac{\partial f(x,y)}{\partial x}\right)$

$= \frac{\partial}{\partial y}\left(g\left(x,y\right)\frac{\partial f(x,y)}{\partial x}\right) - \frac{\partial}{\partial x}\left(g\left(x,y\right)\frac{\partial f(x,y)}{\partial y}\right)$.

Using these representations, FDSc estimates of the Jacobian are

$\bullet \mathrm{J}_1\left(f\left(x_j,y_k\right),g\left(x_j,y_k\right)\right) = \left(\frac{f_{j+1,k}-f_{j-1,k}}{2\Delta x}\right)\left(\frac{g_{j,k+1}-g_{j,k-1}}{2\Delta y}\right)$

$-\left(\frac{g_{j+1,k}-g_{j-1,k}}{2\Delta x}\right)\left(\frac{f_{j,k+1}-f_{j,k-1}}{2\Delta y}\right) + O\left(\Delta x\right)$

$\bullet \mathrm{J}_2\left(f\left(x_j,y_k\right),g\left(x_j,y_k\right)\right) = \frac{1}{4\Delta x\Delta y}\left(f_{j+1,k}\left(g_{j+1,k+1}-g_{j+1,k-1}\right)\right.$

$-f_{j-1,k}\left(g_{j-1,k+1}-g_{j-1,k-1}\right) - f_{j,k+1}\left(g_{j+1,k+1}-g_{j-1,k+1}\right)$

$\left.+f_{j,k,l,m}\left(g_{j+1,k-1}-g_{j-1,k-1}\right)\right) + O\left(\Delta x\right)$

$\bullet \mathrm{J}_3\left(f\left(x_j,y_k\right),g\left(x_j,y_k\right)\right) = \frac{1}{4\Delta x\Delta y}\left(g_{j,k+1}\left(f_{j+1,k+1}-f_{j-1,k+1}\right)\right.$

$-g_{j,k,l,m}\left(f_{j+1,k-1}-f_{j-1,k-1}\right) - g_{j+1,k}\left(f_{j+1,k+1}-f_{j+1,k-1}\right)$

$\left.+g_{j-1,k}\left(f_{j-1,k+1}-f_{j-1,k-1}\right)\right) + O\left(\Delta x\right)$

where the $O\left(\Delta x\right)$ terms are of the form $\frac{\Delta x}{2}\frac{\partial^2 h(\cdot)}{\partial x^2}$ or $\frac{\Delta y}{2}\frac{\partial^2 h(\cdot)}{\partial y^2}$.

As discussed in [17, Chapter 10], the Arakawa Jacobian will be utilised where $\mathrm{J}\left(f\left(x_j,y_k\right),g\left(x_j,y_k\right)\right) = \frac{1}{3}\left(\mathrm{J}_1\left(f\left(x_j,y_k\right),g\left(x_j,y_k\right)\right) + \mathrm{J}_2\left(f\left(x_j,y_k\right),g\left(x_j,y_k\right)\right)\right.$

$\left.+\mathrm{J}_3\left(f\left(x_j,y_k\right),g\left(x_j,y_k\right)\right)\right)$ and this Jacobian conserves enstrophy, vorticity, and mean kinetic energy. Using this information yields the nonlinear term, $\mathrm{J}\left(F\left(x_j,y_k,z_l,t_m\right),\mathcal{Q}\left(x_j,y_k,z_l,t_m\right)\right)$

$= \frac{1}{12\lambda_y\Delta x^2}\left(\left(F_{j+1,k,l,m}-F_{j-1,k,l,m}\right)\left(\mathcal{Q}_{j,k+1,l,m}-\mathcal{Q}_{j,k-1,l,m}\right) + F_{j+1,k,l,m}\right.$

$\times\left(\mathcal{Q}_{j+1,k+1,l,m}-\mathcal{Q}_{j+1,k-1,l,m}\right) - \left(\mathcal{Q}_{j+1,k,l,m}-\mathcal{Q}_{j-1,k,l,m}\right)\left(F_{j,k+1,l,m}-F_{j,k-1,l,m}\right)$

$-F_{j-1,k,l,m}\left(\mathcal{Q}_{j-1,k+1,l,m}-\mathcal{Q}_{j-1,k-1,l,m}\right) - F_{j,k+1,l,m}\left(\mathcal{Q}_{j+1,k+1,l,m}-\mathcal{Q}_{j-1,k+1,l,m}\right)$

$+F_{j,k-1,l,m}\left(\mathcal{Q}_{j+1,k-1,l,m}-\mathcal{Q}_{j-1,k-1,l,m}\right) + \mathcal{Q}_{j,k+1,l,m}\left(F_{j+1,k+1,l,m}-F_{j-1,k+1,l,m}\right)$

$-\mathcal{Q}_{j,k-1,l,m}\left(F_{j+1,k-1,l,m}-F_{j-1,k-1,l,m}\right) - \mathcal{Q}_{j+1,k,l,m}\left(F_{j+1,k+1,l,m}-F_{j+1,k-1,l,m}\right)$

$\left.+\mathcal{Q}_{j-1,k,l,m}\left(F_{j-1,k+1,l,m}-F_{j-1,k-1,l,m}\right)\right)$. Substituting approximations and errors yields the desired result. □

5.2.2 Computational molecules

Using (1.8) to replace $\frac{\partial Q(x,y,z_l,t)}{\partial t}$ with $\frac{\Delta_f Q(x,y,z_l,t)}{\Delta t} + \frac{\Delta t}{2}\frac{\partial^2 Q(r,\cdot)}{\partial t^2}$ and expand using the relevant $Q\left(x,y,z_l,t\right)$ expression yields:

$\bullet$Früh Process: $\nabla^2 F\left(x,y,z_l,t_{k+1}\right) = \mathtt{f}\Delta F\left(x,y,z_l,t_{k+1}\right) + \nabla^2 F\left(x,y,z_l,t_k\right)$

$-\mathtt{f}\Delta F\left(x,y,z_l,t_k\right) + \Delta t\left(-\mathrm{J}\left(F\left(x,y,z_l,t_k\right),\mathcal{Q}\left(x,y,z_l,t_k\right)\right) - \frac{\sqrt{\mathcal{E}}}{2\theta_{\mathcal{A}}}\nabla^2 F\left(x,y,z_l,t_k\right)\right.$

$\left.+\frac{1}{\varkappa}\nabla^2\mathcal{Q}\left(x,y,z_l,t_k\right)\right) + \Delta t\omega\left(x,y,z,t_m\right)\frac{\partial^3 W(x,y,z,t_m)}{\partial x\partial y\partial t} + \frac{\Delta t^2}{2}\frac{\partial^2 Q(r,\cdot)}{\partial t^2}$.

$\bullet$Haines and Holland Process: $\nabla^2 F\left(x,y,z_l,t_{k+1}\right) = \mathtt{f}F\left(x,y,z_l,t_{k+1}\right)$

$-\mathtt{f}F\left(x,y,z_{\neq l},t_{k+1}\right) + \nabla^2 F\left(x,y,z_l,t_k\right) - \mathtt{f}F\left(x,y,z_l,t_k\right) + F\mathtt{f}\left(x,y,z_{\neq l},t_k\right)$

$+\Delta t\left(-\mathrm{J}\left(F\left(x,y,z_l,t_k\right),\mathcal{Q}\left(x,y,z_l,t_k\right)\right) + \mathtt{1}_{l=1}u\left(x,y,z_l,t_k\right)\right.$

$-\left(a+S\left(x\right)\right)\nabla^2\left(F\left(x,y,z_l,t_k\right)-F^I\left(x,y,z_l,t_k\right)\right) + \frac{\Delta t^2}{2}\frac{\partial^2 Q(r,\cdot)}{\partial t^2}$

$\left.+\alpha\nabla^4\left(F\left(x,y,z_l,t_k\right)-F^I\left(x,y,z_l,t_k\right)\right)\right) + \Delta t\omega\left(x,y,z_l,t_k\right)\frac{\partial^3 W(x,y,z_l,t_k)}{\partial x\partial y\partial t}$.

$\bullet$Lee Process: $\nabla^2 F\left(x,y,z_l,t_{k+1}\right) = \nabla^2 F\left(x,y,z_l,t_k\right) - (-1)^l\left(\frac{\Delta F(x,y,z_1,t_{k+1})}{2}\right)$

$+(-1)^l\left(\frac{\Delta F(x,y,z_1,t_k)}{2}\right) + \Delta t\omega\left(x,y,z_l,t_k\right)\frac{\partial^3 W(x,y,z_l,t_k)}{\partial x\partial y\partial t} + \frac{\Delta t^2}{2}\frac{\partial^2 Q(r,\cdot)}{\partial t^2}$

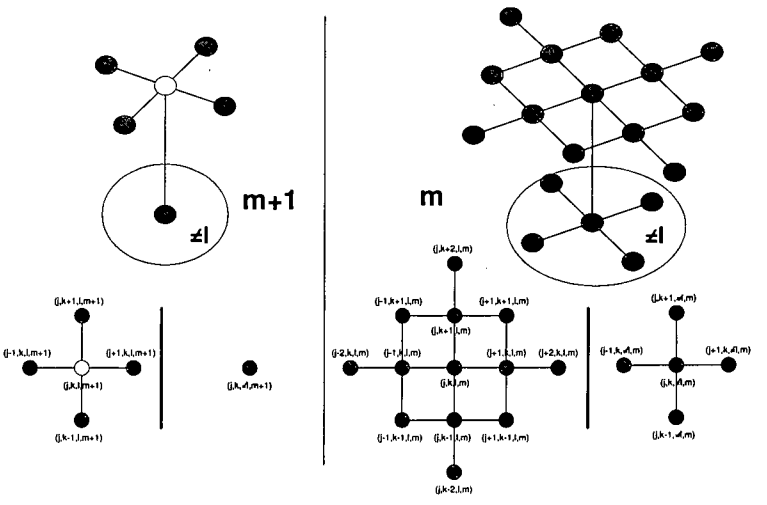

Figure 5.3: QG computational molecule

$+\Delta t\left(-\mathrm{J}\left(F\left(x,y,z_l,t_k\right),\mathcal{Q}\left(x,y,z_l,t_k\right)\right)-\frac{(-1)^l}{30}\left(\frac{\Delta F(x,y,z_1,t_k)}{2}-f\left(y\right)\right)\right.$

$\left.-1_{l=2}a_m\bigtriangledown^2F\left(x,y,z_2,t_m\right)-0.006\bigtriangledown^6F\left(x,y,z_l,t_k\right)\right).$

•Or equivalently $\bigtriangledown^2F\left(x,y,z_l,t_{k+1}\right)=\upsilon_1\left(x_j,y_k,z_l,t_{m+1}\right)+\upsilon_2\left(x_j,y_k,z_l,t_m\right)$

$+\Delta t\omega\left(x_j,y_k,z_l,t_m\right)\frac{\partial^3W\omega(x_j,y_k,z_l,t_m)}{\partial x\partial y\partial t}+O\left(\Delta t^2\right)$, where $\left\{\upsilon_1\left(\cdot,t_{m+1}\right),\upsilon_2\left(\cdot,t_m\right)\right\}$ are a collection of functionals from the QG process, such that the $\upsilon_2\left(x_j,y_k,z_l,t_m\right)$ terms are a weighted two space dimension hyperbolic process.

Using these processes, a computational molecule can be evaluated where the coefficients for the t_{m+1} layer will be singled out from the $\frac{\partial\mathcal{Q}(x_j,y_k,z_l,t_m)}{\partial t}$ term; thus $\frac{\partial\mathcal{Q}(x_j,y_k,z_l,t_m)}{\partial t}=\upsilon_1\left(x_j,y_k,z_l,t_{m+1}\right)+\upsilon_2\left(x_j,y_k,z_l,t_m\right)$

$+\omega_{j,k,l,m}\frac{\mathbb{W}\left(\mathrm{D}_{j,k,l,m}\right)}{\Delta x\Delta y\Delta t}=\frac{1}{\Delta t}\left(-\frac{2}{\Delta x^2}\left(1+\frac{1}{\lambda_y^2}\right)\left(\widehat{F}_{j,k,l,m+1}-\widehat{F}_{j,k,l,m}\right)\right.$

$+\frac{1}{\Delta x^2}\left(\left(\widehat{F}_{j+1,k,l,m+1}-\widehat{F}_{j+1,k,l,m}\right)+\left(\widehat{F}_{j-1,k,l,m+1}-\widehat{F}_{j-1,k,l,m}\right)\right.$

$\left.+\frac{1}{\lambda_y^2}\left(\left(\widehat{F}_{j,k+1,l,m+1}-\widehat{F}_{j,k+1,l,m}\right)+\left(\widehat{F}_{j,k-1,l,m+1}-\widehat{F}_{j,k-1,l,m}\right)\right)\right)$

$\left.-\alpha\left(\widehat{F}_{j,k,l,m+1}-\widehat{F}_{j,k,\neq l,m+1}\right)+\mathfrak{e}\left(\widehat{\mathcal{Q}}_{j,k,l,m+1}\right)-\mathfrak{e}\left(\widehat{\mathcal{Q}}_{j,k,l,m}\right)+\frac{\lambda_t\Delta x}{2}\frac{\partial^2\mathcal{Q}_{j,k,l,m}}{\partial t^2}\right)$

$+\alpha\Delta\widehat{F}_{j,k,l,m}$. Reducing the right hand side yields

$\frac{1}{\Delta t}\frac{2}{\Delta x^2}\left(1+\frac{1}{\lambda_y^2}\right)\widehat{F}_{j,k,l,m+1}+\frac{\alpha}{\Delta t}\widehat{F}_{j,k,l,m+1}=\widehat{\upsilon}_1\left(x_j,y_k,z_l,t_{m+1}\right)+\widehat{\upsilon}_2\left(x_j,y_k,z_l,t_m\right)$

$+\omega_{j,k,l,m}\frac{\mathbb{W}\left(\mathrm{D}_{j,k,l,m}\right)}{\Delta x\Delta y\Delta t}+\frac{1}{\Delta t}\left(\frac{2}{\Delta x^2}\left(1+\frac{1}{\lambda_y^2}\right)\widehat{F}_{j,k,l,m}\right.$

$+\frac{1}{\Delta x^2}\left(\left(\widehat{F}_{j+1,k,l,m+1}-\widehat{F}_{j+1,k,l,m}\right)+\left(\widehat{F}_{j-1,k,l,m+1}-\widehat{F}_{j-1,k,l,m}\right)\right.$

$\left.+\frac{1}{\lambda_y^2}\left(\left(\widehat{F}_{j,k+1,l,m+1}-\widehat{F}_{j,k+1,l,m}\right)+\left(\widehat{F}_{j,k-1,l,m+1}-\widehat{F}_{j,k-1,l,m}\right)\right)\right)$

$\left.+\alpha\widehat{F}_{j,k,\neq l,m+1}+\alpha\Delta\widehat{F}_{j,k,l,m}+\mathfrak{e}\left(\widehat{\mathcal{Q}}_{j,k,l,m+1}\right)-\mathfrak{e}\left(\widehat{\mathcal{Q}}_{j,k,l,m}\right)+\frac{\lambda_t\Delta x}{2}\frac{\partial^2\mathcal{Q}_{j,k,l,m}}{\partial t^2}\right)$

and cancellation yields $\widehat{F}_{j,k,l,m+1}=\frac{2}{C_\dagger}\left(1+\frac{1}{\lambda_y^2}\right)\widehat{F}_{j,k,l,m}$

$-\frac{\lambda_t\Delta x^2}{C_\dagger}\left(\widehat{\upsilon}_1\left(x_j,y_k,z_l,t_{m+1}\right)+\widehat{\upsilon}_2\left(x_j,y_k,z_l,t_m\right)+\omega_{j,k,l,m}\frac{\mathbb{W}\left(\mathrm{D}_{j,k,l,m}\right)}{\Delta x\Delta y\Delta t}\right)$

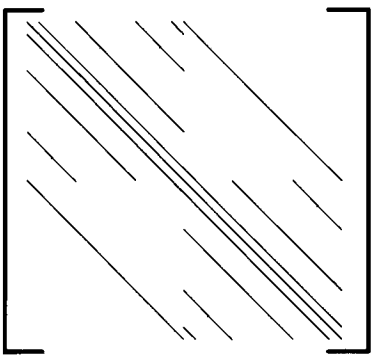

Figure 5.4: $\mathcal{Q}_{j,k,l,m}$ matrix

$+\frac{1}{C_\dagger}\left(\widehat{F}_{j+1,k,l,m+1}+\widehat{F}_{j-1,k,l,m+1}+\frac{1}{\lambda_y^2}\left(\widehat{F}_{j,k+1,l,m+1}+\widehat{F}_{j,k-1,l,m+1}\right)\right)$
$-\frac{1}{C_\dagger}\left(\widehat{F}_{j+1,k,l,m}+\widehat{F}_{j-1,k,l,m}+\frac{1}{\lambda_y^2}\left(\widehat{F}_{j,k+1,l,m}+\widehat{F}_{j,k-1,l,m}\right)\right)$
$+\frac{\Delta x^2}{C_\dagger}\left(\alpha\widehat{F}_{j,k,\neq l,m+1}+\alpha\Delta\widehat{F}_{j,k,l,m}+\mathfrak{e}\left(\widehat{\mathcal{Q}}_{j,k,l,m+1}\right)-\mathfrak{e}\left(\widehat{\mathcal{Q}}_{j,k,l,m}\right)\right.$
$\left.+\frac{\lambda_t\Delta x}{2}\frac{\partial^2\mathcal{Q}_{j,k,l,m}}{\partial t^2}\right)$. Hence $\widehat{F}_{j,k,l,m+1}=\widehat{v}_1\left(x_j,y_k,z_l,t_{m+1}\right)+\widehat{v}_2\left(x_j,y_k,z_l,t_m\right)$
$+\frac{1}{C_\dagger}\left(\widehat{F}_{j+1,k,l,m+1}+\widehat{F}_{j-1,k,l,m+1}+\frac{1}{\lambda_y^2}\left(\widehat{F}_{j,k+1,l,m+1}+\widehat{F}_{j,k-1,l,m+1}\right)\right)$
$+\frac{\Delta x^2}{C_\dagger}\left(\alpha\widehat{F}_{j,k,\neq l,m+1}+\mathfrak{e}\left(\widehat{\mathcal{Q}}_{j,k,l,m+1}\right)\right)-\frac{\lambda_t\Delta x^2}{C_\dagger}\omega_{j,k,l,m}\frac{\mathbb{W}\left(\mathtt{D}_{j,k,l,m}\right)}{\Delta x\Delta y\Delta t}$,

where $C_\dagger=2\left(1+\frac{1}{\lambda_y^2}\right)+\Delta x^2\alpha$. Figure 5.3 demonstrates the form of a computational molecule where $\widehat{F}_{j,k,l,m+1}$ is the point being evaluated and the explicit FDSc matrix for this molecule is shown in Figure 5.4. The left hand side of Figure 5.3 is a $t=(m+1)\,\Delta t$ additive elliptic computational molecule while the right hand side of Figure 5.3 is the $t=m\Delta t$ two space dimensional hyperbolic computational molecule.

Example 5.2.13. *Refer to the Früh Process and Figure 5.3 where:*
•*(5.3) yields* $\frac{1}{\Delta t}\left(-\frac{2}{\Delta x^2}\left(1+\frac{1}{\lambda_y^2}\right)\left(\widehat{F}_{j,k,l,m+1}-\widehat{F}_{j,k,l,m}\right)\right.$
$+\frac{1}{\Delta x^2}\left(\left(\widehat{F}_{j+1,k,l,m+1}-\widehat{F}_{j+1,k,l,m}\right)+\left(\widehat{F}_{j-1,k,l,m+1}-\widehat{F}_{j-1,k,l,m}\right)\right.$
$\left.+\frac{1}{\lambda_y^2}\left(\left(\widehat{F}_{j,k+1,l,m+1}-\widehat{F}_{j,k+1,l,m}\right)+\left(\widehat{F}_{j,k-1,l,m+1}-\widehat{F}_{j,k-1,l,m}\right)\right)\right)$
$-\alpha\Delta\widehat{F}_{j,k,l,m+1}+\alpha\Delta\widehat{F}_{j,k,l,m}+\mathfrak{e}\left(\widehat{\mathcal{Q}}_{j,k,l,m+1}\right)-\mathfrak{e}\left(\widehat{\mathcal{Q}}_{j,k,l,m}\right)+\frac{\lambda_t\Delta x}{2}\frac{\partial^2\mathcal{Q}_{j,k,l,m}}{\partial t^2}\Big)=$
$-\frac{1}{12\lambda_y\Delta x^2}\left(\left(\widehat{F}_{j+1,k,l,m}-\widehat{F}_{j-1,k,l,m}\right)\left(\widehat{\mathcal{Q}}_{j,k+1,l,m}-\widehat{\mathcal{Q}}_{j,k-1,l,m}\right)\right.$
$-\left(\widehat{\mathcal{Q}}_{j+1,k,l,m}-\widehat{\mathcal{Q}}_{j-1,k,l,m}\right)\left(\widehat{F}_{j,k+1,l,m}-\widehat{F}_{j,k-1,l,m}\right)+O\left(\Delta x\right)$
$+\widehat{F}_{j+1,k,l,m}\left(\widehat{\mathcal{Q}}_{j+1,k+1,l,m}-\widehat{\mathcal{Q}}_{j+1,k-1,l,m}\right)-\widehat{F}_{j-1,k,l,m}\left(\widehat{\mathcal{Q}}_{j-1,k+1,l,m}-\widehat{\mathcal{Q}}_{j-1,k-1,l,m}\right)$
$-\widehat{F}_{j,k+1,l,m}\left(\widehat{\mathcal{Q}}_{j+1,k+1,l,m}-\widehat{\mathcal{Q}}_{j-1,k+1,l,m}\right)+\widehat{F}_{j,k-1,l,m}\left(\widehat{\mathcal{Q}}_{j+1,k-1,l,m}-\widehat{\mathcal{Q}}_{j-1,k-1,l,m}\right)$
$+\widehat{\mathcal{Q}}_{j,k+1,l,m}\left(\widehat{F}_{j+1,k+1,l,m}-\widehat{F}_{j-1,k+1,l,m}\right)-\widehat{\mathcal{Q}}_{j,k-1,l,m}\left(\widehat{F}_{j+1,k-1,l,m}-\widehat{F}_{j-1,k-1,l,m}\right)$
$\left.-\widehat{\mathcal{Q}}_{j+1,k,l,m}\left(\widehat{F}_{j+1,k+1,l,m}-\widehat{F}_{j+1,k-1,l,m}\right)+\widehat{\mathcal{Q}}_{j-1,k,l,m}\left(\widehat{F}_{j-1,k+1,l,m}-\widehat{F}_{j-1,k-1,l,m}\right)\right)$

$$+\max\left(\left|\widehat{\mathcal{Q}}(Y)\right| \mathfrak{eg}\left(\widehat{F}(X)\right), \left|\widehat{F}(Y)\right| \mathfrak{eg}\left(\widehat{\mathcal{Q}}(X)\right)\right) + \tfrac{\sqrt{\mathcal{E}}}{2\theta_{\mathcal{A}}}\tfrac{2}{\Delta x^2}\left(1+\tfrac{1}{\lambda_y^2}\right)\widehat{F}_{j,k,l,m}$$
$$-\tfrac{\sqrt{\mathcal{E}}}{2\theta_{\mathcal{A}}}\tfrac{1}{\Delta x^2}\left(\widehat{F}_{j+1,k,l,m}+\widehat{F}_{j-1,k,l,m}+\tfrac{1}{\lambda_y^2}\left(\widehat{F}_{j,k+1,l,m}+\widehat{F}_{j,k-1,l,m}\right)\right)$$
$$-\tfrac{\sqrt{\mathcal{E}}}{2\theta_{\mathcal{A}}}\tfrac{1}{\Delta x^2}\left(\mathfrak{e}\left(\widehat{F}_{j+1,k,l,m}\right)+\mathfrak{e}\left(\widehat{F}_{j-1,k,l,m}\right)+\tfrac{1}{\lambda_y^2}\left(\mathfrak{e}\left(\widehat{F}_{j,k+1,l,m}\right)+\mathfrak{e}\left(\widehat{F}_{j,k-1,l,m}\right)\right)\right)$$
$$+\tfrac{\sqrt{\mathcal{E}}}{2\theta_{\mathcal{A}}}\tfrac{21}{\Delta x^2}\left(1+\tfrac{1}{\lambda_y^2}\right)\mathfrak{e}\left(\widehat{F}_{j,k,l,m}\right)+\tfrac{\Delta x^2}{12}\tfrac{\partial^4 F(\cdot)}{\partial x^4}+\tfrac{\Delta y^2}{12}\tfrac{\partial^4 F(\cdot)}{\partial y^4}$$
$$-\tfrac{1}{\varkappa}\tfrac{2}{\Delta x^2}\left(1+\tfrac{1}{\lambda_y^2}\right)\widehat{\mathcal{Q}}_{j,k,l,m}+\tfrac{1}{\varkappa}\tfrac{1}{\Delta x^2}\left(\widehat{\mathcal{Q}}_{j+1,k,l,m}+\widehat{\mathcal{Q}}_{j-1,k,l,m}+\tfrac{1}{\lambda_y^2}\left(\widehat{\mathcal{Q}}_{j,k+1,l,m}+\widehat{\mathcal{Q}}_{j,k-1,l,m}\right)\right)$$
$$-\tfrac{1}{\varkappa}\tfrac{2}{\Delta x^2}\left(1+\tfrac{1}{\lambda_y^2}\right)\mathfrak{e}\left(\widehat{\mathcal{Q}}_{j,k,l,m}\right)+\tfrac{\Delta x^2}{12}\tfrac{\partial^4 \mathcal{Q}_{j,k,l,m}}{\partial x^4}+\tfrac{\Delta y^2}{12}\tfrac{\partial^4 \mathcal{Q}_{j,k,l,m}}{\partial y^4}$$
$$+\tfrac{1}{\varkappa}\tfrac{1}{\Delta x^2}\left(\mathfrak{e}\left(\widehat{\mathcal{Q}}_{j+1,k,l,m}\right)+\mathfrak{e}\left(\widehat{\mathcal{Q}}_{j-1,k,l,m}\right)+\tfrac{1}{\lambda_y^2}\left(\mathfrak{e}\left(\widehat{\mathcal{Q}}_{j,k+1,l,m}\right)+\mathfrak{e}\left(\widehat{\mathcal{Q}}_{j,k-1,l,m}\right)\right)\right)$$

•*(5.4) yields* $\widehat{\mathcal{Q}}_{j,k,l,m} = -\tfrac{2}{\Delta x^2}\left(1+\tfrac{1}{\lambda_y^2}\right)\widehat{F}_{j,k,l,m}$
$$+\tfrac{1}{\Delta x^2}\left(\widehat{F}_{j+1,k,l,m}+\widehat{F}_{j-1,k,l,m}+\tfrac{1}{\lambda_y^2}\left(\widehat{F}_{j,k+1,l,m}+\widehat{F}_{j,k-1,l,m}\right)\right)$$
$$+\tfrac{1}{\Delta x^2}\left(\mathfrak{e}\left(\widehat{F}_{j+1,k,l,m}\right)+\mathfrak{e}\left(\widehat{F}_{j-1,k,l,m}\right)+\tfrac{1}{\lambda_y^2}\left(\mathfrak{e}\left(\widehat{F}_{j,k+1,l,m}\right)+\mathfrak{e}\left(\widehat{F}_{j,k-1,l,m}\right)\right)\right)$$
$$-\tfrac{2}{\Delta x^2}\left(1+\tfrac{1}{\lambda_y^2}\right)\mathfrak{e}\left(\widehat{F}_{j,k,l,m}\right)+\tfrac{\Delta x^2}{12}\tfrac{\partial^4 F(\cdot)}{\partial x^4}+\tfrac{\Delta y^2}{12}\tfrac{\partial^4 F(\cdot)}{\partial y^4}+\mathcal{B}\left(y_0+k\lambda_y\Delta x\right)$$
$$-\mathfrak{f}\left(\widehat{F}_{j,k,l,m}-\widehat{F}_{j,k,\neq l,m}\right)-\mathfrak{f}\left(\mathfrak{e}\left(\widehat{F}_{j,k,l,m}\right)-\mathfrak{e}\left(\widehat{F}_{j,k,\neq l,m}\right)\right).$$

5.2.3 Numerical approximations

Remark 5.2.14. *Due to the predominant influence of a second order Laplacian operator, a Picard-Lindelöf Iteration scheme will be utilised where multigrid methods have proven to be popular in numerical evaluations.*

In 1922, Richardson was the first to discretise geophysical fluid dynamics over a spherical domain, transform the spherical coordinates into a flat plane, and derive approximations as a progression in time. As can be seen in the computational molecule, there is a hyperbolic and elliptic nature to the QG FDSc where the canonical elliptic five point FDSc (3.10) occurs in the t_{m+1} layer with a two space dimensional hyperbolic characteristic expansions occurring in the t_m layer. Thus, when constructing an estimate, the hyperbolic terms of the QG FDSc will be viewed as a deterministic functional with the remaining functionals equate to an additive elliptic scheme. Unlike Chapter 2, where propagation is a function of time, the noise and hyperbolic terms are dampened due to the elliptic nature of the t_{m+1} level; hence each QG level in time is reduced to an additive elliptic scheme. When implementing a numerical scheme for $\widehat{F}_{j,k,l,m+1}$ and $\widehat{F}_{j,k,\neq l,m+1}$; refer to Figure 5.5:

(1) For the initial FDSy step calculating $\widehat{\mathcal{Q}}_{m=0}$ from $\widehat{F}_{m=0}$ utilise $\widehat{\mathcal{Q}}_m = \beth_0\left(\widehat{F}_m\right)$, where $\widehat{\mathcal{Q}}_{j,k,l,m} = \nabla^2 F(x,y,z,t) + g(\cdot)$.

(2) To progress in time from $\widehat{\mathcal{Q}}_m \to \widehat{\mathcal{Q}}_{m+1}$ utilise $\widehat{\mathcal{Q}}_{m+1} = \beth_1\left(\widehat{F}_m, \widehat{\mathcal{Q}}_m\right)$, where $\widehat{\mathcal{Q}}(x_j, y_k, z_l, t_{m+1}) = \widehat{\mathcal{Q}}(x_j, y_k, z_l, t_m) + \Delta t\left(\frac{\partial \mathcal{Q}(x,y,z,t)}{\partial t}\right) = \widehat{\mathcal{Q}}(x_j, y_k, z_l, t_m)$

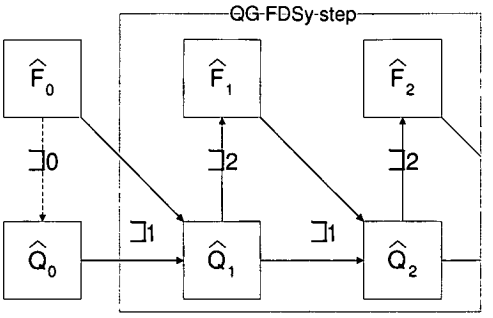

Figure 5.5: QG FDSy method

$$+\Delta t\left(-\mathrm{J}\left(F\left(x,y,z,t\right),\mathcal{Q}\left(x,y,z,t\right)\right)+\omega\left(x,y,z,t\right)\tfrac{\partial^3 W(x,y,z,t)}{\partial x\partial y\partial t}\right)$$
$$+\Delta t v\left(\mathcal{Q}\left(x,y,z,t\right),F'\left(x,y,z,t\right),F\left(x,y,z,t\right),x,y,z,t\right).$$

(3) Calculate the flow via $\widehat{F}_{m+1}=\beth_2\left(\widehat{\mathcal{Q}}_{m+1}\right)$, where
$\bigtriangledown^2 F\left(x_j,y_k,z_l,t_{m+1}\right)=\widehat{\mathcal{Q}}\left(x_j,y_k,z_l,t_{m+1}\right)+f\left(\cdot\right)$.

(4) Repeat as necessary.

In attempting to prove discretised convergence results, utilise Lemma 3.2.3, where $Y_k\in\delta\mho\left|_{t_{m+1}}\right.$, such that, $\widehat{H}_{\delta\mho_k}\left(X;Y_k\right)=\widehat{G}\left(X;Y_k\right)\left(\sum_{X_j\in\delta\mho|_{t_{m+1}}}\widehat{G}\left(X,X_j\right)\right)^{-1}$. As per Lemma 3.2.4, approximations for (5.15) are accomplished via:

$$\widehat{F}\left(X\right)=\sum_{Y_k\in\mho}\widehat{G}\left(X;Y_k\right)v\left(\widehat{F}\left(Y_j\right),Y_j\right)\mathfrak{M}\left(\mathtt{D}_k\right)$$
$$+\sum_{Y_k\in\mho}\widehat{G}\left(X;Y_k\right)\omega\left(Y_k\right)\mathbb{W}\left(\mathtt{D}_k\right)+\sum_{Y_k\in\delta\mho}\widehat{H}_{\delta\mho_k}\left(X;Y_k\right)F_{\delta\mho}\left(Y_k\right). \tag{5.16}$$

Given (QGAIC) and a consistent FDSc for a QG process, then using the elliptic results of Chapter 3, a unique discretized elliptic Green's function exists for each $\widehat{F}_{t=m+1}$ domain since the $\widehat{F}_{t=m}$ values remain constant. Assuming that at least two different approximation $\widehat{F}_{j,k,l,m+1}$ values exist using the same FDSc, domain, and previous $\left\{\widehat{F}_n\mid n\leq m\right\}$ approximations, then either the Green's function, Poisson kernel, or a $\widehat{F}_n$ value are not equivalent for each $\widehat{F}_{j,k,l,m+1}$ estimate. Since the elliptic Green's function is determined uniquely by the geometry of the domain and driving functionals, this implies a contradiction, hence the assumption is incorrect and only one approximation grid exists.

Refer to Section D.3 for a graphical representation of an approximation to a representative process. As described in Chapter 4, modifications of the a priori methods are directly applicable; thus the Blow-up method, $\widehat{G\mathtt{Q}}$ method, Symmetry method, and $\left\|X,Y\right\|_2^d$ method are extremely beneficial. Since often the domain of a QG system is a rectangle in the $\{x,y\}$ plane, then by symmetry, only $\frac{MN}{4}$ discretised Green's functions need to be either stored or approximated.

Bibliography

[1] E.J. Allen, S.J. Novosel, and Z. Zhang, *Finite Element and Difference Approximation of Some Linear Stochastic Partial Differential Equations*, Stochastics and Stochastic Reports **64** (1998), 117–142.

[2] W.F. Ames, *Nonlinear Partial Differential Equations in Engineering*, Academic Press, London, 1965.

[3] Ludwig Arnold, *Stochastic Differential Equations: Theory and Applications*, John Wiley and Sons, London, 1974, Translation of Stochastiche Differentialgleichengen.

[4] Fred Espen Benth and Jon Gjerde, *Convergence for Finite Element Approximations of Stochastic Partial Differential Equations*, Journal of Stochastic Reports **63** (1998), 313–326.

[5] Thomas E. Booth, *Exact Monte Carlo Solution of Elliptic Partial Differential Equations*, Journal of Computational Physics **39** (1981), 396–404.

[6] ———, *Regional Monte Carlo Solution of Elliptic Partial Differential Equations*, Journal of Computational Physics **47** (1982), 281–290.

[7] James R. Brannan, Jinqiao Duan, and Thomas Wanner, *Dissipative Quasi-Geostrophic Dynamics under Random Forcing*, Journal of Mathematical Analysis and Applications **228** (1998), no. 1, 221–233.

[8] R. Buckdahn and E. Pardoux, *Monotonicity Methods for White Noise Driven Quasi-Linear SPDEs*, Diffusion Processes and Related Problems in Analysis **1** (1990), 219–233.

[9] R. Cairoli and John B. Walsh, *Stochastic integrals in the plane*, ACTA Mathematica **134** (1975), 111–183.

[10] Claudio M. Canuto, Alfio Quarteroni Yousuff Hussaini, and Thomas A. Zang, *Spectral Methods in Fluid Dynamics*, Springer-Verlag, London, 1988.

[11] Mark Capiński and Dariusz Gatarek, *Stochastic equations in Hilbert space with application to Navier-Stokes equations in any dimension*, Journal of Functional Analysis **126** (1994), 26–35.

[12] Rene Carmona and David Nualart, *Random Non-Linear Wave Equations: Propagation of Singularities*, The Annals of Probability **16** (1988), no. 2, 730–751.

[13] ———, *Random Non-Linear Wave Equations: Smoothness of Solutions*, Probability Theory and Related Fields **79** (1988), 469–508.

[14] Peter Constantin and Jiahong Wu, *Behavior of solutions of two dimensional quasi-geotrophic equations*, SIAM Journal of Mathematical Analysis **30** (1999), no. 5, 937–948.

[15] Robert C. Dalang and N.E. Frangos, *The Stochastic Wave Equation in Two Spatial Dimensions*, The Annals of Probability **26** (1998), no. 1, 187–212.

[16] Jinqiao Duan and Peter E. Kloeden, *Dissipative quasi-geostrophic dynamics under temporally almost periodic forcing*, Journal of Mathematical Analysis and Applications **236** (1999), no. 1, 74–85.

[17] D.P. Laurie editor, *Numerical Solution of Partial Differential Equations: Theory, Tools and Case Studies*, Birkhuser, Stuttgard, 1983, Summer Seminar Series held at CSIR, Bretoria, 8-10 FEB 82.

[18] William H. Beyer editor, *CRC Standard Mathematical Tables and Formulas*, 29 ed., CRC Press, Ann Arbor, 1991.

[19] J. Douglas Faires and Richard L. Burden, *Numerical Methods*, PWS Publishing Company, Boston, 1993.

[20] Carme Florit and David Nualart, *Diffusion approximation for hyperbolic stochastic differential equations*, Stochastic Processes and their Applications **65** (1996), 1–15.

[21] George E. Forsythe and Wolfgang R. Wasow, *Finite Difference Methods for Partial Differential Equations*, John Wiley and Sons, London, 1960.

[22] W.G. Früh, *Low-order models of wave interactions in the transition to baroclinic chaos*, European Geophysical Society - Nonlinear Processes in Geophysics **3** (1996), 130–165.

[23] M. Röckner G. Da Prato (editor), N.V. Krylöv and J. Zabczyk, *Stochastic PDE's and Kolmogorov Equations in Infinite Dimensions.*, Springer, Berlin, 1998.

[24] T.C. Gard, *Introduction to Stochastic Differential Equations*, Marcel Dekker, New York, 1988.

[25] P. Grisvard, *Elliptic Problems in Nonsmooth Domains*, Pitman Advanced Publishing Program, London, 1985.

[26] Wolfgang Hackbusch, *Convergence of Multi-Grid Iterations Applied to Difference Equations*, Mathematics of Computation **34** (1980), no. 150, 425–440.

[27] ———, *Multi-Grid Methods and Applications*, Springer-Verlag, Heidelberg, 1985.

[28] ———, *Elliptic Differential Equations - Theory and Numerical treatment*, Springer-Verlag, London, 1992.

[29] K. Haines and A. J. Holland, *Vacillation cycles and blocking in a channel*, Q.J.R. Meteorol. Soc. **200** (1996), 1–22.

[30] Bruce Hajek, *Stochastic Equations of Hyperbolic Type and a Two-Parameter Stratonovich Calculus*, The Annals of Probability **10** (1982), 451–463.

[31] David Halliday and Robert Resnick, *Fundamentals of Physics*, Third Extended ed., John Wiley and Sons, New York, 1988.

[32] George J. Haltiner and Roger Terry Williams, *Numerical Prediction and Dynamic Meteorology*, Second ed., John Wiley and Sons, New York, 1980.

[33] Francis B. Hilderbrand, *Finite-Difference Equations and Simulations*, Prentice-Hall, Englewood Cliffs (NJ), 1968.

[34] Helge Holden, Bernt Øskendal, Jan Uboe, and Tusheng Zhang, *Stochastic Partial Differential Equations, A Modeling, White Noise Functional Approach*, Birkhäuser, Woodbine (NJ), 1996.

[35] Leon W. Couch II, *Digital and Analog Communications Systems*, Fifth ed., Prentice Hall, Upper Saddle River, New Jersey, 1997.

[36] Robert Jensen and Pierre Louis Lions, *Some Asymptotic Problems in Fully Nonlinear Elliptic Equations and Stochastic Control*, Annali Della Scuola Normale Superiore Di Pisa **Xi,1** (1984), 129–176.

[37] G. Jumarie, *Input-Output Stability Criteria for a Broad Class of Stochastic Nonlinear Distributed Systems Defined Green's Function*, Journal of Dynamic Systems, Measurement, and Control (1975), 83–91.

[38] Wilfred Kaplan, *Advanced Calculus*, Third ed., Addison - Wesley Publishing Company, London, 1984.

[39] Peter E. Kloeden and Eckhard Platen, *Numerical Solutions of Stochastic Differential Equations*, Second ed., Springer, Berlin, 1995.

[40] N.V. Krylöv, *Lectures on Elliptic an Parabolic Equations in Hölder Spaces*, American Mathematical Society, U.S.A., 1996.

[41] Hui-Hsiung Kuo, *White Noise Distribution Theory*, CRC Press, London, 1996.

[42] Sukyoung Lee, *Maintenance of Multiple Jets in Baroclinic Flow*, Journal of the Atmostpheric Sciences **54** (1997), 1726–1738.

[43] Stephen R. Lewis, *A Quasi-Geostrophic Numerical Model of a Rotating Internally Heated Fluid*, Geophys. Astrophys. Fluid Dynam. **65** (1992), 31–55.

[44] Moshe Marcus and Victor J. Mizel, *Stochastic Hyperbolic Systems and the Wave Equation*, Stochastics and Stochastic Reports **Volume 36** (1991), 225–244.

[45] W.H. McCrea and F.J. W. Whipple, *Random Paths in two and three dimensions*, Proc. Roy. Soc. Edinburgh **60** (1940), 281–298.

[46] Robert McOwen, *Partial Differential Equations: Methods and Applications*, Prentice Hall, London, 1996.

[47] Richard E. Meyer, *Introduction to Mathematical Fluid Dynamics*, John Wiley and Sons, London, 1971.

[48] K.W. Morton and D.F. Mayers, *Numerical Solution of Partial Differential Equations*, Cambridge University Press, Cambridge, 1994.

[49] T. S. Motzkin and Wolfgang R. Wasow, *On the approximation of linear elliptic differential equations by difference equations with positive coefficients.*, J. Math. Physics **31** (1953), 253–259.

[50] Carl Mueller, *Long time existence for the wave equation with a noise term*, The Annals of Probability **25** (1997), no. 1, 133–151.

[51] J.R. Norris, *Twisted Sheets*, Journal of Functional Analysis **132** (1995), 273–334.

[52] David Nualart and Samy Tindel, *Quasilinear stochastic elliptic equations with reflection*, Stochastic Processes and their Applications **57** (1995), 73–82.

[53] Joseph Pedlosky, *Geophysical Fluid Dynamics*, Springer - Verlag, New York, 1979.

[54] K.O. Friedrichs R. Courant and H. Lewy, *Über die parzielle Differentialgleichungen der mathematische*, Physik. Math. Ann. **100** (1928), 32–74.

[55] John A. Rice, *Mathematical Statistics and Data Analysis*, Duxbury Press, Belmont, California, 1995.

[56] Calres Rovira and Marta Sanz-Solé, *The Law of the Solution to a Nonlinear Hyperbolic SPDE*, Journal of Theoretical Probability **Volume 9** (1996), no. Number 4, 863–901.

[57] John C. Strikwerda, *Finite Difference Schemes and Partial Differential Equations*, Wadsworth and Brooks/Coll Advanced Books + Software, Pacific Grove, California, 1989.

[58] Richard P. Kendall Todd Dupont and H.H. Rachford Jr., *An Approximate Factorization Procedure for Solving Self-Adjoint Elliptic Difference Equations*, SIAM Journal of Numerical Analysis **5** (1968), no. 3, 559–573.

[59] Donald W. Trim, *Applied Partial Differential Equations*, PWS-Kent Publishing Company, Boston, 1990.

[60] John B. Walsh, *An Introduction to Stochastic Partial Differential Equations*, vol. Lecture Series Notes in Mathematics Volume 1180, Springer, Berlin, 1986.

[61] Wolfgang R. Wasow, *On the truncation error in the solution of Laplace's equation by finite differences*, J. Research Nat. Bur. Standards **48** (1952), 345–348.

[62] ———, *Discrete approximations to elliptic differential equations.*, Z. Angew. Math. Phys. **6** (1955), 81–97.

[63] ———, *The accuracy of difference approximations to plane Dirichlet problems with piecewise analytic boundary values*, Quart. Appl. Math. **15** (1957), 53–63.

[64] David Williams, *Probability with Martingales*, Cambridge University Press, Cambridge, 1991.

Appendix A

Notation

Table A.1: Standard Notation for Probability

Notation	Definition
$\{\Omega, \mathcal{F}, \mathbb{P}\}$	probability triple
Ω	sample space
$\mathcal{F}$	a σ-algebra with a filtration $\mathcal{F}_t$
$\overline{\alpha}$	an average of α
$\alpha \mid \beta$	α given β
$\mathbb{C}(\alpha, \beta)$	covariance
$\mathbb{E}(\alpha)$	expectation
$\mathfrak{f}(\alpha)$	probability density function
$\mathfrak{f}_{\mathcal{N}(\mu,\sigma^2)}$	Normal pdf
$\mathfrak{F}(\alpha)$	continuous distribution function
iid	independent identically distributed
$\mathcal{M}$	a strong martingale as defined in [9]
$\sim \mathcal{N}(\mu, \sigma^2)$	Normal distribution with mean μ and variance σ^2
$\mathbb{P}(\alpha)$	probability
ρ	correlation coefficient
$\mathcal{SM}$	a semi-martingale
$\sim \mathcal{U}[a, b]$	uniform distribution over the range $[a, b]$
$\mathbb{V}(\alpha)$	variance

Table A.2: Stochastic partial differential equations

Notation	Description
$\int \alpha dW$	Ito Integral
$\int \alpha \circ dW$	Stratonovich Integral
$\frac{\partial g(x,y)}{\partial x}$	partial derivative
$\mathfrak{C}^{(n)}$	refer to Notation 1.1.2
$\bigtriangledown^n(\cdot)$	the nth order Laplacian operator
$\Delta^n(\cdot)$	an n^{th} order difference operator
$\vartheta(j;k)$	FDSc influence from $\wp_j$ to $\wp_k$
$\mathfrak{DT}^{(n)}_{(X)}(\cdot)$	deterministic Taylor expansion operator of order n
$\mathfrak{eg}(\cdot), \mathfrak{es}(\cdot), \mathfrak{e}(\cdot)$	Global, stopping, and general error notation
FDSc	Finite Difference Scheme
FDSy	Finite Difference System
FESy	Finite Element System
$G(\cdot)$	Green's function
$\mathfrak{H}(\cdot)$	hyperbolic operator
$H(\cdot)$	Poisson kernel
$\mathtt{J}(\cdot)$	Jacobian operator
λ_t	$\frac{C\Delta t}{\Delta x}$
$P(m,n)$	refer to Definition 2.2.16
$\mathtt{RC}(r)$	rate of convergence
$\mathtt{sr}(\cdot)$	spectral radius
$\upsilon(\cdot)$	real valued function for pseudo-deterministic terms
$\omega(\cdot)$	real valued function for stochastic terms
$\beth(\cdot)$	FDSy notation

Table A.3: General Notation

Notation	Description
1_{text}	indicator function
$[0]$	zero matrix
α, β, a, b, c	arbitrary real variables
α_{text}	a function or variable α dependent upon *text*
$\lvert\alpha\rvert$	absolute value of a function or variable
$[{}_m^n a_{j,k}]$	a matrix centered on $a_{j,k}$
$[A], [B]$	matrices
$[A^{-1}]$	inverse of a matrix
$[A^T]$	transpose of a matrix
$\mathtt{card}\,(\cdot)$	cardinality of a set or space
$\complement\,(\cdot)$	complement of a set or space
$C, K, L, \lambda, \aleph$	positive real constants
$f(\cdot), g(\cdot), h(\cdot), u(\cdot),$ $\upsilon(\cdot), \omega(\cdot), \Upsilon(\cdot), \xi(\cdot), \zeta(\cdot)$	real valued functions
$F(X)$	a solution to a process
$\widehat{F}(X)$	approximation of a solution
$g(Y)\mid_{(X)}$	function evaluated at X
$\Delta.g(\cdot)$	difference operator, refer to Table 1.2
$\widetilde{g}(\cdot)$	Fourier or discrete Fourier transform of g
i	$\sqrt{-1}$
$[I]$	identity matrix
j, k, l, m, n, o	integer counting variables
δ_{text}	Kroneker delta function
$\mathfrak{M}(\cdot)$	Lebesgue measure of a set or space
$O(\alpha)$	Big-Oh notation
process	a mathematical model in $\mathbb{R}^d$ space
r, s	arbitrary real variables or time in Chapter 2
system	a finite set of equations in $\mathbb{Z}^d$ space
θ	a bounded variable where $0 \leq \theta \leq 1$
$F_{j,k,l,m}$	discretised notation for $F(x_j, y_k, z_l, t_m)$
ϖ	complex variable
$[V]$	vector
$\chi(\cdot)$	Chi-squared statistic

Table A.4: Geometry

Notation	Description
1_X	unit source in a domain located at X
$\delta\mho$	boundary of a domain
$\delta\mho_l$	the boundary sub-space mapped to $\wp_l \in \mathbb{Z}^d$
$\mho$	interior of a domain
d	dimension of a process or space
domain	polygonally connected domain
$\mathtt{D}_\wp$	an $\mathbb{R}^d$ sub-space that is mapped to $\wp_{\mathbb{Z}^d}$
$DoD(\cdot)$	Domain of Dependence
$DoI(\cdot)$	Domain of Influence
$DoR(\cdot)$	Domain of Rotation
M, N	number of divisions of a restricted $\mathbb{R}^1$ region
$\wp$	geometric point
$\wp_\mho$	interior point
$\wp_{\delta\mho}$	boundary point
$\wp_\complement$	exterior point
$\mathtt{Qpath}(\cdot)$	Program C.3.6
$\mathbb{R}^d$	Euclidean d dimensional space
$\mathbb{R}^d_{+t}$	$\mathbb{R}^{d-1} \times [0, \infty]$
$RoI(\cdot)$	Region of Influence
$\mathtt{S}_2(\cdot)$	d dimensional sphere in $\mathbb{R}^d$ space
$\mathtt{S}_1(\cdot)$	d dimensional sphere in $\mathbb{Z}^d$ space
t	orthogonal space dimension denoting time
$\|V\|_a$	the l^a norm of a vector
Δx	discretisation constant for $\mathbb{Z}^d$
$\lambda_y, \lambda_z, \lambda_t$	uniform $\mathbb{Z}^d_{\Delta x}$ constants where $\lambda_\alpha \frac{\Delta\alpha}{\Delta x}$
(x_j, y_k, z_l, t_m)	$(j\Delta x, k\Delta y, l\Delta z, m\Delta t) = (j\Delta x, k\lambda_y\Delta x, l\lambda_z\Delta x, m\lambda_t\Delta x)$
x, y, z	orthogonal space dimensions
X, Y	$\mathbb{R}^d$ position vectors in Euclidean space
Z	normal vector to a boundary in the exterior of a domain
$\mathbb{Z}^d_{\Delta x}$	discretised d dimensional space

Table A.5: QG Notation

Notation	Description
$\mathcal{A}$	the axis rate of rotation
bg	the Berger number
$\mathcal{B}$	the Beta-plane coefficient
$\mathcal{C}$	coriolis effect
$\mathcal{D}$	depth of a fluid or layer
el	elocity
en	enstrophy
$\mathcal{E}$	$\frac{\nu}{AL^2} = \frac{Ro}{Re}$: Ekman number
fr	friction
F	stream function
f	$\frac{V^2}{gL}$: Froude Number
grad	gradient
$\mathcal{G}$	acceleration due to gravity
$\mathcal{H}$	entropy
$\mathcal{M}$	mass
$\mathcal{P}$	pressure
$\mathcal{Q}$	potential vorticity
ρ_{MV}	$\frac{\Delta M}{\Delta V}$: Density
$\mathcal{T}$	temperature
$\theta_{\mathcal{A}}$	the Rossby Number
$\theta_{\mathcal{D}}$	the aspect ratio
$\mathcal{U}$	flow
ν	viscosity
$\mathcal{V}$	vorticity
$\varkappa$	Reynolds number
Υt	barotropic component
Υc	baroclinic component
∂_{conv}	convective derivative

Appendix B

Supplementary proofs and information

B.1 Chapter 2

Lemma 2.1.13: [13, Proposition II.2]: Given (HAIC) where $\upsilon(\cdot)$ and $\omega(\cdot)$ are locally Lipschitz, one can find a constant K_L such that:

$$|\upsilon(F(X),X)-\upsilon(F(Y),Y)|+|\omega(F(X),X)-\omega(F(Y),Y)|\leq K_L\|X-Y\|_2 \tag{B.1}$$

for all $\{X,Y\}\in DoD(x,t)\subset[-L,L]$. Then there exists at most one weak solution.

Proof. Let $F(y,s)$ and $G(y,s)$ be two weak solutions. For each $\mathfrak{C}^\infty$-function with compact support contained in in the domain, say $g(y,s)$, set $f(x,t)=\iint\limits_{DoD\cup DoI} g(y,s)\,dyds$. $f(\cdot)\in\mathfrak{C}^{(\infty)}$ has compact support in $\mathbb{R}^2_{+t}$ and satisfies $g(x,t)=\mathfrak{H}^2(f(x,t),1.0)$. Using $f(\cdot)$ in (2.9) with $F(x,t)$ and $G(x,t)$ we obtain the relation

$$\begin{aligned}\iint\limits_{DoD\cup DoI} g(y,s)\,H(y,s)\,dyds=\iint\limits_{DoD\cup DoI}(\omega(F(y,s),y,s)-\omega(G(y,s),y,s))\\ \times f(y,s)\,dW(y,s)+\iint\limits_{DoD\cup DoI}(\upsilon(F(y,s),y,s)-\upsilon(G(y,s),y,s))\,f(y,s)\,dyds\end{aligned} \tag{B.2}$$

for $H(x,t)=F(x,t)-G(x,t)$. For each integer m the random set $E_m=\left\{(x,t)\in\mathbb{R}^2_{+t};\ \sup\limits_{(y,s)\in\mho(x,t)}(|F(y,s)|+|G(y,s)|)<m\right\}$ is such that $1_{E_m}(x,t)$ is $\mathcal{F}_t$ measurable for all $(x,t)\in\mathbb{R}^2_{+t}$. Using an approximate identity $\{\Im_a;a>0\}$ in the plane and $H(x,t)$ being continuous, we have: $H(x,t)=\lim\limits_{n\to\infty}\iint_{\mathbb{R}^2_{+t}}H(y,s)\,\Im_{\frac{1}{n}}(t-s,x-y)\,dyds$ for each $(x,t)\in\mathbb{R}^2_{+t}$. Consequently, if

$(x,t) \in DoI(z,r)$ are fixed, for each $a > 0$ we have: $\mathbb{E}\left(1_{E_m}(x,t+a)\left|H(x,t)\right|^2\right)$

$$\leq \lim_{n\to\infty}\inf \mathbb{E}\left(1_{E_m}(x,t+a)\left|\iint_{\mathbb{R}^2_{+t}} H(y,s)\,\Im_{\frac{1}{n}}(x-y,t-s)\,dyds\right|^2\right)$$

By Fatou's Lemma

$$\leq 2\lim_{n\to\infty}\inf \mathbb{E}\left(1_{E_m}(x,t+a)\left|\iint_{\mathbb{R}^2_{+t}} \left(\omega\left(F(y,s),y,s\right)\right) - \omega\left(G(y,s),y,s\right) f_n(y,s)\,dW(y,s)\right|^2\right)$$

$$+2\lim_{n\to\infty}\inf \mathbb{E}\left(1_{E_m}(x,t+a)\left|\iint_{\mathbb{R}^2_{+t}} \left(\upsilon\left(F(y,s),y,s\right) - \upsilon\left(G(y,s),y,s\right)\right) f_n(y,s)\,dyds\right|^2\right)$$

By using (B.2) with $g(\cdot,\cdot) = \Im_{\frac{1}{n}}(x-\cdot,t-\cdot)$, for n large enough and with

$f_n(y,s) = \iint_{\mathbb{R}^2_{+t}} \Im_{\frac{1}{n}}(x-\alpha,t-\beta)\,1_{\upsilon(\alpha,\beta)}(y,s)\,d\alpha d\beta$

$$\leq 2\lim_{n\to\infty}\inf \mathbb{E}\left(\left|\iint_{\mathbb{R}^2_{+t}} \left(\omega\left(F(y,s),y,s\right) - \omega\left(G(y,s),y,s\right)\right) 1_{E_m}(y,s)\, f_n(y,s)\,dW(y,s)\right|^2\right)$$

$$+2\lim_{n\to\infty}\inf \mathbb{E}\left(\left|\iint_{DoI(x,t)} \left(\upsilon\left(F(y,s),y,s\right) - \upsilon\left(G(y,s),y,s\right)\right) 1_{E_m}(y,s)\, f_n(y,s)\,dyds\right|^2\right)$$

due to the local properties of the integrals and the Lipschitz assumption

$$\leq K(m,z,r)\lim_{n\to\infty}\inf \iint_{\mathbb{R}^2_{+t}} \left|\mathbb{E}\left(1_{E_m}(y,s)\left|H(y,s)\right|^2\right) f_n ys\right|^2 dyds. \qquad \text{(B.3)}$$

Note that $\lim_{n\to\infty} f_n(y,s) = 1_{DoI(x,t)}(y,s)$ for any point (y,s) away from the boundary of $DoI(x,t)$ which is of Lebesgue's measure zero. Moreover, $|f_n(y,s)| \leq 1$ and $|H(y,s)|^2 1_{E_m}(y,s) \leq m$ for all integers m, so utilising Lebesgue's dominated convergence theorem and (B.3), we have:

$\lim_{n\to\infty} \iint_{DoD\cup DoI} \mathbb{E}\left(1_{E_m}(y,s)\,H(y,s)^2\right) f_n(y,s)^2\,dyds = \iint_{DoD\cup DoI} \mathbb{E}\left(1_{E_m}(y,s)\left|H(y,s)\right|^2\right) dyds,$

$\mathbb{E}\left(1_{E_m}(x,t+a)\left|H(x,t)\right|^2\right) \leq K(m,z,r) \iint_{DoD\cup DoI} \mathbb{E}\left(1_{E_m}(y,s)\left|H(y,s)\right|^2\right) dyds,$

and $\mathbb{E}\left(1_{E_m}(x,t)\left|H(x,t)\right|^2\right) \leq K(m,z,r) \iint_{DoD\cup DoI} \mathbb{E}\left(1_{E_m}(y,s)\left|H(y,s)\right|^2\right) dyds.$

Letting $a \to 0$ and using Fatou's Lemma, recursion gives $\mathbb{E}\left(1_{E_m}\left|H(x,t)\right|^2\right) = 0$.

Hence, $H(\cdot) = 0$ almost surely on E_m, but since m is arbitrary, $H(\cdot) = 0$ a.s. □

Notation B.1.1. *$\mathcal{M}$ is a 'martingale' will be interpreted as a strong martingale as defined in [9]. The reader is referred to [39, Section 2.3], [60, Chapter 2], and [64] for a more thorough discussion on martingales.*

Lemma 2.1.14: [13, Proposition II.3]: Given (HAIC), then for each $\mathcal{F}_0$-measurable continuous process $F(x,t)_0$ satisfying: $\iint_{DoI(x,t)} \mathbb{E}\left(\left|F(y,s)_0\right|^2\right) dyds < \infty$ then there exists a unique continuous solution to the integral equation

$$F(x,t) = F(x,t)_0 + \iint_{DoD\cup DoI} \upsilon\left(F(y,s),y,s\right) dyds + \iint_{DoD\cup DoI} \omega\left(F(y,s),y,s\right) dW(y,s).$$

Proof. Use a Picard-Lindelöf iterative scheme to construct a solution such that $n \geq 1$, $F(x,t)_{n+1} = F(x,t)_0 + \frac{1}{2C} \iint\limits_{DoI(x,t)} \upsilon(F(y,s)_n, y, s)\, dyds$
$+\frac{1}{2C} \iint\limits_{DoI(x,t)} \omega(F(y,s)_n, y, s)\, dW(y,s)$. The process $F(X)_n$ is $\mathcal{F}_z$ adapted and $\iint\limits_{DoI(x,t)} \omega\left(F(y,s)_{n-1}, y, s\right) dW(y,s)$ is a two-parameter martingale with respect to (2.6). Use the two-parameter version of the maximal inequality to obtain:
$\mathbb{E}\left(\sup\limits_{DoD \cup DoI} \left|F(y,s)_{n+1} - F(y,s)_n\right|^2 \right)$
$\leq \mathbb{E}\left(\sup\limits_{DoD \cup DoI} \left| \frac{1}{2C} \iint\limits_{DoI(x,t)} \left(\upsilon(F(y,s)_n, y, s) - \upsilon\left(F(y,s)_{n-1}, y, s\right)\right) dyds \right.\right.$
$\left.\left. + \frac{1}{2C} \iint\limits_{DoD \cup DoI} \left(\omega(F(y,s)_n, y, s) - \omega\left(F(y,s)_{n-1}, y, s\right)\right) dW(y,s) \right|^2 \right)$
$\leq K_{(x,t)} \mathbb{E}\left(\left| \iint\limits_{DoD \cup DoI} \left(\upsilon(F(y,s)_n, y, s) - \upsilon\left(F(y,s)_{n-1}, y, s\right)\right) dyds \right|^2 \right)$
$+ K_{(x,t)} \mathbb{E}\left(\left| \iint\limits_{DoD \cup DoI} \left(\omega(F(y,s)_n, y, s) - \omega\left(F(y,s)_{n-1}, y, s\right)\right) dW(y,s) \right|^2 \right)$
$\leq K_{(x,t)} \iint\limits_{DoD \cup DoI} \mathbb{E}\left(\left|F(y,s)_n - F(y,s)_{n-1}\right|^2 \right) dyds$ and through recursion
$\mathbb{E}\left(\sup\limits_{DoD \cup DoI} \left|F(y,s)_{n+1} - F(y,s)_n\right|^2 \right) \leq K_{(x,t)} \frac{t^{2n}}{n!} \iint\limits_{DoD \cup DoI} \mathbb{E}\left(\left|F(y,s)_0\right|^2\right) dyds$, hence,
$\sum\limits_{n=0}^{\infty} \mathbb{E}\left(\sup\limits_{DoD \cup DoI} \left|F(y,s)_{n+1} - F(y,s)_n\right|^2 \right) < \infty$. This implies the local uniform convergence of $F(x,t)_0 + \sum\limits_{n=0}^{\infty} \left(F(x,t)_{n+1} - F(x,t)_n\right)$ to a process $F(x,t)$ which is continuous and satisfies (2.8). □

Lemma 2.1.16: [13, Proposition II.4]: Given (HAIC) are fulfilled, then the unique solution of the integral equation (2.8) is a weak solution of (2.1) in the sense of Definition 2.1.12.

Proof. $F(x,t)$ denotes the unique solution of (2.8) and is $\mathcal{F}_{(x,t)}$ and $\mathcal{F}_t$-measurable since $\mathcal{F}_{(x,t)} \subset \mathcal{F}_t$. If $f(y,s) \in \mathfrak{C}^{(\infty)}$ with compact support on $DoD \cup DoI$
$\iint\limits_{\mathbb{R}^2_{+t}} \left(\frac{\partial^2 f(x,t)}{\partial t^2} - \frac{\partial^2 f(x,t)}{\partial x^2} \right) \iint\limits_{DoI(x,t)} \left(\upsilon(F(y,s), y, s)\, dyds + \omega(F(y,s), y, s)\, dW(y,s)\right) dxdt$
$= \iint\limits_{\mathbb{R}^2_{+t}} \left(\int\limits_s^t \int\limits_{y-(t-s)}^{y+(t-s)} \mathfrak{H}^2(f(x,t), 1.0)\, dxdt \right)$
$\times \left(\omega(F(y,s), y, s)\, dW(y,s) + \upsilon(F(y,s), y, s)\right) dyds$
$= \iint\limits_{\mathbb{R}^2_{+t}} f(y,s) \left(\omega(F(y,s), y, s)\, dW(y,s) + \upsilon(F(y,s), y, s)\, dyds\right) dyds \quad (B.4)$

using a standard version of Fubini's Theorem for stochastic integrals. Moreover,

$$\frac{1}{2}\iint\limits_{DoI(x,t)} \mathfrak{H}^2\left(f\left(x,t\right),1.0\right)\left(F_{\delta\upsilon}\left(x+t,0\right)+\overset{\backprime}{F}_{\delta\upsilon}\left(x-t,0\right)\right)dxdt + \int\limits_{DoD(x,t)} \frac{\partial f\left(y,0\right)}{\partial t} F_{\delta\upsilon}\left(y,0\right)dy = 0 \tag{B.5}$$

by simple integration by parts. Finally we similarly have:

$$\frac{1}{2}\iint\limits_{DoI(x,t)} \left(\mathfrak{H}^2\left(f\left(x,t\right),1.0\right)\right)\Upsilon\left(x-t,x+t\right)dxdt - \int\limits_{DoD(x,t)} f\left(x,0\right)\Upsilon\left(dx\right) = 0 \tag{B.6}$$

for each deterministic continuous σ-finite measure Υ. Using (B.6) with Υ defined by $\Upsilon\left(E^*\right) = \mathbb{E}\left(1_E \mu\left(E^*\right)\right)$ for $E^* \in \mathcal{B}_f\left(\mathbb{R}\right)$ for each $B \in \mathcal{F}$ we can put (B.4), (B.5), and (B.6) together with (2.8) to check (2.9). □

Corollary 2.1.17: Given (HAIC), there exists a unique solution to (2.8).

Proof. Assume that there are two solutions to (2.8) such that $F\left(x,t\right) \neq G\left(x,t\right)$, then $\frac{F(\zeta(x,t),0)+F(\xi(x,t),0)}{2} + \frac{1}{2C}\int\limits_{DoD(x,t)} \frac{\partial F(y,s)}{\partial s}\mid_{s=0} dy + \frac{1}{2C}\iint\limits_{DoI(x,t)} \upsilon\left(F\left(y,s\right),y,s\right)dyds$
$+\frac{1}{2C}\iint\limits_{DoI(x,t)} \omega\left(F\left(y,s\right),y,s\right)dW\left(y,s\right) \neq +\frac{1}{2C}\iint\limits_{DoI(x,t)} \omega\left(G\left(y,s\right),y,s\right)dW\left(y,s\right)$
$+\frac{G(\zeta(x,t),0)+G(\xi(x,t),0)}{2} + \frac{1}{2C}\int\limits_{DoD(x,t)} \frac{\partial G(y,t)}{\partial t}\mid_{t=0} dy + \frac{1}{2C}\iint\limits_{DoI(x,t)} \upsilon\left(G\left(y,s\right),y,s\right)dyds.$
Since the initial conditions are equivalent such that $F_{j,0} = G_{j,0}$ and $\frac{\partial F(y,s)}{\partial s}\mid_{s=0} = \frac{\partial G(y,t)}{\partial t}\mid_{t=0}$, cancellation of constants and deterministic terms yields
$\iint\limits_{DoI(x,t)} \upsilon\left(F\left(y,s\right),y,s\right)dyds + \iint\limits_{DoI(x,t)} \omega\left(F\left(y,s\right),y,s\right)dW\left(y,s\right) \neq$
$\iint\limits_{DoI(x,t)} \upsilon\left(G\left(y,s\right),y,s\right)dyds + \iint\limits_{DoI(x,t)} \omega\left(G\left(y,s\right),y,s\right)dW\left(y,s\right)$. In order for the inequality to be true either $\iint\limits_{DoI(x,t)} \upsilon\left(F\left(y,s\right),y,s\right)dyds \neq \iint\limits_{DoI(x,t)} \upsilon\left(G\left(y,s\right),y,s\right)dyds$ or $\iint\limits_{DoI(x,t)} \omega\left(F\left(y,s\right),y,s\right)dW\left(y,s\right) \neq \iint\limits_{DoI(x,t)} \omega\left(G\left(y,s\right),y,s\right)dW\left(y,s\right)$. There exists (y,s) such that $\{F\left(y,s\right) \neq G\left(y,s\right) \mid DoI\left(y,s\right) \subset DoI\left(x,t\right)\}$. Using a recursive argument leads to a contradiction with the initial conditions where $F\left(x,0\right) \neq G\left(x,0\right)$ almost surely. □

Lemma 2.2.6: Analogous to the deterministic problem, if $\lambda = 1$, then
$F\left(x_j,t_k\right) = \lambda^2\left(F_{j+1,k-1} + F_{j-1,k-1}\right) + 2\left(1-\lambda^2\right)F_{j,k-1} - F_{j,k-2}$
$+\frac{\lambda}{2C}\iint\limits_{\mathtt{D}_{j,k-1}} \upsilon\left(F\left(y,s\right),y,s\right)dyds + \frac{\lambda}{2C}\iint\limits_{\mathtt{D}_{j,k-1}} \omega\left(F\left(y,s\right),y,s\right)dW\left(y,s\right).$

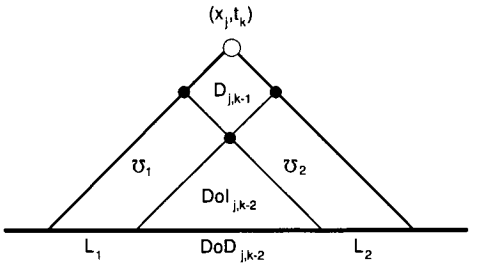

Figure B.1: $\mho_{j,k}$ for Lemma 2.2.6

Proof. From (2.8), $F(x_j,t_k) = \frac{F(\zeta(x_j,t_k),0)+F(\xi(x_j,t_k),0)}{2} + \frac{1}{2C}\int\limits_{DoD(x_j,t_k)} \frac{\partial F(y,s)}{\partial s}\mid_{s=0} dy$
$+\frac{1}{2C}\iint\limits_{DoI(x_j,t_k)} \upsilon(F(y,s),y,s)\,dyds + \frac{1}{2C}\iint\limits_{DoI(x_j,t_k)} \omega(F(y,s),y,s)\,dW(y,s)$. Adding 0 in the form of $(1-1)\left(\frac{F(\zeta(x_j,t_{k-2}),0)}{2} + \frac{F(\xi(x_j,t_{k-2}),0)}{2} + \int\limits_{DoD(x_j,t_{k-2})} \frac{\partial F(y,s)}{\partial s}\mid_{s=0} dy\right)$
$+\frac{1-1}{2C}\left(\iint\limits_{DoI(x_j,t_{k-2})} \upsilon(F(y,s),y,s)\,dyds + \iint\limits_{DoI(x_j,t_{k-2})} \omega(F(y,s),y,s)\,dW(y,s)\right)$
and breaking the integral over the t_{k-2} term yields $F(x_j,t_k) = \frac{F(\xi(x_j,t_k),0)}{2}$
$+\frac{F(\zeta(x_j,t_{k-2}),0)}{2} + \frac{F(\xi(x_j,t_{k-2}),0)}{2} + \frac{F(\zeta(x_j,t_k),0)}{2} - \frac{F(\zeta(x_j,t_{k-2}),0)}{2} - \frac{F(\xi(x_j,t_{k-2}),0)}{2}$
$+\frac{1}{2C}\left(\int\limits_{L_1} \frac{\partial F(y,s)}{\partial s}\mid_{s=0} dy + (2-1)\int\limits_{DoD(x_j,t_{k-2})} \frac{\partial F(y,s)}{\partial s}\mid_{s=0} dy + \int\limits_{L_2} \frac{\partial F(y,s)}{\partial s}\mid_{s=0} dy\right)$
$+\frac{1}{2C}(2-1)\iint\limits_{DoI(x_j,t_{k-2})} \upsilon(F(y,s),y,s)\,dyds + \omega(F(y,s),y,s)\,dW(y,s)$
$+\frac{1}{2C}\iint\limits_{\mho_1} \upsilon(F(y,s),y,s)\,dyds + \omega(F(y,s),y,s)\,dW(y,s)$
$+\frac{1}{2C}\iint\limits_{\mho_2} \upsilon(F(y,s),y,s)\,dyds + \omega(F(y,s),y,s)\,dW(y,s)$
$+\frac{1}{2C}\iint\limits_{D_{j,k-1}} \upsilon(F(y,s),y,s)\,dyds + \omega(F(y,s),y,s)\,dW(y,s)$.
Using (2.8) to combine terms yields $F(x_j,t_k) = F_{j-1,k-1} + F_{j+1,k-1} - F_{j,k-2}$
$+\frac{1}{2C}\iint\limits_{D_{j,k-1}} \upsilon(F(y,s),y,s)\,dyds + \frac{1}{2C}\iint\limits_{D_{j,k-1}} \omega(F(y,s),y,s)\,dW(y,s)$. □

Remark 2.2.7: When $\lambda \neq 1$, then Lemma 2.2.6 is not necessarily true such that
$F(x_j,t_k) \neq \lambda^2(F_{j+1,k-1} + F_{j-1,k-1}) + 2(1-\lambda^2)F_{j,k-1} - F_{j,k-2}$
$+\frac{1}{2C}\iint\limits_{D_{j,k-1}} \upsilon(F(x,y),x,y)\,dxdy + \frac{1}{2C}\iint\limits_{D_{j,k-1}} \omega(F(x,y),x,y)\,dW(x,y)$ since breaking the domain into components expressed in Figure B.2,
$\lambda^2(F_{j+1,k-1} + F_{j-1,k-1}) + 2(1-\lambda^2)F_{j,k-1} - F_{j,k-2}$
$+\frac{1}{2C}\iint\limits_{D_{j,k-1}} \upsilon(F(x,y),x,y)\,dxdy + \frac{1}{2C}\iint\limits_{D_{j,k-1}} \omega(F(x,y),x,y)\,dW(x,y)$
$= \lambda^2\int\limits_{L_1} \frac{\partial F(y,s)}{\partial s}\mid_{s=0} dy + (2-2\lambda^2+\lambda^2)\int\limits_{L_2} \frac{\partial F(y,s)}{\partial s}\mid_{s=0} dy$
$+(2-2\lambda^2+\lambda^2+\lambda^2-1)\int\limits_{DoD_{j,k-2}} \frac{\partial F(y,s)}{\partial s}\mid_{s=0} dy$

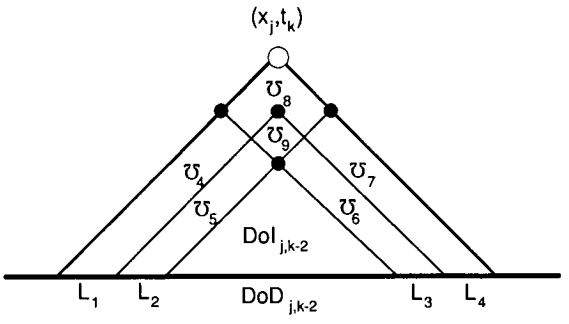

Figure B.2: $\upsilon_{j,k}$ for Lemma 2.2.7

$$
\begin{aligned}
&+\left(2-2\lambda^2+\lambda^2\right)\int\limits_{L_3}\tfrac{\partial F(y,s)}{\partial s}\mid_{s=0}dy+\lambda^2\int\limits_{L_4}\tfrac{\partial F(y,s)}{\partial s}\mid_{s=0}dy\\
&+\lambda^2\iint\limits_{\upsilon_4}v\left(F\left(y,s\right),y,s\right)dyds+\omega\left(F\left(y,s\right),y,s\right)dW\left(y,s\right)\\
&+\left(2-2\lambda^2+\lambda^2\right)\iint\limits_{\upsilon_5}v\left(F\left(y,s\right),y,s\right)dyds+\omega\left(F\left(y,s\right),y,s\right)dW\left(y,s\right)\\
&+\left(2-2\lambda^2+\lambda^2\right)\iint\limits_{\upsilon_6}v\left(F\left(y,s\right),y,s\right)dyds+\omega\left(F\left(y,s\right),y,s\right)dW\left(y,s\right)\\
&+\lambda^2\iint\limits_{\upsilon_7}v\left(F\left(y,s\right),y,s\right)dyds+\omega\left(F\left(y,s\right),y,s\right)dW\left(y,s\right)\\
&+\iint\limits_{\upsilon_8}v\left(F\left(y,s\right),y,s\right)dyds+\omega\left(F\left(y,s\right),y,s\right)dW\left(y,s\right)\\
&+\left(2-2\lambda^2+1\right)\iint\limits_{\upsilon_9}v\left(F\left(y,s\right),y,s\right)dyds+\omega\left(F\left(y,s\right),y,s\right)dW\left(y,s\right)\\
&+\left(2-2\lambda^2+\lambda^2+\lambda^2-1\right)\tfrac{1}{2C}\iint\limits_{DoI_{j,k-1}}v\left(F\left(y,s\right),y,s\right)dyds+\omega\left(F\left(y,s\right),y,s\right)dW\left(y,s\right)
\end{aligned}
$$

Subtracting this result from $\frac{F\left(\zeta_{j,k},0\right)+F\left(\xi_{j,k},0\right)}{2}+\frac{1}{2C}\int\limits_{DoD_{j,k}}\frac{\partial F(y,s)}{\partial s}\mid_{s=0}dy$

$$
\begin{aligned}
&+\tfrac{1}{2C}\iint\limits_{DoI_{j,k}}v\left(F\left(y,s\right),y,s\right)dyds+\tfrac{1}{2C}\iint\limits_{DoI_{j,k}}\omega\left(F\left(y,s\right),y,s\right)dW\left(y,s\right)\text{ yields}\\
&=\left(1-\lambda^2\right)\left(\int\limits_{L_1}\tfrac{\partial F(y,s)}{\partial s}\mid_{s=0}dy-\int\limits_{L_2}\tfrac{\partial F(y,s)}{\partial s}\mid_{s=0}dy\right)\\
&-\left(1-\lambda^2\right)\int\limits_{L_3}\tfrac{\partial F(y,s)}{\partial s}\mid_{s=0}dy+\left(1-\lambda^2\right)\int\limits_{L_4}\tfrac{\partial F(y,s)}{\partial s}\mid_{s=0}dy\\
&+\left(1-\lambda^2\right)\iint\limits_{\upsilon_4}v\left(F\left(y,s\right),y,s\right)dyds+\omega\left(F\left(y,s\right),y,s\right)dW\left(y,s\right)\\
&-\left(1-\lambda^2\right)\iint\limits_{\upsilon_5}v\left(F\left(y,s\right),y,s\right)dyds+\omega\left(F\left(y,s\right),y,s\right)dW\left(y,s\right)\\
&-\left(1-\lambda^2\right)\iint\limits_{\upsilon_6}v\left(F\left(y,s\right),y,s\right)dyds+\omega\left(F\left(y,s\right),y,s\right)dW\left(y,s\right)\\
&+\left(1-\lambda^2\right)\iint\limits_{\upsilon_7}v\left(F\left(y,s\right),y,s\right)dyds+\omega\left(F\left(y,s\right),y,s\right)dW\left(y,s\right)\\
&-\left(2-2\lambda^2\right)\iint\limits_{\upsilon_9}v\left(F\left(y,s\right),y,s\right)dyds+\omega\left(F\left(y,s\right),y,s\right)dW\left(y,s\right).
\end{aligned}
$$

It is easy to see that as $\lambda^2\rightarrow 1$ the induced error will decrease, but since $\lambda^2\neq 1$ and $\Delta x\neq 0$ the expression does not uniquely equal 0.

Remark B.1.2. *Due to the importance of the size of the matrices, let* $\left[{}_n^m\alpha_{j,k}\right]$

denote a matrix with m columns and n rows centered on $\alpha_{j,k}$. In order to remain centered on given variables, matrices of different sizes can be added together provided the matrices are 'padded' with 0's. For example, given $[{}^{m}_{n}\alpha_{j,k}]$, $\alpha_{j,k}$ is the element in the $\lceil \frac{m}{2} \rceil$ column and $\lceil \frac{n}{2} \rceil$ row and when adding matrices, let

$$[A] = [{}^{5}_{3}a_{j,k}] = \begin{bmatrix} a_{j-2,k+1} & a_{j-1,k+1} & a_{j,k+1} & a_{j+1,k+1} & a_{j+2,k+1} \\ a_{j-2,k} & a_{j-1,k} & a_{j,k} & a_{j+1,k} & a_{j+2,k} \\ a_{j-2,k-1} & a_{j-1,k-1} & a_{j,k-1} & a_{j+1,k-1} & a_{j+2,k-1} \end{bmatrix}$$

and $[V^T] = [b^T_{j,k}] = [b_{j,k+2}, b_{j,k+1}, b_{j,k}, b_{j,k-1}, b_{j,k-2}]$, *then* $[{}^{5}_{3}A] + [{}^{1}_{5}V]$

$$= \begin{bmatrix} 0 & 0 & b_{j,k+2} & 0 & 0 \\ a_{j-2,k+1} & a_{j-1,k+1} & a_{j,k+1}+b_{j,k+1} & a_{j+1,k+1} & a_{j+2,k+1} \\ {}^{5}_{5} \; a_{j-2,k} & a_{j-1,k} & a_{j,k}+b_{j,k} & a_{j+1,k} & a_{j+2,k} \\ a_{j-2,k-1} & a_{j-1,k-1} & a_{j,k-1}+b_{j,k-1} & a_{j+1,k-1} & a_{j+2,k-1} \\ 0 & 0 & b_{j,k-2} & 0 & 0 \end{bmatrix}.$$

Notation B.1.3. *Using Notation 2.2.4, let* $[B^m_n] = \prod_{j=1}^{m} [A_{n+2(j-1)}]$, $0 < \{m, n\}$.

Lemma 2.2.9: When $\lambda = 1$, $[{}^{n+2m}_{n}B^m_n] = [{}^{n+2m}_{n}$ MPR $({}^{m}_{\cdot})]$.

Proof. Given: $[{}^{n+2m}_{n}B^m] = \prod_{j=1}^{m} [{}_{n+2(j-1)}A]$ evaluating by hand yields:

$$[{}_{n}B^1] = [{}_{n}A] = \begin{bmatrix} 1 & 0 & 1 & 0 & \dots & 0 \\ {}^{n+2}_{n} & & & \ddots & & \\ 0 & \dots & 0 & 1 & 0 & 1 \end{bmatrix} = [{}^{n+2}_{n}MPR({}^{1}_{\cdot})]$$

$$[{}_{n}B^2] = \begin{bmatrix} 1 & 0 & 2 & 0 & 1 & 0 & \dots & 0 \\ {}^{n+4}_{n} & & & \ddots & & & & \\ 0 & \dots & 0 & 1 & 0 & 2 & 0 & 1 \end{bmatrix} = [{}^{n+4}_{n}MPR({}^{2}_{\cdot})]$$

Assuming that $[B^j_n]$ holds for all n, then $[B^{j+1}_n] = [B^j_n]\,[A_{n+2j}]$

$$= \begin{bmatrix} \binom{j}{0} & 0 & \binom{j}{1} & 0 & \binom{j}{2} & \cdots & 0 & \binom{j}{j-1} & 0 & \binom{j}{j} & 0 & \dots \\ & & & & & \ddots & & & & & & \\ \dots & 0 & \binom{j}{0} & 0 & \binom{j}{1} & 0 & \binom{j}{2} & \cdots & 0 & \binom{j}{j-1} & 0 & \binom{j}{j} \end{bmatrix} \begin{bmatrix} 1 & 0 & 1 & 0 & \dots \\ & & & \ddots & \\ \dots & 0 & 1 & 0 & 1 \end{bmatrix}$$

$$= \begin{bmatrix} \binom{j}{0} & 0 & \binom{j}{0}+\binom{j}{1} & 0 & \cdots & \binom{j}{j-1}+\binom{j}{j} & 0 & \binom{j}{j} & 0 \\ & & & \ddots & & & & & \\ 0 & \binom{j}{0} & 0 & \binom{j}{0}+\binom{j}{1} & 0 & \cdots & \binom{j}{j-1}+\binom{j}{j} & 0 & \binom{j}{j} \end{bmatrix}$$

$$= \begin{bmatrix} \binom{j+1}{0} & 0 & \binom{j+1}{1} & 0 & \cdots & \binom{j+1}{j} & 0 & \binom{j+1}{j+1} & 0 & \dots & 0 \\ & & & & & \ddots & & & & & \\ 0 & \dots & 0 & \binom{j+1}{0} & 0 & \binom{j+1}{1} & 0 & \binom{j+1}{2} & \cdots & 0 & \binom{j+1}{j+1} \end{bmatrix}$$

$[B^{j+1}_n] = [$ MPR $({}^{j+1}_{\cdot})]$. The result follows from a recursive argument. □

Lemma 2.2.11: $\int\limits_{DoD_{j,k}} u(y,0)\,dy = \sum\limits_{DoD_{j,k}}^{n}\left(\int\limits_{x_{n-1}}^{x_{n+1}} u(y,0)\,dy\right)$ and let $\Upsilon(z,r)$ denote either $dzdr$ or $dW(z,r)$, such that $\iint\limits_{DoI_{j,k}} u(v(y,s),y,s)\,\Upsilon(z,r)$

$= \sum\limits_{DoI_{j,k}}^{n}\left(\iint\limits_{\mathtt{D}_n} u(v(y,s),y,s)\,\Upsilon(z,r)\right)$.

Proof. By inspection of Figures 2.5 and 2.6, Definitions 2.1.7 and 2.1.8, Notation 2.2.10; breaking the $DoD_{j,k}$ into intervals of length $2\Delta x$ and skipping adjacent points over the DoI and integrating yields the desired result. □

Corollary 2.2.12: $\mathfrak{M}(DoI_{j,k}) = \left(\frac{k}{2} + \sum\limits_{l=1}^{k-1} l\right)\mathfrak{M}(\mathtt{D}) = \frac{k^2}{2}\mathfrak{M}(\mathtt{D})$ and

$\mathfrak{M}\left(DoI_{j,k} - \sum\limits_{DoD(j;k)}^{n} \mathtt{D}_{n,0}\right) = \frac{k^2-k}{2}\mathfrak{M}(\mathtt{D})$.

Proof. Let $h(k)$ = the number of $\mathtt{D}$ regions in domain. Using Definition 2.1.8, and inspection of Figures 2.6 and 2.5; $\mathfrak{M}(DoI_{j,0}) = 0$, $\mathfrak{M}(DoI_{j,1}) = \frac{\mathfrak{M}(\mathtt{D})}{2}$, and $\mathfrak{M}(DoI_{j,2}) = 2\mathfrak{M}(\mathtt{D})$, thus $h(0) = 0$, $h(1) = \frac{1}{2}$, and $h(2) = 2$. For a general k, assume true for all $j < k$; the problem is reduced to recurrence relation $h(k) = 2h(k-1) - h(k-2) + 1 = 2\left(\frac{(k-1)^2}{2}\right) - \left(\frac{(k-2)^2}{2}\right) + 1 = \frac{k^2}{2}$. For the second result, repeat Corollary 2.2.12 but remove the $\mathtt{D}_{n,0}$ regions from the sum. □

Lemma 2.2.15: Expanding $F(y,s)$ around $F(x_j,t_{k-2})$ (refer to Figure 2.7) yields $F(y,s) = F(x_j,t_{k-1}) + f(y,s) + g(y,s) + h(y,s)$.

Proof. From (2.8), $F(y,s) = \frac{F(\zeta(y,s),0)+F(\xi(y,s),0)}{2} + \frac{1}{2C}\int\limits_{DoD(y,s)} \frac{\partial F(z,r)}{\partial r}\,|_{r=0}\,dz$

$+\frac{1}{2C}\iint\limits_{DoI(y,s)} v(F(z,r),z,r)\,dzdr + \frac{1}{2C}\iint\limits_{DoI(y,s)} \omega(F(z,r),z,r)\,dW(z,r)$.

Breaking up the (y,s) integrals in terms of integrals involving $\{(x_j,t_{k-2}), L_{1,2}, \mho_{1,2,3}\}$ gives: $F(y,s) = (1-1)\frac{F(\xi_{j,k-1},0)+F(\zeta_{j,k-1},0)}{2} + \frac{F(\zeta(y,s),0)+F(\xi(y,s),0)}{2}$

$+\frac{1}{2C}\int\limits_{DoD(x_j,t_{k-2})} \frac{\partial F(z,r)}{\partial r}\,|_{r=0}\,dz + \frac{1}{2C}\iint\limits_{DoI_{j,k-2}} v(F(z,r),z,r)\,dzdr$

$+\frac{1}{2C}\iint\limits_{DoI(x_j,t_{k-2})} \omega(F(z,r),z,r)\,dW(z,r) + \frac{1}{2C}\int\limits_{L_1+L_2} \frac{\partial F(z,r)}{\partial r}\,|_{r=0}\,dz$

$+\frac{1}{2C}\left(\iint\limits_{\mho_1(y,s)} v(F(z,r),z,r)\,dzdr + \iint\limits_{\mho_2(y,s)} v(F(z,r),z,r)\,dzdr\right)$

$+\frac{1}{2C}\left(\iint\limits_{\mho_1(y,s)} \omega(F(z,r),z,r)\,dW(z,r) + \iint\limits_{\mho_2(y,s)} \omega(F(z,r),z,r)\,dW(z,r)\right)$

$+\frac{1}{2C}\left(\iint\limits_{\mho_3(y,s)} v(F(z,r),z,r)\,dzdr + \iint\limits_{\mho_3(y,s)} \omega(F(z,r),z,r)\,dW(z,r)\right)$. Collecting terms yields: $F(y,s) = F(x_j,t_{k-2}) - \frac{F(\xi_{j,k-2},0)+F(\zeta_{j,k-2},0)}{2} + \frac{F(\xi(y,s),0)+F(\zeta(y,s),0)}{2}$

$$+\tfrac{1}{2C}\int\limits_{L_1(y,s)+L_2(y,s)}\frac{\partial F(z,r)}{\partial r}\mid_{r=0}dz$$
$$+\tfrac{1}{2C}\iint\limits_{\mho_1(y,s)+\mho_2(y,s)+\mho_3(y,s)}\upsilon\left(F\left(z,r\right),z,r\right)dzdr$$
$$+\tfrac{1}{2C}\int\limits_{\mho_1(y,s)+\mho_2(y,s)+\mho_3(y,s)}\omega\left(F\left(z,r\right),z,r\right)dW\left(z,r\right),\text{ hence the desired results.}$$

□

Lemma 2.2.17: $P\left(k+1,n\right)=\left[A_n\right]P\left(k,n+2\right)-P\left(k-1,n\right)$.

Proof. By Definition 2.2.16, $0<n$ and $1<k$.

•Let $k=2l+1$. $\left[A_n\right]P\left(k,n+2\right)-P\left(k-1,n\right)=$

$$=\left[A_n\right]\sum_{j=l}^{2l}\left(-1\right)^j\binom{j}{2(j-l)}\left[B_n^{2(j-l)}\right]-\sum_{j=l}^{2l-1}\left(-1\right)^{j+1}\binom{j}{2(j-l)+1}\left[B_n^{2(j-l)+1}\right].$$

$$=\sum_{j=l}^{2l}\left(-1\right)^j\binom{j}{2(j-l)}\left[A_n\right]\left(\prod_{k=1}^{2(j-l)}\left[A_{n+2+2(k-1)}\right]\right)$$
$$-\sum_{j=l}^{2l-1}\left(-1\right)^{j+1}\binom{j}{2(j-l)+1}\left(\prod_{k=1}^{2(j-l)+1}\left[A_{n+2(k-1)}\right]\right)$$

$$=\sum_{j=l}^{2l}\left(-1\right)^j\binom{j}{2(j-l)}\left(\prod_{k=0}^{2(j-l)}\left[A_{n+2,k}\right]\right)-\sum_{j=l}^{2l-1}\left(-1\right)^{j+1}\binom{j}{2(j-l)+1}\left(\prod_{k=0}^{2(j-l)}\left[A_{n+2k}\right]\right)$$

$$=\sum_{j=l}^{2l-1}\left(-1\right)^j\left(\left(\binom{j}{2(j-l)}+\binom{j}{2(j-l)+1}\right)\prod_{k=0}^{2(j-l)}\left[A_{n+2k}\right]+\left(-1\right)^{2l}\binom{2l}{2l}\prod_{k=0}^{2(j-l)}\left[A_{n+2k}\right]\right)$$

$$=\sum_{j=l}^{2l-1}\left(-1\right)^j\binom{j+1}{2(j-l)+1}\prod_{k=0}^{2(j-l)}\left[A_{n+2,k}\right]+\prod_{k=0}^{2l}\left[A_{n+2k}\right]$$

$$=\sum_{j=l}^{2l}\left(-1\right)^j\left(\binom{j+1}{2(j-l)+1}\prod_{k=0}^{2(j-l)}\left[A_{n+2,k}\right]\right)=\sum_{j=l}^{2l}\left(-1\right)^j\binom{j+1}{2(j-l)+1}\prod_{k=1}^{2(j-l)+1}\left[A_{n+2(k-1)}\right]$$

$$=\sum_{j=l}^{2l}\left(-1\right)^j\binom{j+1}{2(j-l)+1}\left[B_n^{2(j-l)+1}\right]=\sum_{j=l+1}^{2(l+1)-1}\left(-1\right)^{j+1}\binom{j}{2(j-l-1)+1}\left[B_n^{2(j-l-1)+1}\right].$$

Hence, $\left[A_n\right]P\left(k,n+2\right)-P\left(k-1,n\right)=\sum\limits_{j=l+1}^{2(l+1)-1}\left(-1\right)^{j+1}\binom{j}{2(j-l-1)+1}\left[B_n^{2(j-l-1)+1}\right]$.

•Let $k=2l$. $\left[A_n\right]P\left(k,n+2\right)-P\left(k-1,n\right)$

$$=\left[A_n\right]\sum_{j=l}^{2l-1}\left(-1\right)^{j+1}\binom{j}{2(j-l)+1}\left[B_{n+2}^{2(j-l)+1}\right]-\sum_{j=l-1}^{2(l-1)}\left(-1\right)^j\binom{j}{2(j-l+1)}\left[B_n^{2(j-l+1)}\right]$$

$$=\sum_{j=l}^{2l-1}\left(-1\right)^{j+1}\binom{j}{2(j-l)+1}\prod_{k=0}^{2(j-l)+1}\left[A_{n+2k}\right]-\sum_{j=l-1}^{2(l-1)}\left(-1\right)^j\binom{j}{2(j-l+1)}\prod_{k=1}^{2(j-l+1)}\left[A_{n+2(k-1)}\right]$$

$$=\sum_{j=l}^{2l-1}\left(-1\right)^{j+1}\binom{j}{2(j-l)+1}\prod_{k=1}^{2(j-l+1)}\left[A_{n+2(k-1)}\right]-\sum_{j=l-1}^{2(l-1)}\left(-1\right)^j\binom{j}{2(j-l+1)}\prod_{k=1}^{2(j-l+1)}\left[A_{n+2(k-1)}\right]$$

$$=\sum_{j=l}^{2l-1}\left(-1\right)^{j+1}\binom{j}{2(j-l)+1}\left[B_n^{2(j-l+1)}\right]-\sum_{j=l-1}^{2(l-1)}\left(-1\right)^j\binom{j}{2(j-l+1)}\left[B_n^{2(j-l+1)}\right]$$

$$=\sum_{j=l}^{2l-1}\left(-1\right)^{j+1}\left(\binom{j}{2(j-l)+1}+\binom{j}{2(j-l+1)}\right)\left[B_n^{2(j-l+1)}\right]+\left(-1\right)^l\binom{l-1}{0}\left[B_n^0\right]$$

$$=\sum_{j=l}^{2l-1}\left(-1\right)^{j+1}\binom{j+1}{2(j-l+1)}\left[B_n^{2(j-l+1)}\right]+\left(-1\right)^l\left[B_n^0\right]$$

$$= \sum_{j=l+1}^{2l} (-1)^j \binom{j}{2(j-l)} \left[B_n^{2(j-l)}\right] + (-1)^l \left[B_n^0\right] = \sum_{j=l}^{2l} (-1)^j \binom{j}{2(j-l)} \left[B_n^{2(j-l)}\right].$$

Hence, $[A_n]\, P(k, n+2) - P(k-1, n) = \sum_{j=l}^{2l} (-1)^j \binom{j}{2(j-l)} \left[B_n^{2(j-l)}\right]$, thus for both cases $P(k+1, n) = [A_n]\, P(k, n+2) - P(k-1, n)$. □

Corollary 2.2.18: When $\lambda = 1$

$$P(k,n) = \begin{bmatrix} & 1 & 0 & 1 & 0 & \cdots & 1 & 0 & 1 & 0 & \ldots & 0 \\ \binom{n+2(k-1)}{n} & & & & & & \ddots & & & & & \\ & 0 & \ldots & 0 & 1 & 0 & 1 & 0 & \cdots & 1 & 0 & 1 \end{bmatrix}.$$

Proof. Setting $k = 1$ for any n it can be shown that

$$P(1,n) = [I] \text{ and } P(2,n) = \begin{bmatrix} 1 & 0 & 1 & 0 & \cdots & 0 \\ & & & \ddots & & \\ 0 & \cdots & 0 & 1 & 0 & 1 \end{bmatrix}.$$

Assume this is true up to and including any k for all n such that

$$P(k,n) = \begin{bmatrix} 1 & 0 & 1 & 0 & \cdots & 1 & 0 & 1 & 0 & \ldots & 0 \\ & & & & & \ddots & & & & & \\ 0 & \ldots & 0 & 1 & 0 & 1 & 0 & \cdots & 1 & 0 & 1 \end{bmatrix}$$

then using Lemma 2.2.17, $P(k+1, n)$

$$= \begin{bmatrix} 1 & 0 & 1 & 0 & \ldots & 0 \\ & & \ddots & & & \\ 0 & \ldots & 0 & 1 & 0 & 1 \end{bmatrix} \begin{bmatrix} 1 & 0 & 1 & 0 & \cdots & 1 & 0 & 1 & 0 & \ldots & 0 \\ & & & & \ddots & & & & & & \\ 0 & \ldots & 0 & 1 & 0 & 1 & 0 & \cdots & 1 & 0 & 1 \end{bmatrix}$$

$$- \begin{bmatrix} 1 & 0 & 1 & 0 & \cdots & 1 & 0 & 1 & 0 & \ldots & 0 \\ & & & & \ddots & & & & & & \\ 0 & \ldots & 0 & 1 & 0 & 1 & 0 & \cdots & 1 & 0 & 1 \end{bmatrix}$$

$$= \begin{bmatrix} 1 & 0 & 2 & 0 & \cdots & 2 & 0 & 1 & 0 & \ldots & 0 \\ & & & & \ddots & & & & & & \\ 0 & \ldots & 0 & 1 & 0 & 2 & 0 & \cdots & 2 & 0 & 1 \end{bmatrix}$$

$$- \begin{bmatrix} 1 & 0 & 1 & 0 & \cdots & 1 & 0 & 1 & 0 & \ldots & 0 \\ & & & & \ddots & & & & & & \\ 0 & \ldots & 0 & 1 & 0 & 1 & 0 & \cdots & 1 & 0 & 1 \end{bmatrix}.$$

In order to subtract the two matrices, the second matrix needs to be padded with 0 columns on both sides to maintain central points such that

$$P(k+1,n) = \begin{bmatrix} 1 & 0 & 2 & 0 & \cdots & 2 & 0 & 1 & 0 & \ldots & 0 \\ & & & & & & \ddots & & & & \\ 0 & \ldots & 0 & 1 & 0 & 2 & 0 & \cdots & 2 & 0 & 1 \end{bmatrix}$$

$$- \begin{bmatrix} 0 & 0 & 1 & 0 & 1 & \cdots & 0 & 1 & 0 & \ldots & 0 \\ & & & & \ddots & & & & & & \\ 0 & \ldots & 0 & 1 & 0 & 1 & \cdots & 0 & 1 & 0 & 0 \end{bmatrix};$$

hence, $P(k,n) = \begin{bmatrix} 1 & 0 & 1 & 0 & \cdots & 1 & 0 & 1 & 0 & \ldots & 0 \\ & & & & & \ddots & & & & & \\ 0 & \ldots & 0 & 1 & 0 & 1 & 0 & \cdots & 1 & 0 & 1 \end{bmatrix}$. □

Lemma 2.2.19: FDSy vectors to (2.8) utilising (2.15) can be expressed as:

$$\left[\widehat{F}_{j,k}\right] = P(k,n)\left[\widehat{F}_{j,1}\right] + \frac{\lambda\mathfrak{M}(\mathtt{D})}{2C}\sum_{l=1}^{k-1} P(l,n)\,\upsilon\left(\left[\widehat{F}_{j,k-l-1}\right],[x_j],(k-l-1)\Delta t\right)$$
$$-P(k-1,n)\left[\widehat{F}_{j,0}\right] + \frac{\lambda}{2C}\sum_{l=1}^{k-1} P(l,n)\left[\mathbb{W}(\mathtt{D}_{j,k-l})\right]\left[\omega\left(\widehat{F}_{j,k-l-1},x_j,(k-l-1)\Delta t\right)\right]. \tag{B.7}$$

Proof. $\widehat{F}_{j,0}$ and $\widehat{F}_{j,1}$ are given, show that (B.7) is true for $k=2$. By (2.14)
$\left[{}_n\widehat{F}_{j,2}\right] = [{}_nA_n]\left[{}_{n+2}\widehat{F}_{j,1}\right] - \left[{}_n\widehat{F}_{j,0}\right] + \frac{\lambda}{2C}\mathfrak{M}(\mathtt{D})\,\upsilon\left(\left[{}_n\widehat{F}_{j,0}\right],[{}_nx_j],0\right)$
$+\frac{\lambda}{2C}\omega\left(\left[{}_n\widehat{F}_{j,0}\right],[{}_nx_j],0\right)[{}_n\mathbb{W}(\mathtt{D}_{j,1})] = [{}_nB_n^1]\left[{}_{n+2}\widehat{F}_{j,1}\right] - \left[{}_n\widehat{F}_{j,0}\right]$
$+\frac{\lambda}{2C}\mathfrak{M}(\mathtt{D})\,\upsilon\left(\left[{}_n\widehat{F}_{j,0}\right],[{}_nx_j],0\right) + \frac{\lambda}{2C}\omega\left(\left[{}_n\widehat{F}_{j,0}\right],[{}_nx_j],0\right)[{}_n\mathbb{W}(\mathtt{D}_{j,1})]$
$= P(2,n)\left[{}_{n+2}\widehat{F}_{j,1}\right] - P(2-1,n)\left[{}_n\widehat{F}_{j,0}\right]$
$+\frac{\lambda}{2C}\mathfrak{M}(\mathtt{D})\,P(1,n)\,\upsilon\left(\left[{}_n\widehat{F}_{j,0}\right],[{}_nx_j],(2-1-1)\Delta t\right)$
$+\frac{\lambda}{2C}P(1,n)\,\omega\left(\left[{}_n\widehat{F}_{j,0}\right],[{}_nx_j],(2-1-1)\Delta t\right)[{}_n\mathbb{W}(\mathtt{D}_{j,2-1})]$.
Repeating this argument for $k=3$ yields
$\left[{}_n\widehat{F}_{j,3}\right] = [{}_nA]\left[{}_{n+2}\widehat{F}_{j,2}\right] - \left[{}_n\widehat{F}_{j,1}\right] + \frac{\lambda\Delta x\Delta t}{C}\upsilon\left(\left[{}_n\widehat{F}_{j,1}\right],[{}_nx_j],\Delta t\right)$
$+\frac{\lambda}{C}\omega\left(\left[{}_n\widehat{F}_{j,1}\right],[{}_nx_j],\Delta t\right)[{}_n\mathbb{W}(\mathtt{D}_{j,2})]$. Substituting in the expansion for $\left[\widehat{F}_{j,2}\right]$ into the $\left[\widehat{F}_{j,3}\right]$ expression and using Lemma 2.2.17 and 2.2.18 yields the desired result. Using the above result and (2.14), when $k=3$ the expansion of the terms equates to (B.7) hence the first two cases are true. In order to show that (B.7) is true for the general case of t_k, assume that the t_{k-1} and t_{k-2} cases are true for all n. From (2.15), $\left[{}_n\widehat{F}_{j,k}\right] = \frac{\lambda\Delta x\Delta t}{C}\upsilon\left(\left[{}_n\widehat{F}_{j,k-2}\right],[{}_nx_j],(k-l-1)\Delta t\right)$
$A_n[{}_{n+2}F_{j,k-1}] - [{}_nF_{j,k-2}] + \frac{\lambda}{2C}\omega\left(\left[{}_n\widehat{F}_{j,k-2}\right],[{}_nx_j],(k-l-1)\Delta t\right)[{}_n\mathbb{W}(\mathtt{D}_{j,k-1})]$
$= A_nP(k-1,n+2)\left[{}_{n+2k-4}\widehat{F}_{j,1}\right] - A_nP(k-2,n+2)\left[{}_{n+2k-6}\widehat{F}_{j,0}\right]$
$+A_n\frac{\lambda}{2C}\mathfrak{M}(\mathtt{D})\sum_{l=1}^{k-2}P(l,n+2)\,\upsilon\left(\left[{}_n\widehat{F}_{j,k-l-2}\right],[{}_nx_j],(k-l-2)\Delta t\right)$
$+A_n\frac{\lambda}{2C}\sum_{l=1}^{k-2}P(l,n+2)\,\omega\left(\left[{}_n\widehat{F}_{j,k-l-2}\right],[{}_nx_j],(k-l-2)\Delta t\right)[{}_n\mathbb{W}(\mathtt{D}_{j,k-l-1})]$
$-P(k-2,n)[{}_{n+2,k-6}F_{j,1}] + P(k-3,n)[{}_{n+2,k-8}F_{j,0}]$
$-\frac{\lambda}{2C}\mathfrak{M}(\mathtt{D})\sum_{l=1}^{k-3}P(l,n)\,\upsilon\left(\left[{}_n\widehat{F}_{j,k-l-3}\right],[{}_nx_j],(k-l-3)\Delta t\right)$
$-\frac{\lambda}{2C}\sum_{l=1}^{k-3}P(l,n)\,\omega\left(\left[{}_n\widehat{F}_{j,k-l-3}\right],[{}_nx_j],(k-l-3)\Delta t\right)[{}_n\mathbb{W}(\mathtt{D}_{j,k-2-l})]$
$+\frac{\lambda}{2C}\mathfrak{M}(\mathtt{D})\,\upsilon\left(\left[{}_n\widehat{F}_{j,k-2}\right],[{}_nx_j],(k-2)\Delta t\right)$
$+\frac{\lambda}{2C}\omega\left(\left[{}_n\widehat{F}_{j,k-2}\right],[{}_nx_j],(k-2)\Delta t\right)[{}_n\mathbb{W}(\mathtt{D}_{j,k-1})]$
$= A_nP(k-1,n+2)\left[{}_{n+2,k-4}\widehat{F}_{j,1}\right] - P(k-2,n)[{}_{n+2,k-6}F_{j,1}]$

$$-A_nP(k-2,n+2)\left[{}_{n+2,k-6}\widehat{F}_{j,0}\right]+P(k-3,n)\left[{}_{n+2,k-8}F_{j,0}\right]$$
$$+\tfrac{\lambda}{2C}\mathfrak{M}(\mathtt{D})\left(A_n\sum_{l=1}^{k-2}P(l,n+2)\,\upsilon\left(\left[{}_n\widehat{F}_{j,k-l-2}(x)\right],[{}_nx_j],(k-l-2)\Delta t\right)\right.$$
$$-\sum_{l=1}^{k-3}P(l,n)\,\upsilon\left(\left[{}_n\widehat{F}_{j,k-l-3}\right],[{}_nx_j],(k-l-3)\Delta t\right)$$
$$\left.+\upsilon\left(\left[{}_n\widehat{F}_{j,k-2}\right],[{}_nx_j],(k-2)\Delta t\right)\right)$$
$$+\tfrac{\lambda}{2C}\left(A_n\sum_{l=1}^{k-2}P(l,n+2)\,\omega\left(\left[{}_n\widehat{F}_{j,k-l-2}\right],[{}_nx_j],(k-l-2)\Delta t\right)[{}_n\mathbb{W}(\mathtt{D}_{j,k-l-1})]\right.$$
$$-\sum_{l=1}^{k-3}P(l,n)\,\omega\left(\left[{}_n\widehat{F}_{j,k-l-3}\right],[{}_nx_j],(k-l-3)\Delta t\right)[{}_n\mathbb{W}(\mathtt{D}_{j,k-l-2})]$$
$$\left.+\omega\left(\left[{}_n\widehat{F}_{j,k-2}\right],[{}_nx_j],(k-2)\Delta t\right)[{}_n\mathbb{W}(\mathtt{D}_{j,k-1})]\right).$$

Using Lemma 2.2.17 $\left[{}_n\widehat{F}_{j,k}\right]=P(k,n)\left[{}_{n+2(k-1)}\widehat{F}_{j,1}\right]-P(k-1,n)\left[{}_{n+2(k-2)}\widehat{F}_{j,0}\right]$

$$+\tfrac{\lambda}{2C}\mathfrak{M}(\mathtt{D})\sum_{l=1}^{k-1}P(l,n)\,\upsilon\left(\left[{}_n\widehat{F}_{j,k-l-1}\right],[{}_nx_j],(k-l-1)\Delta t\right)$$
$$+\tfrac{\lambda}{2C}\sum_{l=1}^{k-1}P(l,n)\,\omega\left(\left[{}_n\widehat{F}_{j,k-l-1}\right],[{}_nx_j],(k-l-1)\Delta t\right)[{}_n\mathbb{W}(\mathtt{D}_{j,k-l})],\text{ hence (B.7)}$$

holds. □

Corollary 2.2.20: Relations of the form

$$\Upsilon_{j,k}=\begin{bmatrix}\lambda^2 & 2(1-\lambda^2) & \lambda^2\end{bmatrix}\begin{bmatrix}\Upsilon_{j-1,k-1}\\ \Upsilon_{j,k-1}\\ \Upsilon JpKm\end{bmatrix}-\Upsilon_{j,k-2}+f(\Upsilon_{j,k-2})$$

with given values of $\{\Upsilon_{j,1},\Upsilon_{j,0}\}$ can be expressed as:

$$[\Upsilon_{j,k}]=P(k,n)[\Upsilon_{j,1}]-P(k-1,n)[\Upsilon_{j,0}]+\tfrac{\lambda}{2C}\sum_{l=1}^{k-1}P(l,n)[f(\Upsilon_{j,k-l-1})].$$

Proof. Repeat Lemma 2.2.19 using the relation

$$\Upsilon_{j,k}=\begin{bmatrix}\lambda^2 & 2(1-\lambda^2) & \lambda^2\end{bmatrix}\begin{bmatrix}\Upsilon_{j-1,k-1}\\ \Upsilon_{j,k-1}\\ \Upsilon_{j+1,k-1}\end{bmatrix}-\Upsilon_{j,k-2}+f(\Upsilon_{j,k-2})\text{ in place of (2.14).}$$

□

Corollary 2.2.21: Given values of $\{[\Upsilon_{j,1}],[\Upsilon_{j,0}]\}$, and $\lambda=1$, (2.18) is expressed as $\Upsilon_{j,k}=\sum_{l=0}^{k}\Upsilon_{j-k+2l,1}-\sum_{l=0}^{k-1}\Upsilon_{j-k+2l+1,0}+\sum_{l=1}^{k-1}\sum_{m=0}^{l-1}f(\Upsilon_{j-l+2m+1,k-l-1})$.

Proof. Use Corollary 2.2.18 to expand the $P(k,1)$ notation and sum the results.

□

Lemma B.1.4. $\frac{F(\zeta(x_j,t_k),0)+F(\xi(x_j,t_k),0)}{2}+\frac{1}{2C}\int\limits_{DoD(x_j,t_k)}\frac{\partial F(z,r)}{\partial r}\,|_{r=0}\,dz$

$$+\tfrac{1}{2C}\sum_{DoD(x_j,t_k)}^{n}\left(\int_{\mathtt{D}_{n,0}}\upsilon(F(z,r),z,r)\,dzdr+\int_{\mathtt{D}_{n,0}}w(F(z,r),z,r)\,dW(z,r)\right)$$
$$-P(k,1)\left[\widehat{F}_{j,1}\right]+P(k-1,1)\left[\widehat{F}_{j,0}\right]=P(k,1)[\mathfrak{e}_{j,1}]-P(k-1,1)[\mathfrak{e}_{j,0}].$$

Proof. Breaking the $DoD\left(x_j,t_k\right)$ into segments of length $2\Delta x$,
$\frac{F(\zeta(x_j,t_k),0)+F(\xi(x_j,t_k),0)}{2}+\frac{1}{2C}\int\limits_{DoD(x_j,t_k)}\frac{\partial F(y,s)}{\partial s}\mid_{s=0}dy$

$+\frac{1}{2C}\sum\limits_{DoD(x_j,t_k)}^{n}\left(\int\limits_{\mathtt{D}_{n,0}}v\left(F\left(z,r\right),z,r\right)dzdr+\int\limits_{\mathtt{D}_{n,0}}w\left(F\left(z,r\right),z,r\right)dW\left(z,r\right)\right)$

$=\frac{1}{2}\left(\widehat{F}\left(\zeta\left(x_j,t_k\right),0\right)+\widehat{F}\left(\xi\left(x_j,t_k\right),0\right)+\mathtt{e}_{\zeta_{j,k},0}+\mathtt{e}_{\xi_{j,k},0}\right)$

$+\frac{1}{2C}\sum\limits_{DoD(x_j,t_k)}^{n}\left(\int\limits_{x_{n-1}}^{x_{n+1}}\frac{\partial F(z,r)}{\partial r}\mid_{r=0}dz+\int\limits_{\mathtt{D}_{n,0}}v\left(F\left(z,r\right),z,r\right)dzdr\right.$

$\left.+\int\limits_{\mathtt{D}_{n,0}}w\left(F\left(z,r\right),z,r\right)dW\left(z,r\right)\right)$. From (2.8),

$F_{n,1}=\frac{F_{n-1,0}+F_{n+1,0}}{2}+\frac{1}{2C}\left(\int\limits_{x_{n-1}}^{x_{n+1}}\frac{\partial F(z,r)}{\partial r}\mid_{r=0}dz+\int\limits_{\mathtt{D}_{n,0}}v\left(F\left(z,r\right),z,r\right)dzdr\right.$

$\left.+\int\limits_{\mathtt{D}_{n,0}}w\left(F\left(z,r\right),z,r\right)dW\left(z,r\right)\right)$. Substitution yields

$\frac{F(\zeta(x_j,t_k),0)+F(\xi(x_j,t_k),0)}{2}+\frac{1}{2C}\int\limits_{DoD_{j,k}}\frac{\partial F(y,s)}{\partial s}\mid_{s=0}dy$

$+\frac{1}{2C}\sum\limits_{DoD(x_j,t_k)}^{n}\left(\int\limits_{\mathtt{D}_{n,0}}v\left(F\left(z,r\right),z,r\right)dzdr+\int\limits_{\mathtt{D}_{n,0}}w\left(F\left(z,r\right),z,r\right)dW\left(z,r\right)\right)$

$=\frac{1}{2}\left(\widehat{F}\left(\zeta\left(x_j,t_k\right),0\right)+\widehat{F}\left(\xi\left(x_j,t_k\right),0\right)+\mathtt{e}_{\zeta_{j,k},0}+\mathtt{e}_{\xi_{j,k},0}\right)+\sum\limits_{DoD_{j,k}}^{n}\left(F_{n,1}-\frac{F_{n-1,0}+F_{n+1,0}}{2}\right)$

$=\frac{1}{2}\left(\widehat{F}\left(\zeta\left(x_j,t_k\right),0\right)+\widehat{F}\left(\xi\left(x_j,t_k\right),0\right)+\mathtt{e}_{\zeta_{j,k},0}+\mathtt{e}_{\xi_{j,k},0}\right)+\sum\limits_{DoD_{j,k}}^{n}\left(\widehat{F}_{n,1}+\mathtt{e}_{n,1}\right)$

$-\sum\limits_{DoD_{j,k-1}}^{n}\left(\widehat{F}_{n,0}+\mathtt{e}_{n,0}\right)-\frac{1}{2}\left(\widehat{F}\left(\zeta\left(x_j,t_k\right),0\right)+\widehat{F}\left(\xi\left(x_j,t_k\right),0\right)+\mathtt{e}_{\zeta_{j,k},0}+\mathtt{e}_{\xi_{j,k},0}\right)$

$=\sum\limits_{DoD_{j,k}}^{n}\left(\widehat{F}_{n,1}+\mathtt{e}_{n,1}\right)-\sum\limits_{DoD_{j,k-1}}^{n}\left(\widehat{F}_{n,0}+\mathtt{e}_{n,0}\right)$

$=P\left(k,1\right)\left[\widehat{F}_{j,1}\right]-P\left(k-1,1\right)\left[\widehat{F}_{j,0}\right]+P\left(k,1\right)\left[\mathtt{e}_{j,1}\right]-P\left(k-1,1\right)\left[\mathtt{e}_{j,0}\right]$. Thus,

$\frac{F(\zeta(x_j,t_k),0)+F(\xi(x_j,t_k),0)}{2}+\frac{1}{2C}\int\limits_{DoD(x_j,t_k)}\frac{\partial F(z,r)}{\partial r}\mid_{r=0}dz$

$+\frac{1}{2C}\sum\limits_{DoD(x_j,t_k)}^{n}\left(\int\limits_{\mathtt{D}_{n,0}}v\left(F\left(z,r\right),z,r\right)dzdr+\int\limits_{\mathtt{D}_{n,0}}w\left(F\left(z,r\right),z,r\right)dW\left(z,r\right)\right)$

$=P\left(k,1\right)\left[\widehat{F}_{j,1}\right]-P\left(k-1,1\right)\left[\widehat{F}_{j,0}\right]+P\left(k,1\right)\left[\mathtt{e}_{j,1}\right]-P\left(k-1,1\right)\left[\mathtt{e}_{j,0}\right]$, where subtraction yields the desired result. □

Corollary B.1.5. $P\left(k,1\right)\left[\mathtt{e}_{j,1}\right]-P\left(k-1,1\right)\left[\mathtt{e}_{j,0}\right]=k\left(\overline{\mathtt{e}_{j,1}}\right)-\left(k-1\right)\left(\overline{\mathtt{e}_{j,0}}\right)$, *where* $\overline{\alpha}$ *denotes the average over the boundary,* $\delta\mho=DoD\left(x_j,t_k\right)$.

Proof. Replace the error terms of $P\left(k,1\right)\left[\mathtt{e}_{j,1}\right]-P\left(k-1,1\right)\left[\mathtt{e}_{j,0}\right]$ with Assumption 2.3.2 and (2.19). Since $\lambda=1$, $P\left(n,1\right)$ is equivalent to n additions. □

Remark B.1.6. *(2.20) can be represented via*

$$[\mathfrak{e}_{j,k}] = P(k,n)[\mathfrak{e}_{j,1}] - P(k-1,n)[\mathfrak{e}_{j,0}] + \sum_{l=1}^{k-1} P(l,n)\left[\Upsilon^{v}_{j,k-l-1} + \Upsilon^{\omega}_{j,k-l-1} + \beta^{v}_{j,k-l-1} + \beta^{\omega}_{j,k-l-1}\right] \tag{B.8}$$

which is a direct result of Lemma 2.2.19, (2.8), and (2.17), such that

$$\mathfrak{e}_{j,k} = \tfrac{F(\zeta(x,t),0)+F(\xi(x,t),0)}{2} + \tfrac{1}{2C}\int_{DoD(x,t)} \tfrac{\partial F(y,s)}{\partial s}\,|_{s=0}\,dy$$
$$+\tfrac{1}{2C}\iint_{DoI(x,t)} v(F(y,s),y,s)\,dyds + \tfrac{1}{2C}\iint_{DoI(x,t)} \omega(F(y,s),y,s)\,dW(y,s)$$
$$-P(k,n)\left[\widehat{F}_{j,1}\right] - \tfrac{\lambda}{2C}\mathfrak{M}(\mathtt{D})\sum_{l=1}^{k-1} P(l,n)\left[v\left(\widehat{F}_{j,k-l-1},x_j,(k-l-1)\Delta t\right)\right]$$
$$+P(k-1,n)\left[\widehat{F}_{j,0}\right] - \tfrac{\lambda}{2C}\sum_{l=1}^{k-1} P(l,n)\left[\mathbb{W}(\mathtt{D}_{j,k-l})\right]\left[\omega\left(\widehat{F}_{j,k-l-1},x_j,(k-l-1)\Delta t\right)\right].$$

Lemma B.1.4 establishes that $P(k,n)[\mathfrak{e}_{j,1}] - P(k-1,n)[\mathfrak{e}_{j,0}]$

$$= \tfrac{F(\zeta(x,t),0)+F(\xi(x,t),0)}{2} + \tfrac{1}{2C}\int_{DoD(x,t)} \tfrac{\partial F(y,s)}{\partial s}\,|_{s=0}\,dy$$
$$+\tfrac{1}{2C}\sum_{DoD(x_j,t_k)}^{n}\left(\int_{\mathtt{D}_{n,0}} v(F(z,r),z,r)\,dzdr + \int_{\mathtt{D}_{n,0}} w(F(z,r),z,r)\,dW(z,r)\right)$$
$$-P(k,1)\left[\widehat{F}_{j,1}\right] + P(k-1,1)\left[\widehat{F}_{j,0}\right] = \sum_{l=0}^{k}\mathfrak{e}_{j-k+2l,1} - \sum_{l=0}^{k-1}\mathfrak{e}_{j-k+2l+1,0}$$

while Lemma 2.2.11 establishes that

$$\sum_{l=1}^{k-1} P(l,n)\left[\Upsilon^{v}_{j,k-l-1} + \Upsilon^{\omega}_{j,k-l-1} + \beta^{v}_{j,k-l-1} + \beta^{\omega}_{j,k-l-1}\right]$$
$$= \tfrac{1}{2C}\iint_{DoI_{j,k}-DoD_{j,k}} v(F(y,s),y,s)\,dyds + \tfrac{1}{2C}\iint_{DoI_{j,k}-DoD_{j,k}} \omega(F(y,s),y,s)\,dW(y,s)$$
$$-\tfrac{1}{2C}\sum_{l=1}^{k-1}\sum_{m=0}^{l-1}\left[v\left(\widehat{F}_{j-l+2m+1,k-l-1},x_{j-l+2m+1},(k-l-1)\Delta t\right)\right]\mathfrak{M}(\mathtt{D})$$
$$-\tfrac{1}{2C}\sum_{l=1}^{k-1}\sum_{m=0}^{l-1}\left[\mathbb{W}(\mathtt{D}_{j-l+2m+1,k-l})\right]\left[\omega\left(\widehat{F}_{j-l+2m+1,k-l-1},x_{j-l+2m+1},(k-l-1)\Delta t\right)\right].$$

B.2 Chapter 3

An arbitrary $\mathbb{Z}^d$ space is constructed by adding individual points to a domain such that the distance between any two points is greater than or equal to an a priori Δx. Hence an 'arbitrary' $\mathbb{Z}^d_{\Delta x}$ space consists of points that fulfill Definition 1.1.3 by being mapped to the natural numbers and this mapping relates to the cardinality of the set and has no correlation with X, the geometric location in $\mathbb{R}^d$. Denote points in an arbitrary space via $g(\wp_j) = g_j$ where Figure B.3 shows a $\mathbb{R}^1$, uniform $\mathbb{Z}^1_{\Delta x}$, and arbitrary $\mathbb{Z}^1_{\Delta x}$ domain of length α and $\Delta x = \frac{\alpha}{24}$; the uniform $\mathbb{Z}^1$ interval has been divided into $M = 24$ discretisations, and the arbitrary $\mathbb{Z}^1$ has been assigned 9 points. Figure B.4 shows a $\mathbb{R}^2$ domain, an arbitrary $\mathbb{Z}^2$ domain that has been discretised into 9 points, and a uniform $\mathbb{Z}^2$ domain where

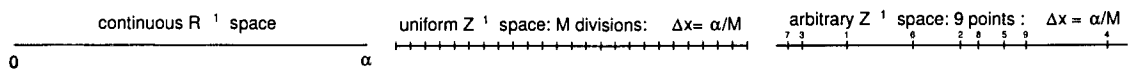

Figure B.3: One-dimensional space grids. Note: $\|X-Y\|_1 = \|X-Y\|_2$

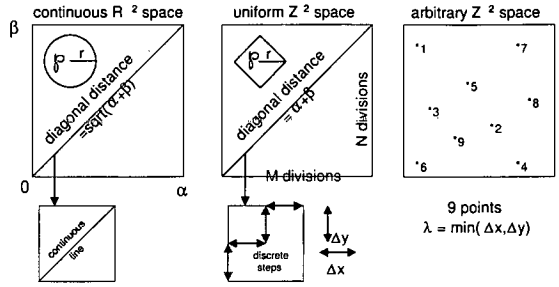

Figure B.4: Two dimensional space grids

the mesh used to cover the region has been divided into M and N orthogonal discretisations.

Notation B.2.1. *Let* $\left\{\widehat{G}_N(j;k), \widehat{G}_{\Delta x}(j;k)\right\}$ *denote an* {*arbitrary , uniform*} $\mathbb{Z}^d$ *FDSy approximation to a Green's function where* $\mathtt{card}(\mho) = N > 0$.

Lemma 3.1.13: Deterministic Existence. Given (EAIC), then a solution to $\{(3.1), \omega(X) = 0\}$ exists as defined by (3.5).

Proof. Refer to [59, page 455] or since $\nabla^2 G(X;Y) = 0$ then

$$\int_{\mho} G(X;Y)\, \upsilon(F(Y),Y)\, dY = \lim_{\Delta x \to 0} \int_{\mho - \mathtt{S}_2(X,\Delta x)} G(X;Y)\, \nabla^2 \upsilon(F(Y),Y)\, dY$$

$$= \lim_{\Delta x \to 0} \int_{\delta\mho - \mathtt{S}_2(X,\Delta x)} \left(G(X;Y) \frac{\partial F(Y)}{\partial Z} - F(Y) \frac{\partial G(X;Y)}{\partial Z} \right) dY$$

$$= \int_{\delta \mathtt{S}_2(X,\Delta x)} \left(G(X;Y) \frac{F(Y)}{\partial Z} - F(Y) \frac{\partial G(X;Y)}{\partial Z} \right) dY - \int_{\delta\mho} F_{\delta\mho}(Y) \frac{G(X;Y)}{\partial Z} dY.$$

Since, $\int_{\delta \mathtt{S}_2(X,\Delta x)} G(X;Y) \frac{F(Y)}{\partial Z} dY \to 0$, $\int_{\delta \mathtt{S}_2(X,\Delta x)} F(Y) \frac{\partial G(X;Y)}{\partial Z} dY$

$$= \int_{\delta \mathtt{S}_2(X,\Delta x)} F(Y) \frac{\partial \xi(X;Y)}{\partial Z} dY - \int_{\delta \mathtt{S}_2(X,\Delta x)} F(Y) \frac{\partial \zeta(X;Y)}{\partial Z} dY,$$

$\int_{\delta \mathtt{S}_2(X,\Delta x)} F(Y) \frac{\partial \xi(X;Y)}{\partial Z} dY \to F(X)$, and $\int_{\delta \mathtt{S}_2(X,\Delta x)} F(Y) \frac{\zeta(X;Y)}{\partial Z} dY \to 0$.

Hence, $\int_{\mho} G(X;Y)\, \upsilon(F(Y),Y)\, dY = F(X) - \int_{\delta\mho} H(X;Y)\, F_{\delta\mho}(Y)\, dY$. □

Lemma 3.1.14: Deterministic Uniqueness. Given (EAIC), then the solution $\{(3.1), \omega(X) = 0\}$, if it exists, is unique.

Proof. Assume that there are two solutions to (3.1), $F_1(X)$ and $F_2(X)$, with the same initial conditions and let $F_3(X) = F_1(X) - F_2(X)$. Then $F_3(X) =$

$\int_{\mho} G(X;Y)\left(v\left(F_1(Y),Y\right)-v\left(F_2(Y),Y\right)\right)dY$. For this term to not be uniquely 0, either two different Green's functions exist for the domain or there exits at least one point such that $F_1(X) \neq F_2(X)$. By definition the Green's function is unique. In order for $F_1(X) \neq F_2(X)$ to exist, there must be a second point Y where $F_1(Y) \neq F_2(Y)$. Using a recursive argument, $F_1(X) \neq F_2(X)$ on the entire domain which contradicts the initial conditions, thus $F_3(X) = 0$. □

Lemma 3.1.22: The Green's function is a symmetric kernel such that $G(X_1, X_2) = G(X_1, X_2)$, i.e. a reciprocity relation exits.

Proof. Using (3.7) and assuming $X_1 \neq X_2$ then $\int_{\mho}\left(G(Y,X_2)\bigtriangledown^2 G(Y,X_1)\right.$
$\left.-G(Y,X_1)\bigtriangledown^2 G(Y,X_2)\right)dY = \int_{\delta\mho}\left(G(Y,X_2)\frac{\partial G(Y,X_1)}{\partial Z} - G(Y,X_1)\frac{\partial G(Y,X_2)}{\partial Z}\right)dY.$
Since this involves a unit source with zero boundary conditions then (3.6) yields
$0 = \int_{\delta\mho}\left(G(Y,X_2)\frac{\partial G(Y,X_1)}{\partial Z} - G(Y,X_1)\frac{\partial G(Y,X_2)}{\partial Z}\right)dY$
$= \int_{\mho}\left(G(Y,X_2)\,1_{X_1=Y} - G(Y,X_1)\,1_{Y=X_2}\right)dY = G(X_2,Y) - G(Y,X_2).$ □

Lemma 3.1.24: [8, Lemma 2.1]: $\int_{\mho} G(\wp_{\mho}, Y)\,\omega(Y)\,dWY$ posses an almost surely continuous modification.

Proof. When $d = 1$, let $x \in [0,a]$, then $\int_0^a G(x,y)\,\omega(y)\,dW(y) = \frac{x}{a}\int_0^a \omega(y)\,dW(y)$
$-\int_0^x \omega(y)\,dW(y)$. This SDE result is well known and will be omitted; see [39].
When $d = 2$, $\mathbb{E}\left(\left|\int_{\mho}\omega(Y)\ln\left(\|X_1-Y\|_2\right)dW(Y) - \int_{\mho}\omega(Y)\ln\left(\|X_2-Y\|_2\right)dW(Y)\right|^2\right)$
$= \int_{\mho}\omega(Y)^2\left|\ln\|X_1-Y\|_2 - \ln\|X-Y\|_2\right|^2 dY \leq \|X_1-X_2\|_2^{2-\alpha}\times$
$\int_{\mho}\omega(Y)^2\left|\ln\|X_1-Y\|_2 - \ln\|X_2-Y\|_2\right|^{\alpha}\left(\int_0^1 \frac{da}{a\|X_1-Y\|_2+(1-a)\|X_2-Y\|_2}\right)^{2-\alpha} dY$
$\leq \|X_1-X_2\|_2^{2-\alpha}\max_{Y\in\mho}\left(\omega(Y)^2\right)\int_{\mho}\left|\ln\|X_1-Y\|_2 - \ln\|X_2-Y\|_2\right|^{\alpha}$
$\left(\frac{1}{\|X_1-Y\|_2}+\frac{1}{\|X_2-Y\|_2}\right)^{2-\alpha} dY \leq K_\alpha \ln\|X_1-X_2\|_2^{2-\alpha}\max_{Y\in\mho}\left(\omega(Y)^2\right)$
$\times\left(\int_{\mho}\left|\ln\|X_1-Y\|_2 - \ln\|X_2-Y\|_2\right|^{q\alpha}dY\right)^{\frac{1}{q}}\left(\int_{\mho}\frac{dY}{\ln\|X_1-Y\|_2^{(2-\alpha)p}}+\int_{\mho}\frac{dY}{\ln\|X_2-Y\|_2^{(2-\alpha)p}}\right)^{\frac{1}{p}}$
where $\frac{1}{q}+\frac{1}{p}=1$ and $1 < p < \frac{2}{2-\alpha}$. Hence, using Assumption 3.1.5:
$\mathbb{E}\left(\left|\int_{\mho}\ln\left(\|X_1-Y\|_2\right)\omega(Y)\,dW(Y) - \int_{\mho}\ln\left(\|X_2-Y\|_2\right)\omega(Y)\,dW(Y)\right|^2\right)$
$\leq K_\alpha\max_{Y\in\mho}\left(\omega(Y)^2\right)\|X_1-X_2\|_2^{1-\alpha}$ and since the difference in the integrals is a normal random variable with 0 mean, using Chebychev's Theorem
$\mathbb{E}\left(\left|\int_{\mho}G(X_1,Y)\,\omega(Y)\,dW(Y) - \int_{\mho}G(X_1,Y)\,\omega(Y)\,dW(Y)\right|^r\right) \leq K_\alpha\|X_1-X_2\|_2^{(1-\alpha)r}.$

Choosing $r > 2$, Kolmogorov's Lemma states that $\int_{\mho} \ln\left(\|X - Y\|_2\right) dW(Y)$ possesses an almost surely continuous modification and having chosen that modification we deduce $\mathbb{E}\left(\int_{\mho} \ln\left(\|S_t - Y\|_2\right) \omega(Y)\, dW(Y)\right)$ is continuous on $\mho$ and

$\frac{1}{\sqrt{2\pi}}\mathbb{E}\left(\int_{\mho} \ln\left(\|W_{X,t} - Y\|_2\right) \omega(Y)\, dW(Y) - \int_{\mho} \ln\left(\|X - Y\|_2\right) \omega(Y)\, dW(Y)\right)$
$= \int_{\mho} \ln\left(\|X - Y\|_2\right) \omega(Y)\, dW(Y) = \int_{\mho} G(X;Y)\, \omega(Y)\, dW(Y)$ with the Brownian sheet being fixed. $d = 3$ mirrors $d = 2$ such that it suffices to check that $h(x) = \int_{\mho} \frac{\omega(Y)}{\|X_1 - Y\|_2} dW(Y)$ posses an almost sure continuous modification. Let $0 < \theta < 1$;

$$\mathbb{E}\left(\left|\int_{\mho} \ln\left(\|X_1 - Y\|_2\right) \omega(Y)\, dW(Y) - \int_{\mho} \ln\left(\|X_2 - Y\|_2\right) \omega(Y)\, dW(Y)\right|^2\right)$$
$$= \int_{\mho} \left|\frac{1}{\|X_1 - Y\|_2} - \frac{1}{\|X_2 - Y\|_2}\right|^2 \omega(Y)^2\, dY$$
$$\leq \int_{\mho} \left|\frac{1}{\|X_1 - Y\|_2} - \frac{1}{\|X_2 - Y\|_2}\right|^{\frac{5+\theta}{4}} \left|\frac{\|X_2 - Y\|_2 - \|X_1 - Y\|_2}{\|X_1 - Y\|_2 \|X_2 - Y\|_2}\right|^{\frac{3+\theta}{4}} \omega(Y)^2\, dY$$
$$\leq \max_{Y \in \mho}\left(\omega(Y)^2\right) \|X_1 - X_2\|_2^{\frac{3-\theta}{4}} \left(\int_{\mho} \left|\frac{1}{\|X_1 - Y\|_2} - \frac{1}{\|X_2 - Y\|_2}\right|^{\frac{5+\theta}{2}} dY\right)^{\frac{1}{2}}$$
$$\times \left(\int_{\mho} \frac{dY}{\left(\|X_1 - Y\|_2 \|X_2 - Y\|_2\right)^{\frac{3+2\theta}{4}}}\right)^{\frac{1}{2}} \leq K_\theta \|X_1 - X_2\|_2^{\frac{3-\theta}{4}} \left(\int_{\mho} \frac{dY}{\|X_2 - Y\|_2^{\frac{5+2\theta}{2}}}\right.$$
$$\left. + \int_{\mho} \frac{dY}{\|X_1 - Y\|_2^{\frac{5+2\theta}{2}}}\right)^{\frac{1}{2}} \left(\int_{\mho} \frac{dY}{\|X_2 - Y\|_2^{3-\theta}}\right)^{\frac{1}{4}} \left(\int_{\mho} \frac{dY}{\|X_1 - Y\|_2^{3-\theta}}\right)^{\frac{1}{4}}.$$ It then follows that

$$\mathbb{E}\left(\left|\int_{\mho} G(X_2, Y)\, \omega(Y)\, dW(Y) - \int_{\mho} G(X_2, Y)\, \omega(Y)\, dW(Y)\right|^2\right) \leq K_\theta \|X_1 - X_2\|_2^{\frac{3-\theta}{4}}.$$

Using moments of Gaussian random variables, for any j, $K_\theta \|X_1 - X_2\|_2^{j\left(\frac{3-\theta}{8}\right)}$
$\geq \mathbb{E}\left(\left|\int_{\mho} G(X_1 - Y)\, \omega(Y)\, dW(Y) - \int_{\mho} G(X_2 - Y)\, \omega(Y)\, dW(Y)\right|^j\right)$. Conclude using Kolmogorov's Lemma to yield the desired result. □

Remark B.2.2. *It follows from the previous proof that* $\int_{\mho} \ln\left(\|X - Y\|_2\right) \omega(Y)\, dW(Y)$ *has Lipschitz paths when* $d = 1$, *Hölder continuous with exponent* $1 - \alpha$ *when* $d = 2$, *and Hölder continuous with exponent* $\frac{3}{8} - \alpha$ *when* $d = 3$.

Lemma 3.1.28: [8, Lemma 2.5]: Given the (EAIC) then (3.5) is the unique solution to (3.1) which is almost surely continuous on $\mho$.

Proof. **Uniqueness.** Let $F_1(x)$ and $F_2(x)$ be two solutions, then$F_1(x) - F_2(x)$
$+ \int_{\mho} G(X;Y)\left(\upsilon\left(F_1(Y)\right) - \upsilon\left(F_2(Y)\right)\right) dY + \int_{\mho} G(X;Y)\left(\omega(Y) - \omega(Y)\right) dY =$
0. Multiplying the appropriate terms of the equation by $\upsilon\left(F_1(X)\right) - \upsilon\left(F_2(X)\right)$, canceling terms, and using Lemma 3.1.26, then $a\left|F_1(X) - F_2(X)\right| \leq 0$ from

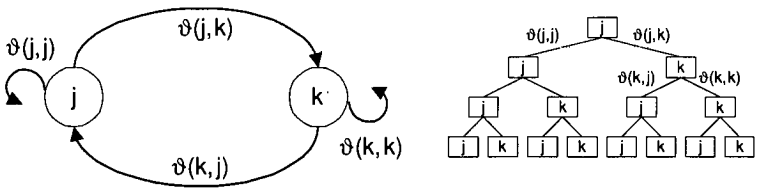

Figure B.5: 2 Point Closed Loop System

which uniqueness follows. This further implies the following uniqueness statement: If $F_1(X)$ and $F_2(X)$ satisfy (3.5) $\mho_j \subset \mathbb{R}^d$, then $F_1(x) = F_2(x)$ i.e. on $\{\mho \cup \mho_j\}$.

Existence Step 1. Suppose that $F(X)$ is bounded, continuous, and non-decreasing. Let W_n be a sequence of processes with trajectories $\int_{\mho} G(X;Y)\, dW_n(Y)$ $\to \int_{\mho} G(X;Y)\, dW(Y)$ almost surely as $n \to \infty$. For each n we consider (3.1) with 0 boundary conditions. The existence of a unique solution follows from Lions [4, Theorem 2.1 p. 171]. $F_n(X)$ fulfills (3.5) and $F_n(X) - F_m(X)$
$+ \int_{\mho} G(X;Y)\, \upsilon(F_n(Y))\, dY - \int_{\mho} G(X;Y)\, \upsilon(F_m(Y))\, dY$
$= \int_{\mho} G(X;Y)\, \omega(Y)\, dW_n(Y) - \int_{\mho} G(X;Y)\, \omega(Y)\, dW_m(Y)$. Multiply both sides by their respective terms and using Lemma 3.1.26 yields $\mathfrak{eg}^2_{n,m} \leq \int_{\mho} G(X;Y)$ $\times (W_n - W_m, \upsilon(F_n) - \upsilon(F_m) + 2a(F_n - F_m))$. Since $\mathbb{E}\left(\int_{\mho} G(X;Y)\,(W_n - W_m)^2\right)$ $\to 0$ as $n, m \to \infty$ and F is bounded, then $\{F_n\}$ is a Cauchy sequence and $F = \lim_{n\to\infty} F_n$ using (3.5).

Existence step 2. Suppose that $F(Y)$ is bounded from below and $F_n(Y) = F(Y) \wedge n$ where $F_n(Y)$ is the unique solution to (3.5). It follows from Lemma 3.1.27 that the sequence $\{F_n(x)\}$ is decreasing for any X, hence converges in $\mathbb{R} \cup -\infty$. Let $\beta_n = \left\{\sup_{\mho} F(X, F_0(X)) \leq n\right\}$. On β_n, $\upsilon(F_m) \leq \upsilon(F_0) \leq n$ and $\upsilon_m(F_m) = \upsilon(F_m)$ on β_m, for $m \geq n$. F_m is the unique solution on β_n to (3.5) and consequently $F_m = F_n$ on β_n where $m \geq n$ and $F_n \to F$.

Existence step 3. Now assume that F is bounded, continuous, and non-decreasing, let $F_n(Y) = F(Y) \vee (-n)$. Repeat the proof in the second step, constructing this time and increasing sequence. □

Lemma 3.2.11: $\widehat{G}_{N+1}(j;j) = \frac{\widehat{G}_N(j;j)}{1-\theta^*_{N+1}} = \frac{1}{1-\theta_{N+1}}$.

Proof. When $\mathtt{card}(\mho) = 1$, there is only one point for the FDSc to act on, hence $\widehat{G}_1(j;j) = 1 + \vartheta(j;j) + \vartheta(j;j)^2 + \cdots = \sum_{l=0}^{\infty} \vartheta(j;j)^l = \frac{1}{1-\theta_1}$; where $\theta_1 = \vartheta(j;j)$. If an explicit scheme is used, $\widehat{G}_1(j;j) = 1$, since $\vartheta(j;j) = 0$, otherwise the initial

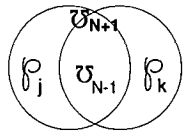

Figure B.6: Venn Diagram for $\mho_{N+1}$

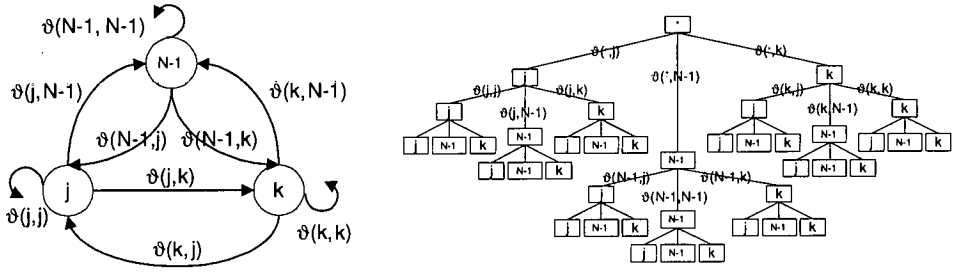

Figure B.7: Schematic and tree for $\mho_{N+1}$

disturbance will grow in size by a factor of $\frac{1}{1-\theta_1}$. When $\mathtt{card}(\mho) = 2$; refer to Figure B.5 and Figure B.6, where $\mho_{N-1} = \emptyset$:

$\widehat{G}_2(k;j) = \sum_{l=0}^{\infty} (\vartheta(k;k))^l \vartheta(k;j) \widehat{G}_2(j;j) = \vartheta(k;j) \widehat{G}_1(k;k) \widehat{G}_2(j;j)$

and $\widehat{G}_2(j;j) = \widehat{G}_1(j;j) + \sum_{l=0}^{\infty} (\vartheta(j;j))^l \widehat{G}_2(k;j) \vartheta(j;k)$

$= \widehat{G}_1(j;j) + \vartheta(j;k) \vartheta(k;j) \widehat{G}_2(j;j) \widehat{G}_1(j;j) \widehat{G}_1(k;k)$. Collecting $\widehat{G}_2(j;j)$ terms yields $\widehat{G}_2(j;j) = \frac{\widehat{G}_1(j;j)}{1-\vartheta(j;k)\vartheta(k;j)\widehat{G}_1(j;j)\widehat{G}_1(k;k)} = \frac{1}{1-\left(\vartheta(j;j)+\vartheta(j;k)\vartheta(k;j)\widehat{G}_1(k;k)\right)}$ where $\{\theta_2^*, \theta_2\} = \left\{\vartheta(j;k)\vartheta(k;j)\widehat{G}_1(j;j)\widehat{G}_1(k;k), \vartheta(j;j) + \vartheta(j;k)\vartheta(k;j)\widehat{G}_1(k;k)\right\}$.

As depicted in Figure B.6, when $\mathtt{card}(\mho_{N+1}) = N+1$, let $\wp_k$ be the new point added to $\mho_N = \{\mho_{N-1} \cup \wp_j\}$, where $\mho_{N-1}$ will be treated as one state, and assume that $\widehat{G}_N(j;j) = \frac{1}{1-\theta_N}$. Thus,

$\widehat{G}_{N+1}(j;j) = \sum_{l=0}^{\infty} \vartheta(j;j)^l \left(\vartheta(j;N-1)\widehat{G}_{N+1}(N-1;j) + \vartheta(j;k)\widehat{G}_{N+1}(k;j)\right)$

$= \widehat{G}_1(j;j)\vartheta(j;N-1)\widehat{G}_{N+1}(N-1;j) + \widehat{G}_1(j;j)\vartheta(j;k)\widehat{G}_{N+1}(k;j)$,

$\widehat{G}_{N+1}(k;j) = \widehat{G}_1(k;k)\vartheta(k;j)\widehat{G}_{N+1}(j;j) + \widehat{G}_1(k;k)\vartheta(k;N-1)\widehat{G}_{N+1}(N-1;j)$,

and $\widehat{G}_{N+1}(N-1;j) = \frac{\vartheta(N-1;j)\widehat{G}_{N+1}(j;j)+\vartheta(N-1;k)\widehat{G}_{N+1}(k;j)}{1-\vartheta(N-1;N-1)}$. Substitution yields

$\left(1 - \frac{\widehat{G}_1(j;j)\vartheta(j;N-1)\vartheta(N-1;j)}{1-\vartheta(N-1;N-1)}\right)\widehat{G}_{N+1}(j;j) = \left(\frac{\widehat{G}_1(j;j)\vartheta(j;N-1)\vartheta(N-1;k)}{1-\vartheta(N-1;N-1)} + \widehat{G}_1(j;j)\vartheta(j;k)\right)\widehat{G}_{N+1}(k;j)$ and $\widehat{G}_{N+1}(k;j) = \left(\widehat{G}_1(k;k)\vartheta(k;j) + \frac{\widehat{G}_1(k;k)\vartheta(k;N-1)\vartheta(N-1;j)}{1-\vartheta(N-1;N-1)}\right)\frac{\widehat{G}_{N+1}(j;j)}{\left(1-\frac{\widehat{G}_1(k;k)\vartheta(k;N-1)\vartheta(N-1;k)}{1-\vartheta(N-1;N-1)}\right)}$.

Remark B.2.3. *It is worth mentioning that* $1 = \frac{1-\vartheta(N-1;N-1)}{1-\vartheta(N-1;N-1)-\widehat{G}_1(j;j)\vartheta(j;N-1)\vartheta(N-1;j)} \times \left(\frac{\widehat{G}_1(j;j)\vartheta(j;N-1)\vartheta(N-1;k)}{1-\vartheta(N-1;N-1)} + \widehat{G}_1(j;j)\vartheta(j;k)\right)\frac{1-\vartheta(N-1;N-1)}{1-\vartheta(N-1;N-1)-\widehat{G}_1(k;k)\vartheta(k;N-1)\vartheta(N-1;k)}$

$\times \left(\widehat{G}_1(k;k)\,\vartheta(k;j) + \frac{\widehat{G}_1(k;k)\vartheta(k;N-1)\vartheta(N-1;j)}{1-\vartheta(N-1;N-1)}\right)$. *This is true only if the reciprocity relationship holds and the FDSc matrix is symmetric; see Lemma 3.2.16.*

Using $\widehat{G}_N(j;j) = \frac{1}{1-\theta_N}$ and the argument from the $\mathtt{card}(\mho) = 2$ case, $\widehat{G}_N(j;j) = \frac{\widehat{G}_1(j;j)}{1-\frac{\vartheta(j;N-1)\vartheta(N-1;j)\widehat{G}_1(j;j)}{1-\vartheta(N-1;N-1)}} = \frac{1}{1-\vartheta(j;j)+\frac{\vartheta(j;N-1)\vartheta(N-1;j)}{(1-\vartheta(N-1;N-1))}} = \frac{1}{1-\theta_N}$. Thus $\widehat{G}_{N+1}(j;j) = \widehat{G}_N(j;j)\left(\frac{\vartheta(j;N-1)\vartheta(N-1;k)}{1-\vartheta(N-1;N-1)} + \vartheta(j;k)\right)\widehat{G}_{N+1}(k;j) = \frac{\widehat{G}_N(j;j)}{1-\theta^*_{N+1}}$; where $\theta^*_{N+1} = 1 - \frac{1-\vartheta(N-1;N-1)}{\widehat{G}_{N+1}(k;j)(\vartheta(j;N-1)\vartheta(N-1;k)+\vartheta(j;k)(1-\vartheta(N-1;N-1)))}$ and $\theta_{N+1} = 1-(1-\theta_N)\left(1-\theta^*_{N+1}\right)$. Further algebraic reduction will be omitted since these results are adequate for this chapter. □

Corollary 3.2.13: Given EAIC, then $\widehat{G}(j;j)$ is a unique constant.

Proof. Let $\left\{\widehat{G}_N(j;j), \widehat{G}^{\dagger}_N(j;j)\right\}$ denote two different Green's function approximations. When $\mathtt{card}(\mho) = 1$, $\widehat{G}_1(j;j) = \widehat{G}^{\dagger}_1(j;j) = \frac{1}{1-\vartheta(j;j)}$ since there is only one point to act upon. Assuming that $\widehat{G}_N(j;j) \neq \widehat{G}^{\dagger}_N(j;j)$ for $\mathtt{card}(\mho) = N$; in order for this to occur at least one $\vartheta(n;m) \neq \vartheta^{\dagger}(n;m)$. This leads to a contradiction, since FDSc $\neq$ FDSc; thus $\widehat{G}_N(j;j) = \widehat{G}^{\dagger}_N(j;j)$. □

Corollary 3.2.14: Given (EAIC), then $\theta_{N+1} < 1$.

Proof. When $\mathtt{card}(\mho) = 1$, $\vartheta(j;j) < 1$, otherwise the FDSc is not consistent.
•When $\mathtt{card}(\mho) = 2$, $\frac{\vartheta(j;j)-\vartheta(j;j)\vartheta(k;k)+\vartheta(j;k)\vartheta(k;j)}{1-\vartheta(k;k)} < 1$ or
$\vartheta(j;j)(1-\vartheta(k;k)) + \vartheta(j;k)\vartheta(k;j) + \vartheta(k;k) < 1$. In an explicit FDSc; $0 + \vartheta(j;k)\vartheta(k;j) + 0 < 1$ almost surely. In an implicit FDSc, $\vartheta(j;j)(1-\vartheta(k;k)) + \vartheta(j;k)\vartheta(k;j) + \vartheta(k;k) < \vartheta(j;j)(1-\vartheta(k;k)) + (1-\vartheta(k;k))\vartheta(k;j) + \vartheta(k;k)$ $= (1-\vartheta(k;k))(\vartheta(j;j)+\vartheta(k;j)) + \vartheta(k;k) \leq (1-\vartheta(k;k))(1) + \vartheta(k;k) = 1$, hence, $\frac{\vartheta(j;j)-\vartheta(j;j)\vartheta(k;k)+\vartheta(j;k)\vartheta(k;j)}{1-\vartheta(k;k)} < 1$ almost surely.
•When $\mathtt{card}(\mho) = N+1$ it suffices to show that $0 < \theta^*_N \leq 1$.
Case 1: For an explicit scheme $\vartheta(l;l) = 0$, $\vartheta(N-1;N-1) + \vartheta(N-1;j)$
$+\vartheta(N-1;k) = 1$ and $\vartheta(\{j \text{ or } k\};\mho_{N-1}) \leq 1$ if $\wp_{\{j \text{ or } k\}}$ is an interior point and $\vartheta(\{j,k\};\mho_{N-1}) < 1$ if an adjacent point. Hence, almost surely true.
Case 2: For an implicit scheme $\theta^*_{N+1} < 1$ almost surely, since $0 < \vartheta(\mho_N;N+1) \leq (1-\vartheta(\mho_N;\mho_N))$ and $\vartheta(N+1;\mho_N) = 1-\vartheta(N+1;N+1)$. □

Corollary 3.2.15: When $\mathtt{card}(\mho) = N \to \infty$, then $\widehat{G}_N(j;j) \to \infty$ if $\wp_j$ is 'well within the interior' and a finite constant if $\wp_j$ is 'close to the interior.'

Proof. Since $\widehat{G}_{N+1}(j;j) = \frac{\widehat{G}_N(j;j)}{1-\theta^*_{N+1}}$, $\lim_{n\to\infty}\widehat{G}_N(j;j) = \widehat{G}_1(j;j)\prod_{n\to\infty}\frac{1}{1-\theta^*_n}$. Thus, it is simply a matter of checking that $0 < \theta^*_{N+1} \leq 1$ and this can be easily verified, using Assumption 3.2.1. If $\theta^*_n \mid \{n > M\}$ is numerically indistinguishable from 0, the growth of the discretised Green's function will remain constant after a finite

series of iterations. Being numerically distinguishable from 0 is dependent upon the radiation principle, round-off error, and location in the domain since points close to the boundary have a limited number of paths that can be utilised in the growth of the Green's function approximation. □

Lemma 3.2.16: Given (EAIC) where $\vartheta(j;k) = \vartheta(k;j)$, in accordance with Lemma 3.1.22 then the reciprocity relation is true such that $\widehat{G}_N(j;k) = \widehat{G}_N(k;j)$.

Proof. When $\mathtt{card}(\mho) = 1$, $\widehat{G}_1(j;k) = \widehat{G}_1(k;j) = \widehat{G}_1(j;j)$ since $\wp_j = \wp_k$. When $\mathtt{card}(\mho) = 2$, $\widehat{G}_2(j;k) = \sum_{l=0}^{\infty} (\vartheta(j;j))^l \vartheta(j;k) \widehat{G}_2(k;k)$
$= \vartheta(j;k) \widehat{G}_1(j;j) \widehat{G}_2(k;k) = \vartheta(k;j) \widehat{G}_1(j;j) \frac{\widehat{G}_1(k;k)}{1-\vartheta(j;k)\vartheta(k;j)\widehat{G}_1(j;j)\widehat{G}_1(k;k)}$
$= \vartheta(k;j) \widehat{G}_1(k;k) \frac{\widehat{G}_1(j;j)}{1-\vartheta(j;k)\vartheta(k;j)\widehat{G}_1(j;j)\widehat{G}_1(k;k)} = \vartheta(k;j) \widehat{G}_1(k;k) \widehat{G}_2(j;j)$
$= \sum_{l=0}^{\infty} (\vartheta(k;k))^l \vartheta(k;j) \widehat{G}_2(j;j) = \widehat{G}_2(k;j)$. Referring to Figure B.6:
•Assume $\vartheta(j;k) = \vartheta(k;j)$ true for $\{\mho_{N-1}, \mho_j, \mho_k\}$. $\mathtt{card}(\mho_{N-1}) = N-1$; $\mho_{N-1} = \{\wp_1, \cdots, \wp_{N-1}\}$. $\mathtt{card}(\mho_j) = \mathtt{card}(\mho_k) = N$; $\mho_j = \{\wp_1, \cdots, \wp_{N-1}, \wp_j\}$, and $\mho_k = \{\wp_1, \cdots, \wp_{N-1}, \wp_k\}$. Let $\mho_{N+1} = \mho_j \cup \mho_k$; $\mathtt{card}(\mho_{N+1}) = N+1$; $\mho_k = \{\wp_1, \cdots, \wp_{N-1}, \wp_j, \wp_k\}$.
Refering to Figure B.7; assume that $\mho_{N-1}$ is one state space and place a unit source at $\cdot = \wp_j$ to yield $\widehat{G}_{N+1}(j;k) = \vartheta(j;j) \widehat{G}_{N+1}(j;k) + \vartheta(j;k) \times$
$\Big(\vartheta(k;j) \widehat{G}_{N+1}(j;k) + \vartheta(k;k) \widehat{G}_{N+1}(k;k) + \vartheta(k;N-1) \widehat{G}_{N+1}(N-1;k)\Big)$
$+\vartheta(j;N-1) \Big(\vartheta(N-1;j) \widehat{G}_{N+1}(j;k) + \vartheta(N-1;k) \widehat{G}_{N+1}(k;k)$
$+\vartheta(N-1;N-1) \widehat{G}_{N+1}(N-1;k)\Big)$. Rearranging terms
$\widehat{G}_{N+1}(j;k) = \frac{1}{1-\vartheta(j;j)-\vartheta(k;j)\vartheta(j;k)-\vartheta(N-1;j)\vartheta(j;N-1)} \times$
$\Big(\vartheta(k;j) \Big(\vartheta(k;k) \widehat{G}_{N+1}(k;k) + \vartheta(N-1;k) \widehat{G}_{N+1}(N-1;k)\Big)$
$+\vartheta(N-1;j) \Big(\vartheta(k;N-1) \widehat{G}_{N+1}(k;k) + \vartheta(N-1;N-1) \widehat{G}_{N+1}(N-1;k)\Big)\Big)$
Using the fact that $\vartheta(m;n) = \vartheta(n;m)$; solving for
$\Big\{\widehat{G}_{N+1}(N-1;k), \widehat{G}_{N+1}(N-1;j), \widehat{G}_{N+1}(j;j), \widehat{G}_{N+1}(k;k)\Big\}$ with some rather tedious algebra yields $\widehat{G}_{N+1}(j;k) = \frac{1}{1-\vartheta(k;k)-\vartheta(j;k)\vartheta(k;j)-\vartheta(N-1;k)\vartheta(k;N-1)} \times$
$\Big(\vartheta(j;k) \Big(\vartheta(j;j) \widehat{G}_{N+1}(j;j) + \vartheta(N-1;j) \widehat{G}_{N+1}(N-1;j)\Big)$
$+\vartheta(N-1;k) \Big(\vartheta(j;N-1) \widehat{G}_{N+1}(j;j) + \vartheta(N-1;N-1) \widehat{G}_{N+1}(N-1;j)\Big)\Big)$
$= \widehat{G}_{N+1}(k;j)$, hence $\widehat{G}_{N+1}(j;k) = \widehat{G}_{N+1}(k;j)$ almost surely. □

Corollary 3.2.17: Given (EAIC), as $\Delta x \to 0$, the difference between two Green's function approximations on the same domain that are a $[V] = [\alpha_j \Delta x]$ distance apart is a constant such that: $\lim_{\Delta x \to 0} \Big(\widehat{G}_{\Delta x}(X;Y) - \widehat{G}_{\Delta x}([X-V],Y)\Big) = \lim_{\Delta x \to 0} \Big(\widehat{G}_{s\Delta x}(X;Y) - \widehat{G}_{s\Delta x}([X-sV],Y)\Big) = K$.

Proof. In the limit as $\Delta x \to 0$, the coefficients for the FDSc are oblivious to the magnitudes of $\{\Delta x, \upsilon(\cdot)\}$. When numerically solving the discretised homogeneous Laplace equation, the influence between two points follows a tree expansion depicted in Figures B.5 and B.7. Hence, the magnitude of $\widehat{G}(X_j; Y_k)$ is function of the number of discrete steps and paths between the points, i.e. a measure proportional to $\theta^{\left(\frac{\|X_j - Y_k\|_1}{\Delta x}\right)}$ and the number of paths that can be used to connect two points. From the radiation principle, points outside a neighborhood $\frac{\|[X-X_2]\|_2}{s\Delta x} \geq \|[\alpha_j]\|_2$ play a diminished role in the evaluation of $\widehat{G}(X;Y)$. Hence, the branching process used to approximate a solution does not utilise a 'distance measure' in the usual sense, only the number of discretised step sizes away. Thus, in the limit, $\Delta\widehat{G}$ represents a series of constants. Given that $\widehat{G}(X;Y) = \theta\widehat{G}(X;X)$ then this explains why $\widehat{G}(X;X) - \widehat{G}(X;Y) = \widehat{G}(X;X) - \theta\widehat{G}(X;X) = \widehat{G}(X;X)(1-\theta)$. □

B.3 Chapter 5

Fluids on the surface of a planet act as a combination of barotropic ('dry air') and baroclinic ('pure water') components where various amounts of water, momentum, and heat are exchanged. Thus, meteorological phenomena should be completely described by a set of highly nonlinear PDE's relying upon Newton's second law of motion, Navier-Stokes equations, law of thermodynamics, and the conservation of energy, mass, and momentum for thin viscous fluids. To visualize the scales involved, if the earth was an apple, the atmosphere and oceans would be approximately the skin of the apple, hence descriptions of the atmosphere involve fluid dynamics with minimal vertical motion relative to large horizontal motion. Due to friction, this thin fluid experience solid body rotation with a planet where winds and currents represent small deviations from this rotation. As discussed in [53, Section 1.3], the non-inertial plane of reference effects fluids by 'forcing' flow to occur parallel to pressure gradients; paired with the prevalence of naturally occurring density stratification, these effects further magnify the thin dynamics of a geophysical process since different density layers rarely interact except for rare global disturbances (volcanoes), strong isotropic systems (hurricanes), and the pycnocline. Thus, the atmosphere may be regarded as a multi-layered thin fluid on a rotating irregular surface experiencing external heating over $O(1000\text{ km})$ areas moving with average horizontal velocities of $O\left(10\frac{\text{km}}{\text{hr}}\right)$.

When describing phenomena such as weather systems, ocean currents, or the flow of magma in the inner earth; the effects of rotation, stratification, and the predominance of nonlinear interactions that involve a number of variables ensure that developing a process, much less evaluating a 'solution,' is an arduous

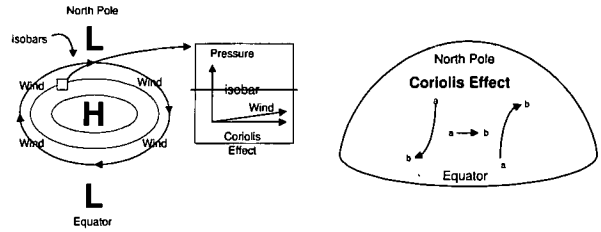

Figure B.8: Coriolis effect on the Northern Hemisphere

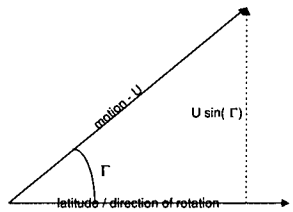

Figure B.9: Vector breakdown of the Coriolis effect

task. Due to this complexity, simplifications are made to develop processes that capture the essence of the physical phenomena, thus these assumptions are not an inherent property of a fluid, but are macro concepts. For example, steady incompressible and inviscid flow are simplifications acceptable for large scale geophysical fluid dynamics since viscosity effects are moot and shock waves do not exist almost surely. Quasi-Geostrophic (QG) processes attempt to describe large-scale geophysical fluid phenomena where the fluid is both incompressible and inviscid. The attribute of 'large scale motions' will be restricted to phenomena where the rate of a fluid element traveling over the length of a domain is significantly less than the rate of rotation of a planet. The Rossby number, $\theta_{\mathcal{A}} = \frac{\|\mathcal{U}\|_2}{2\mathcal{A}L}$, is a measure of the non-inertial plane of reference's effect upon the motion, where the magnitude of the Rossby number is inversely proportional to the effect the rotation has upon the process. Thus, only phenomena with low Rossby numbers ($\theta_{\mathcal{A}} \leq 1$) will be considered, where a planet's rotation plays a significant role in the movement of the fluid. On earth, the effect of the low Rossby number is the seeming force called the Coriolis Effect, where objects appear to experience a force that is orthogonal to the rotation of the earth and pushes from (left to right) / (right to left) if one is in the northern / southern hemisphere; refer to Figure B.8

Remark B.3.1. *For the Coriolis effect, only consider the velocity of the process normal to the direction of rotation. Unless otherwise specified, the rate of rotation for the earth is* $\mathcal{A} = 7.3 \times 10^{-5} s^{-1}$ *and the magnitude of the acceleration can be*

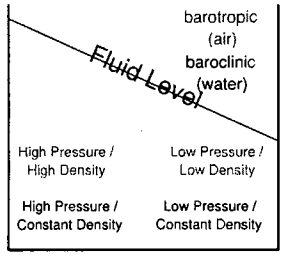

Figure B.10: Barotropic and Baroclinic

estimated at $C = 2\mathcal{A}\sin(\Gamma) \approx 2A \times U$, *where* Γ *is the angle from the equator; refer to Figure B.9.*

Remark B.3.2. *The Poincaré inequality holds for these boundary conditions. Solid stationary walls with no-slip boundary conditions,* $\mathcal{U} = 0$ *and either constant temperatures* $T = T_{wall}$ *or adiabatic conditions* $\frac{\partial T}{\partial Z} = 0$ *are utilised, where Ekman layers at the lid and base are due to the ageostrophic effects of having a 'hard' surface. One cannot 'cut' or sever a fluid's boundary and the boundary of a fluid 'sticks' to non-fluid surfaces; refer to works by Rutherford and [47, page 6].*

B.3.0.1 Baroclinic and barotropic components

Although a spectral approach will not be used in this text, all fluids have barotropic and baroclinic components, where:

•The baroclinic component of a fluid, $\Upsilon\mathtt{c}(x, y, z, t)$, represents the dynamics of fluid similar to pure water, where the components of pressure and density do not coincide such that $\nabla\rho_{MV} \times \nabla\mathcal{P} \neq 0$. For example, the density at the bottom of a glass of water is the same as the density at the top, but the pressure is greater at the bottom of the glass.

•The barotropic component of a fluid, $\Upsilon\mathtt{t}(x, y, z, t)$, represents the dynamics of a compressible fluid similar to pure dry air. The components of pressure and density coincide such that $\nabla\rho_{MV} \times \nabla\mathcal{P} = 0$. For example, the density and pressure of dry air at the bottom of a glass is more than at the top.

Notation B.3.3. *In a two-level system, the first barotropic and baroclinic modes are given by* $\Upsilon\mathtt{t}(x, y, z, t) = \frac{F(x,y,z_l,t)+F\left(x,y,z_{\neq l},t\right)}{2}$ *and* $\Upsilon\mathtt{c}(x, y, z, t) = \frac{F(x,y,z_l,t)-F\left(x,y,z_{\neq l},t\right)}{2}$. *Let* $\mathtt{1}_{=l}$ *denotes the indicator function if the level for the variable is the same as the level in question and* $\mathtt{1}_{\neq l}$ *if the level is different.*

Due to spectral properties, stream function processes are often separated into baroclinic and barotropic components, such that waves can be decoupled. Since the fluid is inviscid, both components cannot support a shearing stress, thus flow runs parallel to isobars and are driven by pressure and the Coriolis effect.

B.3.1 Inviscid shallow-water processes

As discussed in [53], when constructing processes, numerous approaches can be taken to describe a phenomena, but the processes considered in this text will utilise a two-layer conservation approach using partial derivatives (Eulerian) vice a convective derivatives (Lagrangian). One of the most prolific processes of describing geophysical fluid dynamics has been the study of inviscid shallow-water models and shear fluid dynamics on a homogenous, incompressible, and inviscid (baroclinic) fluid as proposed by Rossby, Pedlosky, et all. In this two-layered shear flow shallow water model, the baroclinic nature of the fluid and mass conservation ensure that $\nabla \mathcal{U} = \frac{\partial \mathcal{U}_x}{\partial x} + \frac{\partial \mathcal{U}_y}{\partial y} + \frac{\partial \mathcal{U}_z}{\partial z} = 0$ while $\|F\|_2 \left(\mathfrak{M}\left(L\right)^{-1}\right) \lll 1$. Given these constraints, $\frac{\partial \mathcal{U}_x}{\partial x} + \frac{\partial \mathcal{U}_y}{\partial y} = 0$ and the vorticity is given by: $[\mathcal{V}] = \begin{bmatrix} \frac{\partial \mathcal{U}_z}{\partial y} \\ -\frac{\partial \mathcal{U}_z}{\partial x} \\ \frac{\partial \mathcal{U}_y}{\partial x} - \frac{\partial \mathcal{U}_x}{\partial y} \end{bmatrix}$. This two-layer approach is the simplest model that maintains baroclinicty and is robust and resilient in that as one eliminates given wave frequencies, other waves transfer the energy flux. The connection between the elliptic processes of Chapter 3 and processes of this chapter are quite apparent, but the connection with the hyperbolic process is not as clear. To illustrate this connection, one of the simplest processes to consider is a two-dimensional model where one of the dimensions is space and the other is time; as in Chapter 2. Processes of this nature can be reduced to the so-called telegrapher's problem $\frac{\partial F(x,t)}{\partial x \partial t} + \frac{F(x,t)}{4} = 0$ which is a hyperbolic process with initial conditions solved on either $\mathbb{R}^2_{+t}$, the positive quadrant, or a semi-finite strip; [21, Section 28.3]. Although simplified, higher dimensional models on a planetary surface possess the same connection where the spherical wrapping of a planet can be modeled with a restricted semi-finite strip with boundary conditions experiencing the reflection property of Chapter 2. In the 1950's Forsythe demonstrated that the solution this process where $x \in [0, L]$ is $F(x,t) = \int_0^L G(x-y,\tau)\, df(y,0)$ where $G(\cdot)$ is a Green's function that represents the characteristic solutions of Chapter 2 and not the Green's function defined in Chapter 3 and 4.

Remark B.3.4. $\frac{\partial_{\text{conv}} g}{\partial_{\text{conv}} t} = \frac{\partial g}{\partial t} + \mathcal{U}\left(\frac{\partial g}{\partial x}, \frac{\partial g}{\partial y}, \ldots\right)$ *denote the convective derivative which is derivative along a fluids trajectory to a particular closed element. Rather than fixing a derivative on a set point in space, the derivative is centered upon a small element in a fluid. Heuristically view a convective derivative as a drop of ink in a stream of water.*

The state variables of density, entropy, friction, and pressure are denoted by ρ_{MV}, $\mathcal{H}$, $\mathtt{fr}$, and $\mathcal{P}$, respectively. Other physical constants include the Berger

number (bg), Reynolds number ($\varkappa$),beta plane coefficient $\mathcal{B}$, viscous dissipation constant ν, Ekman dissipation constant $\mathcal{E}$ and the Froude Number (f) which is a quantitative measure of the relative importance of rotation and stratification on a fluid. Vorticity is a measure of the curl of a velocity vector, enstrophy is the total mean square vorticity and the low Rossby number implies that the relative vorticity is small compared to the planetary vorticity, where flows almost surely experience a significant vorticity vector, which is non-divergent. If the curl of $\mathcal{U}$ is 0, then the flow is irrotational and the circulation is 0 on every closed path. A vortex filament is a line in the fluid that parallels the vorticity vector. Let:

•$\mathcal{U}(x,y,z,t) = \begin{bmatrix} \mathcal{U}_x(x,y,z,t) \\ \mathcal{U}_y(x,y,z,t) \\ \mathcal{U}_z(x,y,z,t) \end{bmatrix}$ denote the velocity of a fluid.

•$\mathcal{V}(x,y,z,t) = \begin{bmatrix} \frac{\partial \mathcal{U}_z}{\partial y} - \frac{\partial \mathcal{U}_y}{\partial z} \\ \frac{\partial \mathcal{U}_x}{\partial z} - \frac{\partial \mathcal{U}_z}{\partial x} \\ \frac{\partial \mathcal{U}_y}{\partial x} - \frac{\partial \mathcal{U}_x}{\partial y} \end{bmatrix}$ denote the vorticity of a fluid.

•$\mathcal{G} = [\mathcal{G}^T] = [0, 0, -\mathcal{G}]$ denote the acceleration due to gravity.

B.3.2 Equations of state

[17, Chapter 10] gives an introduction to enforcing conservation laws in a FDSy to ensure that mass, energy, momentum, vorticity, and enstrophy are conserved. From Assumption 5.1.8 the domain is a closed system and friction is negligible within the interior. Incompressible denotes that the ρ_{MV} is a constant and independent of the temperature and inviscid implies $\nu = 0$. Tangential stress implies a non-zero viscosity and energy and mass cannot be created or destroyed and it is impossible to convert heat into work at a constant temperature. This implies that complete information for a process at set time is known if the stream function, two thermodynamic variables, and an equation of state are given. The basic hydrodynamic equations for a barotropic atmosphere are the equation of motion relative to a non-inertial plane of reference (Newton's second law), the continuity equation (conservation of mass), the equation of state for dry air and the thermodynamic equations may be written as follows.

•The momentum equation: $\frac{\partial \mathcal{U}}{\partial t} = \alpha \mathtt{grad}\mathcal{P} - 2\mathcal{A} \times \mathcal{U} + \mathcal{G} + \mathtt{f}r$

•Conservation of mass: $\frac{\partial \rho_{MV}}{\partial t} = -\mathtt{grad} \cdot (\rho_{MV}\mathcal{U})$ given $\rho_{MV} = \frac{1}{\alpha}$ and $\mathcal{P}\alpha = \beta\mathcal{T}$

•First law of thermodynamics - conservation of energy: $h = c\frac{\partial \mathcal{T}}{\partial t} + \mathcal{P}\frac{\partial \alpha}{\partial t}$

where α is the specific volume, β is the barotropic gas constant for dry air, c is the specific heat at a constant volume, and h is the diabatic heating. These equations may be written in terms of various coordinate systems and although they are capable of solution, as shown in [53, Chapter 4], further simplification can be conducted. For example, using the hydrostatic relation $\frac{1}{\rho_{MV}}\frac{\partial \mathcal{P}}{\partial z} + \mathcal{G} = 0$ to

derive forms identical to the simplified Navier-Stokes equation. The $d = 2$ steady Navier-Stokes equations for an incompressible fluid in conservative form are:
$\bullet \frac{\partial(\mathcal{U}_x^2)}{\partial x} + \frac{\partial(\mathcal{U}_x\mathcal{U}_y)}{\partial y} + \frac{\partial}{\partial x}\left(\frac{\mathcal{P}}{\rho_{MV}}\right) = \nu\left(\nabla^2\mathcal{U}_x\right) \qquad \bullet \alpha^2\left(\frac{\partial \mathcal{U}_x}{\partial x} + \frac{\partial \mathcal{U}_y}{\partial y}\right)$
$\bullet \frac{\partial(\mathcal{U}_y^2)}{\partial y} + \frac{\partial(\mathcal{U}_x\mathcal{U}_y)}{\partial x} + \frac{\partial}{\partial y}\left(\frac{\mathcal{P}}{\rho_{MV}}\right) = \nu\left(\nabla^2\mathcal{U}_y\right)$
where α is a reference velocity introduced to homogenize the eigen values of the system. If the process is inviscid the Navier-Stokes equations reduce to the Euler Equations where: $\bullet \frac{\partial \mathcal{P}}{\partial t} + v \cdot \nabla + \gamma \mathcal{P} \nabla \cdot v = 0.$
$\bullet \frac{\partial \rho_{MV} u}{\partial t} + \nabla \cdot (\rho_{MV} uu) + \nabla = 0 \qquad \bullet \frac{\partial \rho_{MV}}{\partial t} + \nabla \cdot (\rho_{MV} v) = 0$
Pressure in this case is not a thermodynamic variable, but it can be considered a LaGrange multiplier that ensures the kinematic constraint of incompressibility, i.e. solenoid of the velocity field. The vorticity is calculated by $\mathcal{V} = \nabla \times u$ and represents approximately half the local rotation rate of the fluid. The additional of the term $\omega \cdot \nabla u$ represents the effects of the vortex stretching and is identically 0 in two-dimensional flows. The vorticity can be combined with the stream function to yield a concise description of the two-dimensional flows where the flow is parallel to curves of constant streamlines. The boundary conditions are $F\left(\wp_{\delta\mho}\right) = 0$ and $\frac{\partial F(\wp_{\delta\mho})}{\partial Z} = 0$, where the elimination of the vorticity leads to the pure stream function $\frac{\partial \mathcal{Q}}{\partial t} + \mathrm{J}\left(F, \mathcal{Q}\right) = \nu\Delta^2 F$ where energy is transferred via convection, not conduction or radiation.

B.3.3 Quasi-Geostrophic existence and uniqueness

The following results are taken directly from [7].

Notation B.3.5. *Let $\langle u, v\rangle$ denote an inner product.*

Use the integral form
$\mathcal{Q}(t) = G(t)\,\mathcal{Q}_0(t) + \int_0^t G(t-s)\,f(\mathcal{Q}(s))\,ds + \int_0^t G(t-s)\,\omega(x,y,t)\,dW(s).$
By defining
$f(\mathcal{Q}) = -\mathcal{E}\mathcal{Q} - \mathcal{B}\frac{\partial F}{\partial x} - \mathrm{J}\left(F, \mathcal{Q}\right)$ and $h(t) = \mathcal{Q}(t) - \int_0^t G(t-s)\,\omega(x,y,t)\,dW(s)$
yields the deterministic mild integral equation
$h(t) = G(t)\,\mathcal{Q}_0 + \int_0^t G(t-s)\,f\left(h(t) + \int_0^t G(t-s)\,\omega(x,y,t)\,dW(s)\right)ds$. In the following, prove the local existence of $h(t)$ by the Banach contraction mapping principle in l^2. Since A generates an analytic semi-group $S(t)$ on l^2 and has only negative eigen values, we have for $a > 0$,
$S(t)(-A)^a = (-A)^a S(t)$ yields $\|(-A)^a S(t)\,u\|_2 \leq \frac{c}{t^a} \cdot \|u\|_2$, hence
$\|S(t)\|_2 \leq K \cdot \|u\|_2$. We first show that $S_0^t S(t-s)\,f(U(s) + W_A(s))\,ds$ makes sense for $U(\cdot) + W_A(\cdot)$ and thus $U(\cdot)$ in $C([0,T]; l^2)$. Recalling that $w = U + W_A$, this follows from the following lemma.

Lemma B.3.6. *[7, Lemma 1]: Define the mapping* $\mathrm{F} : C([0,T];H_0^1) \to C([0,T];l^2)$ *by* $(\mathrm{F}(w))(t) = \int_0^t G(t-s) f(w(s))\,ds$ *where* $t \in [0,T]$ *and* $w \in C([0,T];H^1)$. *The* F *is continuous, and it can be extended t a continuous mapping from the space* $C([0,T];l^2)$ *to* $C([0,T];l^2)$. *Furthermore, the image of the extended mapping is contained in* $C([0,T];H^a)$ *for* $a \in \left[0,\frac{1}{2}\right)$.

Proof. The continuity of $\mathrm{F} : C([0,T];H_0^1) \to C([0,T];l^2)$ is obvious. As for extending the domain of f let $\{ww_2\} \in C([0,T];l^2)$ be arbitrary. Using the above abbreviations $w = \nabla^2 F$ and $w_2 = \nabla^2 F_2$, we get $f(w) - f(w_2) = \mathcal{E}(w_2 - w) + \mathcal{B}(F_2 - F) + \frac{\partial F}{\partial x}\frac{\partial (w_2 - w)}{\partial y} + \frac{\partial (F_2 - F)}{\partial x}\frac{\partial w_2}{\partial y} - \frac{\partial F}{\partial y}\frac{\partial (w_2 - w)}{\partial x} + \frac{\partial (F - F_2)}{\partial y}\frac{\partial w_2}{\partial x}$. Let $a \in [0,1)$ and consider an arbitrary $\psi \in D((-A)^a)$. Then the above identity implies

$J = \langle (-A)^a \psi, \int_0^t G(t-s) f(w(s))\,ds - \int_0^t G(t-s) f(w_2(s))\,ds \rangle$

$= \int_0^t \langle G(t-s)(-A)^a \psi, \left[\mathcal{E}(w_2 - w) + \mathcal{B}\frac{\partial (F_2 - F)}{\partial x} + \frac{\partial F}{\partial x}\frac{\partial (w_2 - w)}{\partial y}\frac{\partial (F_2 - F)}{\partial x}\frac{\partial w_2}{\partial y}\right.$

$\left. - \frac{\partial F}{\partial y}\frac{\partial (w_2 - w)}{\partial x} + \frac{\partial (F - F_2)}{\partial y}\frac{\partial w_2}{\partial x}\right](s)\rangle ds = \int_0^t (J_1 + J_2 + J_3 + J_4 + J_5 + J_6)\,ds$. Let

- $J_1 = \langle G(t-s)(-A)^a \psi, (\mathcal{E}(w_2 - w))](s)\rangle$
- $J_2 = \langle G(t-s)(-A)^a \psi, \left[\mathcal{B}\frac{\partial (F_2 - F)}{\partial x}\right](s)\rangle$
- $J_3 = \langle G(t-s)(-A)^a \psi, \left[\frac{\partial F}{\partial x}\frac{\partial (w_2 - w)}{\partial y}\right](s)\rangle$
- $J_4 = \langle G(t-s)(-A)^a \psi, \left[\frac{\partial (F_2 - F)}{\partial x}\frac{\partial w_2}{\partial y}\right](s)\rangle$
- $J_5 = \langle G(t-s)(-A)^a \psi, \left[-\frac{\partial F}{\partial y}\frac{\partial (w_2 - w)}{\partial x}\right](s)\rangle$
- $J_6 = \langle G(t-s)(-A)^a \psi, \left[\frac{\partial (F - F_2)}{\partial y}\frac{\partial w_2}{\partial x}\right](s)\rangle$.

and estimate $|J_j|$ such that

- $|J_1| = |\langle G(t-s)(-A)^a \psi, \mathcal{E}(w_2 - w)\rangle| \le \mathcal{E}\,\|G(t-s)(-A)^a \psi\|_2 \cdot \|w_2 - w\|_2$

$\le rK(t-s)^{-a} \cdot \|\psi\|_2 \cdot \|w_2 - w\|_2$

- $|J_2| = \left|\langle G(t-s)(-A)^a \psi, \left[\mathcal{B}\frac{\partial (F_2 - F)}{\partial x}\right](s)\rangle\right|$

$\le \mathcal{B}\,\|G(t-s)(-A)^a \psi\|_2 \cdot \left\|\frac{\partial (F_2 - F)}{\partial x}\right\|_2 \le \mathcal{B}K(t-s)^{-a}\,\|\psi\|_2 \cdot \|w_2 - w\|_2$ where we have used the Poincaré inequality, on $\frac{\partial (F_2 - F)}{\partial x}$ which has 0 mean. Using the Cauchy-Schwartz inequality $|\langle u, v\rangle| \le \|u\|\,\|v\|$ we also obtain

- $|J_3| = \left|\langle G(t-s)(-A)^a \psi, \left[\frac{\partial F}{\partial x}\frac{\partial (w_2 - w)}{\partial y}\right](s)\rangle\right|$

$= \left|\langle \frac{\partial D}{\partial y}\left((G(t-s)(-A)^a \psi)\frac{\partial F}{\partial x}, w_2 - w\right)\rangle\right|$

$\le \left|\langle \frac{\partial D}{\partial y}(G(t-s)(-A)^a \psi)\frac{\partial F}{\partial x}, w_2 - w\rangle\right| + \left|\langle (G(t-s)(-A)^a \psi)\frac{\partial^2 F}{\partial x \partial y}, w_2 - w\rangle\right|$

$\le \left\|\frac{\partial D}{\partial y}(G(t-s)(-A)^a \psi)\frac{\partial F}{\partial x}\right\| \cdot \|w_2 - w\| + \|G(t-s)(-A)^a \psi\|_\infty \cdot \left\|\frac{\partial^2 F}{\partial x \partial y}\right\| \cdot \|w_2 - w\|$.

As for estimating $\left\|\frac{\partial D}{\partial y}(G(t-s)(-A)^a \psi)\frac{\partial F}{\partial x}\right\|$ we get

$\left\|\frac{\partial D}{\partial y}(G(t-s)(-A)^a \psi)\frac{\partial F}{\partial x}\right\| \le \left\|\frac{\partial D}{\partial y}(G(t-s)(-A)^a \psi)\right\|_{\frac{1}{4}} \cdot \left\|\frac{\partial F}{\partial x}\right\|_{\frac{1}{4}}$

$\leq K \left\| \frac{\partial D}{\partial y} \left(G\left(t-s\right) \left(-A\right)^{a} \psi \right) \right\|_{H^{\frac{1}{2}}} \cdot \left\| \frac{\partial F}{\partial x} \right\|_{H^{1}} \leq K \left\| \left(G\left(t-s\right) \left(-A\right)^{a} \psi \right) \right\|_{H^{\frac{3}{2}}} \cdot \left\| w \right\|$
$\leq K \left\| A^{\frac{3}{4}+b} G\left(t-s\right) \left(-A\right)^{a} \psi \right\| \cdot \left\| w \right\| \leq K \left(t-s\right)^{-\left(\frac{3}{4}+b+a\right)} \left\| \psi \right\| \cdot \left\| w \right\|$, where we have used the inequality $\left\| uv \right\| \leq \left\| u \right\|_{\frac{1}{4}} \left\| v \right\|_{\frac{1}{4}}$, the continuity of the mapping $\frac{\partial D}{\partial y} : H^{\frac{3}{2}} \rightarrow H^{\frac{1}{2}}$, the embedding $D\left(\left(-A\right)^{\frac{3}{4}+b} \right) H^{\frac{3}{2}}$ for arbitrary $b > 0$, and the facts that $H^{\frac{1}{2}}$ and H^{1} are embedded in l^{4}. Furthermore, $\left\| G\left(t-s\right) \left(-A\right)^{a} \psi \right\|_{\infty} \leq K \left\| G\left(t-s\right) \left(-A\right)^{a} \psi \right\|_{H^{1+b}} \leq K \left\| G\left(t-s\right) \left(-A\right)^{\frac{1}{2}+b} \left(-A\right)^{a} \psi \right\|$
$\leq K \left(t-s\right)^{-\left(\frac{1}{2}+b+a\right)} \left\| \psi \right\|$ because of the smoother property of the semi-group G and the embeddings $D\left(\left(-A\right)^{\frac{1}{2}+b} \right) \rightarrow H^{1+b} \rightarrow l^{\infty}$ for arbitrary $b > 0$. Thus,

- $\left| J_3 \leq K \left(t-s\right)^{-\left(\frac{3}{4}+b+a\right)} + K \left(t-s\right)^{-\left(\frac{1}{2}+b+a\right)} \right| \cdot \left\| \psi \right\| \cdot \left\| w \right\| \cdot \left\| w - w_2 \right\|$
- $\left| J_4 \leq K \left(t-s\right)^{-\left(\frac{3}{4}+b+a\right)} + K \left(t-s\right)^{-\left(\frac{1}{2}+b+a\right)} \right| \cdot \left\| \psi \right\| \cdot \left\| w_2 \right\| \cdot \left\| w - w_2 \right\|$
- $\left| J_5 \leq K \left(t-s\right)^{-\left(\frac{3}{4}+b+a\right)} + K \left(t-s\right)^{-\left(\frac{1}{2}+b+a\right)} \right| \cdot \left\| \psi \right\| \cdot \left\| w \right\| \cdot \left\| w - w_2 \right\|$
- $\left| J_6 \leq K \left(t-s\right)^{-\left(\frac{3}{4}+b+a\right)} + K \left(t-s\right)^{-\left(\frac{1}{2}+b+a\right)} \right| \cdot \left\| \psi \right\| \cdot \left\| w_2 \right\| \cdot \left\| w - w_2 \right\|$

Thus we have $\left| J \right| \leq \int_{0}^{t} \left(\left| J_1 \right| + \left| J_2 \right| + \left| J_3 \right| + \left| J_4 \right| + \left| J_5 \right| + \left| J_6 \right| \right) ds$
$\leq \frac{\mathcal{E}K+\mathcal{B}K}{1-a} \cdot t^{1-a} \cdot \left\| \psi \right\| \cdot \sup_{0 \leq s \leq t} \left\| w\left(s\right) - w_2\left(s\right) \right\| + \left(\frac{8K}{1-4b-4a} \cdot t^{\frac{1}{4}-b-a} + \frac{4K}{1-2b-2a} \cdot t^{\frac{1}{42}-b-a} \right) \cdot \left\| \psi \right\| \cdot \sup_{0 \leq s \leq t} \left(\left\| w\left(s\right) \right\| + \left\| w_2\left(s\right) \right\| \right) \cdot \sup_{0 \leq s \leq t} \left\| w\left(s\right) - w_2\left(s\right) \right\|$ providing the positive constants $\left\{ a, b \right\}$ satisfy $0 < a + b < \frac{1}{4}$. This finally implies that

$\int_{0} tG\left(t-s\right) f\left(w\left(s\right)\right) - \int_{0} tG\left(t-s\right) f\left(w_2\left(s\right)\right) \in D\left(\left(-A\right)^{a}\right)$ for $0 < a < \frac{1}{4}$ and

$\left\| \left(\left(-A\right)^{a}\right) \left(\int_{0} tG\left(t-s\right) f\left(w\left(s\right)\right) - \int_{0} tG\left(t-s\right) f\left(w_2\left(s\right)\right) \right) \right\|$
$\leq \frac{\mathcal{E}K+\mathcal{B}K}{1-a} \cdot t^{1-a} \cdot \left\| \psi \right\| \cdot \sup_{0 \leq s \leq t} \left\| w\left(s\right) - w_2\left(s\right) \right\| + \left(\frac{8K}{1-4b-4a} \cdot t^{\frac{1}{4}-b-a} + \frac{4K}{1-2b-2a} \cdot t^{\frac{1}{2}-b-a} \right) \cdot \left\| \psi \right\| \cdot \sup_{0 \leq s \leq t} \left(\left\| w\left(s\right) \right\| + \left\| w_2\left(s\right) \right\| \right) \cdot \sup_{0 \leq s \leq t} \left\| w\left(s\right) - w_2\left(s\right) \right\|$. Especially for $a = 0$ we obtain $\left\| \int_{0} tG\left(t-s\right) f\left(w\left(s\right)\right) - \int_{0} tG\left(t-s\right) f\left(w_2\left(s\right)\right) \right\|$
$\leq \left(K + \mathcal{B}K\right) \cdot t \cdot \sup_{0 \leq s \leq t} \left\| w\left(s\right) - w_2\left(s\right) \right\| + \left(\frac{8K}{1-4b} \cdot t^{\frac{1}{4}-b} + \frac{4K}{1-2b} \cdot t^{\frac{1}{2}-b} \right) \cdot \left\| \psi \right\|$
$\cdot \sup_{0 \leq s \leq t} \left(\left\| w\left(s\right) \right\| + \left\| w_2\left(s\right) \right\| \right) \cdot \sup_{0 \leq s \leq t} \left\| w\left(s\right) - w_2\left(s\right) \right\|$ for every $0 < b < \frac{1}{4}$. □

Concluding from the above lemma that $\int_{0} tG\left(t-s\right) f\left(U\left(s\right)\right) + W_A\left(s\right)$, considered as a mapping with the argument $U\left(\cdot\right)$ can be extended to a bounded map from $C\left(\left[0,T\right], l^{2}\left(D\right)\right)$ into itself. To obtain that a unique local solution $U\left(t\right)$ has a unique local solution $w\left(x,y,t\right)$ on $\left[0,\tau\right)$, by the Banach contraction mapping principle, the solution $w\left(x,y,t\right) \in C\left(\left[0,\tau\right]; l^{2}\left(D\right)\right)$ as well as $w\left(x,y,t\right) \in C\left(\left[0,\tau\right]; H^{a}\left(D\right)\right)$ for arbitrary $a \in \left[0, \frac{1}{2}\right)$.

Theorem 5.1.10: [7, Theorem 1]: Using (QGAIC), then for the initial conditions considered in this text, there exists a unique global solution to (5.1) when

$\omega(X)W(X) = \omega(X)W(t)$.

Proof. Let $U = \nabla^2 u$ and $V = \nabla^2 v$ Because of the smoothing effect of the sectorial operator A, and the fact that f is locally Lipschitz in U from $H_0^{m+1} \cap H^{2(m+1)}$ to $H_0^m \cap H^{2m}$ for $m = \{0,1,2\}$, we conclude that the solution is $H_0^m \cap H^{2m}$ for $m = \{0,1,2\}$ and hence U is a strong solution. Estimating the norm $\|U(t)\|$, multiply by u and integrate over D to get

$\frac{1}{2}\frac{\partial \|U\|^2}{\partial t} = -v\int\limits_D |\nabla U|^2 - \mathcal{E}\int\limits_D (U+V)U - \mathcal{B}\int\limits_D \left(\frac{\partial u}{\partial x} + \frac{\partial v}{\partial x}\right)U - \int\limits_D \mathrm{J}(u+v, U+V)$

$= -v\|\nabla U\|^2 - \mathcal{E}\int\limits_D (U^2+UV) - \mathcal{B}\int\limits_D \left(\frac{\partial u}{\partial x}U + \frac{\partial v}{\partial x}U\right)$

$+\int\limits_D \left(-\frac{\partial u}{\partial x}\frac{\partial V}{\partial y}U + \frac{\partial u}{\partial y}\frac{\partial V}{\partial x}U - \frac{\partial v}{\partial x}\frac{\partial V}{\partial y}U + \frac{\partial v}{\partial y}\frac{\partial V}{\partial x}U\right)$ where we have used the fact that $\int\limits_D \mathrm{J}(u,F)U = \int\limits_D \mathrm{J}(v,F)U = 0$ via integration by parts. We estimate the right hand side term by term

$\bullet -\mathcal{E}\int\limits_D (U+V)U \le \mathcal{E}(1+L\|V\|_\infty)\|U\|^2$

$\bullet -\mathcal{B}\int\limits_D \left(\frac{\partial u}{\partial x} + \frac{\partial v}{\partial x}\right)U \le \mathcal{B}\int\limits_D \frac{1}{2}\left(\frac{\partial u}{\partial x}^2 + U^2 + \frac{\partial v}{\partial x}^2 + V^2\right)$

$\le \mathcal{B}K\left(\|U\|^2 + \|V\|^2\right) \le \mathcal{B}K\left(\|U\|^2 + \|V\|_\infty^2\right)$ where we have used the Poincaré inequality on $\frac{\partial u}{\partial x}$ and $\frac{\partial v}{\partial x}$ which have 0 mean.

$\int\limits_D -\frac{\partial u}{\partial x}\frac{\partial V}{\partial y}U = \int\limits_D \frac{\partial\left(\frac{\partial u}{\partial x}U\right)}{\partial y}V = \int\limits_D \left(\frac{\partial^2 u}{\partial x \partial y}UV + \frac{\partial u}{\partial x}\frac{\partial U}{\partial y}V\right)$

$\le \|V\|_\infty \int\limits_D \left|\frac{\partial^2 u}{\partial x\partial y}U\right| + \int\limits_D \left(\left|\frac{\partial u}{\partial x}\right| \cdot \|V\|_\infty\right)\left|\frac{\partial U}{\partial y}\right|$

$\le \|V\|_\infty \int\limits_D \frac{1}{2}\left(\frac{\partial^2 u}{\partial x\partial y}^2 + U^2\right) + \int\limits_D \left(\frac{1}{2\alpha}\frac{\partial u}{\partial x}^2 \|V\|_\infty^2 \frac{\alpha}{2}\frac{\partial U}{\partial y}^2\right)$

$\le \frac{K}{2}\|V\|_\infty\left(1 + \frac{1}{a}\|V\|_\infty\right) + \|U\|^2 + \frac{\alpha}{2}\|\nabla U\|^2$. Since $\int\limits_D \frac{\partial^2 u}{\partial x\partial y}^2$ is bounded by $K\int\limits_D \nabla^2 u^2 = KS_D U^2$. We also have used the Young inequality to get that $\left(\left|\frac{\partial u}{\partial x}\right|\|V\|_\infty\right)\left|\frac{\partial U}{\partial y}\right| \le \frac{1}{2\alpha}\frac{\partial u}{\partial x}^2\|V\|_\infty^2 + \frac{\alpha}{2}\frac{\partial U}{\partial y}^2$, for any real positive number $\alpha > 0$. Similarly we have $\int\limits_D \frac{\partial u}{\partial y}\frac{\partial V}{\partial x}U \le \frac{K}{2}\|V\|_\infty\left(1 + \frac{1}{\alpha}\|V\|_\infty\right)\|U\|^2 + \frac{\alpha}{2}\|\nabla U\|^2$

$\int\limits_D -\frac{\partial v}{\partial x}\frac{\partial V}{\partial y}U = \int\limits_D \frac{\partial \frac{\partial v}{\partial x}U}{\partial y}V = \int\limits_D \left(\frac{\partial^2 v}{\partial x\partial y}UV + \frac{\partial v}{\partial x}\frac{\partial U}{\partial y}V\right)$

$\le \|V\|_\infty \int\limits_D \frac{1}{2}\left(\frac{\partial^2 v}{\partial x\partial y}^2 + U^2\right) + \int\limits_D \left(\frac{1}{2\alpha}\frac{\partial v}{\partial x}^2\|V\|_\infty^2 + \frac{\alpha}{2}\frac{\partial U}{\partial y}^2\right)$

$\le \frac{1}{2}\|V\|_\infty\|U\|^2 + K\|V\|_\infty\|V\|^2 + \frac{K}{\alpha}\|V\|_\infty^2\|V\|^2 + \frac{\alpha}{2}\|\nabla U\|^2$

$\le \frac{1}{2}\|V\|_\infty\|U\|^2 + K\|V\|_\infty^3 + \frac{K}{\alpha}\|V\|_\infty^4 + \frac{\alpha}{2}\|\nabla U\|^2$

$\int\limits_D -\frac{\partial v}{\partial Y}\frac{\partial V}{\partial X}U \le \frac{1}{2}\|V\|_\infty\|U\|^2 + K\|V\|_\infty^3 + \frac{K}{\alpha}\|V\|_\infty^4 + \frac{\alpha}{2}\|\nabla U\|^2$.

Combining these results yields $\frac{1}{2}\frac{\partial \|U\|}{\partial t}^2 \le (-v+2\alpha)\cdot\|\nabla U\|^2$

$+\left(\mathcal{E}(1+K\|V\|_\infty) + \mathcal{B}K + K\|\mathbb{V}\|_\infty\left(1+\frac{1}{\alpha}\|V\|_\infty\right) + \|V\|_\infty\right)\cdot\|U\|^2 + \mathcal{B}K\|V\|_\infty^2 + 2K\|V\|_\infty^3 + \frac{2}{\alpha}K\|V\|_\infty^4$. Taking $\alpha = v/2$, we obtain $\frac{1}{2}\frac{\partial\|U\|}{\partial t}^2 \le A(t)\cdot\|U(t)\|^2 + B(t)$ where $A(t) = \left(\mathcal{E}(1+K\|V\|_\infty) + \mathcal{B}K + K\|\mathbb{V}\|_\infty\left(1+\frac{1}{\alpha}\|V\|_\infty\right) + \|V\|_\infty\right) > 0$

and $B(t) = 2\mathcal{B}K\|V\|_\infty^2 + 4K\|V\|_\infty^3 + \frac{8}{v}K\|V\|_\infty^4 > 0$. Hence by the Gronwall inequality we obtain $\|U(t)\|^2 \leq \|w_0\|^2 e^{\int_0^t A(s)ds} + \int_0^t B(s) e^{\int_s^t A(\mathcal{E})dr} ds$ where $t \in (0,T)$. Note that $H_0^3(D)$ is embedded in $C_0(D)$, the trajectories of $W_A(t)$ can be uniformly approximate on any finite interval $[0,T]$ by functions V in $C([0,T]; H_0^3(D))$ and $D(A)$ is dense in $l^2(D)$. Thus, the boundedness estimate is true for any local solution $U(t)$. This shows that the unique local solution does not blow up on any finite intervals. □

Appendix C

Computer code

Although not all of the programs are necessary when implementing a particular system, the following is intended as a guide for the construction of the algorithms presented in this text. Allocating code with respect to private and public access is at the discretion of the programmer.

•The following C++ 'header files' are assumed: `stdio.h`, `iomanip.h`, `math.h`, `iostream.h`, `fstream.h`, `stdlib.h`, and `time.h`. If using a different language, please utilise appropriate header files to ensure similar functionality.

•The following files are specifically created for numerical implementations and assumed when designing systems: `functions.cpp`, `time_class.cpp`, `fft.cpp`, `vector.cpp`, `comp_num.cpp`, `comp_vec.cpp`, `matrix_3d.cpp`, `matrix_2d.cpp`, `chi_test.cpp`, `max_min.cpp`, `random_gen.cpp`, `path.cpp`, `square.cpp`, and `space.cpp`. The last three classes are numerical implementations of the Brownian path, Brownian sheet, and Brownian space; refer to Propositions C.2.1 - C.2.3.

C.1 Notation

Algorithms have been coded in JAVA and C++, but will be presented in pseudo-code to utilise the notation of this text and free the reader from a particular language syntax. Refer to the following examples.

Program C.1.1. *The function* $\omega(\cdot)$ *is a generic function returning a real value and the constant* `char TYPE_of_`ω `= {'a','m','g','d'}` *determines if* $\omega(\cdot)$ *is an additive, multiplicative, general, or 0 functional, respectively.*

ω `(real` $\widehat{F}$`, vector` X`) : real`

```
{
   if TYPE_of_ω = d then return (0);
   if TYPE_of_ω = a then return (ω(X));
   if TYPE_of_ω = m then return (ω(X)F̂);
```

```
   if TYPE_of_ω = g then return (ω(F̂, X));
}
```

Thus in C++, Program C.1.1 could be:

```
double w_func(double F, double x, double y, double z)
{ double tempval = 0.0;
   if (TYPE_of_w =='a')
     tempval = 2x + y − 3z ∗ z;
   if (TYPE_of_w =='m')
     tempval = ((2x + y − 3z ∗ z) ∗ F);
   if (TYPE_of_w =='g')
     tempval = ((2x + y − 3z ∗ z) ∗ F ∗ F − F);
   return(tempval); }
```

Program C.1.2. *For an example of a user defined class, the following $d = 2$ matrix class is dynamically allocated and incremented by Δx.*

```
class matrix_2d
{
   double Δx, Δy, A(·);
     matrix_2d(int Mx, Ny; double α, L) %% Constructor function.
     {
       Δx = L/(Mx−1);    Δy = λy Δx;    A = new vector double [Mx];
       for j = 0 to Mx
       {
         Aj = new vector double [Ny];
         for k = 0 to Ny
           Aj,k = α;
       }
       if print_it=1 then print "Create matrix_2d";
     }
     ~matrix_2d() %% Destructor function.
     {
       if print_it=1 then print "Destruct matrix_2d";
       for j = 0 to Mx
         delete Aj;
       delete A;
     }
%% Functions that belong in this class are placed here.
};
```

C.1.1 Constants

The following constants will be utilised and denote `integer` int_{max} as the maximum positive integer that can be expressed on a given computer.

`double` π `= 3.14159265358979323846264338;`

`double` e `= 2.71828182845904523536028747;`

`int char_offset = 304;`

`int print_it = 0;` %% Set to 1 to print results to the screen.

`int dec_places = 9;` %% The number of decimal places requested when printing out results. The maximum value is dependent upon the number of significant digits being utilised on the computer.

`int noise_generations = 1;` %% The number of noise generations used to derive an approximation. Set equal to 1 if a pathwise approximation is required or a higher number if a non-pathwise approximation is required.

`double` $\Delta x = \frac{L}{M_x - 1}$; %% The corresponding Δx for M_x where $x \in [0, L]$.

`int` $M_{small} = 5$; %% The 'roughest' M_x grid considered.

`double` λ `= 1.0;` %% the hyperbolic CFL condition

`double` C_{hyp} `> 0;` %% The speed of propagation

`int hyp_STYLE_of_INIT = 1;` %% Allows different initialization schemes to be utilised when evaluating adjacent points $\widehat{F}(x_j, \Delta t)$.

`int hyp_STYLE_of_SOL = 1;` %% Set to 0 if a P approximation is sought or 1 if a approximation is sought over the DoI.

`double` $\lambda_y = \lambda_z = 1;$

`double es = 5e-12;`

`int e_STYLE_of_INIT = 1;` %% A variable that allows for different initialization schemes to be utilised when evaluating the discretised boundary.

`int e_STYLE_of_SOL = 2;` %% A variable that allows for different FDSy's to be utilised: SOR, multigrid, Jacobi, etc.

`double` $\vartheta = \left(2\left(1 + \lambda_y^2 + \lambda_z^2\right)\right)^{-1}$; %% The canonical FDSc's of (3.9) through (3.11) will be assumed.

`double` λ_t `= 0.001;`

`char QGprocess = 'f';` %% 'h' 'l' = Designates whether a Früh, Haines and Holland, or Lee process is being modeled.

`int save = 1e7;` %% Save $\left[\widehat{F}(\cdot)\right]$ and any other required information every 'save'th time iteration.

`int QGruns = 1e10;` %% The number of time iterations required before a model terminates.

C.1.2 Goodness of fit

Program C.1.3. *A test for goodness of fit using a Pearson Chi-square test, where* $\chi^2(\mathfrak{e}) = \sum_{j=1}^{\mathrm{card}(\mho_{\Delta x})} = \frac{\left|\widehat{F}_{\theta\Delta x}(\wp_j) - \widehat{F}_{\Delta x}(\wp_j)\right|^2}{\widehat{F}_{\theta\Delta x}(\wp_j)}$.

```
chi_2_test (matrix_2d F̂_{θΔx}, F̂_{Δx}(·); integer M_x, N_y): real
{
  real α = 0, χ² = 0;
  for j = 0 to M_x
    for k = 0 to N_y
    {
      if F̂_{θΔx}(jΔx, kΔt) ≠ 0 then χ² = χ² + |F̂_{θΔx}(jΔx,kΔt) − F̂_{Δx}(jΔx,kΔt)|² / F̂_{θΔx}(jΔx,kΔt);
      if F̂_{θΔx}(jΔx, kΔt) = 0 then α = |F̂_{Δx}(jΔx, kΔt)|²;
    }
  if α ≥ α_critical then
    print "Questionable test:" (χ², α);
  return (χ²);
}
```

C.2 Numerical generation of Brownian spaces

A method for numerically generating a white noise stochastic space is accomplished by dividing a domain into mutually exclusive subspaces and generating a series of mean-zero Gaussian random variables. As standard notation, let $\alpha \mid \beta$ denote α given β, $\mathfrak{M}(\cdot)$ denote the Lebesgue measure, and denote the Normal distribution via $\mathfrak{f}_{\mathcal{N}(\mu,\sigma^2)}(s) = \frac{1}{\sqrt{2\pi\sigma^2}} e^{\frac{-(s-\mu)^2}{2\sigma^2}}$. Mutually exclusive sub-domains, $\mathtt{D}_j$, have independent and stationary increments such that:

- $W(0) = 0$, $\mathbb{W}(\mathtt{D}_j) \sim \mathcal{N}(0, \mathfrak{M}(\mathtt{D}_j))$, and $W(\cdot)$ is continuous.
- Given $\mathtt{D}_k \subset \mathtt{D}_j$ then $\mathbb{E}(\mathbb{W}(\mathtt{D}_j) \mid \mathbb{W}(\mathtt{D}_k)) = \mathbb{W}(\mathtt{D}_k)$, $\mathbb{V}(\mathbb{W}(\mathtt{D}_j) \mid \mathbb{W}(\mathtt{D}_k)) = \mathfrak{M}(\mathtt{D}_j - \mathtt{D}_k)$, and $\mathbb{C}(\mathbb{W}(\mathtt{D}_j), \mathbb{W}(\mathtt{D}_k)) = \mathfrak{M}(\mathtt{D}_j \cap \mathtt{D}_k)$.
- $\mathbb{E}\left(\mathbb{W}(\mathtt{D}_j)^4\right) = 3\mathfrak{M}(\mathtt{D}_j)^2$.

The initial generation of $W(X)$ given $\mathbb{Z}^d_{\Delta x}$ is a straightforward procedure, while the refinement of $W(X)$ is not; as demonstrated via the following propositions.

Proposition C.2.1. *Assuming a Brownian path, $W(x)$, has been created with $\mathfrak{M}(\mathtt{D}_j) = \Delta x$; when the path decreases in step size to $\mathfrak{M}(\mathtt{D}_k) = \frac{\Delta x}{2}$, the stationary increments of $\mathbb{W}(\mathtt{D}_j) \sim \mathcal{N}(0, \mathfrak{M}(\mathtt{D}_j))$ refine to $\mathbb{W}_2(\mathtt{D}_k \mid \mathbb{W}(\mathtt{D}_j)) \sim \mathcal{N}\left(\frac{\mathbb{W}(\mathtt{D}_j)}{2}, \frac{1}{4}\mathfrak{M}(\mathtt{D}_j)\right)$ and $\mathbb{W}_2(\mathtt{D}_{k+1} \mid \mathbb{W}(\mathtt{D}_j)) = \mathbb{W}(\mathtt{D}_j) - \mathbb{W}(\mathtt{D}_k)$, where $k = 2j$. A possible refinement*

scheme would consist of $\mathbb{W}_2\left(\mathtt{D}_k \mid \mathbb{W}(\mathtt{D}_j)\right) = \frac{\mathbb{W}(\mathtt{D}_j)}{2} + \alpha$ *and* $\mathbb{W}_2\left(\mathtt{D}_{k+1} \mid \mathbb{W}(\mathtt{D}_j)\right) = \frac{\mathbb{W}(\mathtt{D}_j)}{2} - \alpha$*; where* $\alpha \sim \mathcal{N}\left(0, \frac{1}{4}\mathfrak{M}\left(\mathtt{D}_j\right)\right)$.

Proof. Given a Brownian path, derive a second process, $W_2(x)$, by utilising a Levy Construction Method conditioned upon the functional values of $\mathbb{W}(\mathtt{D}_j)$. Hence, $\mathbb{E}(\mathbb{W}_2(\mathtt{D}_k) \mid \mathbb{W}(\mathtt{D}_j)) = \frac{\mathbb{W}(\mathtt{D}_j)}{2}$ and $\mathbb{V}(\mathtt{D}_k) = \frac{\Delta x}{2}$, to yield
$\mathbb{E}(\mathbb{V}(\mathbb{W}_2(\mathtt{D}_k) \mid \mathbb{W}(\mathtt{D}_j))) = \frac{\Delta x}{2} - \mathbb{V}\left(\frac{\mathbb{W}(\mathtt{D}_j)}{2}\right) = \frac{\Delta x}{4}$; refer to Figure C.1. □

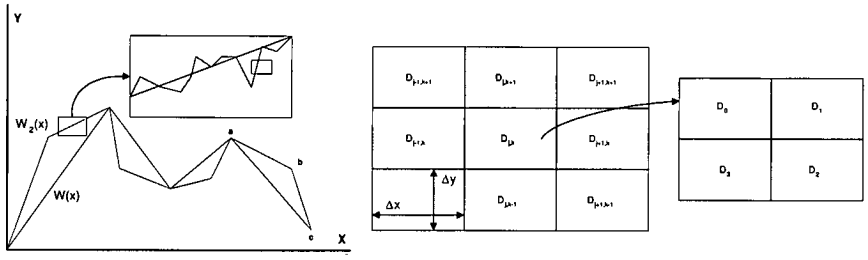

Figure C.1: Levy construction: Brownian path and sheet divisions

Proposition C.2.2. *Assuming a two-dimensional Brownian sheet has been created where* $\mathtt{D}_{j,k}$ *consists of rectangular shape regions with central differences. In order to construct the Levy refinement scheme depicted in Figure C.1, let* $\mathtt{D}_{j,k}$ *be the union of the four restricted rectangular regions labeled* $\{\mathtt{D}_0, \mathtt{D}_1, \mathtt{D}_2, \mathtt{D}_3\}$. *A possible refinement scheme would consist of:* $\mathbb{W}(\mathtt{D}_0) = \frac{\mathbb{W}(\mathtt{D}_{j,k})}{4} + \frac{\alpha}{2} + \beta_1$, $\mathbb{W}(\mathtt{D}_1) = \frac{\mathbb{W}(\mathtt{D}_{j,k})}{4} + \frac{\alpha}{2} - \beta_1$, $\mathbb{W}(\mathtt{D}_2) = \frac{\mathbb{W}(\mathtt{D}_{j,k})}{4} - \frac{\alpha}{2} + \beta_2$, $\mathbb{W}(\mathtt{D}_3) = \frac{\mathbb{W}(\mathtt{D}_{j,k})}{4} - \frac{\alpha}{2} - \beta_2$*; where* $\alpha \sim \mathcal{N}\left(0, \frac{1}{4}\mathfrak{M}(\mathtt{D}_{j,k})\right)$ *and* $\beta_{\{1,2\}} \sim \mathcal{N}\left(0, \frac{1}{8}\mathfrak{M}(\mathtt{D}_{j,k})\right)$.

Proof. Let $E = \mathtt{D}_0 \cup \mathtt{D}_1$ or $\mathtt{D}_2 \cup \mathtt{D}_3$, $\alpha \sim \mathcal{N}\left(0, \frac{\Delta x \Delta y}{4}\right)$, and $\beta \sim \mathcal{N}\left(0, \frac{\Delta x \Delta y}{8}\right)$. Due to Martingale properties; $\mathbb{V}(\mathbb{W}(\mathtt{D}_{j,k})) = \Delta x \Delta y$, $\mathbb{V}(\mathbb{W}(E)) = \frac{\Delta x \Delta y}{2}$, and $\mathbb{V}(\mathbb{W}(\mathtt{D}_{0,1,2,3})) = \frac{\Delta x \Delta y}{4}$. Assuming that $\mathbb{W}(\mathtt{D}_{j,k})$ is given, use the ergodic drift to yield: $\mathbb{E}(\mathbb{W}(E) \,|\mathbb{W}(\mathtt{D}_{j,k})) = \frac{\mathbb{W}(\mathtt{D}_{j,k})}{2}$ and $\mathbb{V}(\mathbb{W}(E) \mid \mathbb{W}(\mathtt{D}_{j,k}))$
$= \mathbb{V}((\mathbb{W}(E))) - \mathbb{V}(\mathbb{E}(E|\mathbb{W}(\mathtt{D}_{j,k}))) = \frac{\Delta x \Delta y}{2} - \mathbb{V}\left(\frac{\mathbb{W}(\mathtt{D}_{j,k})}{2}\right) = \frac{\Delta x \Delta y}{2} - \frac{\Delta x \Delta y}{4} =$
$\frac{\Delta x \Delta y}{4}$. Let $\mathbb{W}(E) = \frac{\mathbb{W}(\mathtt{D}_{j,k})}{2} \pm \alpha$ such that $\mathbb{E}(\mathbb{W}(\mathtt{D}_j) \mid \mathbb{W}(E)) = \frac{\mathbb{W}(E)}{2}$ and $\mathbb{V}(\mathbb{W}(\mathtt{D}_j) \,|\mathbb{W}(E)) = \mathbb{V}(\mathbb{W}(\mathtt{D}_j)) - \mathbb{V}(\mathbb{E}(\mathbb{W}(\mathtt{D}_j) \mid \mathbb{W}(E))) = \frac{\Delta x \Delta y}{4} - \mathbb{V}\left(\frac{A}{2}\right) =$
$\frac{\Delta x \Delta y}{4} - \frac{\mathbb{V}(A)}{4} = \frac{\Delta x \Delta y}{4} - \frac{\Delta x \Delta y}{8} = \frac{\Delta x \Delta y}{8}$. Hence, $\mathbb{W}(\mathtt{D}_j) = \frac{\frac{\mathbf{w}(\mathtt{D}_{j,k})}{2} \pm \alpha}{2} \pm \beta = \frac{\mathbb{W}(\mathtt{D}_{j,k})}{4} \pm \frac{\alpha}{2} \pm \beta$, yielding: $\mathbb{W}(\mathtt{D}_0) = \frac{\mathbb{W}(\mathtt{D}_{j,k})}{4} + \frac{\alpha}{2} + \beta_1$, $\mathbb{W}(\mathtt{D}_1) = \frac{\mathbb{W}(\mathtt{D}_{j,k})}{4} + \frac{\alpha}{2} - \beta_1$, $\mathbb{W}(\mathtt{D}_2) = \frac{\mathbb{W}(\mathtt{D}_{j,k})}{4} - \frac{\alpha}{2} + \beta_2$, and $\mathbb{W}(\mathtt{D}_3) = \frac{\mathbb{W}(\mathtt{D}_{j,k})}{4} - \frac{\alpha}{2} - \beta_2$. □

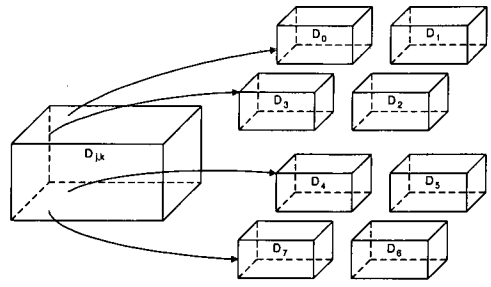

Figure C.2: Brownian space divisions

Proposition C.2.3. *Assuming a three-dimensional Brownian space has been created where* $\mathtt{D}_{j,k,l}$ *consists of rectangular shape regions with central differences. In order to construct the Levy refinement scheme depicted in Figure C.2, let* $\mathtt{D}_{j,k,l}$ *be the union of the eight restricted rectangular regions* $\{\mathtt{D}_0, \cdots, \mathtt{D}_7\}$*, where each of the* $\mathtt{D}_n$ *is adjacent to* $\wp_{j,k,l}$*. A possible refinement scheme would consist of:*

$\mathbb{W}(\mathtt{D}_0) = \frac{\mathbb{W}(\mathtt{D}_{j,k,l})}{8} + \frac{\alpha}{4} + \frac{\beta_1}{2} + a_1$, $\mathbb{W}(\mathtt{D}_1) = \frac{\mathbb{W}(\mathtt{D}_{j,k,l})}{8} + \frac{\alpha}{4} + \frac{\beta_1}{2} - a_1$,

$\mathbb{W}(\mathtt{D}_2) = \frac{\mathbb{W}(\mathtt{D}_{j,k,l})}{8} + \frac{\alpha}{4} - \frac{\beta_1}{2} + a_2$, $\mathbb{W}(\mathtt{D}_3) = \frac{\mathbb{W}(\mathtt{D}_{j,k,l})}{8} + \frac{\alpha}{4} - \frac{\beta_1}{2} - a_2$,

$\mathbb{W}(\mathtt{D}_4) = \frac{\mathbb{W}(\mathtt{D}_{j,k,l})}{8} - \frac{\alpha}{4} + \frac{\beta_2}{2} + a_3$, $\mathbb{W}(\mathtt{D}_5) = \frac{\mathbb{W}(\mathtt{D}_{j,k,l})}{8} - \frac{\alpha}{4} + \frac{\beta_2}{2} - a_3$,

$\mathbb{W}(\mathtt{D}_6) = \frac{\mathbb{W}(\mathtt{D}_{j,k,l})}{8} - \frac{\alpha}{4} - \frac{\beta_2}{2} + a_4$, $\mathbb{W}(\mathtt{D}_7) = \frac{\mathbb{W}(\mathtt{D}_{j,k,l})}{8} - \frac{\alpha}{4} - \frac{\beta_2}{2} - a_4$; *where*

$\alpha \sim \mathcal{N}\left(0, \frac{1}{4}\mathfrak{M}(\mathtt{D}_{j,k,l})\right)$, $\beta_{\{1,2\}} \sim \mathcal{N}\left(0, \frac{1}{8}\mathfrak{M}(\mathtt{D}_{j,k,l})\right)$, *and* $a_{\{1,2,3,4\}} \sim \mathcal{N}\left(0, \frac{1}{16}\mathfrak{M}(\mathtt{D}_{j,k,l})\right)$.

Proof. Repeat Proposition C.2.1 using the sub-domains $\{\mathtt{D}_0 \cup \mathtt{D}_1 \cup \mathtt{D}_2 \cup \mathtt{D}_3\}$ and $\{\mathtt{D}_4 \cup \mathtt{D}_5 \cup \mathtt{D}_6 \cup \mathtt{D}_7\}$. Then utilise Proposition C.2.2 on each sub-domain. □

C.2.1 Normal random variables

The following pseudo-random number generator algorithms are taken from code written by Dr. Jessica Gaines. As per her instructions, please do not distribute and contact University of Edinburgh Department of Mathematics and Statistic if interested in utilising the following code.

Program C.2.4. *The following is a general construction of a user-defined class.*

```
class jrandom
{
    jrandom(void) %% Constructor function.
    { %% Seed the random-number generator with current time
      srand( (unsigned)time( NULL));
      if print_it=1 then print "Construct jrandom RV functions.";
    }
    ~jrandom() %% Destructor function.
```

```
    { %% Destruct the appropriate objects.
      if print_it=1 then print "Destruct jrandom ";
    }
%% Functions that belong in this class are placed here.
};
```

Program C.2.5. *Sample random functions.*

```
random_int ( void ):  integer
{   return(rand(·)); }
and
random( void ):  real
{   return (random_int(·) (int^-1_max)); }
```

Program C.2.6. *Returns a uniform random deviate between 0.0 and 1.0. Set idum to any negative value to initialize or reinitialize the sequence. Uses no system-supplied routines and shuffles numbers.*

```
ran2(long idum):  real
{
   integer MJ = 714025, IA = 1366, IC = 150889;
   long α, V_98, newdum;    integer iff = 0;
   if (idum < 0 or iff = 0) then
   {
     iff = 1;
     if print_it=1 then print "Initializing";
     if (idum = (IC − (idum)) %MJ < 0) then idum = (− (idum));
     for j = 1 to 97
       idum = (IA (idum) + IC) %MJ;    V_j = (idum);
     idum = (IA (idum) + IC) %MJ;    α = newdum = idum;
   }
   j =  integer ((1+97.0*α)/MJ);
   if (j > 97 or j < 1) then print "RAN2:  Error in j value.";
   α = V_j;    newdum = (IA newdum + IC) %MJ;    V_j = newdum;
   return (α/MJ);
}
```

Program C.2.7. *Routine to return a uniform random deviate between 0.0 and 1.0; set idum to any negative value to initialize or reinitialize the sequence.*

```
ran3(integer idum): real
{
   integer M_BIG = 10^9, MSEED = 161803398, MZ = 0;
   integer inext, inextp, iff = 0;    long ma_56, mj, mk;
   if (idum < 0 or iff = 0) then
   {
     iff = 1;
     if print_it=1 then print "Initializing";
     mj = MSEED - (idum);
     mj% = M_BIG;    ma_55 = mj;    mk = 1;
     for o =1 to 54
     {
       j = (21 * o)%55;      ma_j = mk;      mk = mj - mk;
       if (mk < MZ) then mk+ = M_BIG;    mj = ma_j;
     }
     for k = 1 to 4
       for o = 1 to 55
       {
         ma_o- = ma (1 + (o + 30)%55);
         if (ma_o < MZ) then ma_o+ = M_BIG;
       }
       inext = 0;      inextp = 31;
     }
     if (++inext = 56) then inext = 1;
     if (++inextp = 56) then inextp = 1;
     mj = ma_inext - ma_inextp;
     if (mj < MZ) then mj+ = M_BIG;
     ma_inext = mj;
     return (mj / M_BIG);
}
```

Program C.2.8. *Returns a normally distributed deviate with a given mean and standard deviation.*

```
SlowN(real μ, σ): real
{
   integer iset=0;   real gset, fac, r, v_1, v_2;
   if iset = 0 then
   {
```

```
      while (r ≥ 1.0);
      { v1 = 2random(·) − 1;    v2 = 2random(·) − 1;    r = v1^2 + v2^2; }
      fac=sqrt((−2.0log(r))/r);    gset=σv1fac + μ;    iset=1;
      return (σv2fac + μ);
   }
   else
   {   iset=0;      return (gset);   }
}
```

C.2.2 Brownian sheet code

A $d = 2$ example will be provided where $\mathbb{W}(\mathtt{D}_{j,k})$ is the random variable mapped to $(x_j, y_k) \in \mathtt{D}_{j,k}$ and $\mathbb{W}(j,k,l)$ is allocated via the scheme depicted in Figure C.1.

Program C.2.9. *Class square for the d=2 Brownian Sheet.*

```
class square
   real σ;   integer Nz, fringe;   matrix_3d W;
     square(integer Mx, Ny; real Δx, Δy) %% Constructor
     {
       Nz = 4;    σ = sqrt((Δx Δy)/4);
       W = new matrix_3d (Mx, Ny, Nz);
       if print_it = 1 then print "Create square";
       reset(·);
       edge(); %% correction for the adjacent points
     }
     ~square() %% Destructor function.
     {
       delete W;
       if (print_it=1) then print "Destruct square ";
     }
%% Functions that belong in this class are placed here.
};
```

Program C.2.10. *Function to reset the Brownian Sheet.*

```
reset( void ):  void
{
   for j = 0 to Mx
     for k = 0 to Ny
       for l = 0 to Nz
```

```
        W(j,k,l) = SlowN(μ,σ); %% μ = 0
    %% Now correct for the boundary
    for j = 0 to M_x
    {
      W(j,0,2) = 0;   W(j,N_y − 1,0) = 0;
      W(j,0,3) = 0;   W(j,N_y − 1,1) = 0;
    }
    for k = 0 to N_y
    {
      W(0,k,0) = 0;     W(M_x − 1,k,1) = 0;
      W(0,k,3) = 0;     W(M_x − 1,k,2) = 0;
    }
```

Program C.2.11. *Get the value of* $\mathbb{W}$(D) *as depicted in Figure C.1.*

```
W(D) (integer j, k):  real
{
   real β = 0;
   if (−1 < j < M_x) then
     if (−1 < k < N_y) then
       for l = 0 to N_z
         β = β + W(j,k,l);
   return (β);
}
```

Program C.2.12. *Condense the noise as* $\Delta x \to 2\Delta x$. *The order of operations is VERY important!*

```
condense_noise(matrix_3d W; integer M_x, N_y; real σ) :  matrix_3d
{
   M_x = 1 + M_x/2;     N_y = 1 + N_y/2;     σ = 2σ;
   edge(); %% correction for the adjacent points
   W(0,0,1) = W(0,0,1) + W(0,1,2) + W(1,1,3) + W(1,0,0);
   for k = 1 to N_y − 1
   {
     W(0,k,2) = W(0,2k,2) + W(0,2k − 1,1) + W(1,2k − 1,0) + W(1,2k,3);
     W(0,k,1) = W(0,2k,1) + W(0,2k + 1,2) + W(1,2k + 1,3) + W(1,2k,0);
   }
   W(0,N_y − 1,2) = W(0,2(N_y − 1),2) + W(0,2(N_y − 1) − 1,1)
```

$+\mathbb{W}(1,2(N_y-1)-1,0)+\mathbb{W}(1,2(N_y-1),3);$

for $j=1$ to M_x-1

{

$\mathbb{W}(j,0,0)=\mathbb{W}(2j,0,0)+\mathbb{W}(2j-1,0,1)+\mathbb{W}(2j-1,1,2)+\mathbb{W}(2j,1,3);$

$\mathbb{W}(j,0,1)=\mathbb{W}(2j,0,1)+\mathbb{W}(2j,1,2)+\mathbb{W}(2j+1,1,3)+\mathbb{W}(2j+1,0,0);$

}

$\mathbb{W}(M_x-1,0,0)=\mathbb{W}(2(M_x-1),0,0)+\mathbb{W}(2(M_x-1)-1,0,1)$

$+\mathbb{W}(2(M_x-1)-1,1,2)+\mathbb{W}(2(M_x-1),1,3);$

for $j=1$ to M_x-1

for $k=1$ to N_y-1

{

$\mathbb{W}(j,k,3)=\mathbb{W}(2j,2k,3)+\mathbb{W}(2j,2k-1,0)$

$+\mathbb{W}(2j-1,2k-1,1)+\mathbb{W}(2j-1,2k,2);$

$\mathbb{W}(j,k,0)=\mathbb{W}(2j,2k,0)+\mathbb{W}(2j-1,2k,1)$

$+\mathbb{W}(2j-1,2k+1,2)+\mathbb{W}(2j,2k+1,3);$

$\mathbb{W}(j,k,2)=\mathbb{W}(2j,2k,2)+\mathbb{W}(2j,2k-1,1)$

$+\mathbb{W}(2j+1,2k-1,0)+\mathbb{W}(2j+1,2k,3);$

$\mathbb{W}(j,k,1)=\mathbb{W}(2j,2k,1)+\mathbb{W}(2j,2k+1,2)$

$+\mathbb{W}(2j+1,2k+1,3)+\mathbb{W}(2j+1,2k,0);$

}

for $j=1$ to M_x-1

{

$\mathbb{W}(j,N_y-1,2)=\mathbb{W}(2j,2(N_y-1),2)+\mathbb{W}(2j,2(N_y-1)-1,1)$

$+\mathbb{W}(2j+1,2(N_y-1)-1,0)+\mathbb{W}(2j+1,2(N_y-1),3);$

$\mathbb{W}(j,N_y-1,3)=\mathbb{W}(2j,2(N_y-1),3)+\mathbb{W}(2j,2(N_y-1)-1,0)$

$+\mathbb{W}(2j-1,2(N_y-1)-1,1)+\mathbb{W}(2j-1,2(N_y-1),2);$

}

for $k=1$ to N_y-1

{

$\mathbb{W}(M_x-1,k,0)=\mathbb{W}(2(M_x-1),2k,0)+\mathbb{W}(2(M_x-1)-1,2k,1)$

$+\mathbb{W}(2(M_x-1)-1,2k+1,2)+\mathbb{W}(2(M_x-1),2k+1,3);$

$\mathbb{W}(M_x-1,k,3)=\mathbb{W}(2(M_x-1),2k,3)+\mathbb{W}(2(M_x-1),2k-1,0))$

$+\mathbb{W}(2(M_x-1)-1,2k-1,1)+\mathbb{W}(2(M_x-1)-1,2k,2);$

}

$\mathbb{W}(M_x-1,N_y-1,3)=\mathbb{W}(2(M_x-1),2(N_y-1),3)$

$+\mathbb{W}(2(M_x-1),2(N_y-1)-1,0)+\mathbb{W}(2(M_x-1)-1,2(N_y-1),2)$

$+\mathbb{W}(2(M_x-1)-1,2(N_y-1)-1,1);$

for $j=0$ to M_x

```
    {
      W(j,0,2) = 0;     W(j,N_y − 1,0) = 0;
      W(j,0,3) = 0;     W(j,N_y − 1,1) = 0;
    }
    for k = 0 to N_y
    {
      W(0,k,0) = 0;     W(M_x − 1,k,1) = 0;
      W(0,k,3) = 0;     W(M_x − 1,k,2) = 0;
    }
    return (W);
}
```

Program C.2.13. *Expand the Brownian Sheet from $2\Delta x \to \Delta x$ as depicted in Proposition C.2.2.*

```
expand_noise(matrix_3d W; integer M_x, N_y; real σ): matrix_3d
{
   real a,b,c,β,σ_2;   matrix_3d W_2, hold;
   edge(); %% If doing a blow up
   M_x = 2(M_x − 1) + 1;     N_y = 2(N_y − 1) + 1;
   σ = σ/2.0;     σ_2 = σ/√2.0;
   W_2 = new matrix_3d(M_x, N_y, N_z); %% new noise grid
   for j = 2 to M_x − 1 %% Add 2 to j with each iteration
     for k = 2 to N_y − 1, %% Add 2 to k with each iteration
     {
       β = (1/4)W(j/2, k/2, 0);     a = (1/2)SlowN(0,σ);
       b = SlowN(0,σ_2);     c = SlowN(0,σ_2);
       W_2(j − 1,k + 1,2) = β − a + c;
       W_2(j,k + 1,3) = β − a − c;
       W_2(j − 1,k,1) = β + a − b;
       W_2(j,k,0) = β + a + b;
       β = (1/4)W(j/2, k/2, 1);     a = (1/2)SlowN(0,σ);
       b = SlowN(0,σ_2);     c = SlowN(0,σ_2);
       W_2(j,k + 1,2) = β − a + c;
       W_2(j + 1,k + 1,3) = β − a − c;
       W_2(j + 1,k,0) = β + a + b;
       W_2(j,k,1) = β + a − b;
       β = (1/4)W(j/2, k/2, 2);     a = (1/2)SlowN(0,σ) ;
       b = SlowN(0,σ_2);     c = SlowN(0,σ_2);
```

$\mathbb{W}_2(j+1,k,3) = \beta - a - c;$

$\mathbb{W}_2(j+1,k-1,0) = \beta + a + b;$

$\mathbb{W}_2(j,k-1,1) = \beta + a - b;$

$\mathbb{W}_2(j,k,2) = \beta - a + c;$

$\beta = \frac{1}{4}\mathbb{W}\left(\frac{j}{2},\frac{k}{2},3\right);$ $\quad a = \frac{1}{2}\texttt{Slow}\mathcal{N}(0,\sigma);$

$b = \texttt{Slow}\mathcal{N}(0,\sigma_2);$ $\quad c = \texttt{Slow}\mathcal{N}(0,\sigma_2);$

$\mathbb{W}_2(j,k-1,0) = \beta + a + b;$

$\mathbb{W}_2(j-1,k-1,1) = \beta + a - b;$

$\mathbb{W}_2(j-1,k,2) = \beta - a + c;$

$\mathbb{W}_2(j,k,3) = \beta - a - c;$

}

for $j = 2$ to $M_x - 1$ %% Add 2 to j with each iteration

{

$\beta = \frac{1}{4}\mathbb{W}\left(\frac{j}{2},0,0\right);$ $\quad a = \frac{1}{2}\texttt{Slow}\mathcal{N}(0,\sigma);$

$b = \texttt{Slow}\mathcal{N}(0,\sigma_2);$ $\quad c = \texttt{Slow}\mathcal{N}(0,\sigma_2);$

$\mathbb{W}_2(j-1,1,2) = \beta - a + c;$

$\mathbb{W}_2(j,1,3) = \beta - a - c;$

$\mathbb{W}_2(j-1,0,1) = \beta + a - b;$

$\mathbb{W}_2(j,0,0) = \beta + a + b;$

$\beta = \frac{1}{4}\mathbb{W}\left(\frac{j}{2},0,1\right);$ $\quad a = \frac{1}{2}\texttt{Slow}\mathcal{N}(0,\sigma);$

$b = \texttt{Slow}\mathcal{N}(0,\sigma_2);$ $\quad c = \texttt{Slow}\mathcal{N}(0,\sigma_2);$

$\mathbb{W}_2(j,1,2) = \beta - a + c;$

$\mathbb{W}_2(j+1,1,3) = \beta - a - c;$

$\mathbb{W}_2(j+1,0,0) = \beta + a + b;$

$\mathbb{W}_2(j,0,1) = \beta + a - b;$

$\beta = \frac{1}{4}\mathbb{W}\left(\frac{j}{2},\frac{N_y-1}{2},2\right);$ $\quad a = \frac{1}{2}\texttt{Slow}\mathcal{N}(0,\sigma);$

$b = \texttt{Slow}\mathcal{N}(0,\sigma_2);$ $\quad c = \texttt{Slow}\mathcal{N}(0,\sigma_2);$

$\mathbb{W}_2(j+1,N_y-1,3) = \beta - a - c;$

$\mathbb{W}_2(j+1,N_y-1-1,0) = \beta + a + b;$

$\mathbb{W}_2(j,N_y-1-1,1) = \beta + a - b;$

$\mathbb{W}_2(j,N_y-1,2) = \beta - a + c;$

$\beta = \frac{1}{4}\mathbb{W}\left(\frac{j}{2},\frac{N_y-1}{2},3\right);$ $\quad a = \frac{1}{2}\texttt{Slow}\mathcal{N}(0,\sigma);$

$b = \texttt{Slow}\mathcal{N}(0,\sigma_2);$ $\quad c = \texttt{Slow}\mathcal{N}(0,\sigma_2);$

$\mathbb{W}_2(j,N_y-2,0) = \beta + a + b;$

$\mathbb{W}_2(j-1,N_y-2,1) = \beta + a - b;$

$\mathbb{W}_2(j-1,N_y-1,2) = \beta - a + c;$

$\mathbb{W}_2(j,N_y-1,3) = \beta - a - c;$

}

for $k = 2$ to $N_y - 1$ %% Add 2 to k with each iteration

{

$\beta = \frac{1}{4}\mathbb{W}\left(\frac{M_x-1}{2}, \frac{k}{2}, 0\right)$; $\quad a = \frac{1}{2}\texttt{Slow}\mathcal{N}(0,\sigma)$;

$b = \texttt{Slow}\mathcal{N}(0,\sigma_2)$; $\quad c = \texttt{Slow}\mathcal{N}(0,\sigma_2)$;

$\mathbb{W}_2(M_x - 2, k+1, 2) = \beta - a + c$;

$\mathbb{W}_2(M_x - 1, k+1, 3) = \beta - a - c$;

$\mathbb{W}_2(M_x - 2, k, 1) = \beta + a - b$;

$\mathbb{W}_2(M_x - 1, k, 0) = \beta + a + b$;

$\beta = \frac{1}{4}\mathbb{W}\left(0, \frac{k}{2}, 1\right)$; $\quad a = \frac{1}{2}\texttt{Slow}\mathcal{N}(0,\sigma)$;

$b = \texttt{Slow}\mathcal{N}(0,\sigma_2)$; $\quad c = \texttt{Slow}\mathcal{N}(0,\sigma_2)$;

$\mathbb{W}_2(0, k+1, 2) = \beta - a + c$;

$\mathbb{W}_2(1, k+1, 3) = \beta - a - c$;

$\mathbb{W}_2(1, k, 0) = \beta + a + b$;

$\mathbb{W}_2(0, k, 1) = \beta + a - b$;

$\beta = \frac{1}{4}\mathbb{W}\left(0, \frac{k}{2}, 2\right)$; $\quad a = \frac{1}{2}\texttt{Slow}\mathcal{N}(0,\sigma)$;

$b = \texttt{Slow}\mathcal{N}(0,\sigma_2)$; $\quad c = \texttt{Slow}\mathcal{N}(0,\sigma_2)$;

$\mathbb{W}_2(1, k, 3) = \beta - a - c$;

$\mathbb{W}_2(1, k-1, 0) = \beta + a + b$;

$\mathbb{W}_2(0, k-1, 1) = \beta + a - b$;

$\mathbb{W}_2(0, k, 2) = \beta - a + c$;

$\beta = \frac{1}{4}\mathbb{W}\left(\frac{M_x-1}{2}, \frac{k}{2}, 3\right)$; $\quad a = \frac{1}{2}\texttt{Slow}\mathcal{N}(0,\sigma)$;

$b = \texttt{Slow}\mathcal{N}(0,\sigma_2)$; $\quad c = \texttt{Slow}\mathcal{N}(0,\sigma_2)$;

$\mathbb{W}_2(M_x - 1, k-1, 0) = \beta + a + b$;

$\mathbb{W}_2(M_x - 1 - 1, k-1, 1) = \beta + a - b$;

$\mathbb{W}_2(M_x - 1 - 1, k, 2) = \beta - a + c$;

$\mathbb{W}_2(M_x - 1, k, 3) = \beta - a - c$;

}

$\beta = \frac{1}{4}\mathbb{W}\left(\frac{M_x-1}{2}, 0, 0\right)$; $\quad a = \frac{1}{2}\texttt{Slow}\mathcal{N}(0,\sigma)$;

$b = \texttt{Slow}\mathcal{N}(0,\sigma_2)$; $\quad c = \texttt{Slow}\mathcal{N}(0,\sigma_2)$;

$\mathbb{W}_2(M_x - 1 - 1, 1, 2) = \beta - a + c$;

$\mathbb{W}_2(M_x - 1, 1, 3) = \beta - a - c$;

$\mathbb{W}_2(M_x - 1 - 1, 0, 1) = \beta + a - b$;

$\mathbb{W}_2(M_x - 1, 0, 0) = \beta + a + b$;

$\beta = \frac{1}{4}\mathbb{W}(0, 0, 1)$; $\quad a = \frac{1}{2}\texttt{Slow}\mathcal{N}(0,\sigma)$;

$b = \texttt{Slow}\mathcal{N}(0,\sigma_2)$; $\quad c = \texttt{Slow}\mathcal{N}(0,\sigma_2)$;

$\mathbb{W}_2(0, 1, 2) = \beta - a + c$;

$\mathbb{W}_2(1, 1, 3) = \beta - a - c$;

$\mathbb{W}_2(1, 0, 0) = \beta + a + b$;

```
    W2 (0,0,1) = β + a − b;
    β = (1/4)W(0, (Ny−1)/2, 2);    a = (1/2)SlowN(0,σ);
    b = SlowN(0,σ2);    c = SlowN(0,σ2);
    W2 (1,Ny − 1,3) = β − a − c;
    W2 (1,Ny − 2,0) = β + a + b;
    W2 (0,Ny − 2,1) = β + a − b;
    W2 (0,Ny − 1,2) = β − a + c;
    β = (1/4)W((Mx−1)/2, (Ny−1)/2, 3);    a = (1/2)SlowN(0,σ);
    b = SlowN(0,σ2);    c = SlowN(0,σ2);
    W2 (Mx − 1,Ny − 1 − 1,0) = β + a + b;
    W2 (Mx − 1 − 1,Ny − 1 − 1,1) = β + a − b;
    W2 (Mx − 1 − 1,Ny − 1,2) = β − a + c;
    W2 (Mx − 1,Ny − 1,3) = β − a − c;
    hold = W;    W = W2;    W2 = hold;
    delete W2;
  }
  return (W);
}
```

Program C.2.14. *Save a Brownian Sheet for later use.*

```
void save_file( matrix_3d W; integer o):  file
{
  integer ones= o%10;
  integer tens = ((o-ones)/10)%10;
  integer hundreds = (o-ones-tens*10)/100;
  char A = char(hundreds+char_offset);
  char B = char(tens +char_offset);
  char C = char(ones +char_offset);
  open print_file('s','q', A, B, C, '.','t','x','t');
  for j = 0 to Mx
    for k = 0 to Ny
      for l = 0 to Nz
        print_file, setprecision(dec_places), W(j,k,l);
  close print_file;
}
```

Program C.2.15. *Output a Brownian sheet for a Maple plot.*

```
maple_print_file(matrix_3d 𝕎; integer o, num):  file
{
   integer ones= o%10;
   integer tens = ((o-ones)/10)%10;
   integer hundreds = (o-ones-tens*10)/100;
   char A = char(hundreds+char_offset);
   char B = char(tens +char_offset);
   char C = char(ones +char_offset);
   open print_file('m','a','p','s', A, B, C, '.','m','w','s');
   ones= num%10;
   tens = ((num-ones)/10)%10;
   B = char(tens +char_offset);
   C = char(ones +char_offset);
   print_file "A"BC":=[[ ";
   for k = N_y - 1 to 0
   {
     for j = 0 to M_x - 1
       print_file,setprecision(dec_places), 𝕎(D)(j,k)", ";
     print_file, setprecision(dec_places), 𝕎(D)(M_x - 1,k) " ],[ ";
   }
   for j = 0 to M_x - 1
     print_file, setprecision(dec_places), 𝕎(D)(j,0) ", ";
   print_file, setprecision(dec_places), 𝕎(D)(M_x - 1,0) " ]]:";
   close print_file;
}
```

Program C.2.16. *Get a Brownian sheet for further manipulation.*

```
get_file(matrix_3d 𝕎; integer o):  matrix_3d
{
   real β = 0;
   integer ones= o%10;
   integer tens = ((o-ones)/10)%10;
   integer hundreds = (o-ones-tens*10)/100;
   char A = char(hundreds+char_offset);
   char B = char(tens +char_offset);
   char C = char(ones +char_offset);
   if print_it=1 then print "Make sure that sq###.txt contains data.";
   open in_file('s','q',A, B, C, '.','t','x','t');
```

```
    for j = 0 to M_x
      for k = 0 to N_y
        for l = 0 to N_z
        {
          in_file >> β;
          W(j,k,l) = β;
        }
    close in_file;
}
```

C.2.3 Rhombic $\mathbb{W}(\mathtt{D})$ discretisations

The following Brownian sheet applies to the FDS of Chapter 2 and utilised the notation of the previous Section. The sub-domains are divided via the scheme depicted in Figure C.3.

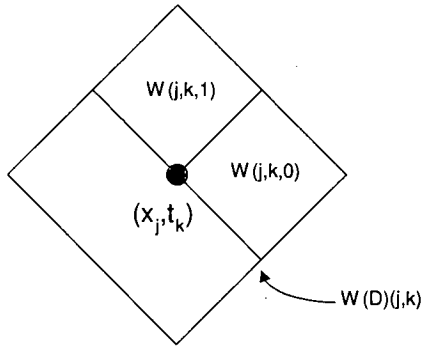

Figure C.3: Brownian sheet allocation

Program C.2.17. *Brownian sheet used for the hyperbolic problem.*

```
class h_rhombic
{
   real σ;    integer N_z;    matrix_3d W;
h_rhombic(integer M_x, N_y; real Δx, Δy) %% Constructor
{
   N_z = 2;    σ = sqrt(ΔxΔy/2);
   W = new matrix_3d (M_x, N_y, N_z);
   reset(·);
   if print_it =1 then print "Create h_rhombic";
}
```

```
~h_rhombic() %% Destructor function
{
   delete 𝕎;
   if print_it=1 then print "Destruct h_rhombic";
}
```

Program C.2.18. *Initialize the Brownian sheet.*

```
reset( void ):  void
{
   for j = 0 to M_x
     for k = 0 to N_y
       for l = 0 to N_z
         𝕎(j,k,l) = SlowN(μ,σ); %% μ = 0
   for j = 0 to M_x
     𝕎(j,0,0) = 𝕎(j,0,0)/2;
   for k = 0 to N_y
   {
     𝕎(0,k,1) = 𝕎(0,k,1)/2;
     𝕎(M_x - 1,k,1) = 𝕎(M_x - 1,k,1)/2;
     𝕎(M_x - 1,k,0) = 0;
   }
}
```

Program C.2.19. *Retrieve* $\mathbb{W}(\mathtt{D})$.

```
𝕎(D) (integer j, k):  real
{
   real β = 0;
   if ((-1 < j < M_x) and (-1 < k < N_y)) then
   {
     if j ≠ 0 then β = 𝕎(j - 1,Y,0);
     if k ≠ 0 then β = β + 𝕎(j,k - 1,1);
     β = β + 𝕎(j,k,0) + 𝕎(j,k,1);
   }
   return (β);
}
```

Program C.2.20. *Condense the grid from* $\Delta x \to 2\Delta x$.

```
condense_noise(matrix_3d W; integer M_x, N_y; real σ): matrix_3d
{
  σ = 2σ;   M_x = (M_x − 1)/2 + 1;   N_y = (N_y − 1)/2 + 1;
  for j = 0 to M_x
    for k = 0 to N_y
    {
      W(j, k, 0) = W(D)(2j + 1, 2k);
      W(j, k, 1) = W(D)(2j, 2k + 1);
    }
}
```

Program C.2.21. *Expand the grid from* $2\Delta x \to \Delta x$.

```
expand_noise(matrix_3d W; integer M_x, N_y; real σ): matrix_3d
{
  M_x = 2(M_x − 1) + 1;   N_y = 2(N_y − 1) + 1;   σ = σ/2;
  for j = 0 to M_x
    for k = 0 to N_y
    {
      W(2j, 2k, 0) = SlowN(0, σ);
      W(2j + 1, 2k, 0) = SlowN(0, σ);
      W(2j + 1, 2k, 1) = SlowN(0, σ);
      W(2j + 1, 2k − 1, 1) = W(j, k, 0) − W(2j, 2k, 0)
        −W(2j + 1, 2k, 0) − W(2j + 1, 2k, 1);
      W(2j − 1, 2k + 1, 0) = SlowN(0, σ);
      W(2j, 2k, 1) = SlowN(0, σ);
      W(2j, 2k + 1, 0) = SlowN(0, σ);
      W(2j, 2k + 1, 1) = W(j, k, 1) − W(2j − 1, 2k + 1, 0)
        −W(2j, 2k, 1) − W(2j, 2k + 1, 0);
    }
}
```

C.2.4 Unit point source

Program C.2.22. *Introduce a unit point source to a two dimensional plane.*

```
delta(matrix_3d W; integer j, k): void
{
  reset(0); %% reset the sheet to 0
  W(j, k, 0) = 0.25;   W(j, k, 1) = 0.25;
```

$\mathbb{W}(j,k,2) = 0.25;$ $\mathbb{W}(j,k,3) = 0.25;$

}

Program C.2.23. *Introduce a unit point source to rhombic discretisation.*

```
void delta(integer j,k)
{
   reset(0); %% reset the sheet to 0
   W(j,k-1,1) = 1;
}
```

C.3 A priori initialization methods

C.3.1 Symmetry considerations

Program C.3.1. *This is a sub-optimal program listing the orientations and the arrangement of points necessary to derive an estimate. To aid readability, let* $\omega(j,k) = \omega(j\Delta x, k\Delta y)$ *and assume* $v(\cdot) = 0$.

```
real pt_eval(matrix_2d F̂(·), Ĝ; square W; integer orientation)
{
   real num = 0, den = 0;
   if (orientation=0) then
   {
     for k = 1 to N_y - 2
     {   num = num + F̂(0,k) Ĝ(1,k) + F̂(M_x - 1,k) Ĝ(M_x - 2,k);
       den = den + Ĝ(1,k) + Ĝ(M_x - 2,k);   }
     for j = 1 to M_x - 2
     {   num = num + F̂(j,0) Ĝ(j,1) + F̂(j,N_y - 1) Ĝ(j,N_y - 2);
       den = den + Ĝ(j,1) + Ĝ(j,N_y - 2);   }
     num = num/den;   den = 0;
     for j = 1 to M_x - 2
       for k = 1 to N_y - 2
         den = den + ω(j,k) W(D)(j,k) Ĝ(j,k);
     num = num + den;
   }
   else if (orientation=1) then
   {
     for k = 1 to N_y - 2
     {   num = num + F̂(k,N_y - 1) Ĝ(1,k) + F̂(k,0) Ĝ(M_x - 2,k);
```

```
    den = den + Ĝ(1,k) + Ĝ(M_x − 2,k);     }
  for j = 1 to M_x − 2
  {   num = num + F̂(0, N_y − 1 − j) Ĝ(j,1)
        + F̂(M_x − 1, N_y − 1 − j) Ĝ(j, N_y − 2);
    den = den + Ĝ(j,1) + Ĝ(j, N_y − 2);     }
  num = num/den;    den = 0;
  for k = (N_y − 1) to 1
    for j = 1 to M_x − 2
      den = den + ω(N_y − k, j) 𝕎(D)(N_y − k, j) Ĝ(j,k);
  num = num + den;
}
else if (orientation=2) then
{
  for k = 1 to N_y − 2
     num = num + F̂(M_x − 1, N_y − 1 − k) Ĝ(1,k)
       + F̂(0, N_y − 1 − k) Ĝ(M_x − 2,k);
    den = den + Ĝ(1,k) + Ĝ(M_x − 2,k);     }
  for j = 1 to M_x − 2
  {   num = num + F̂(M_x − 1 − j, N_y − 1) Ĝ(j,1)
       + F̂(M_x − 1 − j, 0) Ĝ(j, N_y − 2);
    den = den + Ĝ(j,1) + Ĝ(j, N_y − 2);     }
  num = num/den;    den = 0;
  for j = (M_x − 1) to 1
    for k = (N_y − 1) to 1
      den = den + ω(M_x − j, N_y − k) 𝕎(D)(M_x − j, N_y − k) Ĝ(j,k);
  num = num + den;
else if (orientation=3) then
{
  for k = 1 to N_y − 2
  {   num = num + F̂(M_x − 1 − k, 0) Ĝ(1,k)
       + F̂(M_x − 1 − k, N_y − 1) Ĝ(M_x − 2,k);
    den = den + Ĝ(1,k) + Ĝ(M_x − 2,k);     }
  for j = 1 to M_x − 2
  {   num = num + F̂(M_x − 1, j) Ĝ(j,1) + F̂(0,j) Ĝ(j, N_y − 2);
    den = den + Ĝ(j,1) + Ĝ(j, N_y − 2);     }
  num = num/den;    den = 0;
  for k = 1 to N_y − 2
    for j = (M_x − 1) to 1
```

$\quad\quad$ den = den + $\omega(k, M_x - j)\,\mathbb{W}(\mathtt{D})(k, M_x - j)\,\widehat{G}(j,k)$;

num = num + den;

}

else if (orientation=4) then

{

for $k = 1$ to $N_y - 2$

{ num = num + $\widehat{F}(M_x - 1, k)\,\widehat{G}(1,k) + \widehat{F}(0,k)\,\widehat{G}(M_x - 2, k)$;

den = den + $\widehat{G}(1,k) + \widehat{G}(M_x - 2, k)$; }

for $j = 1$ to $M_x - 2$

{ num = num + $\widehat{F}(M_x - 1 - j, 0)\,\widehat{G}(j,1)$

$+\widehat{F}(M_x - 1 - j, N_y - 1)\,\widehat{G}(j, N_y - 2)$;

den = den + $\widehat{G}(j,1) + \widehat{G}(j, N_y - 2)$; }

num = $\frac{\text{num}}{\text{den}}$; den = 0;

for $j = (M_x - 1)$ to 1

for $k = 1$ to $N_y - 2$

den = den + $\omega(M_x - j, k)\,\mathbb{W}(\mathtt{D})(M_x - j, k)\,\widehat{G}(j,k)$;

num = num + den;

}

else if (orientation=5) then

{

for $k = 1$ to $N_y - 2$

{ num = num + $\widehat{F}(k,0)\,\widehat{G}(1,k) + \widehat{F}(k, N_y - 1)\,\widehat{G}(M_x - 2, k)$;

den = den + $\widehat{G}(1,k) + \widehat{G}(M_x - 2, k)$; }

for $j = 1$ to $M_x - 2$

{ num = num + $\widehat{F}(0,j)\,\widehat{G}(j,1) + \widehat{F}(M_x - 1, j)\,\widehat{G}(j, N_y - 2)$;

den = den + $\widehat{G}(j,1) + \widehat{G}(j, N_y - 2)$; }

num = $\frac{\text{num}}{\text{den}}$; den = 0;

for $k = 1$ to $N_y - 2$

for $j = 1$ to $M_x - 2$

den = den + $\omega(k,j)\,\mathbb{W}(\mathtt{D})(k,j)\,\widehat{G}(j,k)$;

num = num + den;

}

else if (orientation=6) then

{

for $k = 1$ to $N_y - 2$

{ num = num + $\widehat{F}(0, N_y - 1 - k)\,\widehat{G}(1,k)$

$+\widehat{F}(M_x - 1, N_y - 1 - k)\,\widehat{G}(M_x - 2, k)$;

den = den + $\widehat{G}(1,k) + \widehat{G}(M_x - 2, k)$; }

```
    for j = 1 to M_x − 2
    {   num = num + F̂(j, N_y − 1) Ĝ(j, 1) + F̂(j, 0) Ĝ(j, N_y − 2);
        den = den + Ĝ(j, 1) + Ĝ(j, N_y − 2);   }
    num = num/den;   den = 0;
    for j = 1 to M_x − 2
      for k = (N_y − 1) to 1
        den = den + ω(j, N_y − k) W(D)(j, N_y − k) Ĝ(j, k);
    num = num + den;
  }
  else if (orientation=7) then
  {
    for k = 1 to N_y − 2
    {   num = num + F̂(M_x − 1 − k, N_y − 1) Ĝ(1, k)
          + F̂(M_x − 1 − k, 0) Ĝ(M_x − 2, k);
        den = den + Ĝ(1, k) + Ĝ(M_x − 2, k);   }
    for j = 1 to M_x − 2
    {   num = num + F̂(M_x − 1, N_y − 1 − j) Ĝ(j, 1)
          + F̂(0, N_y − 1 − j) Ĝ(j, N_y − 2);
        den = den + Ĝ(j, 1) + Ĝ(j, N_y − 2);   }
    num = num/den;   den = 0;
    for k = (N_y − 1) to 1
      for j = (M_x − 1) to 1
        den = den + ω(N_y − k, M_x − j) W(D)(N_y − k, M_x − j) Ĝ(j, k);
    num = num + den;
  }
  return(num);
}
```

C.3.2 Blow-up method

The following programs will utilise a simplistic version of the Blow-up method. When implementing this method, one should correct for points 'close to the boundary' and then normalize the influence vector by dividing by $\widehat{G}_N(X_j; X_j)$. The size of the influence vector can also be adjusted depending upon the domain and nature of the driving noise.

Program C.3.2. *Example function used for the elliptic* $\mathbb{Z}^2$ *grid where* $\widehat{G}(j,k;j,k)$ *is approximated using the FDSc (3.10).*

```
blow_up_5p (integer M_x):  real
{
   if M_x = 3 then return(1.0);
   if M_x = 5 then return(1.5);
   else return (1.5 + 0.45 (log_2 (M_x) − 2));
}
```

Program C.3.3. *$\widehat{G}_N(X_j; X_j)$ is estimated and then Corollary 3.2.17 is utilised to create a vector of $\widehat{G}(\cdot)$ values where: $\widehat{G}_o = \widehat{G}_N(j,k;j,k) - \Delta\widehat{G}_N(j,k;j-o,k)$.*

```
void set_influence (integer M_x) :  vector
{
     Ĝ_N (X_j; X_j) = blow_up_5p (M_x);
     Ĝ = vector [l^1_radius];
     Ĝ_0 = Ĝ_N (X_j; X_j);
     Ĝ_1 = Ĝ_0 − 1.00000;   Ĝ_2 = Ĝ_1 − 0.45352;   Ĝ_3 = Ĝ_2 − 0.26760;
     Ĝ_4 = Ĝ_3 − 0.18685;   Ĝ_5 = Ĝ_4 − 0.14364;   Ĝ_6 = Ĝ_5 − 0.11685;
     Ĝ_7 = Ĝ_6 − 0.09859;   Ĝ_8 = Ĝ_7 − 0.08529;   Ĝ_9 = Ĝ_8 − 0.07517;
     Ĝ_10 = Ĝ_9 − 0.06722;   Ĝ_11 = Ĝ_10 − 0.060780;   continue ···;
     for j = 0 to l^1_radius, ++j
       if Ĝ_j < 0 then Ĝ_j = 0;
}
```

Program C.3.4. *Using the radiation principle, only points within a restricted neighborhood will be considered. A spline function, trapezoidal method, or some other approximation technique can be used to interpolate $\widehat{G}_{l^2}(\alpha)$ when $\alpha \in (n\Delta x, n+1\Delta x)$.*

```
real Ginfluence (real α ) :  real
{
     integer base = integer (α/Δx);
     if (base < l^1_radius) then return (Ĝ_base);
     else return(0);
}
```

C.3.3 $\widehat{G}\mathtt{Q}$ method

Regardless of the magnitude of Δx, distances in a uniform $\mathbb{Z}^d$ are traversed using an l^1 norm since paths occur on jumps parallel to an axis. For example, a particle traveling the diagonal of the $\mathbb{R}^2$ rectangular domain of Figure 1.3 would cover a distance of $\sqrt{\alpha^2+\beta^2}$, while a particle in a uniform $\mathbb{Z}^2$ travels a distance of $|\alpha| + |\beta|$. Since multiple paths of the same l^1 distance can be constructed in

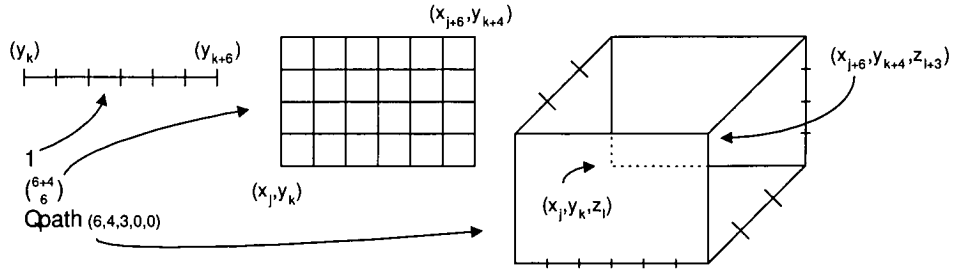

Figure C.4: Minimum l^1 distance paths for domains

a uniform $\mathbb{Z}^d$; ideally, every conceivable path over every distance is accounted for when constructing a numerical approximation. Although impractical for numerical evaluations due to the infinite number of distinct paths for even trivial domains, Program C.3.6 determines the number of minimum distance l^1 paths between two uniform $\mathbb{Z}^d$ points; refer to Figure C.4.

Remark C.3.5. *In order to implement a* $\|X, Y\|_2^{-d}$ *method, utilise* $\|X, Y\|_2^{-d}$ *in place of* $\mathtt{Q}(X; Y)$ *in the following algorithms.*

Program C.3.6. *A recursive function that determines the number of minimum distance* l^1 *paths in a restricted convex sub-domain between two uniform* $\mathbb{Z}^d$ *points* $(x_a, y_b, z_\alpha, t_\beta)$ *and* $(x_{a+l}, y_{b+m}, z_{\alpha+n}, t_{\beta+o})$*, where* $\{a, b, \alpha, \beta\}$ *are integers.*

```
function Qpath (integer l, m, n, o, sum) : integer
{
   l = |l|, m = |m|, n = |n|, o = |o|; integer branch = 0;
% If all counters are 0 but one, then only one Z^1 path.
   If {(l + m + n + o) = max(l, m, n, o)} then branch = 1;
   else
   { % Recursive calls to cover the different branching paths
       If l > 0 then branch = branch + Qpath(l − 1, m, n, o, sum);
       If m > 0 then branch = branch + Qpath(l, m − 1, n, o, sum);
       If n > 0 then branch = branch + Qpath(l, m, n − 1, o, sum);
       If o > 0 then branch = branch + Qpath(l, m, n, o − 1, sum);
   }
   return (sum + branch);
}
```

•If $d = 1$, then there is only one path between x_j and x_k such that $\mathtt{Qpath}(\cdot) = 1$.
•If $d = 2$, then the number of paths between (x_j, y_k) and (x_{j+l}, y_{k+m}) is algebraically reduced to $\mathtt{Qpath}(l, m, 0, 0, 0) = \binom{l+m}{l} = \binom{l+m}{m}$.

•If $d > 2$ then the number of paths between X_j and X_k experiences geometric growth. For example, when $d = 3$: $\texttt{Qpath}(1,1,1,0,0) = 6$, $\texttt{Qpath}(1,2,3,0,0) = 60$, $\texttt{Qpath}(2,2,2,0,0) = 90$, and $\texttt{Qpath}(3,3,3,0,0) = 1680$.

Program C.3.7. *A $\widehat{GQ}$ function which is not corrected for the number of adjacent points. If $\|\cdot\|_1 \leq O(\Delta x)(50\Delta x)$, then an exact calculation is recommended, otherwise an approximation is highly recommended. When $\Delta x \neq \Delta y \neq \Delta z \neq \Delta t$ a weighting scheme for ϑ can be implemented.*

```
GQ (integer j, k, l, m, n, o; real ϑ):  real
{
   integer α = |j − m| + |k − n| + |l − o|; %% the l¹ norm
   return (ϑ^α × Qpath(|j − m|, |k − n|, |l − o|, 0, 0));
}
```

Program C.3.8. *This is a simplistic realisation of the $\widehat{GQ}$ where the Qpath Program C.3.6 has been replaced by an equivalent binomial coefficient. An adjustment for adjacent points are included given a square domain is assumed.*

```
real GQ( integer j, k, m, n, card(℘adjacent)) :  real
{
   real α = 0;    integer o, counter;
   o = |j − m| + |k − n|;    counter = min(|j − m|, |k − n|);
   if o < 50 then α = ϑ^o (o−2+card(℘adjacent) choose counter); %% exact calculation
   else α = ϑ^o (o−2+card(℘adjacent) choose counter); %% approximation
   return (α);
}
```

Program C.3.9. *A simple implementation on a rectangular domain.*

```
matrix2d GQ( matrix2d F) :  matrix2d
{
     for k = 1 to N_y − 2, ++k
       for j = 1 to M_x − 1, ++j
         F_{j,k} = DET(j, k) + STO(j, k);
}
```

Program C.3.10. *This program approximates values of $\sum_{\delta\upsilon} \widehat{H}(X)\,\widehat{F}_{\delta\upsilon}(X)$ using the $\widehat{GQ}(\cdot)$ results and to estimate $\widehat{H}(X)$.*

```
real DET^(integer J,K; real F^_δU(·)) :  real
{
   real β = 0, num = 0, den = 0;
   for j = 1 to M_x − 2, ++j
   {
     β = GQ^(J,K,j,0,ϑ,1);
     den = den + β;     num = num + βF^_δU(j,0);
     β = GQ^(J,K,j,N_y − 1,ϑ,1);
     den = den + β;     num = num + βF^_δU(j,N_y − 1);
   }
   for k = 1 to N_y − 2, ++k
   {
     β = GQ^(J,K,0,k,ϑ,1);
     den = den + β;     num = num + βF^_δU(0,k);
     β = GQ^(J,K,M_x − 1,k,ϑ,1);
     den = den + β;     num = num + βF^_δU(M_x − 1,k));
   }
   if (|num| < 0.00001) then return (0);
   else return(num/den);
}
```

Program C.3.11. *This program approximates values of* $\widehat{G}$ *using the* $\widehat{GQ}(\cdot)$ *results and derives an estimate for the functionals of the system.*

```
real STO^(integer J,K) :  real
{
   real β = 0, num = 0;
   for j = 1 to M_x − 2, ++j
     for k = 1 to N_y − 2, ++k
     {
       β = GQ^(J,K,j,k,ϑ);
       if (j ≠ J or k ≠ K) then
         num = num + β(υ(jΔx,kΔy)𝔐(D) + ω(jΔx,kΔy)𝕎(D)(j,k));
     }
   return(Ĝ(J,K;J,K)ϑ(υ(F̂(·),JΔx,KΔy)𝔐(D)
   +ω(JΔx,KΔy)𝕎(D)(J,K)) + λ_yϑnum)
}
```

C.3.4 GPS method

Program C.3.12. *This is a sub-optimal program showing the orientation of points with respect to the discretised Green's function. A method for estimating the influence from the driving functionals* $\{\upsilon(\cdot), \omega(\cdot)\}$ *is omitted.*

```
void 8GPS(matrix_2d [F̂], [Ĝ]; square [𝕎]) :  matrix_2d
{
   real num = 0;    real den = 0;
   for j = 1 to M_x − 2, ++j
     for k = 1 to N_y − 2, ++k
     {
       num = Ĝ(℘_0; j, k) F̂(℘_0); %% orientation=0
       den = Ĝ(℘_0; j, k);
       num = num + Ĝ(℘_0; N_y − k, j) F̂(℘_1); %% orientation=1
       den = den + Ĝ(℘_0; N_y − k, j);
       num = num + Ĝ(℘_0; M_x − j, N_y − k) F̂(℘_2); %% orientation=2
       den = den + Ĝ(℘_0; M_x − j, N_y − k);
       num = num + Ĝ(℘_0; k, M_x − j) F̂(℘_3); %% orientation=3
       den = den + Ĝ(℘_0; k, M_x − j);
       num = num + Ĝ(℘_0; M_x − j, k) F̂(℘_4); %% orientation=4
       den = den + Ĝ(℘_0; M_x − j, k);
       num = num + Ĝ(℘_0; k, j) F̂(℘_5); %% orientation=5
       den = den + Ĝ(℘_0; k, j);
       num = num + Ĝ(℘_0; j, N_y − k) F̂(℘_6); %% orientation=6
       den = den + Ĝ(℘_0; j, N_y − k);
       num = num + Ĝ(℘_0; N_y − k, M_x − j) F̂(℘_7); %% orientation=7
       den = den + Ĝ(℘_0; N_y − k, M_x − j);
       F̂_{j,k} = num/den + {Ĝ_N(·), υ(·) 𝔐(D), ω(·) 𝕎(D)(·)};
     }
   return ([F̂]);
}
```

Appendix D

Figures

Although the numerical work to verify the results of this chapter have involved uniform $\mathbb{Z}^2$ with a few billion interior points, in order to show visible changes, only rough domains will be presented.

D.1 Hyperbolic system

Figures D.1 through D.6 represent a numerical refinement of a uniform $\mathbb{Z}^2$ rectangular domain $(x,t) \in \left\{[0,1] \times \left[0, \frac{1}{2}\right]\right\}$ where $\mathfrak{H}^2\left(F\left(x,t\right),1\right) = F\left(x,t\right) + 2F\left(x,t\right)\frac{\partial^2 W(x,t)}{\partial x \partial t}$, $F\left(x,0\right) = \sin\left(2\pi x + 2\pi t\right) = \sin\left(2\pi x\right)$, and $\frac{\partial F(x,t)}{\partial t} \mid_{t=0} = 2\pi\cos\left(2\pi x\right)$. Using the 513×257 numerical approximation of the process as the 'numerical solution,' Table D.1 gives a quick comparison of the different numerical refinements where $\chi^2\left(\mathfrak{e}\right)$ is a standard Pearson's chi-square statistic and $\max\left(\mathfrak{eg}\right)$ is the maximum global error taken over the DoI. Since the chi-square statistic yields a p-value of approximately 1, this indicates that even rough $\mathbb{Z}^2_{\Delta x}$ approximations are good approximations to the numerical solution.

Grid Size	$\chi^2\left(\mathfrak{e}\right)$	$\max\left(\mathfrak{eg}\right)$
(513×257)	0	0
(257×129)	0.00123126	0.0254
(129×65)	0.00368544	0.05111
(65×33)	0.00863931	0.1013
(33×17)	0.0192065	0.2574
(17×9)	0.044964	0.577
(9×5)	0.129365	1.155

Table D.1: $\mathbb{Z}^d_{\Delta x}$ comparisons

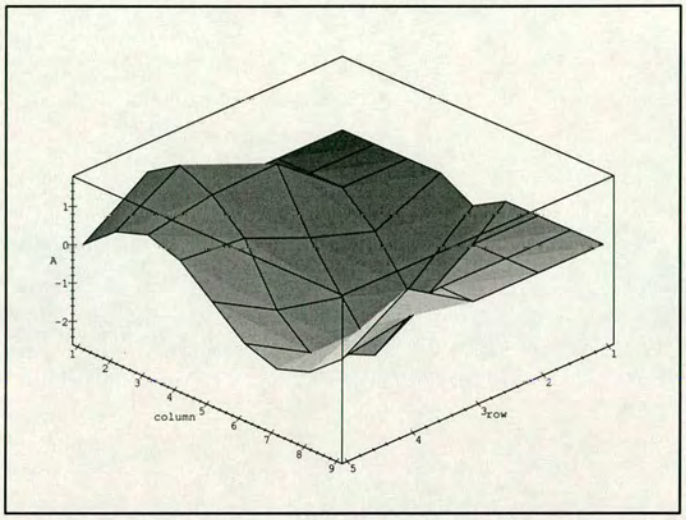

Figure D.1: $\Delta x = \frac{1}{8}$

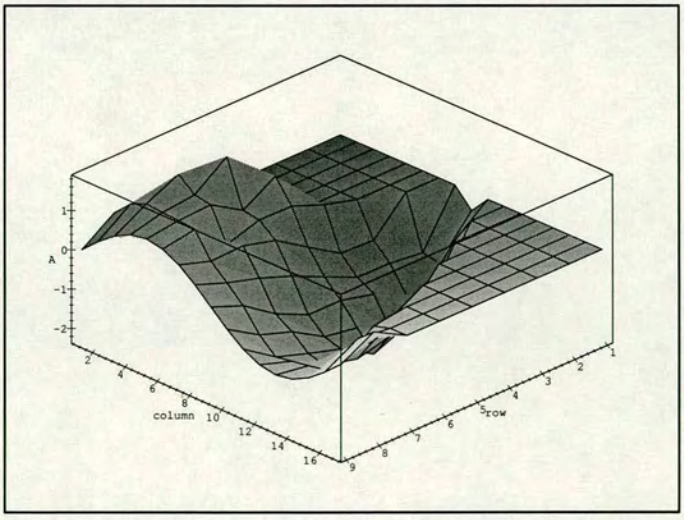

Figure D.2: $\Delta x = \frac{1}{16}$

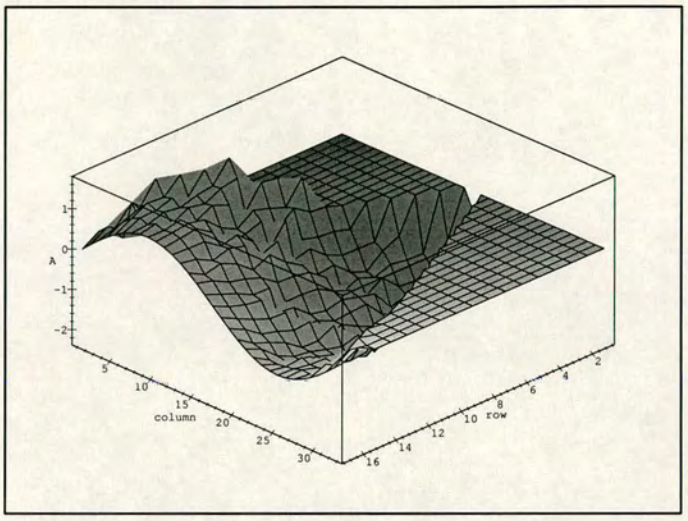

Figure D.3: $\Delta x = \frac{1}{32}$

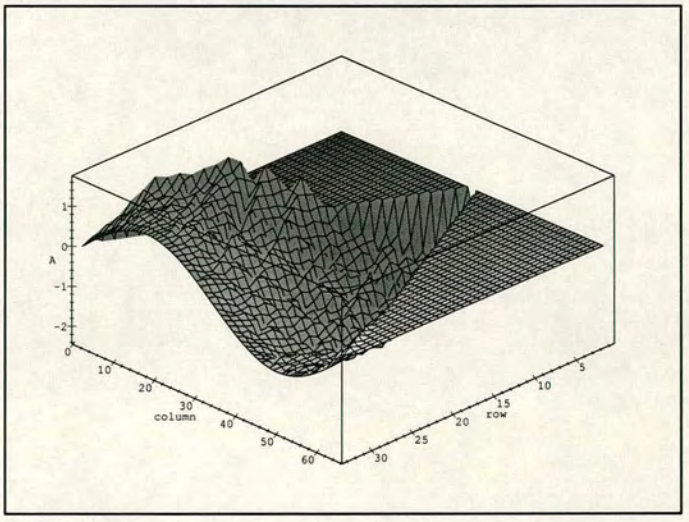

Figure D.4: $\Delta x = \frac{1}{64}$

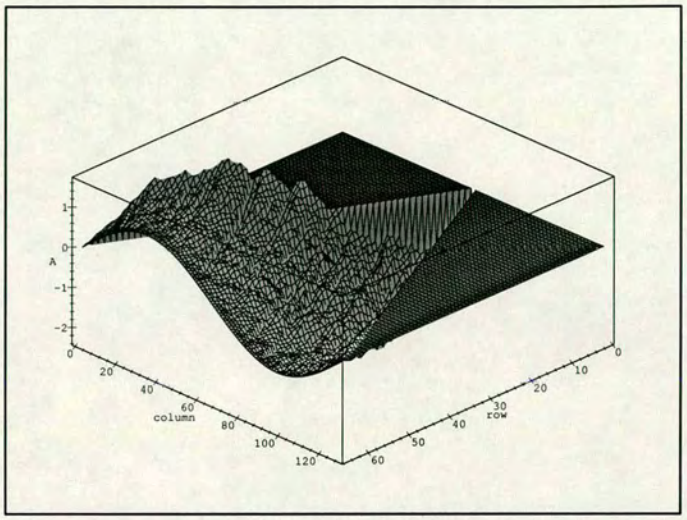

Figure D.5: $\Delta x = \frac{1}{128}$

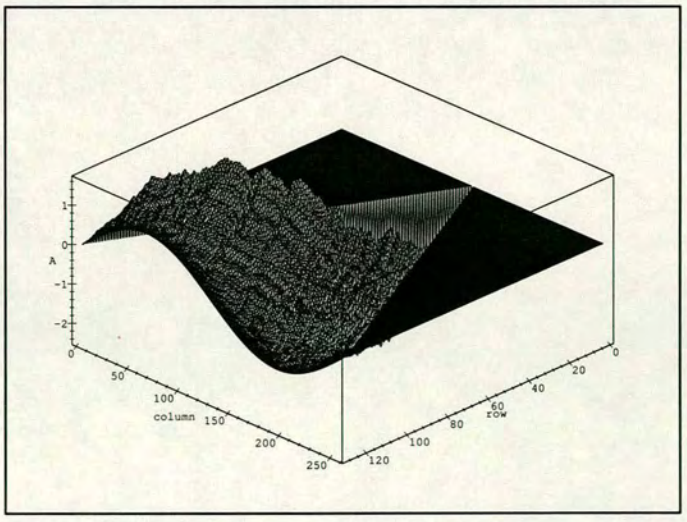

Figure D.6: $\Delta x = \frac{1}{256}$

D.2 Elliptic systems

To illustrate the discretised Green's function Lemma's, let:

•Figure D.7, depicts a Kroneker delta function located at $\left(\frac{1}{2}, \frac{1}{2}\right)$. Often called a 'unit point source,' this will be utilised to derive the discretised Green's function.

•Figures D.8 through D.12 represent the growth of a Green's function 'close to the boundary' to show that the function experiences limited growth.

•Figures D.13 through D.17 represent discretised Green's functions on a unit square $\mathbb{Z}^2$ grid.

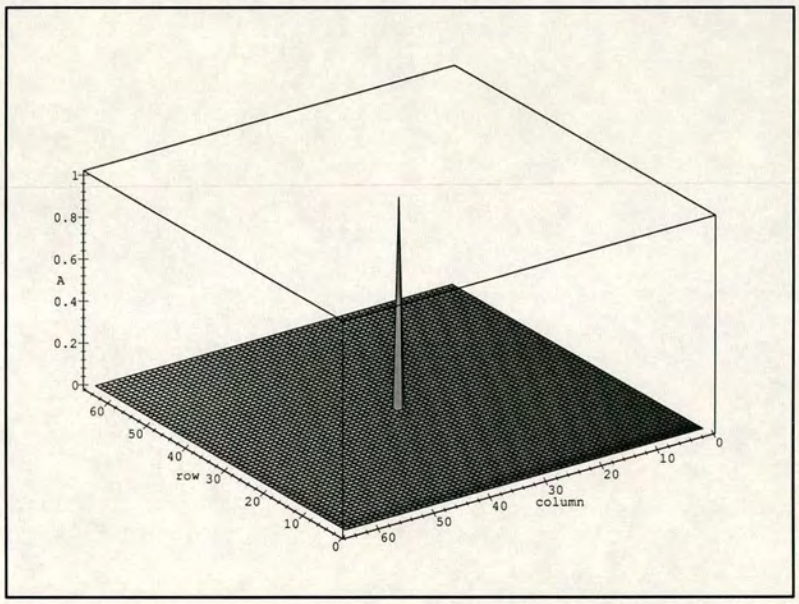

Figure D.7: $\delta_{\left(\frac{1}{2},\frac{1}{2}\right)}$ in $\mathbb{Z}^2_{\frac{1}{64}}$

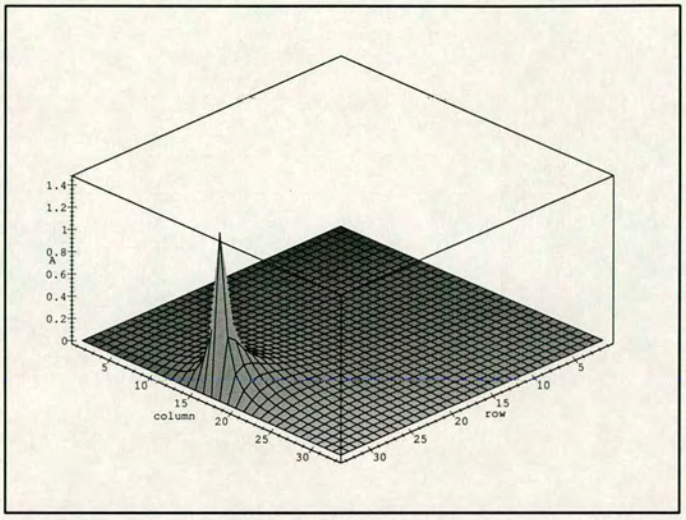

Figure D.8: $\widehat{G}\left(\frac{1}{2}, \Delta y; j, k\right) \mathfrak{M}(\mathtt{D})$ on $\mathbb{Z}^2_{33\times 33}$

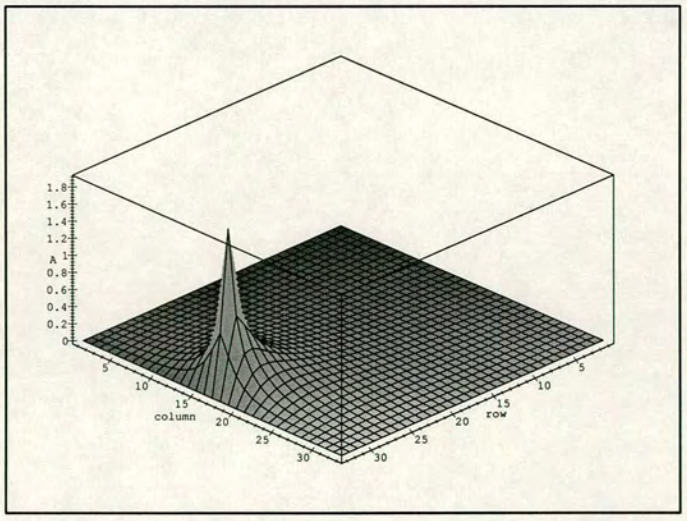

Figure D.9: $\widehat{G}\left(\frac{1}{2}, 2\Delta y; j, k\right) \mathfrak{M}(\mathtt{D})$ on $\mathbb{Z}^2_{33\times 33}$

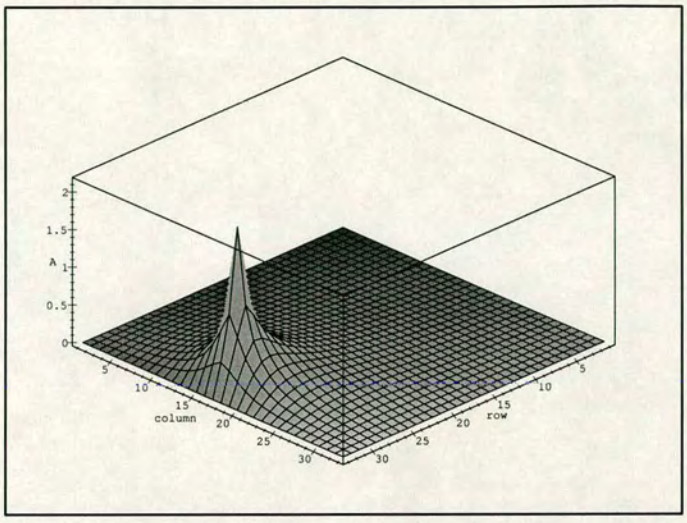

Figure D.10: $\widehat{G}\left(\frac{1}{2}, 3\Delta y; j, k\right) \mathfrak{M}(\mathtt{D})$ on $\mathbb{Z}^2_{33\times 33}$

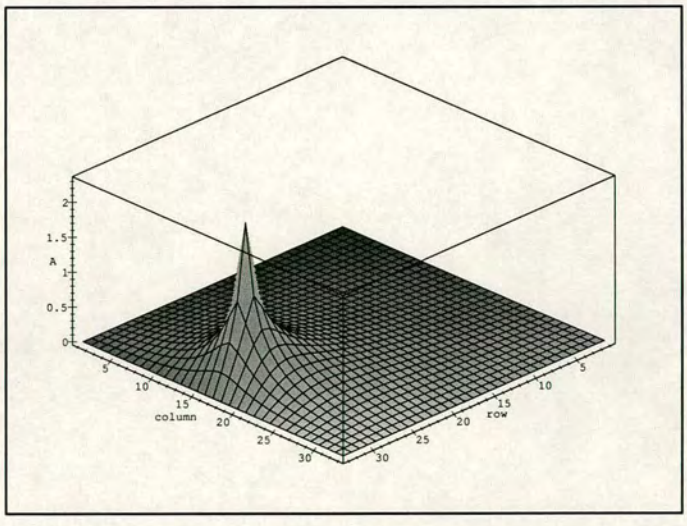

Figure D.11: $\widehat{G}\left(\frac{1}{2}, 4\Delta y; j, k\right) \mathfrak{M}(\mathtt{D})$ on $\mathbb{Z}^2_{33\times 33}$

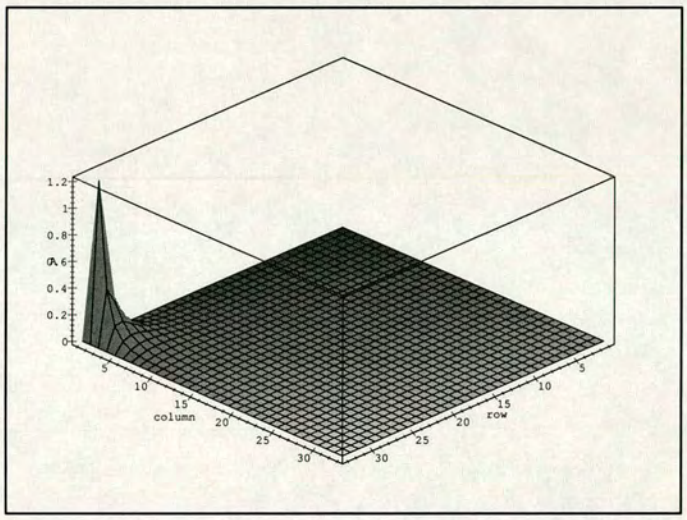

Figure D.12: $\widehat{G}\left(\Delta x, \Delta y; j, k\right) \mathfrak{M}\left(\mathtt{D}\right)$ on $\mathbb{Z}_{33\times 33}^{2}$

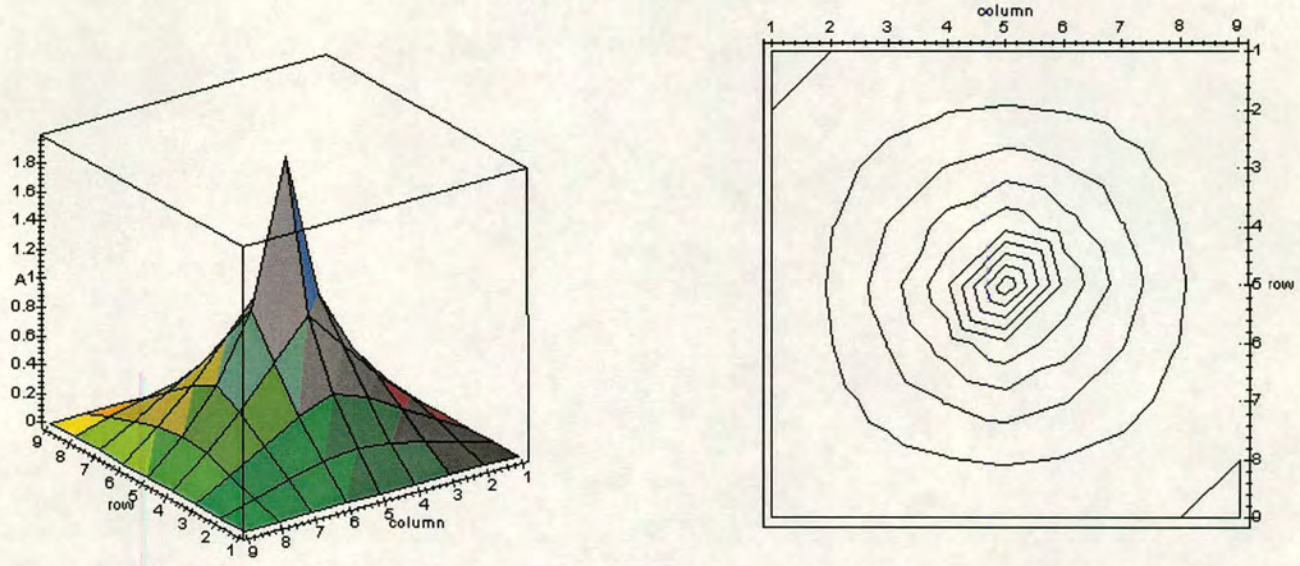

Figure D13: Discretised Green's Function on a 9x9 grid

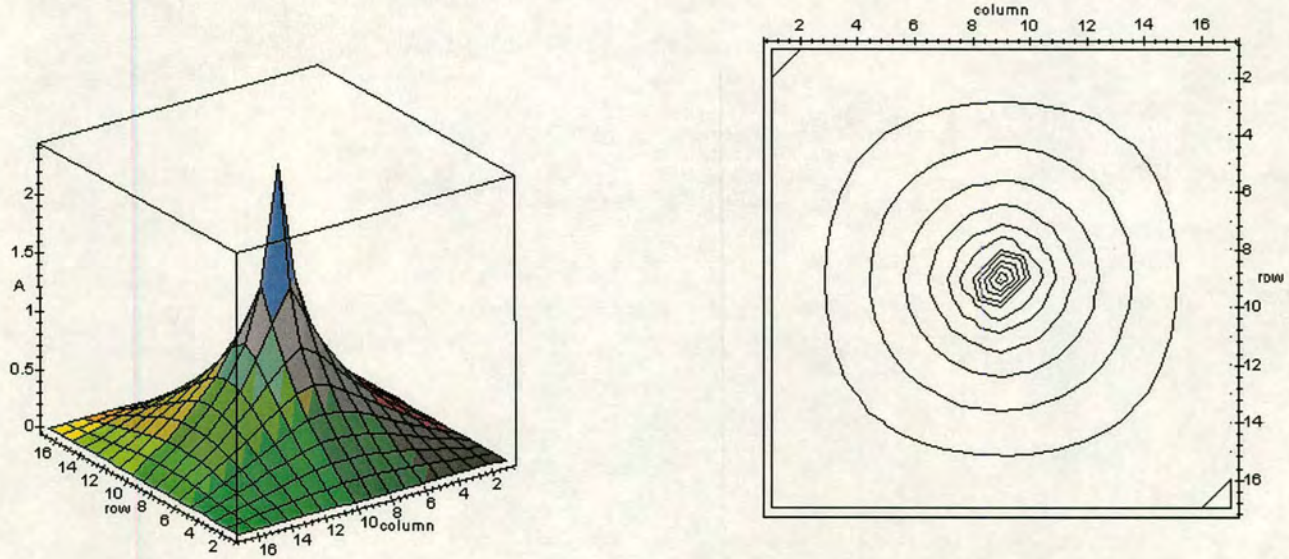

Figure D14: Discretised Green's Function on a 16x16 grid

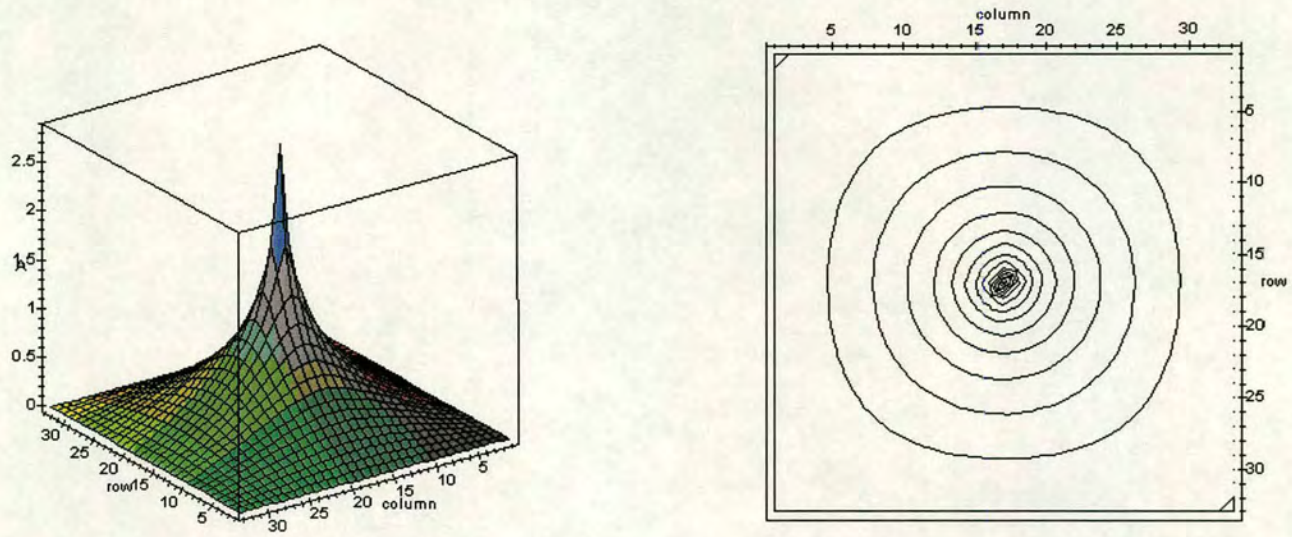

Figure D15: Discretised Green's Function on a 33x33 grid

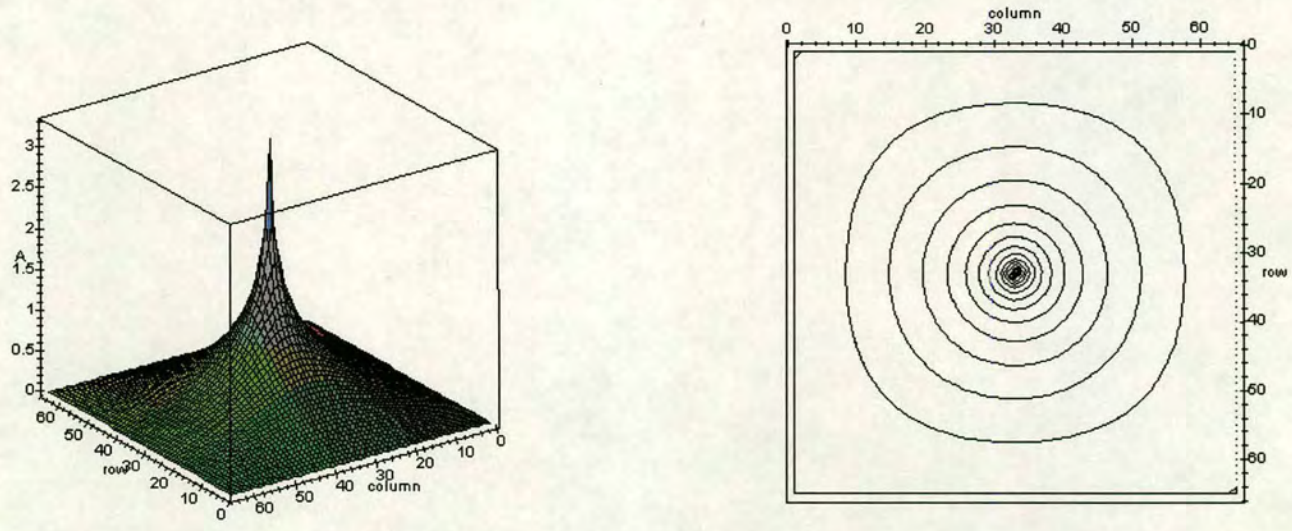

Figure D16: Discretised Green's Function on a 65x65 grid

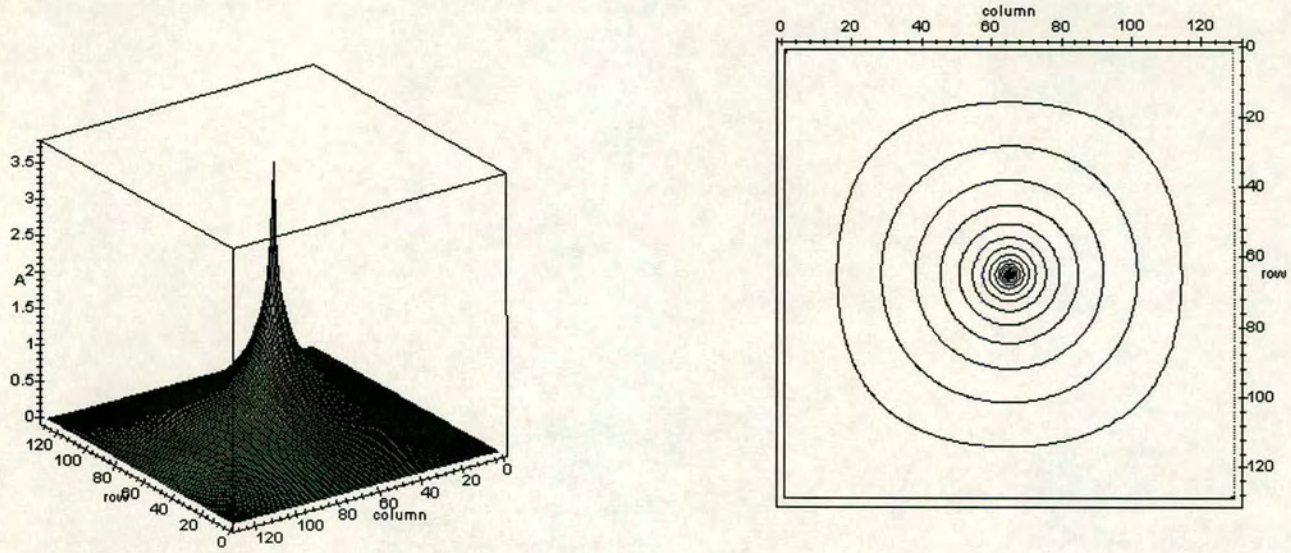

Figure D17: Discretised Green's Function on a 129x129 grid

D.2.1 $Z^2_{\Delta x=\frac{1}{512}}$ examples

Using a Z^2 unit square grid on {[0,1]x[0,1]} where $\Delta x=\Delta y=\frac{1}{512}$, approximate $\delta^2 F(x,y)=\frac{\partial^2 W(x,y)}{\partial x\,\partial y}$ via an iterative FDSy using {FDSc = (3.11), $e_{stop}=2x10^{-14}$}. The following two figures represent the $\mathbb{W}_{BM}(\Omega)$ used to drive the system.

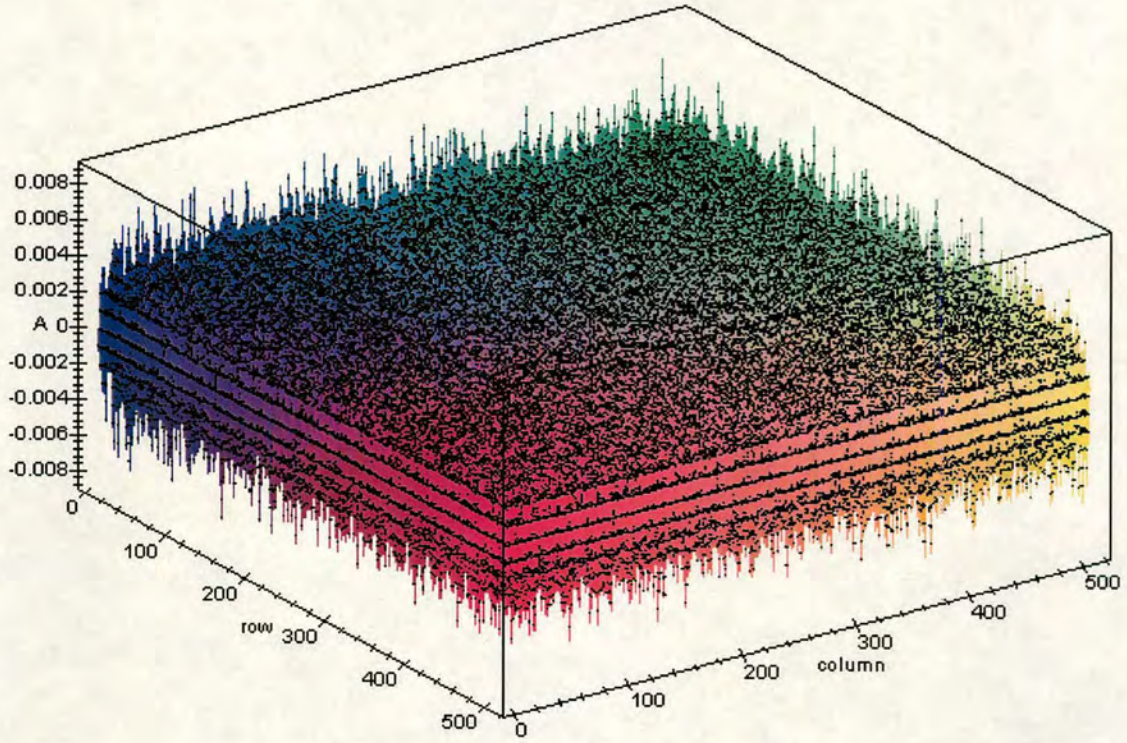

Plot of $\mathbb{W}_{BM}(D)$ using file elsq004.txt

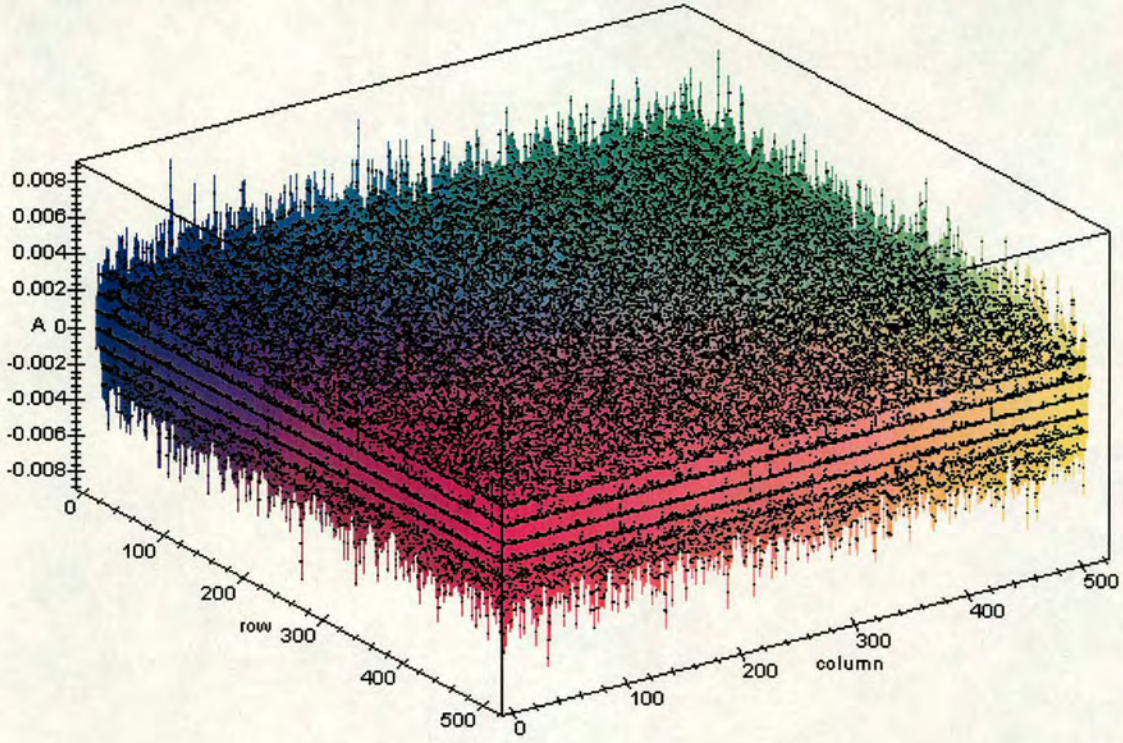

Plot of $W_{BM}(\Omega)$ using file elsq005.txt

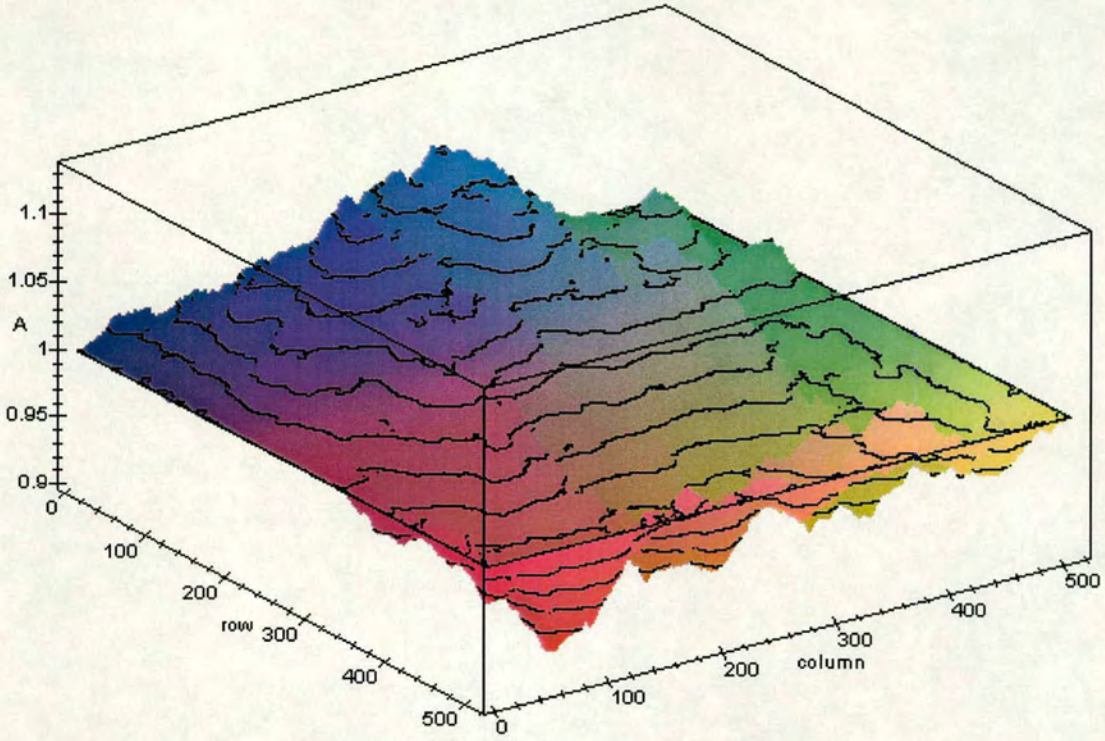

Elliptic additive noise system driven by elsq004.txt with a linear boundary $F_{\delta\Omega}(x,y)=1$.

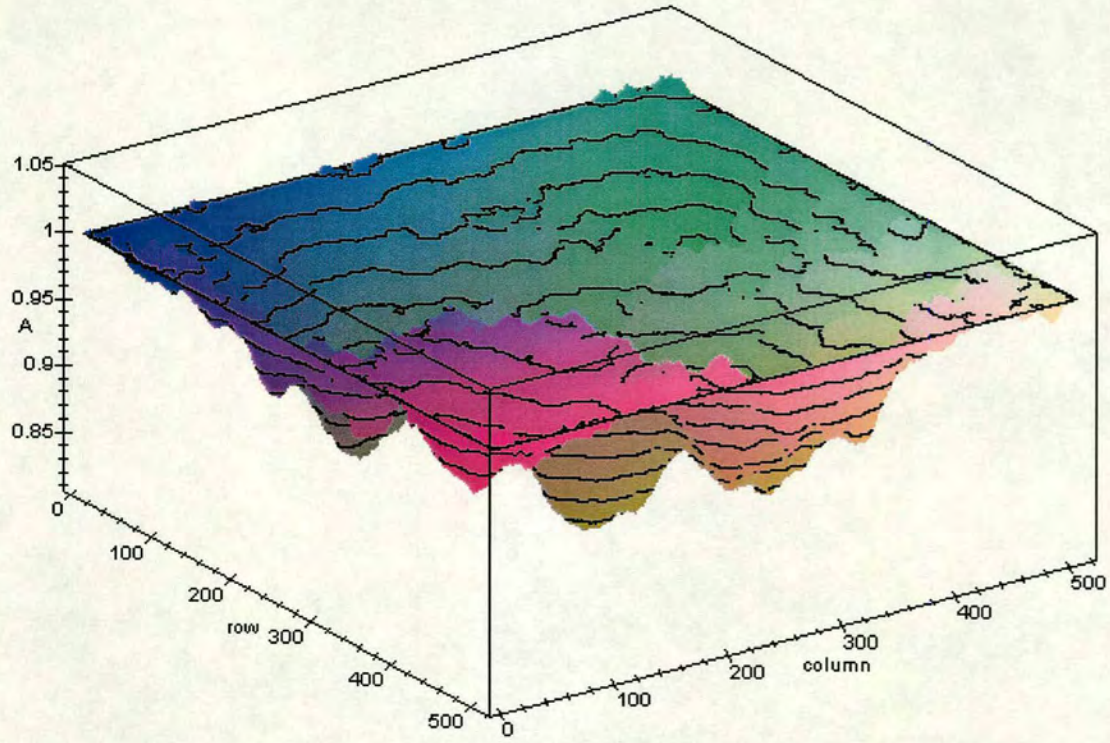

Elliptic additive noise system driven by elsq005.txt with a linear boundary $F_{\delta\Omega}(x,y)=1$.

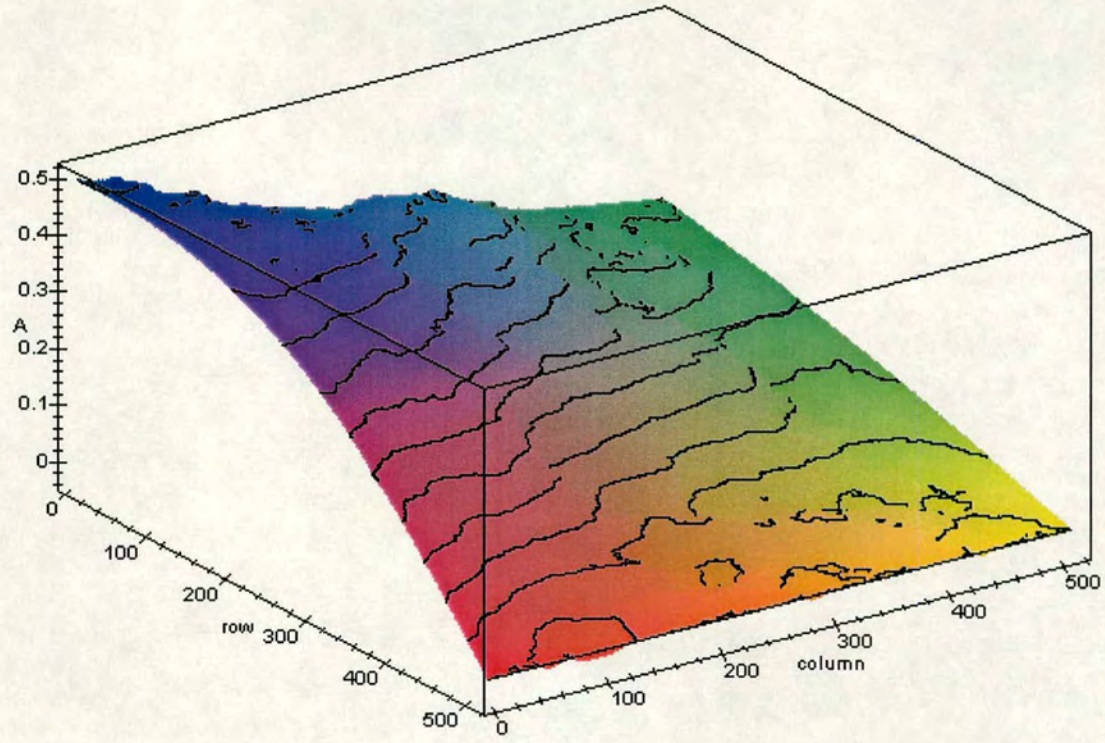

Elliptic additive noise system driven by elsq004.txt with a non-linear boundary $F_{\delta\Omega}(x,y)=\frac{y}{(1+x)^2+y^2}$.

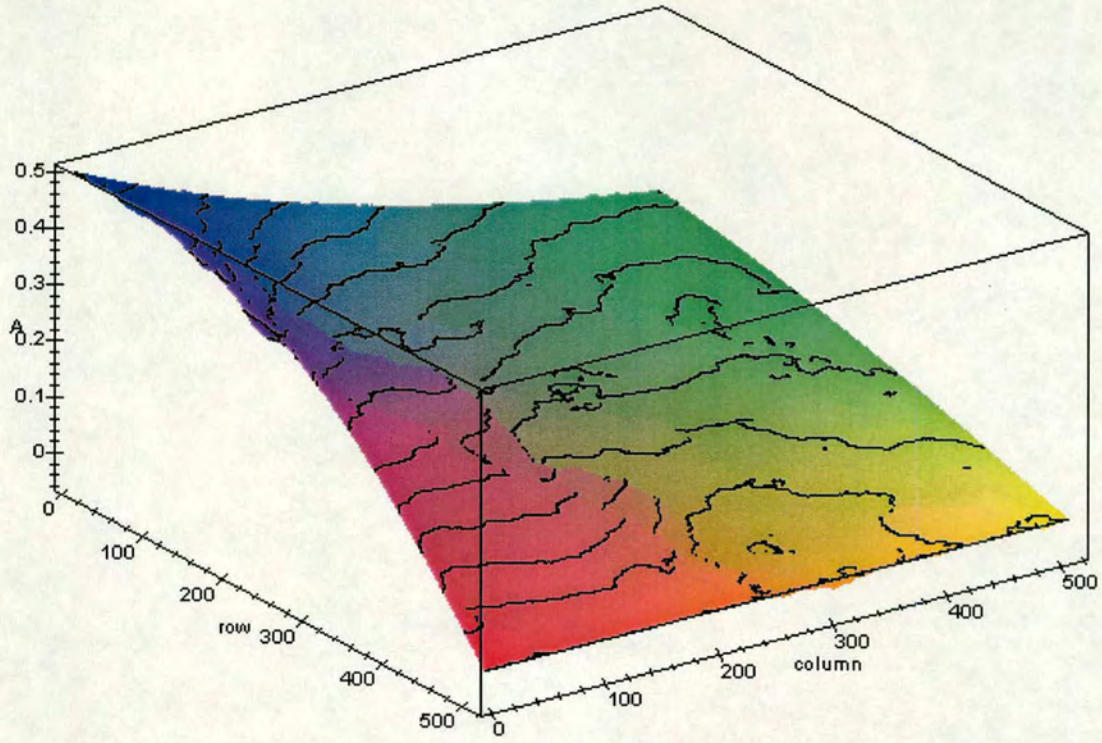

Elliptic additive noise system driven by elsq005.txt with a non-linear boundary $F_{\delta\Omega}(x,y)=\frac{y}{(1+x)^2+y^2}$.

Utilize a Z^2 unit square grid on $\{[0,1]x[0,1]\}$ where $\Delta x=\Delta y = \frac{1}{512}$ and approximate $\delta^2 F(x,y) = F(x,y)\frac{\partial^2 W(x,y)}{\partial x\, \partial y}$ via $\{FDSc = (3.11), e_{stop}=2x10^{-14}\}$.

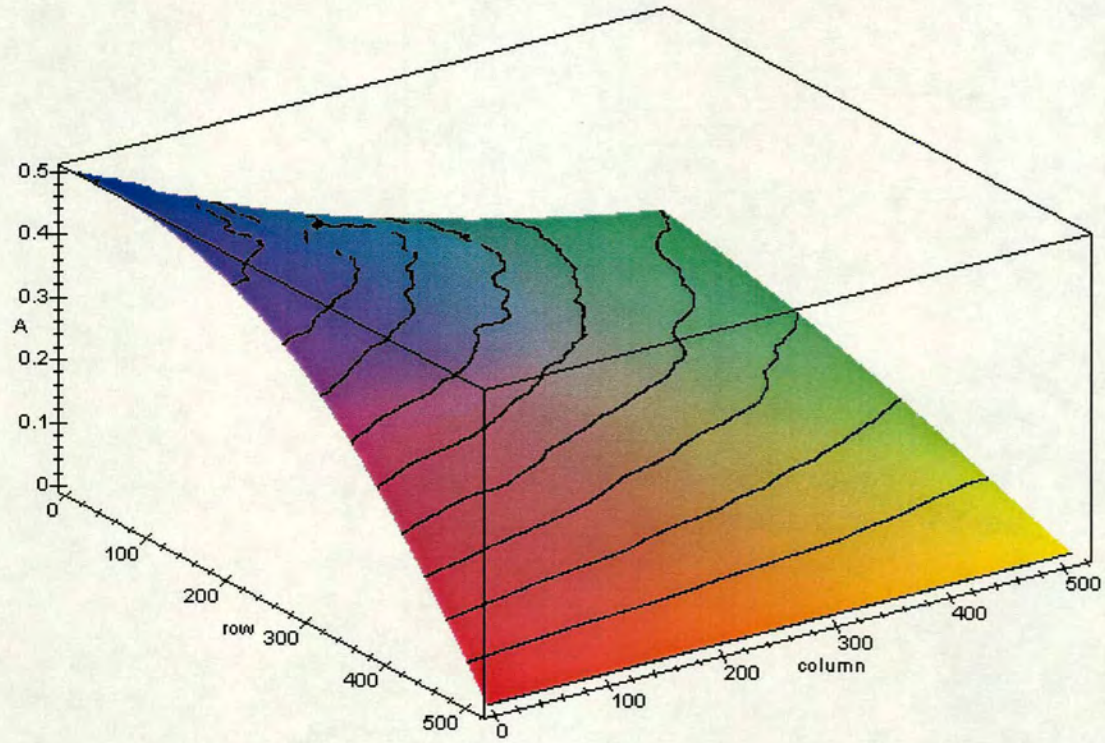

Elliptic multiplicative noise system driven by elsq004.txt with a non-linear boundary $F_{\delta\Omega}(x,y)=\frac{y}{(1+x)^2+y^2}$.

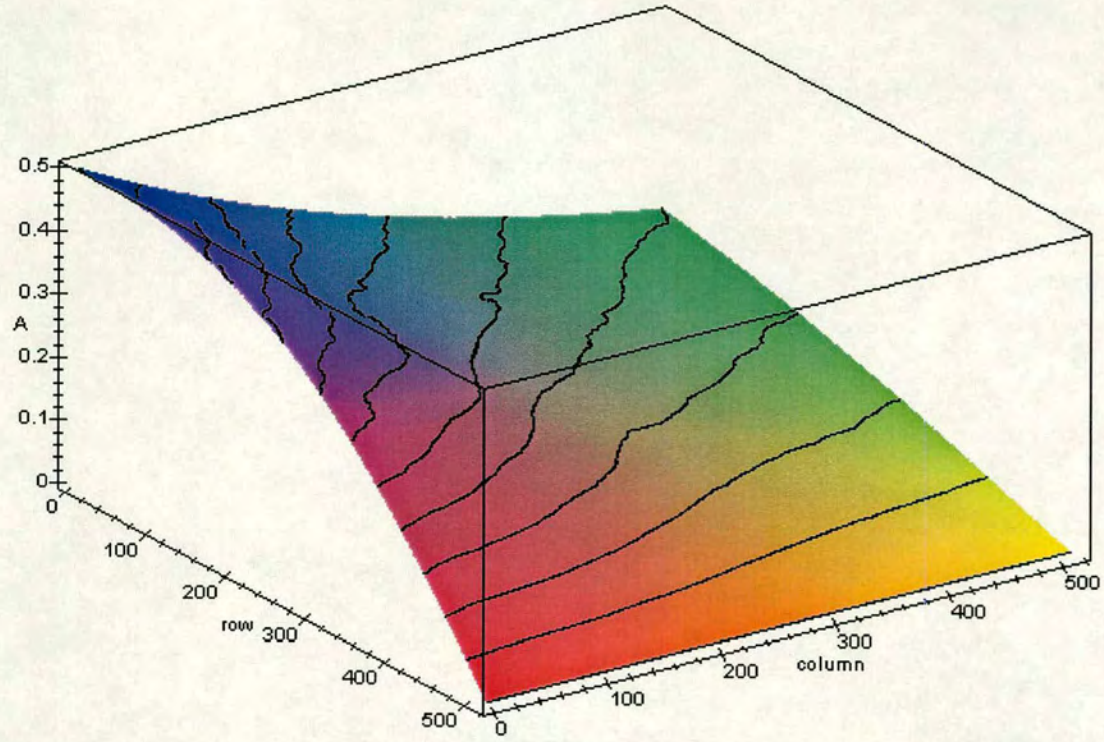

Elliptic multiplicative noise system driven by elsq005.txt with a non-linear boundary $F_{\delta\Omega}(x,y)=\frac{y}{(1+x)^2+y^2}$.

D.3 Quasi-Geostrophic system

Using a Z^2 unit square grid on {[0,1]x[0,1]} where $\Delta x=\Delta y = \frac{1}{129}$ and $\Delta t = \frac{1}{1000}\Delta x$; approximate the Früh QG process with 0 boundary conditions and $\epsilon_{stop}=5\text{x}10^{-12}$ using the process:

$$\frac{\partial Q(x,y,z,t)}{\partial t} = -J(F(x,y,z,t),Q(x,y,z,t)) - 0.2\Delta^2 F(x,y,z,t) + 0.32\Delta^2 Q(x,y,z,t) + 2\frac{\partial^3 W(x,y,z,t)}{\partial x \partial y \partial t}$$

where $Q(x,y,z,t) = \Delta^2 F(x,y,z,t) + 0.1y - 90\Delta F(x,y,z,t)$.

Level 0

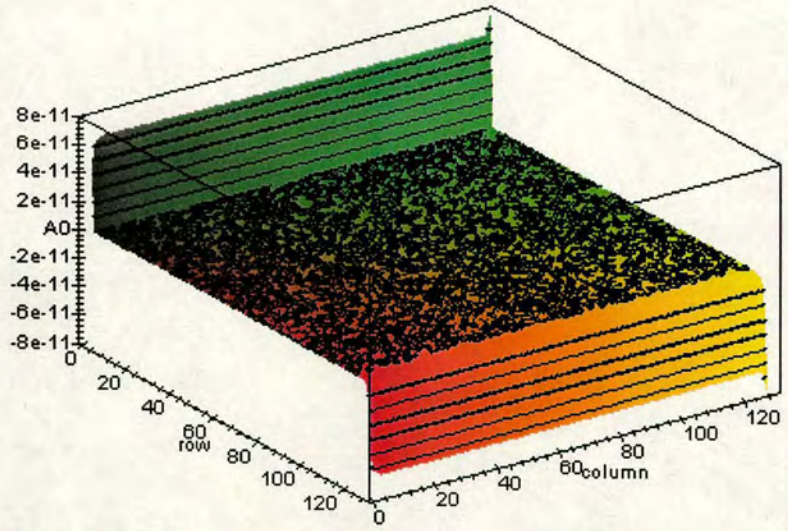

Level 1

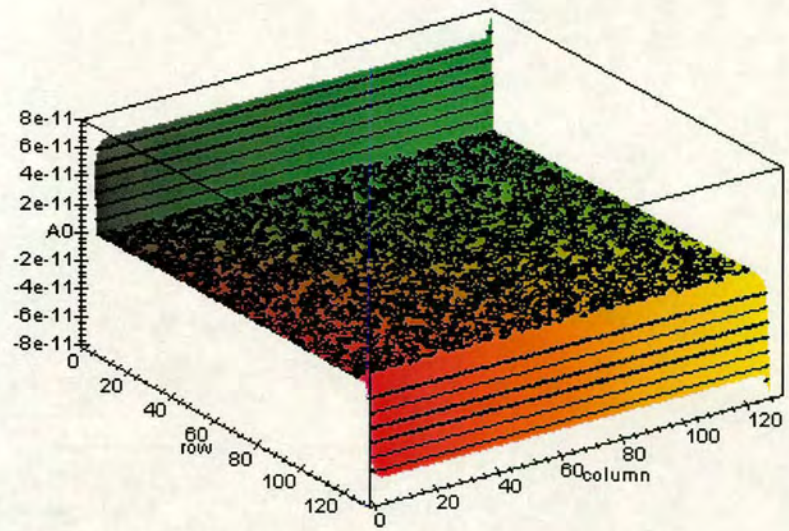

t = 0.001 time unit

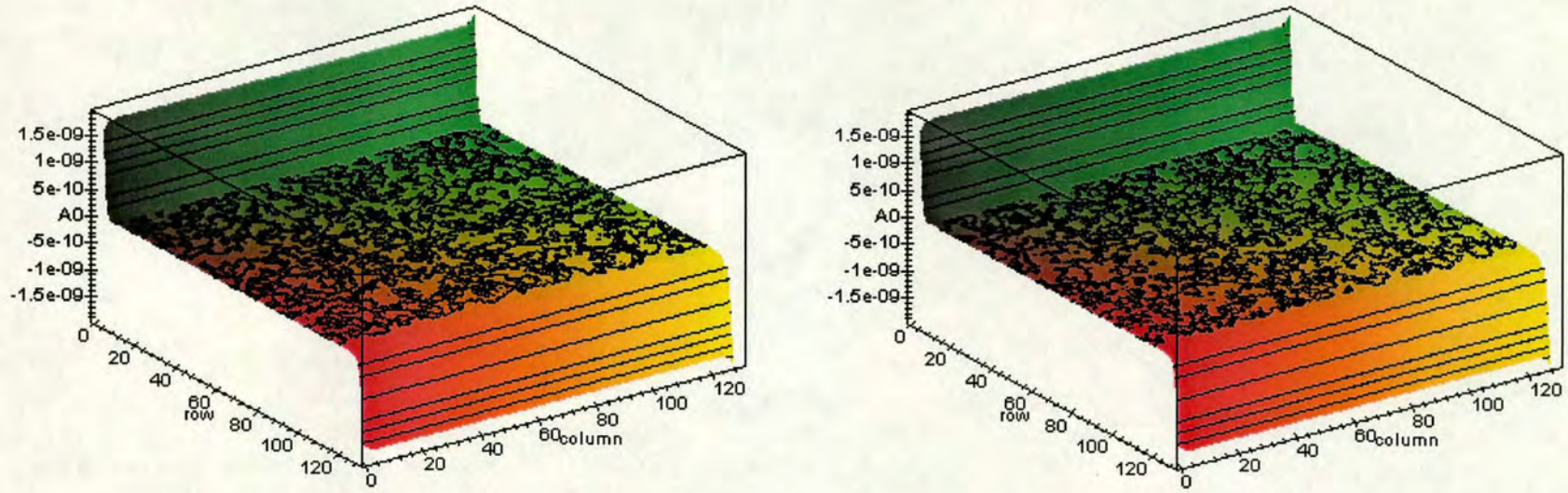

t=0.01 time unit

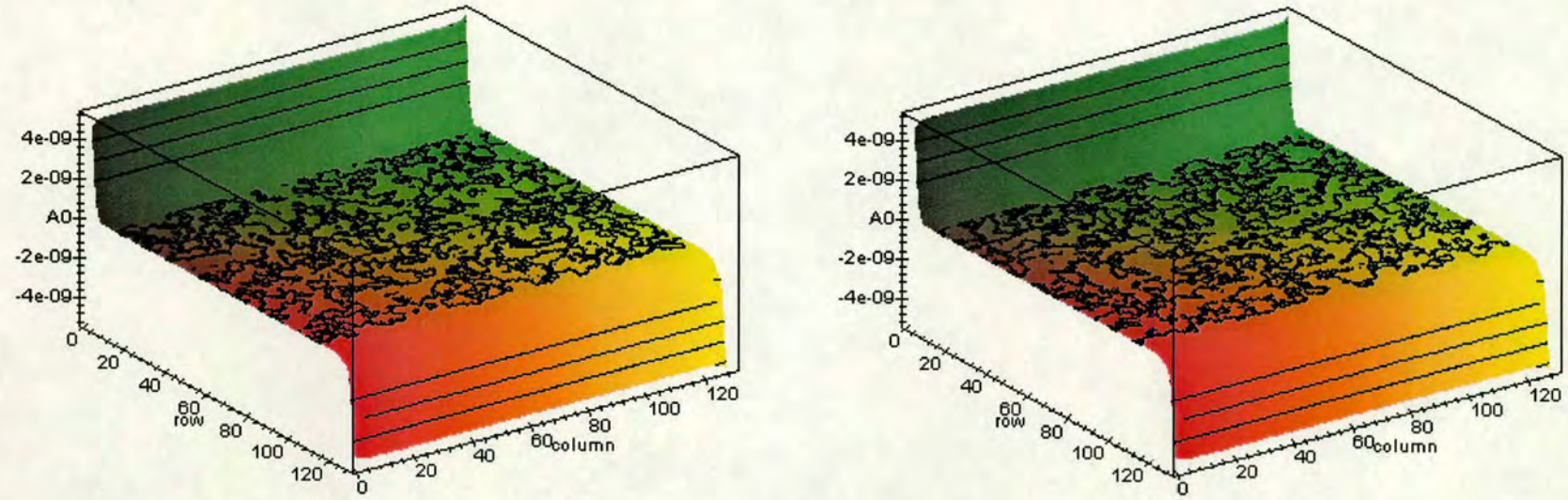

t=0.02 time unit

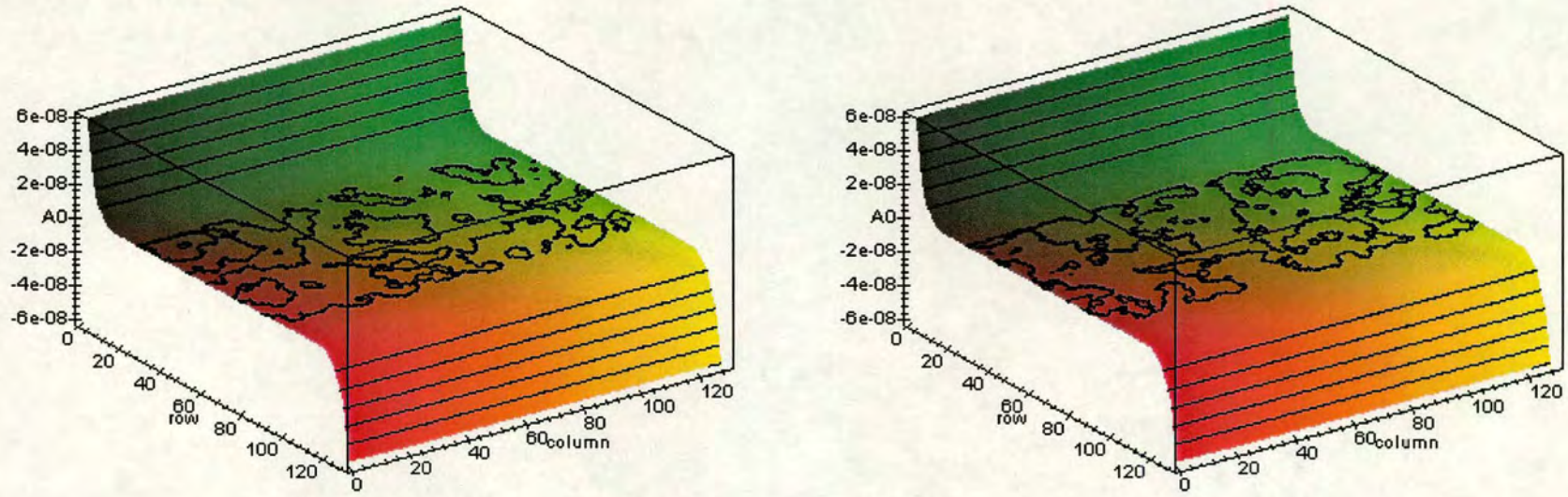

t=0.03 time unit

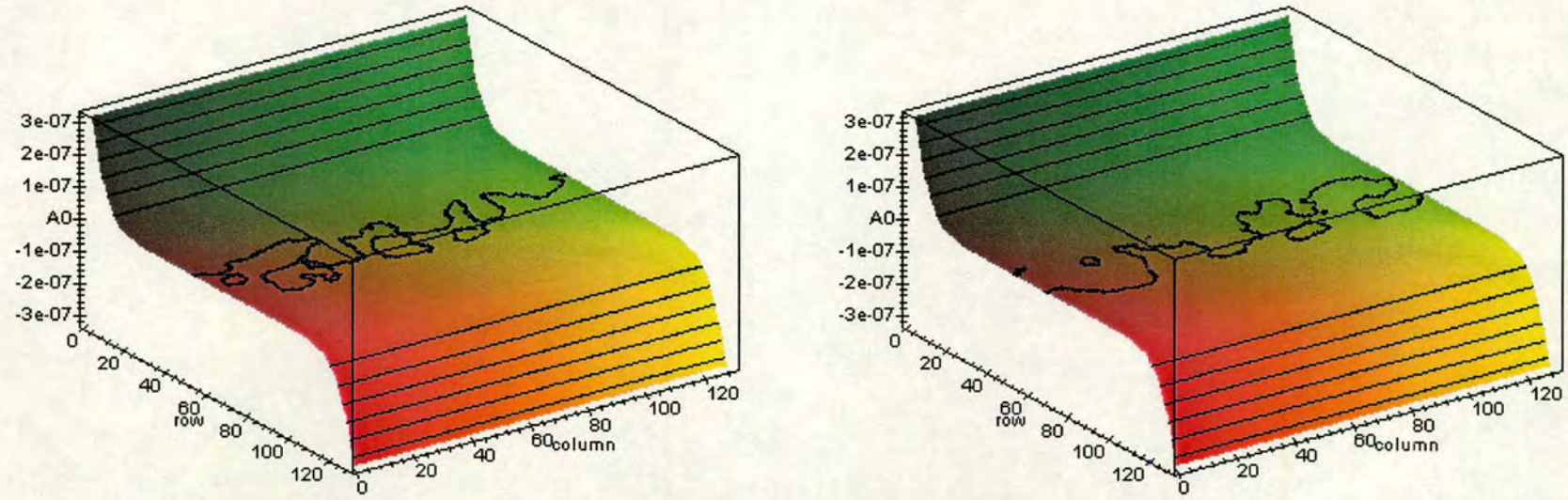

t=0. 1 time unit

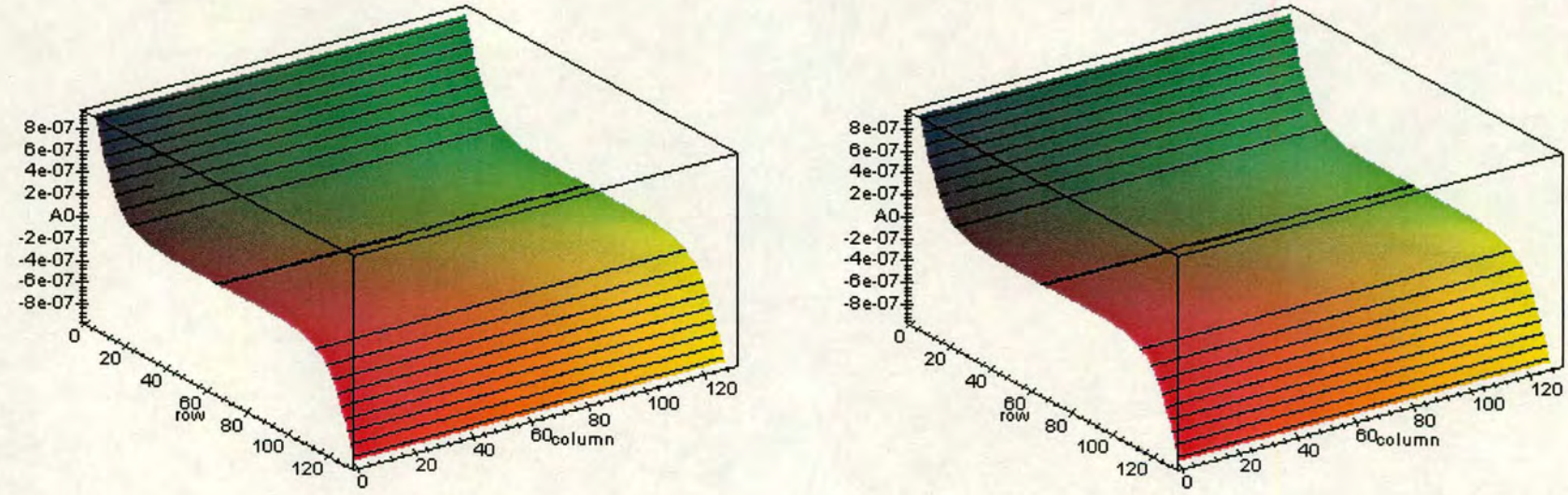

t=0.3 time unit

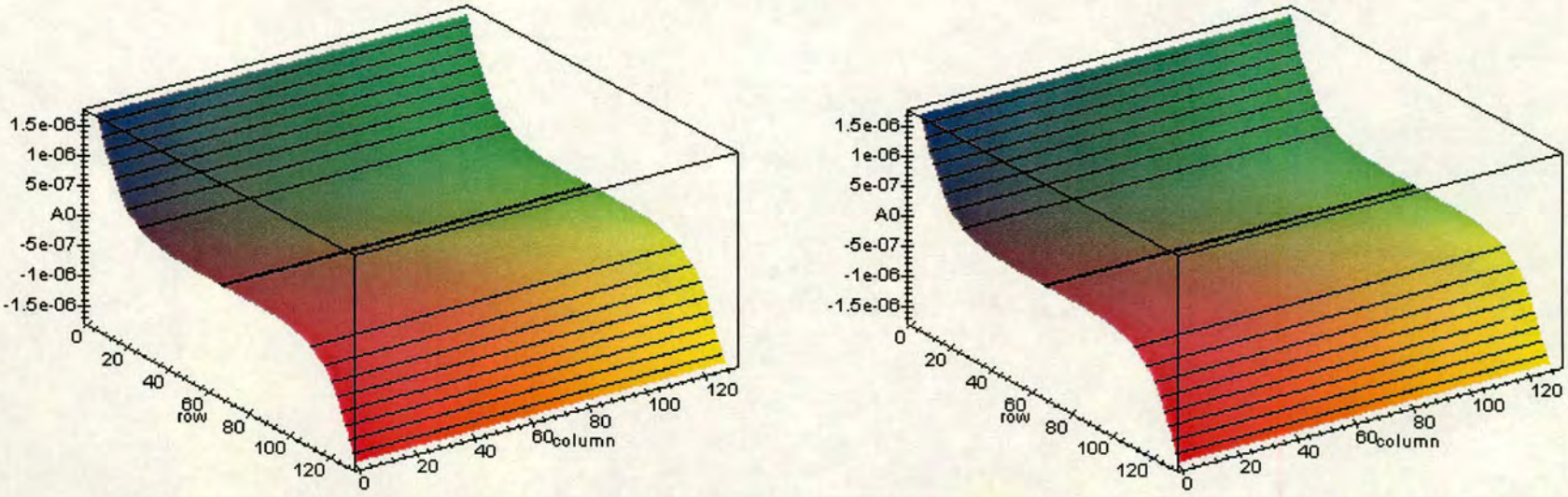

t=0.6 time unit

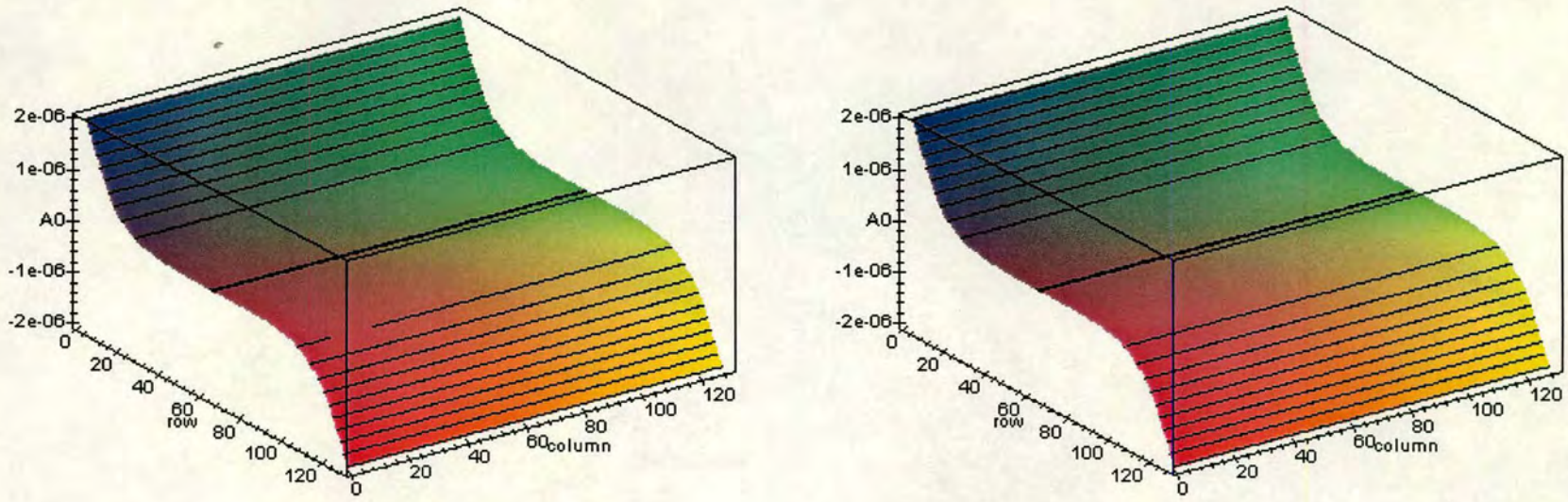

t=0.9 time unit

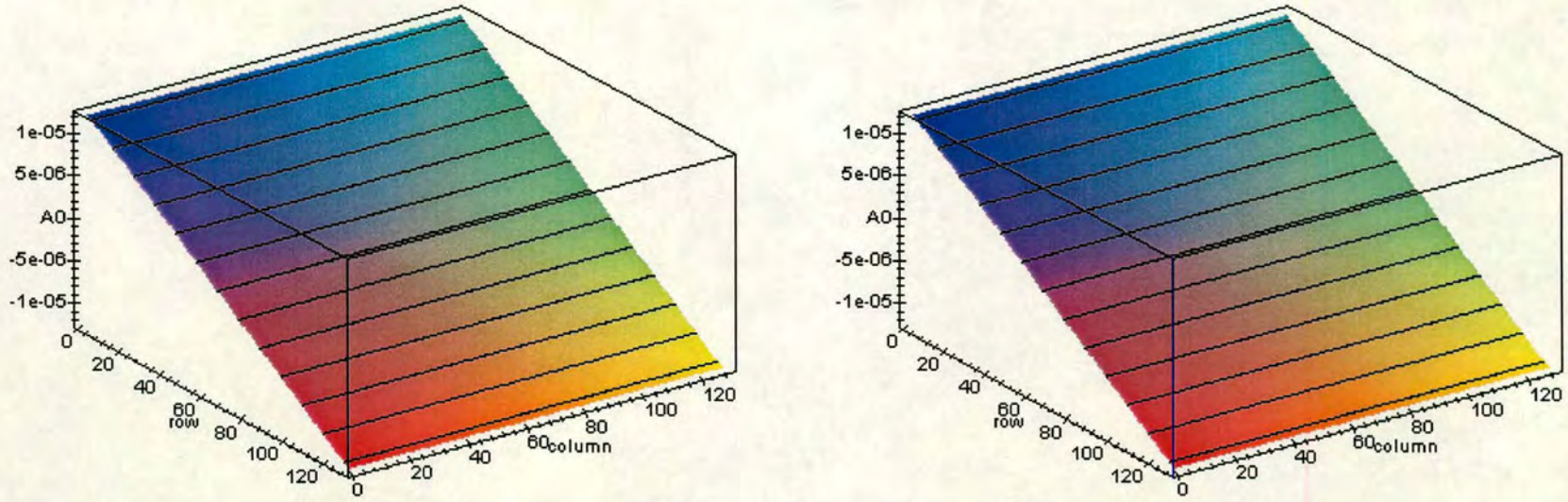

t=1.0 time unit